Silesian University of Technology

Faculty of Energy and Environmental Engineering

Department of Water and Wastewater Engineering

Ph.D. Thesis

Degradation of natural and anthropogenic pollutant on surface water in aspect of self-cleaning phenomenon

Author:

MSc, Bhautik Dave

Supervisor:

Dr. hab. Inz. Ewa Lobos-Moysa, prof. PS

Gliwice, 2026

Motivation and Inspiration

1. Bhagavad Gita on Knowledge and Discipline – The Inspiration

Sanskrit:
श्रद्धावान् लभते ज्ञानं तत्परः संयतेन्द्रियः।
ज्ञानं लब्ध्वा परां शान्तिमचिरेणाधिगच्छति॥

Hindi:
श्रद्धावान और संयमी, जो इन्द्रियों पर नियंत्रण रखते हैं, ज्ञान प्राप्त करते हैं; और ज्ञान प्राप्त करके वे परम शांति को शीघ्र ही प्राप्त करते हैं।

English:
The faithful and disciplined, who control their senses, attain knowledge; through knowledge, they reach supreme peace.

2. Arjuna and Krishna Dialogue – The Energy

Sanskrit (adapted):
अर्जुन: हे कृष्ण, सर्वं मम विपरीतम् अस्ति।
कृष्ण: हे अर्जुन, सर्वं जयिष्यति, अहं तव संगतिरेव अस्मि।

Hindi:
अर्जुन: हे कृष्णा, सब मेरे विपरीत हैं।
कृष्णा: हे अर्जुन, सब हारेंगे, मैं तुम्हारे साथ हूँ।

English:
Arjun: Hey Krishna, everything is against me.
Krishna: Hey Arjun, everything will be won, I am with you.

3. Life as a Journey of Higher Truth – The Conclusion

Sanskrit (adapted):
जीवनं असत्यात् सत्यं प्रति न, किन्तु निम्नसत्यात् उच्चसत्यं प्रति यात्रा अस्ति।

Hindi:
"जीवन असत्य से सत्य की ओर नहीं, बल्कि निम्न सत्य से उच्च सत्य की ओर की यात्रा है।"

English:
"Life is not a journey from untruth to truth, but from a lower truth to a higher truth."

Dedicated to my parents and wife.

Acknowledgments

I wish to express my profound and sincere gratitude to my supervisor, Prof. Ewa Lobos Moysa, whose exceptional guidance, unwavering support, and profound knowledge have been invaluable throughout my doctoral journey. Her patience, encouragement, and insightful mentorship have not only shaped the trajectory of my research but also enriched my personal and professional growth. I am deeply appreciative of the time, wisdom, and dedication she has generously invested in my development as a researcher.

I am indebted to my colleagues and collaborators, whose cooperation and intellectual contributions have significantly enhanced the quality of my work. In particular, I would like to acknowledge Nisarg Mehta, Ruchi Upadhyay, Anna Kuznik, Edyta Kudlek-Tymoszuk, Wioletta Przystas, Marcelina Jureczko, Irena Korus, Advait Mehta, Rushikesh Joshi, Vicky Jain, and Abdullah Maqsood, Małgorzata Kwiatosz, and Aleksandra Bernaczek for their consistent support, guidance, and encouragement. Your collaborative spirit, constructive feedback, and mentoring have been a source of inspiration and motivation.

I extend my heartfelt appreciation to all those with whom I have had the privilege of working over the years. Your knowledge, insights, and encouragement have played a pivotal role in enriching my research experience and fostering my growth as a scholar. Above all, I owe an immense debt of gratitude to my parents, and my family. Your unwavering love, care, and belief in my abilities have been the foundation of my journey. The opportunities, guidance, and encouragement you have provided have sustained me through every challenge and milestone.

Finally, my deepest and most heartfelt gratitude goes to my wife, Krutika. From the moment she entered my life, she has been an unwavering source of strength, encouragement, and solace. Her patience, steadfast support, and boundless love, especially during the most challenging periods of my doctoral journey, have been a beacon of hope and resilience. Words alone cannot capture the depth of my appreciation for her presence, understanding, and unwavering faith in me.

Abstract

The increasing presence of emerging contaminants (ECs) in aquatic environments poses a persistent challenge to natural self-cleaning processes and conventional wastewater treatment systems. In natural aquatic systems, self-cleaning processes operate passively and are strongly constrained by environmental variability, whereas this research addresses self-cleaning as a deliberately engineered and biologically intensified process. Compounds such as caffeine, nicotine, methylparaben (MeP), and trichlorocarbanilide (TCC) exhibit diverse physicochemical properties and are often incompletely attenuated in surface waters due to dilution, nutrient limitation, ecological competition, and environmental variability. Although microbial self-cleaning contributes to contaminant transformation, its efficiency under uncontrolled environmental conditions remains limited. This doctoral research aimed to enhance biologically driven self-cleaning processes through pollutant-specific microbial selection, wastewater-based microbial adaptation, and integration of adapted fungal and bacterial systems within an engineered constructed wetland framework.

The study was conducted at two sequential scales: lab-scale experiments and a pilot-scale constructed wetland system. The originality of this research was the use of synthetic wastewater formulated to resemble polluted surface and wastewater matrices, which served simultaneously as a model contaminated water system and the sole nutrient source for microbial growth. By imposing nutrient limitation, this approach forced direct coupling between microbial growth and contaminant metabolism, thereby improving environmental relevance and scalability beyond laboratory-optimized media. This strategy was intentionally designed to move beyond laboratory-optimized media and to enhance pollutant degradation by forcing microorganisms to utilize wastewater-derived nutrients while metabolizing target contaminants.

At the lab scale, the biodegradation potential of the white-rot fungus *Trametes versicolor* toward caffeine and nicotine was evaluated under controlled, nutrient-limited conditions. Experiments were conducted at an initial contaminant concentration of 100 mg L^{-1} using chemically extracted caffeine and nicotine from natural sources. The effects of temperature (25 and 37 °C), pH (strongly acidic and moderately acidic), and medium composition (potato dextrose broth, synthetic wastewater, and complex natural matrices) were systematically

assessed. Due to prolonged fungal adaptation phases and slow biomass development, biodegradation was evaluated using an endpoint-based approach after 45 days of incubation, as fungal-mediated degradation is cumulative rather than kinetically rapid. Pollutant identity and removal were confirmed using spectroscopic techniques such as FT-IR, ^{1}H NMR, and ^{13}C NMR qualitatively and quantitatively.

Caffeine removal reached 97-98% under moderately acidic conditions and in synthetic wastewater at 25 °C, coinciding with maximal fungal biomass formation. High removal efficiencies were maintained in synthetic wastewater even at 37 °C, demonstrating that wastewater-derived nutrients not only sustained fungal growth but also enhanced long-term degradation performance under nutrient-limited conditions. Nicotine removal exceeded 98% under optimal conditions (25 °C, pH ~5.20, synthetic wastewater), with reduced performance observed only under combined thermal and acidic stress. Across all systems, a strong positive relationship was observed between fungal biomass accumulation and cumulative contaminant removal, confirming that adaptation to wastewater directly promoted microbial growth at scale and enhanced biodegradation efficiency.

Continuing further, a lab-scale study investigated the biodegradation of MeP and TCC by a defined bacterial consortium comprising *Alcaligenes* sp. and *Rhodococcus* sp. Experiments were conducted at an initial concentration of 100 mg L^{-1} over a 120-hour incubation period in nutrient broth and synthetic wastewater. High-Performance Thin-Layer Chromatography (HPTLC) was used to quantitatively monitor both pollutants. MeP degradation reached approximately 89% in nutrient broth and 83% in synthetic wastewater, with enhanced mid-stage degradation in synthetic wastewater following bacterial acclimation to the nutrient-limited matrix. In contrast, TCC exhibited rapid degradation, exceeding 97% removal by 96 hours and complete disappearance by 120 hours in both media. These results demonstrate that synthetic wastewater supports efficient bacterial growth and enhances the degradation of both moderately and highly recalcitrant pollutants without external nutrient supplementation.

Upscaling was performed using pilot-scale biomimetic constructed wetlands planted with *Phragmites australis*. Wastewater-adapted fungal (*Trametes versicolor*), bacterial (*Pseudomonas aeruginosa*), and combined microbial systems were integrated into the wetland matrix, operated and analysed for seven weeks under batch conditions using synthetic wastewater containing mixed pollutants (caffeine, MeP, and TCC at 100 mg L^{-1}). Prior tolerance testing

confirmed microbial survivability under mixed-pollutant stress. All biologically active wetlands exhibited sustained plant growth, stable near-neutral pH, and persistent microbial activity, confirming successful system accumulation and ecological stability.

Pollutant removal was evaluated at weeks 4 and 7 using ^{1}H and ^{13}C NMR spectroscopy, where analytically feasible. Caffeine was completely removed by week 4 in bacterial and consortium wetlands and by week 7 in the fungal wetland. MeP exhibited degradation in the fungal wetland 89% at week 4, while complete removal was achieved in all wetlands by week 7. The combined fungal–bacterial system did not universally outperform monocultures during the initial adaptation phase but reduced adaptation time, achieved faster system stabilization, and provided balanced degradation performance across chemically distinct pollutants, demonstrating functional complementarity rather than additive synergy. It enhanced methylparaben removal compared to bacteria alone, while showing similar performance to the bacterial system for caffeine degradation. TCC could not be quantified by NMR due to solubility limitations; however, stable wetland operation and high removal of other pollutants indicate favourable conditions for biodegradation of selected pollutants.

Overall, this research demonstrates that targeted microbial adaptation to synthetic wastewater enhances pollutant degradation by enabling microbial growth and metabolic activity using wastewater-derived nutrients. By linking laboratory-scale optimization with pilot-scale validation in constructed wetlands, the study establishes a scalable, sustainable strategy that actively intensifies microbial self-cleaning beyond passive natural attenuation in contaminated aquatic systems. Collectively, this work reframes surface-water self-cleaning from a passive natural phenomenon into a deliberately engineered, biologically intensified process for contaminant attenuation.

Keywords: emerging contaminants; synthetic wastewater; enhanced biodegradation; microbial adaptation; constructed wetlands; fungal degradation; bacterial consortia; self-cleaning systems

Streszczenie

Rosnąca obecność zanieczyszczeń pojawiających się (emerging contaminants, ECs) w środowiskach wodnych stanowi trwałe wyzwanie dla naturalnych procesów samooczyszczania oraz konwencjonalnych systemów oczyszczania ścieków. W naturalnych ekosystemach wodnych procesy samooczyszczania przebiegają pasywnie i są silnie ograniczone zmiennością środowiskową, podczas gdy niniejsze badania traktują samooczyszczanie jako proces celowo projektowany i biologicznie intensyfikowany. Związki takie jak kofeina, nikotyna, metyloparaben (MeP) oraz triklorokarbanilid (TCC) charakteryzują się zróżnicowanymi właściwościami fizykochemicznymi i często ulegają niepełnej eliminacji w wodach powierzchniowych na skutek rozcieńczenia, ograniczeń nutrientowych, konkurencji ekologicznej oraz zmienności warunków środowiskowych. Chociaż mikrobiologiczne procesy samooczyszczania przyczyniają się do transformacji zanieczyszczeń, ich efektywność w warunkach niekontrolowanych pozostaje ograniczona. Celem niniejszej rozprawy doktorskiej było wzmocnienie biologicznie napędzanych procesów samooczyszczania poprzez selekcję mikroorganizmów specyficznych względem zanieczyszczeń, adaptację mikrobiologiczną do ścieków oraz integrację zaadaptowanych układów grzybowych i bakteryjnych w ramach zaprojektowanego systemu mokradeł sztucznych.

Badania przeprowadzono w dwóch następujących po sobie skalach: laboratoryjnej oraz pilotażowej, obejmującej system mokradeł sztucznych. Oryginalność pracy polegała na zastosowaniu syntetycznych ścieków zaprojektowanych w celu odwzorowania zanieczyszczonych wód powierzchniowych i ścieków, które jednocześnie pełniły funkcję modelowego układu wodnego oraz jedynego źródła składników odżywczych dla wzrostu mikroorganizmów. Wprowadzenie ograniczeń nutrientowych wymusiło bezpośrednie sprzężenie wzrostu mikroorganizmów z metabolizmem zanieczyszczeń, zwiększając tym samym relewantność środowiskową oraz potencjał skalowania w porównaniu z mediami laboratoryjnymi zoptymalizowanymi pod kątem wzrostu. Strategia ta została celowo zaprojektowana w celu odejścia od klasycznych pożywek laboratoryjnych oraz wzmocnienia degradacji zanieczyszczeń poprzez zmuszenie mikroorganizmów do wykorzystania składników odżywczych pochodzących ze ścieków przy jednoczesnym metabolizowaniu docelowych związków.

Na etapie laboratoryjnym oceniono potencjał biodegradacyjny grzyba białej zgnilizny *Trametes versicolor* wobec kofeiny i nikotyny w kontrolowanych warunkach ograniczenia nutrientowego. Eksperymenty prowadzono przy początkowym stężeniu zanieczyszczeń wynoszącym 100 mg L^{-1}, wykorzystując chemicznie wyekstrahowaną kofeinę i nikotynę pochodzenia naturalnego. Systematycznie badano wpływ temperatury (25 i 37 °C), pH (silnie kwaśne oraz umiarkowanie kwaśne) oraz składu medium (bulion ziemniaczano-glukozowy, syntetyczne ścieki oraz złożone matryce naturalne). Ze względu na długotrwałe fazy adaptacji grzybów oraz powolny przyrost biomasy, biodegradację oceniano metodą punktu końcowego po 45 dniach inkubacji, ponieważ degradacja grzybowa ma charakter kumulatywny, a nie szybki kinetycznie. Tożsamość i stopień usunięcia zanieczyszczeń potwierdzano jakościowo i ilościowo przy użyciu technik spektroskopowych, takich jak FT-IR, ^1H NMR oraz ^13C NMR.

Usunięcie kofeiny osiągnęło poziom 97–98% w warunkach umiarkowanie kwaśnych oraz w syntetycznych ściekach w temperaturze 25 °C, co korelowało z maksymalnym przyrostem biomasy grzybowej. Wysoka skuteczność usuwania była utrzymywana w syntetycznych ściekach również w temperaturze 37 °C, co wskazuje, że składniki odżywcze pochodzące ze ścieków nie tylko podtrzymywały wzrost grzybów, lecz także poprawiały długoterminową efektywność degradacji w warunkach ograniczenia nutrientowego. Usuwanie nikotyny przekraczało 98% w warunkach optymalnych (25 °C, pH ~5,20, syntetyczne ścieki), przy czym spadek wydajności obserwowano jedynie przy jednoczesnym stresie termicznym i kwaśnym. We wszystkich badanych układach zaobserwowano silną dodatnią zależność pomiędzy akumulacją biomasy grzybowej a skumulowanym usuwaniem zanieczyszczeń, co potwierdza, że adaptacja do ścieków bezpośrednio wspiera wzrost mikroorganizmów w skali większej oraz zwiększa efektywność biodegradacji.

W kolejnym etapie przeprowadzono laboratoryjne badania biodegradacji MeP i TCC z wykorzystaniem zdefiniowanego konsorcjum bakteryjnego obejmującego *Alcaligenes* sp. oraz *Rhodococcus* sp. Eksperymenty prowadzono przy początkowym stężeniu 100 mg L^{-1} przez okres 120 godzin w pożywce odżywczej oraz w syntetycznych ściekach. Do ilościowego monitorowania obu zanieczyszczeń zastosowano wysokosprawną chromatografię cienkowarstwową (HPTLC). Degradacja MeP osiągnęła około 89% w pożywce odżywczej oraz 83% w syntetycznych ściekach, przy czym w syntetycznych ściekach zaobserwowano

intensyfikację degradacji w środkowej fazie procesu po adaptacji bakterii do matrycy ubogiej w składniki odżywcze. W przeciwieństwie do MeP, TCC wykazywał bardzo szybką degradację, przekraczając 97% usunięcia po 96 godzinach i ulegając całkowitemu zanikowi po 120 godzinach w obu mediach. Wyniki te dowodzą, że syntetyczne ścieki skutecznie wspierają wzrost bakterii oraz sprzyjają degradacji zarówno umiarkowanie, jak i silnie recalcitrantnych zanieczyszczeń bez konieczności zewnętrznego suplementowania składników odżywczych.

Etap skalowania przeprowadzono z wykorzystaniem laboratoryjnych biomimetycznych mokradeł sztucznych obsadzonych *Phragmites australis*. Do matrycy mokradeł wprowadzono układy grzybowe (*Trametes versicolor*), bakteryjne (*Pseudomonas aeruginosa*) oraz układ łączony, które eksploatowano i analizowano przez siedem tygodni w warunkach okresowych (batch), stosując syntetyczne ścieki zawierające mieszaninę zanieczyszczeń (kofeina, MeP i TCC po 100 mg L^{-1}). Wcześniejsze testy tolerancji potwierdziły zdolność mikroorganizmów do przetrwania w warunkach stresu wielozanieczyszczeniowego. Wszystkie biologicznie aktywne mokradła wykazywały stabilny wzrost roślin, utrzymanie pH w zakresie bliskim obojętnemu oraz trwałą aktywność mikrobiologiczną, co potwierdza skuteczną akumulację układu i stabilność ekologiczną.

Usuwanie zanieczyszczeń oceniano w 4. i 7. tygodniu przy użyciu spektroskopii ^1H i ^13C NMR, tam gdzie było to analitycznie możliwe. Kofeina została całkowicie usunięta do 4. tygodnia w mokradłach bakteryjnych i konsorcjalnych oraz do 7. tygodnia w mokradle grzybowym. Metyloparaben ulegał degradacji w mokradle grzybowym na poziomie 89% w 4. tygodniu, natomiast całkowite usunięcie we wszystkich mokradłach osiągnięto do 7. tygodnia. Układ łączony grzybowo-bakteryjny nie wykazywał jednoznacznej przewagi nad monokulturami w początkowej fazie adaptacji, jednak skracał czas adaptacji, umożliwiał szybszą stabilizację systemu oraz zapewniał zrównoważoną skuteczność degradacji wobec chemicznie odmiennych zanieczyszczeń, co wskazuje na komplementarność funkcjonalną, a nie addytywną synergię. Układ ten poprawiał usuwanie metyloparabenu w porównaniu z samym systemem bakteryjnym, przy jednoczesnej porównywalnej skuteczności wobec kofeiny. Ze względu na ograniczenia rozpuszczalności TCC nie mógł być ilościowo oznaczony metodą NMR; jednak stabilna praca mokradeł oraz wysoka skuteczność usuwania pozostałych zanieczyszczeń wskazują na sprzyjające warunki dla biodegradacji wybranych związków.

Podsumowując, niniejsze badania dowodzą, że celowana adaptacja mikroorganizmów do syntetycznych ścieków intensyfikuje degradację zanieczyszczeń poprzez umożliwienie wzrostu i aktywności metabolicznej przy wykorzystaniu składników odżywczych pochodzących ze ścieków. Łącząc optymalizację laboratoryjną z walidacją w skali pilotażowej w systemach mokradeł sztucznych, praca ta ustanawia skalowalną i zrównoważoną strategię aktywnej intensyfikacji mikrobiologicznego samooczyszczania, wykraczającą poza pasywną naturalną atenuację w zanieczyszczonych ekosystemach wodnych. Całościowo badania te redefiniują samooczyszczanie wód powierzchniowych jako proces celowo projektowany i biologicznie wzmacniany, a nie wyłącznie zjawisko naturalne.

Słowa kluczowe: zanieczyszczenia pojawiające się; syntetyczne ścieki; wzmocniona biodegradacja; adaptacja mikrobiologiczna; mokradła sztuczne; degradacja grzybowa; konsorcja bakteryjne; systemy samooczyszczania

Table of Contents

Publications Included in the Doctoral Thesis

The presented doctoral thesis consists of 4 monothematic papers listed below.

1. **Dave Bhautik***, Łobos-Moysa Ewa; *A comprehensive review of caffeine and nicotine as emerging environmental contaminants in water systems*; Architecture Civil Engineering Environment; 2025; vol. 18, no. 2; pp. 171–190; (MNiSW: 70 points, IF: 0.4)

2. **Dave, B.*,** Łobos-Moysa, E., Kuźnik, A.; Enhancing fungal adaptation for efficient caffeine degradation in wastewater: biomimetic approach and environmental optimization; *Desalination and Water Treatment*; 2024; 321; 1–16; (MNiSW:100 points, IF:1.0)

3. **Dave Bhautik***, Łobos-Moysa Ewa, Kuźnik Anna; *Nicotine degradation by Trametes versicolor: insights from diverse environmental stressors and wastewater medium*; Molecules; 2025; vol. 30, no. 12; pp. 1–20 (Article no. 2658); (MNiSW: 140 points, IF: 4.6)

4. **Dave Bhautik***, Łobos-Moysa Ewa, Kuźnik Anna, Maqsood A., Appiah A. N. S., Krzeszowski S., Joshi R.; *Enhancing microbial biodegradation of PPCPs in wastewater via natural self-purification in a novel constructed wetland system*; Sustainability; 2026; vol. 18, no. 1; pp. 1–18 (Article no. 548); (MNiSW: 100 points, IF: 3.9)

*Corresponding author

Additional Scientific Activities

Conference Presentations

1. **Dave Bhautik,** Łobos-Moysa Ewa, Kuźnik Anna, Biodegradation of emerging contaminants, cosmetic ingredients, butylated hydroxy anisole, and benzophenone by sp. *Trametes versicolor*, 5th International Conference on Sustainable Technologies for Water and Wastewater Treatment, Vellore Institute of Technology, India, 2023 (Oral Presentation).

2. **Dave Bhautik,** Łobos-Moysa Ewa, Kuźnik Anna, Natural nicotine extraction, determination from tobacco leaves, and its microbial biodegradation through sp. *Trametes versicolor*, 5th International Conference on Sustainable Technologies for Water and Wastewater Treatment, Vellore Institute of Technology, India, 2023 (Oral Presentation).

3. **Dave Bhautik,** Thakar Milan, Łobos-Moysa Ewa, Sindhav Gaurang, Joshi Rushikesh, Advanced HPTLC approach for comprehensive and accurate analysis of parabens and triclocarban in wastewater, Hydro(geo)logia: The Scientific Conference, 18 October 2024, Sosnowiec, Poland. Book of Abstracts, pp. 6-7.

4. **Dave Bhautik,** Łobos-Moysa Ewa, Kuźnik Anna, Enhancing fungal adaptation for efficient caffeine degradation in wastewater: biomimetic approach and environmental optimization, Mikrozanieczyszczenia w środowisku człowieka, 18-20 September 2024, Częstochowa, Poland. Book of Abstracts, pp. 59-59.

5. Łobos-Moysa Ewa, **Dave Bhautik,** Kuźnik Anna, Występowanie i przemiany kofeiny i nikotyny podczas kontrolowanego samooczyszczania się wód powierzchniowych, Mikrozanieczyszczenia w środowisku człowieka, 18-20 September 2024, Częstochowa, Poland. Book of Abstracts, pp. 104-104.

6. **Dave Bhautik,** Microbial consortia-driven paraben degradation: a comparative study of synthetic wastewater and nutrient broth using HPTLC, 5th International Conference

Strategies toward Green Deal Implementation - Water, Raw Materials & Energy in Green Transition 2024, Poland (Poster Presentation).

7. **Dave Bhautik,** Łobos-Moysa Ewa, Kuźnik Anna, Microbial biodegradative constructed wetlands for effective micropollutant remediation, Young Science Beyond Borders 2024, PAN, Poland. pp. 24-25. ISBN 978-83-66847-97-2.

8. **Dave Bhautik,** Łobos-Moysa Ewa, Evaluating sand-based clay for adsorption of caffeine, methylparaben, and trichlorocarbanilide across aqueous media, The 9th International Electronic Conference on Water Sciences, 11-14 November 2025 (Online). Program and Abstract Book, Article number: sciforum-151570, pp. 164-164.

9. **Dave Bhautik,** Łobos-Moysa Ewa, Kuźnik Anna, Appiah Augustine Nana Sekyi, Biomimetic constructed wetland for microbial degradation of caffeine, paraben, and triclocarban in synthetic wastewater, WETPOL 2025: 11th International Symposium on Wetland Pollutant Dynamics and Control, 7-11 September 2025, Gdansk, Poland. Book of Abstract, pp. 95-95 (Poster Presentation).

Book Chapters

1. **Dave Bhautik**; Biodegradation of industrial wastewater and effluent; Werle S., Ferdyn-Grygierek J. (eds.); Ochrona klimatu i środowiska, nowoczesna energetyka: wybrane aspekty; Politechnika Śląska; 2022; pp. 129–143; ISBN 978-83-7880-863-3. (MNiSW: 20 points)

2. **Dave Bhautik**, Łobos-Moysa Ewa, Thakar Milan S., Trivedi Pooja, Sindhav Gaurang M., Joshi Rushikesh; High performance thin layer chromatography: detection, quantification, and implementation in assessing pollutants and environmental fate; Werle S., Ferdyn-Grygierek J. (eds.); Ochrona klimatu i środowiska, nowoczesna energetyka: wybrana problematyka; Politechnika Śląska; 2024; pp. 140–162; ISBN 978-83-7880-969-2. (MNiSW: 20 points)

3. **Dave Bhautik**, Bapodara Janki, Saran Aditya, Łobos-Moysa Ewa; Isolation and identification of N_2-fixing symbiotic and endosymbiotic bacteria from Pleurotus ostreatus; Pikoń K., Lewandowski M. (eds.); Contemporary problems of power engineering and environmental protection 2024; Politechnika Śląska; 2025; pp. 92–102; ISBN 978-83-964116-7-9. (MNiSW: 5 points)

Other Scientific Publications

1. **Dave Bhautik***, Łobos-Moysa Ewa, Kuźnik Anna; *Comparative analysis of cosmetic ingredient degradation: fungal vs. bacterial activity in diverse media as potential replacements*; International Biodeterioration & Biodegradation; 2024; vol. 191; pp. 1–14 (Article no. 105795); (MNiSW: 140 points, IF: 4.1)

2. Upadhyay Ruchi*, Przystaś Wioletta, **Dave Bhautik;** *Mycoremediation of synthetic dyes: a comprehensive review on contaminant alleviation mechanisms, kinetic study and toxicity analysis*; International Journal of Environmental Science and Technology; 2025; vol. 22; pp. 521–538; (MNiSW: 70 points, IF: 3.4)

3. Kamińska, G.*, **Dave, B.,** Appiah, A. N. S., Majewska, J.; Exploitation of bentonite and halloysite fixed bed columns – removal of organic micropollutants and microbiological regeneration; *Desalination and Water Treatment*; 2024; 322; 1–8; (MNiSW:100 points, IF:1.0)

Nomenclature

^{0}C	Degree Celsius
δ	Chemical Shift (NMR)
λ_{max}	Maximum Absorption Wavelength
cm	Centimetre
g	Gram
h	Hour
Hz	Hertz
J	Coupling Constant (NMR)
L	Liter
mg	Milligram
MHz	Megahertz
min	Minute
mL	Millilitre
ng	Nanogram
nm	Nanometre
ppm	Parts Per Million
$\mathbf{R}_f$	Retention Factor
rpm	Revolutions Per Minute
v/v	Volume per Volume
µL	Microliter

List of Abbreviations

ABC	ATP-Binding Cassette (transporter)
CDCl3	Deuterated Chloroform
CFU	Colony Forming Unit
CW	Constructed Wetland
DMSO	Dimethyl Sulfoxide
EC	Emerging Contaminant
FAD	Flavin Adenine Dinucleotide
FTIR	Fourier Transform Infrared Spectroscopy
GC-MS	Gas Chromatography-Mass Spectrometry
HPLC	High-Performance Liquid Chromatography
HPTLC	High-Performance Thin-Layer Chromatography
HRT	Hydraulic Retention Time
ICH	International Council for Harmonisation
LC-MS	Liquid Chromatography-Mass Spectrometry
LiP	Lignin Peroxidase
LOD	Limit of Detection
LOQ	Limit of Quantification
MBBR	Moving Bed Biofilm Reactor
MeP	Methylparaben
MnP	Manganese Peroxidase
NA	Nutritional Agar
NB	Nutrient Broth
NMR	Nuclear Magnetic Resonance
PDA	Potato Dextrose Agar
PPCPs	Pharmaceuticals and Personal Care Products
RSD	Relative Standard Deviation
SDBS	Spectral Database for Organic Compounds
SEM	Scanning Electron Microscopy
SWW	Synthetic Wastewater
TCC	Trichlorocarbanilide (Triclocarban)
TDS	Total Dissolved Solids

TLC Thin-Layer Chromatography

TMS Tetramethylsilane

TPs Transformation Products

UV Ultraviolet

Chapter 1: Introduction

Water is a fundamental resource for ecological integrity, human health, and socioeconomic development. However, population growth, urbanization, industrialization, and changes in consumption patterns have placed unprecedented pressure on natural and engineered water systems. Among the most persistent challenges facing aquatic environments is the continuous input of chemically diverse contaminants that are not fully removed by natural attenuation processes or conventional treatment infrastructure. These substances, commonly referred to as emerging contaminants (ECs), include pharmaceuticals, personal care products, lifestyle-related compounds, and industrial additives that occur at low concentrations but can exert disproportionate ecological and toxicological impacts [1,2].

In contaminated water systems, ECs are continuously introduced through diffuse and point sources such as domestic discharges, urban runoff, and industrial activities. Their physicochemical diversity and biological activity enable persistence and interaction with aquatic organisms, potentially disrupting ecological processes and food webs. Conventional water management strategies have proven insufficient for addressing this challenge, as many ECs resist complete mineralization and remain detectable even after treatment [3]. These limitations have intensified interest in nature-based solutions that harness biological processes for sustainable and low-energy water quality improvement.

Microbial self-cleaning processes play a central role in the natural attenuation of organic contaminants in aquatic environments; in this context, self-cleaning refers specifically to biologically mediated transformation and degradation rather than physical processes such as dilution or sorption [4]. However, the effectiveness of natural microbial self-cleaning is inherently constrained by environmental variability, nutrient limitation, and ecological competition. Although laboratory studies have demonstrated that selected bacterial and fungal species possess enzymatic capabilities to degrade specific contaminants under controlled conditions, such systems typically rely on nutrient-rich growth media and simplified experimental conditions. Consequently,

translating microbial degradation strategies into environmentally relevant and cost-effective applications remains limited [5].

Constructed wetlands offer a promising ecological platform by integrating physical filtration, biological transformation, and system stability; however, in most existing applications, contaminant removal relies primarily on passive attenuation and naturally occurring microbial communities [6]. This reliance limits treatment efficiency, reproducibility, and functional control. The present dissertation addresses this limitation by developing an engineered microbial self-cleaning strategy that intensifies biologically driven degradation through the deliberate use of specialist fungal and bacterial degraders adapted to wastewater-based growth conditions. By employing the intrinsic nutrient content of synthetic wastewater as the sole growth resource, this approach avoids dependence on external culture media and enables microbial adaptation under controlled yet environmentally relevant conditions. The adapted microbial systems are subsequently integrated into constructed wetland platforms, allowing systematic evaluation of pollutant degradation from laboratory scale to constructed wetland-scale ecological systems. This work represents a shift from passive reliance on natural attenuation toward the intentional design of biologically driven treatment systems for enhanced and system-scale removal of emerging contaminants in contaminated water matrices.

Chapter 2: Literature Review

2.1 Emerging Contaminants in Surface Water Systems: Occurrence and Environmental Relevance

Water is fundamental to life, ecological stability, and socio-economic development; however, increasing anthropogenic pressure has significantly compromised its quality and availability. Global water consumption has doubled over the past few decades due to population growth, urbanization, industrial expansion, and agricultural intensification [7]. These pressures, exacerbated by climate change, have altered hydrological regimes and transformed water from a renewable resource into an increasingly constrained commodity [8]. As a consequence, maintaining water quality has emerged as a central challenge for environmental sustainability, particularly in surface water bodies that support drinking water supply, irrigation, and aquatic ecosystems.

Among the most persistent threats to surface water quality is the widespread occurrence of emerging contaminants (ECs), a heterogeneous group of biologically active compounds that are not routinely monitored or fully regulated. ECs encompass pharmaceuticals, personal care products, lifestyle compounds, and industrial chemicals that enter aquatic environments through domestic, agricultural, and industrial activities [1]. In contrast to many conventional pollutants, ECs are often designed for chemical stability and biological activity, enabling persistence in aquatic systems even at trace concentrations. Their continuous release, coupled with incomplete attenuation, has led to their characterization as pseudo-persistent contaminants in water environments.

The scale of global chemical production underscores the magnitude of this challenge. Between 1930 and 2000, annual chemical production increased from approximately 1 million tons to over 400 million tons [9]. Currently, an estimated 80,000-100,000 chemical substances circulate in the global environment, with approximately 1,500 new compounds introduced annually [10]. A substantial fraction of these chemicals ultimately reaches rivers, lakes, reservoirs, groundwater, and coastal waters, where they interact with natural biogeochemical cycles. Surface waters,

therefore, function as both recipients and conduits for EC transport across environmental compartments [11,12].

Although ECs are typically detected at low concentrations (ng/L to µg/L), growing evidence indicates that chronic exposure can pose significant risks to aquatic organisms and ecosystem functioning. Numerous studies have reported the occurrence of ECs in freshwater systems, urban streams, estuaries, groundwater, and marine environments, where they can disrupt endocrine regulation, microbial community structure, and trophic interactions [3,13–15]. Continuous contaminant input can exceed the intrinsic attenuation capacity of aquatic systems, thereby challenging the natural microbial self-cleaning potential of surface waters (Figure 1).

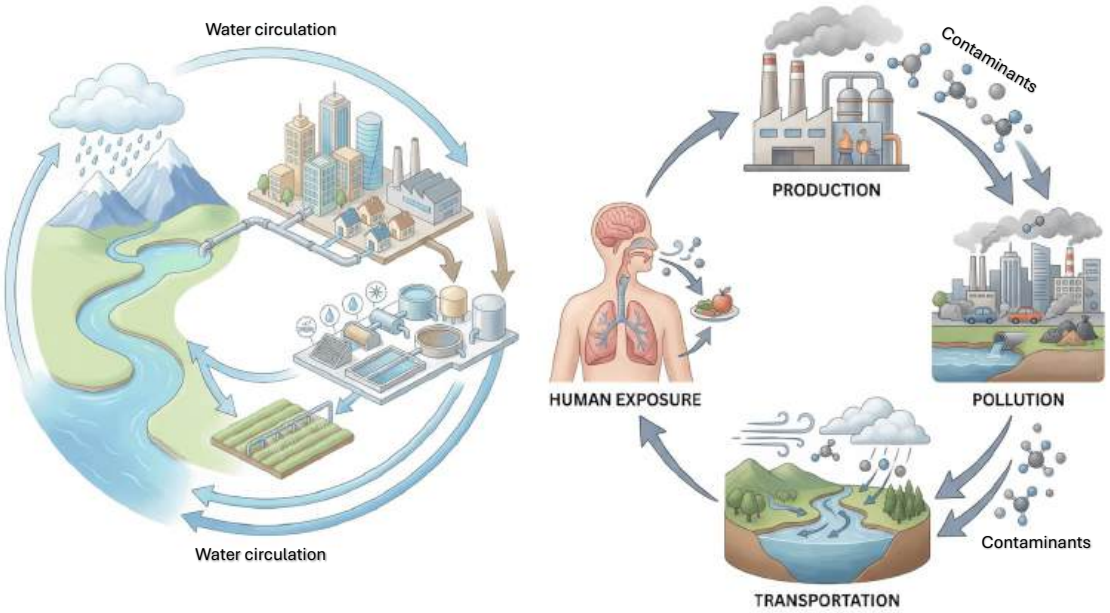

Figure 1. Contaminant exposure, transportation through water circulation

The environmental distribution and fate of ECs are governed by multiple interacting factors, including consumption patterns, population density, land use, hydrological conditions, and compound-specific physicochemical properties [11,12]. Following release, ECs are transported through the water cycle and may accumulate in sediments, soils, vegetation, and biota, thereby prolonging their environmental residence time. This circulation emphasizes the need for treatment approaches that promote true contaminant degradation rather than simple phase transfer within aquatic systems.

In response to these concerns, international organizations and regulatory bodies such as the European Union (EU), the United States Environmental Protection Agency (USEPA), and the World Health Organization (WHO) have identified priority contaminants and highlighted the urgent need for improved mitigation strategies. However, regulatory control alone is insufficient to address the continuous introduction of novel compounds and the complexity of aquatic environments. Consequently, increasing attention has been directed toward nature-based, biologically driven solutions that enhance microbial degradation.

Natural microbial communities play a central role in attenuating organic contaminants, yet their effectiveness is frequently constrained by ecological competition, the low abundance of specialist degraders, and fluctuating environmental conditions. Strengthening intrinsic microbial self-cleaning mechanisms through targeted biological processes and engineered ecological systems, therefore, represents a promising pathway for protecting water quality. This conceptual framework underpins the present research, which seeks to enhance microbial biodegradation of representative natural and anthropogenic contaminants using controlled model water systems and constructed wetlands as scalable representations of self-cleaning processes in contaminated aquatic environments.

2.2 Classification of Target Pollutants in Aquatic Systems: Natural and Anthropogenic Contaminants

Emerging contaminants (ECs) detected in aquatic environments originate from diverse sources and can be broadly classified as natural or anthropogenic (synthetic) compounds. This distinction is relevant for understanding differences in environmental occurrence, physicochemical behaviour, and susceptibility to microbial degradation. Compounds of differing origin often exhibit contrasting persistence, solubility, and bioavailability, which in turn influence their attenuation and treatment behaviour in aquatic systems.

From a biodegradation perspective, classifying ECs into natural and anthropogenic groups provides a rational framework for evaluating microbial self-cleaning processes and for designing targeted biological treatment strategies. Natural ECs, although derived from biological or lifestyle-related sources, may still exhibit environmental persistence

due to continuous release and incomplete degradation. In contrast, anthropogenic compounds are typically synthetic, structurally complex, and often more resistant to microbial transformation. These distinctions are particularly relevant when assessing microbial degradation under environmentally relevant and model water conditions.

Table 1. Physical and chemical properties of caffeine, nicotine, methylparaben, and trichlorocarbanilide

Property	**Caffeine**	**Nicotine**	**Methyl paraben**	**Trichlorocarbanilide (Triclocarban)**
IUPAC Name	1,3,7-Trimethylpurine-2,6-dione	(S)-3-(1-Methylpyrrolidin-2-yl)pyridine	Methyl 4-hydroxybenzoate	3-(4-Chlorophenyl)-1-(3,4-dichlorophenyl)urea
Molecular Formula	C8H10N4O2	C10H14N2	C8H8O3	C13H9Cl3N2O
Molar Mass	194.19 g/mol	162.23 g/mol	152.15 g/mol	315.59 g/mol
Physical State (at 20°C)	White crystalline powder (odourless, bitter)	Colourless to pale yellow oily liquid (turns brown in air)	White crystalline powder	Fine white powder or white plates
Melting Point	235 - 238 °C	-79 °C	125 - 128 °C	255 - 257 °C
Boiling Point	178 °C (sublimes)	247 °C (decomposes)	270 - 280 °C (decomposes)	~344 °C (estimated)
Solubility (in Water)	Moderate (21.6 g/L at 25°C); increases significantly with heat	Miscible (below 60°C); soluble	Low (2.5 g/L at 25°C)	Very Low (~0.11 mg/L at 20°C); practically insoluble

Log Kow (Partition Coeff.)	-0.07 (Hydrophilic)	1.17	1.96	3.63 - 4.9 (Lipophilic)
Chemical Structure	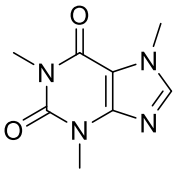	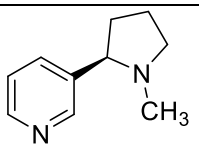	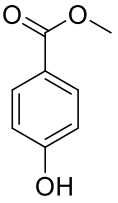	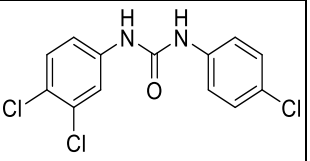

The selected target compounds—caffeine, nicotine, methylparaben, and trichlorocarbanilide-span a broad range of molecular weights, solubilities, and hydrophobicities (Table 1). These physicochemical differences are expected to influence microbial accessibility, transport behaviour, and degradation kinetics, thereby providing a representative basis for evaluating biodegradation performance across compounds of varying origin and complexity.

2.2.1 Caffeine

Caffeine is one of the most widely consumed psychoactive substances worldwide and is present in coffee, tea, cacao products, and numerous beverages and food items [16]. Due to its widespread use and continuous release, caffeine has emerged as a persistent environmental contaminant. It enters aquatic systems primarily through domestic wastewater, urban runoff, and agricultural discharges, where it is often incompletely removed by conventional treatment processes [17]. As a result, caffeine is frequently used as an indicator compound to track pharmaceuticals and personal care products (PhACs) in aquatic environments [18].

Consumption patterns directly influence environmental loading. Average daily caffeine intake has been reported at 271.7 mg/day across European countries, with intake exceeding 350 mg/day in certain regions, such as Austria [19–21]. Although dietary consumption varies by age group and cultural habits, the environmental consequences remain consistent: continuous input of caffeine into wastewater streams and into receiving water bodies.

Numerous studies have documented caffeine across a wide range of aquatic environments, confirming its persistence beyond point-source discharges. Reported concentrations in river systems typically range from 0.007 to 49.60 μg/L, with elevated levels observed downstream of urbanized catchments [22]. Comparable concentrations have been measured in bay waters (0.01-1.60 μg/L) and estuarine systems (0.04-5.00 μg/L), indicating transport from inland waters to coastal environments [23–30]. Detection of caffeine in coastal seawater at concentrations of 0.045-0.33 μg/L further demonstrates its environmental mobility [31,32]. In Europe, including Poland, caffeine has been consistently reported in rivers and drinking water sources, reflecting regional wastewater inputs and hydrological conditions [22,33] (Table 2).

The widespread occurrence of caffeine across freshwater, estuarine, and marine systems highlights its resistance to complete natural attenuation and underscores its suitability as a model compound for evaluating microbial degradation processes. Its hydrophilic character, continuous loading, and partial biodegradability make caffeine particularly relevant for assessing biologically driven degradation under controlled model water conditions. Consequently, caffeine serves as an appropriate natural contaminant for investigating the performance of engineered microbial systems designed to enhance self-cleaning processes in contaminated aquatic environments.

Table 2. Reported caffeine concentrations in different aquatic matrices

Water System / Matrix	**Location**	**Reported Concentration (ng/L)**	**Primary Source Attribution**	**Reference**
River water	Rudawa River, Poland	14.0 - 852.0	Municipal wastewater discharge	[34]
River water	Danube River, Europe	Avg: 137; Max: 1467	Urban and industrial discharges	[35]
River water	Danube tributaries, Europe	Avg: 406; Max: 6798	Diffuse and point-source inputs	[35]
River water	Lippe River, Germany	<10 - 420	Wastewater effluent and runoff	[36]

River water	Seine River, France	3.2 - 186.9	Urban wastewater discharge	[37]
River water	Upper Iguassu River, Brazil	1,200 - 124,350	Untreated domestic wastewater	[38]
Estuarine systems	USA, Canada, China, Portugal	40 - 5,000	Upstream anthropogenic inputs	[23–25,27–29]
Coastal seawater	Mediterranean & Atlantic coasts (Europe)	45 - 330	Wastewater discharge, coastal runoff	[31,32]

2.2.2 Nicotine

Nicotine (3-(1-methyl-2-pyrrolidinyl) pyridine) is the dominant alkaloid in tobacco, accounting for approximately 90% of total alkaloid content and occurring at concentrations between 0.3% and 3% in tobacco leaves, depending on plant variety and growth conditions [39–41]. It is a water-soluble, hygroscopic compound with high environmental mobility, facilitating its rapid transfer from terrestrial sources into aquatic systems [42,43]. Although nicotine is biosynthesized naturally in plant roots, its presence in aquatic environments is predominantly driven by anthropogenic activities, including tobacco cultivation, cigarette consumption, and improper disposal of tobacco-related waste [44].

Nicotine enters aquatic environments primarily through urban runoff, agricultural drainage, and wastewater discharge, where its high solubility promotes transport into rivers, canals, lakes, and groundwater systems. Monitoring studies have reported nicotine concentrations ranging from 12.6 to 947 ng/L in reclaimed water, up to 9,340 ng/L in surface waters, and approximately 164 ng/L in groundwater, confirming its persistence across multiple aquatic compartments [45]. A comprehensive monitoring campaign conducted in Berlin detected nicotine in all investigated surface water bodies, including rivers, canals, lakes, and ponds, with concentrations ranging from 7 to 1,469

ng/L, highlighting the role of diffuse urban sources such as cigarette butt leaching and stormwater runoff [46].

Environmental concentrations of nicotine are influenced by hydrological conditions, seasonal variability, and local human activity patterns, as well as treatment-related factors such as hydraulic retention time and microbial activity [45,47]. While wastewater treatment plants can achieve partial nicotine removal, particularly during secondary and tertiary treatment stages, complete degradation is rarely observed. As a result, nicotine residues are frequently detected in treated effluents and receiving waters [48–50]. This incomplete removal contributes to the continuous reintroduction of nicotine into aquatic environments and limits the effectiveness of conventional treatment approaches.

The widespread occurrence, high mobility, and partial biodegradability of nicotine make it a relevant natural-origin contaminant for studies investigating biologically driven degradation processes in contaminated water matrices. Compared to structurally complex synthetic antimicrobials, nicotine exhibits relatively higher biodegradability, making it a suitable benchmark compound for evaluating microbial adaptation and degradation performance under nutrient-limited conditions. Consequently, nicotine provides a useful contrast to more recalcitrant anthropogenic pollutants and supports functional assessment of microbial self-cleaning processes in engineered aquatic treatment systems (Table 3).

Table 3. Nicotine concentrations in different aquatic matrices

Water System / Matrix	**Location / Region**	**Reported Concentration (ng/L)**	**Primary Source Attribution**	**Reference**
Lakes, ponds, rivers, canals, brooks (surface waters)	Berlin, Germany	7 - 1,469	Cigarette butt leaching, urban runoff	[46]
Reclaimed water	Europe (various locations)	12.6 - 947	Treated municipal	[51,52]

			wastewater reuse	
Surface water (rivers)	Europe (multiple river systems)	Up to 9,340	Agricultural runoff, wastewater discharge	[47]
Wastewater effluent	Europe	ng/L - µg/L range	Incomplete WWTP removal	[50]
Wastewater influent/effluent	UK, Europe	Variable (treatment dependent)	Domestic sewage, tobacco product waste	[48,49]

In contrast to natural emerging contaminants, anthropogenic pollutants are synthetic chemicals designed for specific functional purposes and often exhibit enhanced chemical stability and antimicrobial properties. These characteristics, while beneficial in consumer and industrial applications, significantly hinder biodegradation in aquatic environments. Among such compounds, methylparaben (MeP) and trichlorocarbanilide (TCC) are particularly relevant due to their widespread use, environmental persistence, and potential toxicity.

2.2.3 Methylparaben (MeP)

Parabens are a group of synthetic alkyl esters of *p*-hydroxybenzoic acid widely used as antimicrobial preservatives in personal care products, pharmaceuticals, food, and industrial formulations due to their chemical stability, low cost, and broad-spectrum antimicrobial activity [53–55]. Among this group, methylparaben (MeP) is the most frequently used compound, owing to its comparatively high water solubility, regulatory acceptance, and lower acute toxicity relative to longer-chain parabens [56]. Nevertheless, increasing evidence indicates that MeP exhibits estrogenic activity, raising concerns regarding endocrine disruption in aquatic organisms and potential long-term human health effects [57–59].

Unlike pollutants restricted to point source wastewater discharges, MeP is now recognized as a ubiquitous contaminant in aquatic environments. Monitoring studies have reported its occurrence in rivers, lakes, coastal waters, and urban runoff, confirming its environmental mobility and persistence. In freshwater systems, MeP concentrations commonly range between 3.4 and 920 ng/L [60–63]. Even higher concentrations have been reported in urban stormwater, reaching up to 13.78 μg/L, highlighting the importance of diffuse nonpoint sources such as surface runoff and urban drainage systems [64]. Comparable levels detected in marine environments, ranging from 4.87 to 104 ng/L, demonstrate the transfer of MeP from inland waters to receiving coastal systems [65–67].

The extensive environmental presence of MeP reflects its widespread use in consumer products, including cosmetics, food packaging materials, sanitary products, and pharmaceutical formulations [68]. Product-level investigations have reported MeP concentrations of 2,840 ng/g in bactericidal creams in the United States [69] and 3,280 μg/g in labelled personal care products in Vietnam [12], illustrating the potential for continuous environmental release through domestic use and disposal. Consequently, MeP enters aquatic systems via household wastewater, urban runoff, landfill leachates, and stormwater discharge, extending its presence beyond wastewater treatment plant (WWTP) boundaries.

Although MeP is widely detected in surface and coastal waters, wastewater systems remain a major pathway for its environmental loading and regional variability. A comprehensive review of pharmaceuticals and personal care products in Polish water bodies by [70] reported exceptionally high MeP concentrations in raw wastewater influents, with a maximum value of 40,898.6 ng/L, among the highest documented in Europe. In contrast, a multi-city European study analyzing wastewater from Antwerp and Brussels (Belgium), Girona (Spain), and Zagreb (Croatia) reported substantially lower concentrations, indicating pronounced regional differences in MeP occurrence [71]. These findings confirm that while WWTPs act as important conduits for MeP transport, environmental loading is strongly influenced by local consumption patterns and treatment performance (Table 4).

The persistence of MeP in aquatic environments, its continuous release from diffuse sources, and its incomplete removal during conventional treatment processes

highlight the limitations of existing water management strategies. Given its documented estrogenic activity, widespread occurrence, and mobility across aquatic compartments, MeP represents a relevant anthropogenic target compound for evaluating biologically driven treatment approaches under environmentally relevant conditions. Its physicochemical properties and environmental behaviour make it particularly suitable for assessing engineered natural treatment systems, such as constructed wetlands, as model platforms for enhanced contaminant attenuation.

Table 4. Reported concentrations of methylparaben (MeP) in aquatic systems

Water System / Matrix	Location	Reported Concentration (ng/L)	Primary Source Attribution	Reference
River water	Europe (multi-site)	3.4 - 920	Urban runoff, wastewater inputs	[60,61]
River water	Japan	4 - 380	Domestic wastewater discharge	[62]
River water	China	6 - 910	Urban runoff and effluent mixing	[63]
Urban stormwater	USA	up to 13,780	Diffuse urban sources	[72]
Coastal seawater	Taiwan	4.87 - 104	Land-sea transport	[65–67]
Wastewater influent	Poland	up to 40,898.6	High PCP consumption	[70]

2.2.4 Trichlorocarbanilide (TCC)

Triclocarban (3,4,4′-trichlorocarbanilide, TCC) is a chlorinated antimicrobial compound extensively used in personal care products, particularly antibacterial soaps and hygiene formulations. Owing to its high chemical stability, hydrophobicity, and resistance to biodegradation, TCC has emerged as a persistent contaminant in aquatic environments, raising concerns about its ecological and human health impacts [73]. Its

physicochemical properties promote partitioning between the aqueous phase, suspended solids, sediments, and biota, thereby facilitating long-term environmental persistence and transport.

Field investigations have confirmed the widespread occurrence of TCC in aquatic environments, particularly downstream of urbanized catchments and wastewater-impacted systems. In Fountain Creek (Colorado, USA), a wastewater-dominated stream, TCC concentrations in surface waters ranged from 4.5 to 47.3 ng/L under both high- and low-flow conditions, demonstrating persistence across variable hydrological regimes [74]. In this system, TCC transport occurred predominantly in the dissolved phase (64-99%), enabling downstream migration and contributing substantially to the TCC load in the receiving Arkansas River. These findings indicate that TCC is not confined to discharge zones but can persist within connected aquatic networks, underscoring its environmental relevance.

In addition to its presence in the water column, TCC exhibits a strong affinity for suspended solids and sediments, where concentrations have been shown to correlate with organic carbon content, indicating potential for long-term storage and delayed release [74]. Previous studies have reported the presence of partial transformation products, including dichlorocarbanilide (DCC), monochlorocarbanilide (MCC), and non-chlorinated carbanilide (NCC), in environmental matrices, suggesting incomplete natural attenuation under environmental conditions rather than complete mineralization [75,76].

Wastewater treatment plants act as important pathways for TCC transport rather than effective sinks. Approximately 79% of influent TCC has been reported to partition into sludge, while only limited fractions undergo transformation during treatment, allowing continued release into receiving waters [77–79]. Influent concentrations ranging from 0.320 to 45.261 µg/L have been documented, with measurable residues persisting in treated effluents and associated aquatic environments [80,81]. These observations highlight the limited capacity of conventional wastewater treatment processes to prevent environmental dissemination of TCC.

The ecological relevance of TCC is further underscored by its documented toxicity to aquatic organisms and its tendency to bioaccumulate, leading to reproductive

disruption and endocrine interference in fish, algae, invertebrates, and aquatic plants [82,83]. In humans, chronic exposure has been associated with alterations in gut microbiota and interference with steroid hormone signalling [84]. Together, these effects, combined with environmental persistence, position TCC among the more problematic antimicrobial contaminants detected in aquatic environments.

The environmental behaviour of TCC, characterized by persistence, hydrophobicity, sediment interactions, and incomplete removal during conventional treatment, makes it a stringent model compound for evaluating biologically driven remediation strategies under environmentally relevant conditions. Its recalcitrant nature provides a robust benchmark for assessing the performance of engineered natural treatment systems, such as constructed wetlands, designed to enhance contaminant attenuation through integrated biological and physicochemical processes.

Table 5. Reported concentrations of trichlorocarbanilide (TCC) in aquatic systems

Water System / Matrix	**Location**	**Reported Concentration**	**Environmental Relevance**	**Reference**
Surface water (stream)	USA	4.5 - 47.3 ng/L	Persistent in flowing waters under variable hydrological conditions	[85]
Surface water	Arkansas River, USA	Up to 76% of downstream load from tributary	Demonstrates long-range transport in surface-water networks	[74,86]
Suspended sediments	Fountain Creek, USA	0.7 - 57.3 ng/g	Strong association with organic matter, storage potential	[74,86]
Bed sediments	Fountain Creek, USA	4.09 ± 5.26 ng/g	Long-term accumulation and delayed release	[74]

Wastewater sludge	China	up to 1,188 ng/g	High retention and secondary environmental release	[81,87–89]

Understanding the physicochemical properties of selected contaminants is fundamental to predicting their environmental fate, transport behaviour, and susceptibility to biological removal. The key properties of caffeine, nicotine, methylparaben (MeP), and trichlorocarbanilide (TCC) are summarized in (Table 5).

The selection of caffeine, nicotine, MeP, and TCC therefore represents a strategic spectrum of contaminants encompassing both natural and synthetic origins, a wide range of physicochemical characteristics, and varying degrees of biodegradability. This classification provides a functional basis for evaluating differences in microbial degradation performance and treatment behaviour under environmentally relevant conditions. By addressing both natural and anthropogenic contaminants, the present research aims to develop a broadly applicable framework for biologically driven self-cleaning processes using controlled model water systems that reflect the complexity of contaminated aquatic environments.

2.3 Limitations of Natural Attenuation and Uncontrolled Microbial Degradation in Aquatic Systems

Aquatic systems possess an inherent capacity for self-cleaning through a combination of natural attenuation processes, including dilution, photodegradation, sorption to sediments, plant uptake, and microbial biodegradation. Together, these processes influence the environmental fate of organic contaminants in rivers, lakes, and reservoirs; however, their effectiveness depends strongly on pollutant loading, hydrological conditions, and microbial community structure [90,91]. With the increasing and continuous input of emerging contaminants (ECs), natural attenuation capacities are frequently exceeded, leading to the persistence and accumulation of biologically active compounds in aquatic environments [92–94].

Among attenuation mechanisms, microbial biodegradation represents the primary biological process capable of transforming organic contaminants and, under favourable conditions, achieving extensive mineralization. In natural aquatic environments,

however, microbial degradation processes are largely uncontrolled and constrained by ecological competition, nutrient availability, and environmental variability. Indigenous microbial communities are typically adapted to utilize readily degradable organic carbon, whereas specialist degraders capable of transforming structurally complex or xenobiotic compounds often occur at low abundance [91,95,96]. As a result, many ECs undergo incomplete transformation in natural systems, leading to the formation of transformation products that may persist and retain biological activity, as reported in previous studies [97–100].

A major limitation to microbial self-cleaning in open aquatic systems is dilution. In surface waters, contaminants are rapidly dispersed to concentrations below those required to sustain microbial growth on the target compound as a primary carbon or energy source. Under such conditions, biodegradation often proceeds through co-metabolic pathways, which are inherently slow, inefficient, and dependent on the presence of alternative substrates [91,95]. This phenomenon provides a mechanistic explanation for the persistence of compounds such as caffeine and nicotine in surface waters despite their inherent biodegradability when continuously introduced at low concentrations [34,101].

Environmental variability further constrains the efficiency of microbial degradation. Parameters such as temperature, oxygen availability, redox conditions, pH, and seasonal hydrological fluctuations exert strong control over microbial metabolism and enzymatic activity [102,103]. Sudden changes in flow regime, pollutant loading, or nutrient availability can disrupt microbial community function and suppress degradation processes, resulting in pronounced spatial and temporal variability in contaminant removal.

Microbial competition represents an additional ecological constraint on the effectiveness of self-cleaning. In natural aquatic environments, fast-growing generalist microorganisms often outcompete specialist degraders for nutrients and space, limiting the establishment and persistence of pollutant-degrading populations [104,105]. This effect is particularly relevant for slow-growing fungi and actinomycetes, whose enzymatic systems can degrade complex organic compounds but typically require stable environmental conditions to function efficiently.

Collectively, these limitations indicate that while natural attenuation plays an essential role in maintaining water quality, it is insufficient to address the growing burden of persistent, biologically active contaminants under current environmental pressures. Enhancing microbial degradation, therefore, requires controlled environments that reduce dilution, stabilize physicochemical conditions, and support the activity of selected degradative microorganisms [106–108]. Engineered ecological treatment systems, such as constructed wetlands, have been proposed as promising platforms for intensifying biologically driven self-cleaning processes under environmentally relevant, controlled conditions, providing the conceptual basis for the approach adopted in this thesis.

2.4 Microbial Self-Cleaning Mechanisms for Pollutant Degradation

Microbial activity represents the dominant biological driver of self-cleaning processes in aquatic environments, enabling the transformation of organic contaminants that cannot be effectively removed by physical or chemical processes alone. Bacteria and fungi represent two distinct but complementary biological systems for the degradation of emerging contaminants (ECs), differing in metabolic strategies, enzyme localization, substrate accessibility, and ecological roles. Understanding these differences at the functional level is essential for developing engineered treatment systems capable of enhanced, reliable pollutant removal.

2.4.1 Bacterial Degradation Mechanisms

Bacteria play a central role in the biodegradation of low-molecular-weight and water-soluble organic contaminants and are widely reported as key degraders of many synthetic pollutants. Their metabolic versatility is associated with a diverse range of intracellular enzymes that catalyse oxidative, reductive, and hydrolytic reactions, enabling pollutant transformation either as growth-linked substrates or through co-metabolic processes. Enzyme systems such as monooxygenases, dioxygenases, dehydrogenases, and hydrolases are commonly implicated in bacterial biodegradation of xenobiotic compounds (Figure 2).

For anthropogenic pollutants, including parabens and trichlorocarbanilide (TCC), bacterial degradation has been reported to involve initial transformation steps such as

hydrolysis or dechlorination, which can increase compound polarity and microbial accessibility. Members of the genera *Pseudomonas*, *Rhodococcus*, *Alcaligenes*, and *Sphingomonas* have been associated with the transformation of phenolic preservatives, antimicrobial agents, and structurally related compounds under laboratory and environmental conditions [96,105]. However, many synthetic compounds exhibit resistance to complete biodegradation due to halogenation, steric hindrance, or limited enzyme affinity, resulting in slow degradation kinetics and incomplete removal.

2.4.2 Fungal Degradation Mechanisms

In contrast to bacteria, fungi, particularly white-rot fungi, utilize extracellular, largely non-specific oxidative enzyme systems that facilitate the transformation of structurally complex, hydrophobic organic compounds. Enzymes such as laccases, manganese peroxidases (MnP), lignin peroxidases (LiP), and versatile peroxidases enable fungi to oxidize a wide range of pollutants without the need for direct cellular uptake [109–111]. These enzyme systems generate reactive intermediates capable of inducing structural modification of organic contaminants (Figure 2).

Fungal systems have been reported to effectively transform natural alkaloids, aromatic compounds, and high-molecular-weight micropollutants with low aqueous solubility under controlled conditions. Compounds such as caffeine and nicotine have been shown in previous studies to be susceptible to fungal-mediated transformation, highlighting the potential role of fungi in degrading biologically derived contaminants. The ability of fungi to act on compounds associated with solid substrates or complex matrices further distinguishes them from bacterial systems and supports their relevance in engineered treatment environments.

2.4.3 Complementarity and Synergistic Interactions Among Microbial Systems

Although bacterial and fungal systems differ in their degradation strategies, these differences create opportunities for functional complementarity. Fungal-mediated transformation of complex or recalcitrant compounds can increase the availability of smaller or more polar products that are more readily transformed by bacterial communities. Conversely, bacterial activity can reduce the accumulation of low-

molecular-weight byproducts that may inhibit fungal enzyme production, contributing to overall process stability. Such complementary interactions form the conceptual basis for dual-microbial systems reported to achieve enhanced pollutant removal compared to single-organism approaches [107,108].

In engineered treatment environments such as constructed wetlands, bacteria and fungi can occupy different ecological niches associated with substrates, plant roots, and aqueous phases. This niche differentiation is proposed to reduce direct competition and support parallel or sequential contaminant transformation processes, thereby enhancing system robustness under variable environmental conditions. Importantly, these interactions reflect functional concepts derived from natural systems rather than explicitly engineered microbial community structures.

2.4.4 Context-Dependent Limitations of Single-Microbial Degradation Systems

Single-species microbial systems can exhibit high degradation efficiency for specific classes of contaminants under controlled laboratory conditions. However, their performance is strongly dependent on environmental stability, pollutant composition, and system scale. In complex aquatic treatment systems, where contaminant mixtures coexist and physicochemical conditions fluctuate, single-organism approaches often lack robustness and adaptability.

Fungal systems, while effective for structurally complex or hydrophobic compounds, may exhibit slower degradation kinetics and sensitivity to environmental conditions such as temperature, oxygen availability, and nutrient supply. Conversely, bacterial systems may efficiently transform small, polar compounds but exhibit limited activity toward bulky or halogenated molecules. These complementary limitations become increasingly apparent during scale-up, where hydraulic variability, substrate heterogeneity, and microbial competition influence overall system performance [112,113].

Accordingly, integration of bacterial and fungal processes within controlled ecological platforms has been proposed as a strategy to improve stability and treatment efficiency. This concept provides the rationale for investigating dual-microbial systems

within engineered environments, such as constructed wetlands, where functional complementarity can be exploited to enhance biologically driven self-cleaning processes under environmentally relevant conditions.

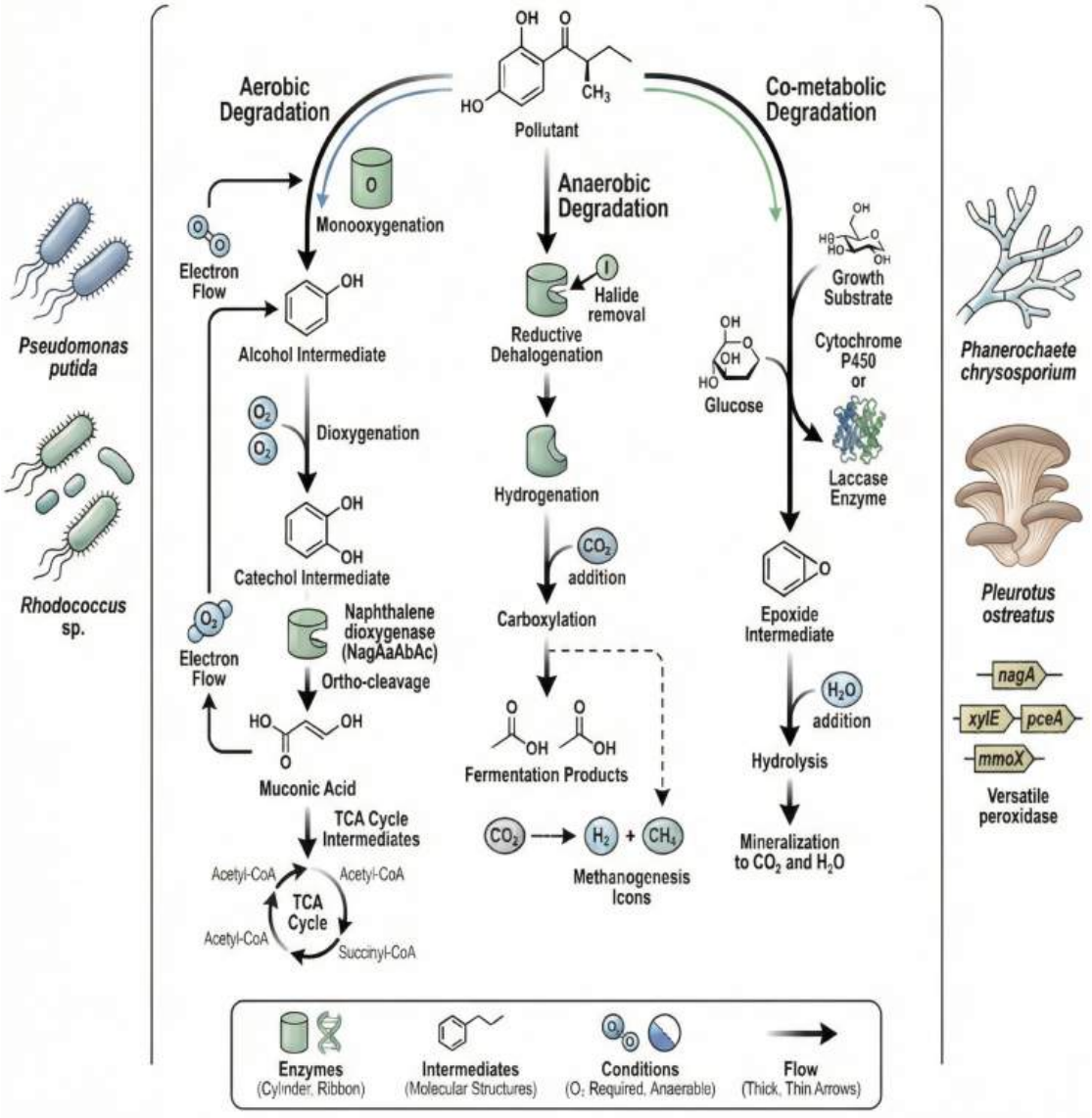

Figure 2. Schematic diagram of the microbial degradation mechanism of pollutants

2.5 Constructed Wetlands as Engineered Self-Cleaning Systems Driven by Microbial Remediation

While natural surface waters possess an intrinsic capacity for self-cleaning, the uncontrolled conditions of open aquatic ecosystems limit the efficiency and consistency of microbial degradation of emerging contaminants (ECs). Constructed wetlands (CWs) represent an engineered extension of these natural processes, designed to provide controlled ecological conditions that enhance biological, physical, and chemical attenuation mechanisms. By mimicking key structural and functional characteristics of natural wetlands, CWs offer a controlled platform for intensifying biologically driven self-cleaning processes in aquatic treatment systems [114,115].

Unlike conventional treatment technologies that rely primarily on physical separation or chemical transformation, CWs function as ecological reactors in which microorganisms play a dominant role in contaminant transformation. The porous substrates, plant root systems, and biofilm-covered surfaces within CWs create heterogeneous environments that support diverse microbial populations and promote sustained biodegradation activity [116,117]. These features facilitate increased microbial biomass, prolonged contact between contaminants and degradative microorganisms, and stabilization of physicochemical conditions required for microbial metabolic activity.

A defining characteristic of CWs is the development of redox gradients and ecological niches within the same treatment unit. Aerobic, anoxic, and anaerobic zones can coexist at micro- and macro-scales, supporting a range of biologically mediated transformation processes. This spatial heterogeneity enables complementary microbial functions to occur in parallel, which is particularly relevant for the attenuation of complex contaminant mixtures that cannot be addressed by a single biological process [118].

Vegetation plays a supporting but critical role in microbial self-cleaning within CWs. Macrophytes provide extensive surface area for microbial colonization, contribute to oxygen transport into the rhizosphere, and release organic exudates that stimulate microbial activity [116,119]. The root-microbe interface thus represents an active zone for microbial transformation, where pollutant bioavailability and metabolic activity can

be enhanced. For most micropollutants, direct plant uptake is a minor removal pathway; instead, vegetation primarily structures microbial habitats and promotes system stability.

Substrate composition further influences microbial performance in CWs by controlling hydraulic behaviour, surface area availability, and adsorption capacity. Porous media such as gravel, sand, and biochar support biofilm development and facilitate extended interaction between contaminants and microbial communities [120,121]. By concentrating pollutants within the wetland matrix, substrates can mitigate dilution effects typical of open surface waters and create conditions more favourable for microbial transformation processes.

From a research perspective, CWs provide an important link between laboratory-scale experiments and environmentally relevant treatment systems. Compared with batch reactors or simplified laboratory setups, CWs enable investigation of biologically driven contaminant attenuation under structured ecological conditions while retaining experimental control [122,123]. However, conventional CWs typically rely on naturally colonized, undefined microbial communities that are often poorly adapted to the targeted degradation of specific micropollutants. This limitation contributes to variable performance and incomplete removal of persistent contaminants [124,125].

Addressing these limitations requires the intentional integration of selected microbial degraders into wetland systems to enhance functional biodegradation capacity under controlled conditions. This concept underpins the present study, which investigates the incorporation of fungal and bacterial degraders into constructed wetland platforms to improve the biologically driven attenuation of representative natural and anthropogenic contaminants.

2.6 Challenges in Scaling Microbial Biodegradation from Laboratory to Field-Scale Systems

Although laboratory-scale studies have demonstrated the potential of microbial systems for degrading a wide range of organic micropollutants, translating these findings into stable, efficient engineered treatment systems remains a significant scientific and technical challenge. Most biodegradation experiments are conducted under controlled lab-scale conditions, where temperature, pH, nutrient availability, and microbial

populations are optimized to favour pollutant removal. Such conditions do not adequately represent the complexity of natural or engineered aquatic environments, where physical, chemical, and biological factors interact dynamically. As a result, degradation efficiencies achieved under laboratory conditions often decline when processes are transferred to larger-scale or open systems [93,97,126].

A major limitation in scaling microbial biodegradation processes is the instability of microbial activity over time. In open or semi-open treatment systems, microbial populations are exposed to washout, ecological competition, predation, and inhibitory effects of transformation products, all of which can reduce sustained degradation performance. Single-microbial systems, while effective under controlled conditions, are particularly susceptible to such disturbances. Consequently, increasing attention has been directed toward microbial consortia, where functional redundancy and complementary metabolic capabilities can enhance system resilience and maintain degradation performance under variable environmental conditions [127,128]. The combined use of bacterial and fungal systems has therefore been proposed as a promising strategy to improve robustness in engineered biodegradation systems.

Another key challenge arises from the variability of environmental conditions and pollutant matrices encountered beyond laboratory settings. Natural and engineered water systems contain complex mixtures of contaminants, natural organic matter, and inorganic constituents that can influence pollutant bioavailability and microbial activity [129]. In addition, fluctuations in pH, oxygen availability, redox conditions, and nutrient levels can substantially affect biodegradation performance [130]. These factors are difficult to reproduce fully at laboratory scale but critically influence the effectiveness of biological treatment systems under environmentally relevant conditions.

From an engineering perspective, integrating microbial degradation processes into scalable treatment systems must also account for hydraulic behaviour, mass transfer limitations, and spatial heterogeneity. Constructed wetlands have been proposed as biomimetic systems capable of integrating physical, chemical, and biological processes to enhance contaminant attenuation [114,131]. However, despite their demonstrated potential, relatively few studies have systematically evaluated the performance of fungal-bacterial systems within constructed wetlands, particularly for mixed natural and anthropogenic micropollutants under variable operational conditions [132,133].

Accordingly, a clear knowledge gap exists between laboratory-scale microbial degradation studies and their application in engineered ecological treatment systems. Addressing this gap requires experimental frameworks that allow microbial adaptation, degradation performance, and system stability to be evaluated across increasing levels of complexity under controlled, yet environmentally relevant, conditions.

2.7 Research Gap and Justification of the Present Study

The literature reviewed in the preceding sections demonstrates that emerging contaminants (ECs) such as caffeine, nicotine, methylparaben (MeP), and trichlorocarbanilide (TCC) are widely detected in aquatic environments and exhibit diverse physicochemical properties, environmental behaviours, and ecological risks. While natural attenuation processes and microbial self-cleaning contribute to regulating contaminant fate, these mechanisms are insufficient to address the increasing load and complexity of pollutants introduced into aquatic systems. Persistent dilution effects, ecological competition, and environmental variability limit the efficiency of natural microbial degradation, resulting in incomplete removal and long-term persistence of biologically active compounds.

Existing research has largely focused on either isolated microbial degradation under laboratory conditions or on the application of constructed wetlands as passive treatment systems that rely on undefined microbial communities. Laboratory studies provide valuable insight into pollutant biodegradation potential but often lack ecological relevance and scalability, whereas wetland-based studies frequently emphasize bulk water quality parameters rather than targeted biodegradation of specific micropollutants. Consequently, a critical disconnect remains between laboratory-scale biodegradation research and its practical application within engineered ecological treatment systems.

Moreover, most studies focus on single classes of contaminants or individual microbial groups, overlooking the functional complementarity between fungi and bacteria. Bacterial systems are typically effective for low-molecular-weight and polar compounds, while fungi, particularly white-rot species, can transform structurally complex and biologically derived contaminants through extracellular oxidative processes. Despite this complementarity, the intentional integration of fungal and bacterial degraders into engineered ecological platforms has received limited systematic

investigation, particularly for mixed contaminant scenarios representative of environmentally relevant pollution.

An additional gap lies in the absence of controlled upscaling frameworks that facilitate the transfer of microbial degradation strategies from laboratory conditions to systems that retain ecological complexity while allowing experimental control. Open surface waters are inherently variable and unsuitable for controlled evaluation, whereas conventional treatment technologies introduce confounding physical and chemical processes that obscure microbial contributions. Constructed wetlands offer an intermediate platform that preserves key ecological processes while enabling structured investigation, yet their potential as intentionally designed microbial self-cleaning systems remains underexplored.

In this context, the present study addresses these gaps by developing and evaluating a dual-microbial biodegradation strategy across multiple experimental scales. Selected fungal and bacterial degraders were first investigated under controlled laboratory conditions using synthetic wastewater as a reproducible model of contaminated water matrices. The adapted microbial systems were subsequently incorporated into a laboratory-scale constructed wetland platform, enabling assessment of microbial performance, functional complementarity, and system stability under increasingly complex and environmentally relevant conditions. Through this integrated approach, the study aims to contribute to the development of biologically driven self-cleaning strategies that bridge the gap between laboratory biodegradation research and engineered ecological treatment systems.

Chapter 3: Research Aim, Objectives, and Scope of the Study

3.1 Scientific Motivation and Rationale

Emerging contaminants (ECs), including pharmaceuticals, personal care products, and lifestyle-related compounds, are increasingly detected in surface water systems worldwide and represent a persistent environmental challenge. Compounds such as caffeine, nicotine, methylparaben (MeP), and trichlorocarbanilide (TCC) enter aquatic environments continuously through domestic, industrial, and diffuse sources, and their diverse physicochemical properties result in variable environmental persistence and incomplete natural attenuation. Although microbial self-cleaning processes operate in surface waters, their efficiency is often insufficient to prevent long-term accumulation of these contaminants due to dilution, nutrient limitation, ecological competition, and fluctuating environmental conditions. In this study, self-cleaning is understood as the biologically mediated transformation and removal of organic contaminants by indigenous or introduced microorganisms, excluding purely physical processes such as dilution, volatilization, or sediment sorption. While such natural self-cleaning processes contribute to contaminant attenuation, they remain largely passive, poorly controllable, and highly variable under environmental conditions.

Conventional wastewater treatment technologies are not specifically designed to remove such micropollutants, and their removal efficiency is often inconsistent. While advanced physicochemical treatment methods can enhance removal, they are associated with high operational costs, energy demand, and potential formation of toxic byproducts. In this context, microbial biodegradation emerges as an environmentally sustainable alternative, offering the potential for low-energy, in situ transformation of organic contaminants; however, its effective application beyond nutrient-rich laboratory media remains constrained by limited microbial adaptation, nutrient availability, and environmental complexity. As a result, translating laboratory-scale biodegradation performance to environmentally relevant water matrices remains challenging.

However, the effective application of microbial processes beyond laboratory conditions remains a key scientific and technological challenge, particularly for

achieving sustained and reliable contaminant degradation in nutrient-limited, dynamically changing aquatic environments.

3.2 Aim of the Study

The primary objective of this doctoral dissertation is to develop and experimentally validate a microbial self-purification strategy designed to enhance the biodegradation of emerging anthropogenic contaminants in surface water environments. Targeted enhancement of microbial communities involved in surface water self-purification, achieved through the selection, adaptation, and integration of contaminant caffeine, nicotine, methylparaben, and triclocarban. -specific fungal and bacterial degraders will significantly increase the biodegradation of emerging anthropogenic contaminants beyond natural attenuation.

This aim is pursued through the integration of adapted microbial degraders into a constructed wetland platform and the systematic evaluation of degradation performance across experimental scales, ranging from laboratory-based studies to a pilot-scale, ecologically relevant treatment system.

This adaptation enables pollutant degradation using the intrinsic nutrient content of wastewater as the sole growth resource, eliminating the need for external nutrient supplementation and supporting the development of low-input, biologically driven treatment strategies.

3.3 Specific Research Objectives

To achieve the stated aim, the following specific objectives are pursued:

1. **Selection and functional evaluation of microbial degraders**
   To evaluate the biodegradation potential and growth performance of selected fungal and bacterial species toward representative natural and anthropogenic emerging contaminants under controlled laboratory conditions.

2. **Investigation of microbial adaptation to wastewater-based growth conditions**

   To investigate the adaptation, growth, and degradation performance of selected fungal and bacterial degraders during transition from nutrient-rich laboratory media to synthetic wastewater, enabling pollutant biodegradation using the intrinsic nutrient content of wastewater as the sole growth resource.

3. **Kinetic and process-level evaluation of biodegradation**

   To quantify biodegradation kinetics and verify biologically driven contaminant removal using validated analytical techniques.

4. **Design and operation of an engineered constructed wetland system**

   To integrate adapted microbial systems into a constructed wetland platform and evaluate pollutant removal under controlled and ecologically relevant operating conditions.

5. **Assessment of microbial synergy and system-level performance**

   To determine the role of microbial complementarity and system stability in enhancing degradation efficiency and operational robustness under mixed-contaminant conditions.

6. **Validation of system-scale performance and reproducibility**

   To demonstrate that microbial degradation performance achieved at laboratory scale can be translated to constructed wetland-scale operation using synthetic wastewater as a model polluted water matrix, establishing a reproducible framework for biologically driven self-cleaning of contaminated water systems.

3.4 Thesis Statement

This dissertation is based on the hypothesis that the natural microbial self-cleaning capacity of contaminated surface water systems is generally insufficient to remove emerging contaminants effectively under real environmental conditions, especially when nutrients are limited. It is proposed that this limitation can be addressed by introducing

pollutant-specific microbial degraders that are well adapted to wastewater conditions and can use wastewater-derived nutrients as their sole growth source.

A central assumption of this work is that proper adaptation of fungal and bacterial degraders to wastewater is essential for sustained microbial growth. Once adapted, these microorganisms are expected to grow at a larger scale within the treatment system, maintain stable metabolic activity, and achieve higher and more consistent contaminant degradation than non-adapted cultures. In contrast, microorganisms not adapted to wastewater conditions are likely to exhibit limited growth and reduced degradation performance due to nutrient stress and environmental constraints.

This thesis further proposes that integrating such wastewater-adapted specialist degraders into constructed wetland systems can actively strengthen natural self-cleaning processes. By supporting microbial growth at scale, these engineered systems are expected to increase degradation efficiency and improve treatment stability, particularly under mixed-contaminant conditions where microbial cooperation between fungal and bacterial degraders becomes important.

Overall, this dissertation asserts that engineered microbial self-cleaning systems based on properly adapted degraders can enable efficient, low-input, and system-scale removal of emerging contaminants in surface water treatment. This approach reduces reliance on external nutrient addition and energy-intensive technologies while remaining suitable for ecologically relevant treatment environments.

3.5 Scope and Limitations of the Study

This study focuses on four representative emerging contaminants: caffeine, nicotine, methylparaben, and trichlorocarbanilide, selected to represent both natural and anthropogenic pollutant classes of environmental relevance. The research is limited to laboratory-scale and constructed wetland-scale investigations using synthetic wastewater as a model polluted water matrix. Field-scale implementation, long-term seasonal variability, and full-scale wetland validation are beyond the scope of this dissertation.

The study does not include microbial isolation, taxonomic profiling, or molecular identification, as the emphasis is placed on functional biodegradation performance and

system-level outcomes rather than microbial characterization. Analytical detection and qualification of contaminants and their degradation were performed using NMR and HPTLC techniques.

The experimental program was implemented in a staged manner to reflect increasing system complexity and the availability of representative microbial systems, as determined through collaborative research. Natural contaminants (caffeine and nicotine) were initially evaluated using fungal systems at laboratory scale, while anthropogenic contaminants (methylparaben and trichlorocarbanilide) were subsequently investigated using bacterial consortia. For constructed wetland-scale experiments, three representative contaminants, caffeine, methylparaben, and trichlorocarbanilide, were selected to assess microbial synergy and system-level performance under mixed-contaminant conditions.

Chapter 4: Research Methodology

4.1 Preparation and Characterization of Target Pollutants

The research methodology was designed and implemented using a staged experimental framework corresponding to increasing levels of system complexity, progressing from laboratory-scale biodegradation experiments to an pilot scale biomimetic constructed wetland system. At the initial stage, fungal degradation experiments were conducted using naturally derived contaminants to evaluate microbial adaptation and degradation behaviour under controlled conditions while retaining environmental matrix complexity. Due to funding constraints during the early phase of the study, caffeine and nicotine were extracted from their natural sources, allowing investigation of pollutant degradation in a form representative of real environmental inputs.

In contrast, anthropogenic contaminants, namely methylparaben (MeP) and trichlorocarbanilide (TCC), were introduced as analytical-grade standards to ensure reproducibility and analytical reliability in bacterial degradation experiments. Based on the outcomes of laboratory-scale studies, a subset of representative pollutants was subsequently selected for integration into the constructed wetland system. This design enabled systematic evaluation of microbial adaptation, synergistic degradation mechanisms, and system-scale performance under mixed-contaminant conditions, consistent with the objectives of intensifying natural microbial self-cleaning processes.

4.1.1 Extraction of Natural Pollutants (Caffeine and Nicotine)

Caffeine and nicotine were extracted from natural sources to reflect their environmental origin and associated matrix complexity, whereas anthropogenic contaminants were used as analytical-grade standards to ensure controlled degradation studies. A liquid-liquid extraction approach was employed to isolate both alkaloids from coffee and tobacco, respectively, following alkaloid extraction principles reported in the literature [134,135].

4.1.1.1 Caffeine Extraction

Ground coffee powder was obtained from locally purchased coffee. For extraction, 1 g of coffee powder was mixed with 20 mL of distilled hot water and stirred on a hot plate at 80 °C for 15 min. To maintain caffeine in its free-base form, the pH of the mixture was adjusted to above 12 using a sodium hydroxide (NaOH) solution. The alkaline extract was transferred to a separating funnel and subjected to liquid-liquid extraction using 15 mL of chloroform. The organic phase containing caffeine was collected and evaporated in a water bath at 60 °C for 15 min. The resulting solid residue was further dried in a hot air oven at 50 °C for 3 h prior to characterization [136] (Figure 3).

Analytical-grade caffeine standard, chloroform, deuterated chloroform ($CDCl_3$), syringe filters, and dimethyl diphenylsilane (internal standard) were obtained from Sigma-Aldrich (Poland).

Figure 3. Graphical representation of caffeine extraction, degradation, and analysis experiments [138]

4.1.1.2 Nicotine Extraction

Raw tobacco material was purchased from a local market and used as the natural source of nicotine. For extraction, 10 g of tobacco was mixed with 150 mL of 40% NaOH solution and mechanically stirred at 250 rpm for 1 h to liberate nicotine into the alkaline medium. The mixture was heated to 50 °C to enhance extraction efficiency while avoiding thermal degradation. After filtration, 30 mL of petroleum ether was added to the filtrate, and the mixture was transferred to a separating funnel for liquid-liquid extraction. The extraction step was repeated to maximize recovery. The collected organic phase was evaporated in a water bath at 45 °C to obtain the nicotine extract [137] (Figure 4).

Reagents, including sodium hydroxide, petroleum ether (98%), anhydrous potassium carbonate, sulfuric acid, and analytical-grade nicotine standard, were purchased from Merck (Poland).

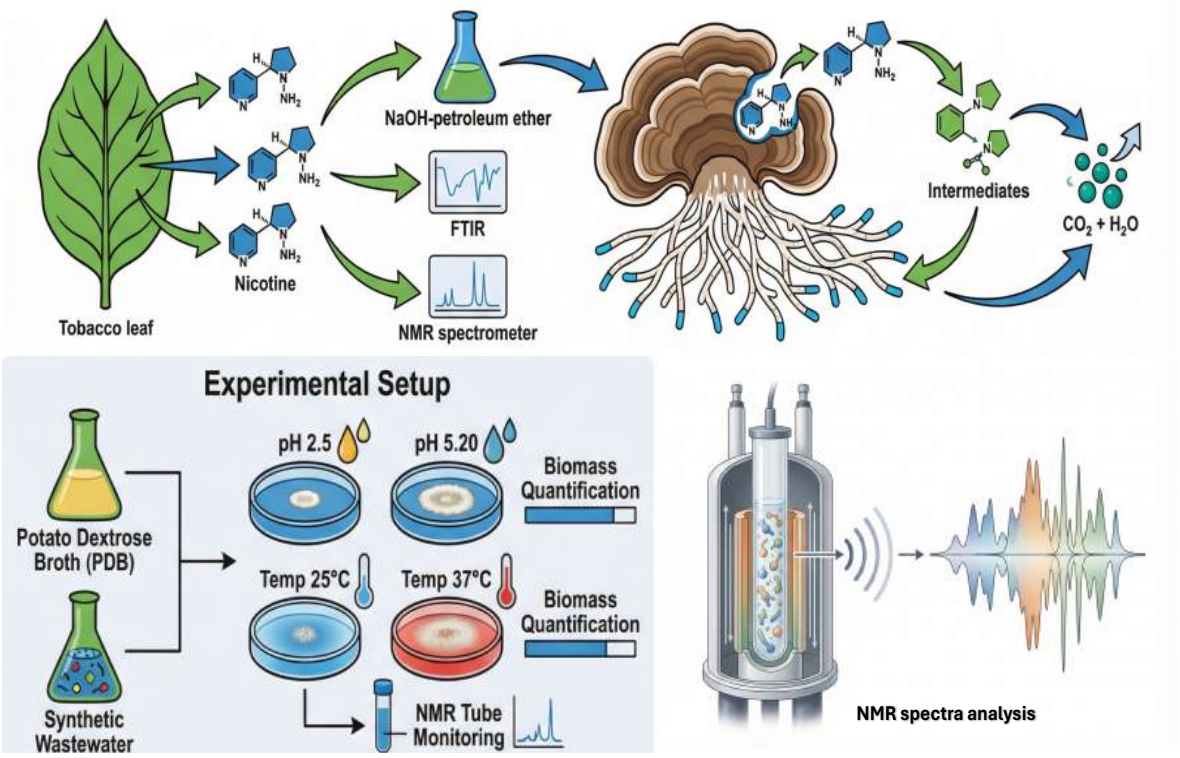

Figure 4. Graphical representation of nicotine extraction, degradation, and analysis experiments

4.1.2 Characterization of Extracted Compounds

Following extraction, the identity and purity of caffeine and nicotine were assessed using spectroscopic techniques prior to biodegradation experiments. Fourier Transform Infrared Spectroscopy (FT-IR) and Nuclear Magnetic Resonance (NMR) spectroscopy were employed to verify structural integrity and to enable subsequent quantitative analysis by comparison with analytical standards.

FT-IR spectra of extracted caffeine and nicotine were recorded using a Nicolet 6700 FT-IR spectrophotometer (Thermo Scientific) equipped with an attenuated total reflectance (ATR) accessory. Prior to analysis, the extracted samples were dried for 24 h at 40 °C in a hot-air oven to remove residual moisture. Spectra were collected over the mid-infrared range, and characteristic functional group vibrations were compared with those of analytical-grade standards to confirm compound identity, following established procedures [134,139].

^{1}H and ^{13}C NMR spectra of caffeine and nicotine were recorded on a Varian 400 spectrometer operating at 400 MHz for ^{1}H and 100 MHz for ^{13}C nuclei. Deuterated chloroform ($CDCl_3$) was used as the solvent. Chemical shifts (δ) for ^{1}H NMR were referenced to tetramethylsilane (TMS) as the internal standard, while ^{13}C NMR chemical shifts were referenced to the solvent resonance of $CDCl_3$ at 77.16 ppm. All chemical shifts are reported in parts per million (ppm), and coupling constants (J) are reported in hertz (Hz).

Dimethyl diphenylsilane was employed as an internal standard for quantitative comparison with analytical-grade reference compounds, enabling verification of compound identity and concentration prior to biodegradation experiments [140–142].

4.1.3 Preparation of Anthropogenic Pollutant Solutions (Methylparaben and Trichlorocarbanilide)

Anthropogenic pollutants selected for this study—methylparaben (MeP) and trichlorocarbanilide (TCC)—were introduced as analytical-grade standards to ensure concentration accuracy, reproducibility, and analytical reliability during biodegradation experiments. Unlike naturally derived pollutants, these compounds were not extracted

from commercial products, as their use in pure form enabled controlled evaluation of bacterial degradation performance without confounding effects from formulation additives or complex matrices.

Methylparaben (methyl 4-hydroxybenzoate; purity 99.0%) and trichlorocarbanilide (purity 98.5%) were obtained from Merck (Poland). Stock solutions of both compounds were prepared in analytical-grade methanol to ensure complete dissolution and precise dosing. For each pollutant, 100 mg of the analytical standard was dissolved in 100 mL of methanol as a primary stock solution.

Prior to biodegradation experiments, appropriate volumes of the stock solutions were diluted with synthetic wastewater to achieve the desired working concentrations. Solvent contributions from methanol were kept constant across experimental systems, and solvent controls were included to exclude solvent-induced effects on microbial activity.

For naturally derived pollutants, the concentrations used in biodegradation experiments were determined by quantitative nuclear magnetic resonance (qNMR) analysis using an internal standard, ensuring accurate and reproducible dosing despite matrix-derived variability. In contrast, concentrations of anthropogenic pollutants were defined directly from analytical-grade stock solutions prepared from certified reference materials. This approach ensured consistency in pollutant loading across all experimental systems while accounting for differences in pollutant origin and preparation.

Pollutant concentrations employed in lab-scale and wetland experiments (typically 100 mg L^{-1} or equivalent dosing from stock solutions) were intentionally higher than those commonly detected in environmental waters. This design choice was made to rigorously evaluate the intrinsic degradation capacity, resilience, and adaptation potential of the selected microbial species under elevated contaminant loads. High initial concentrations enabled clear assessment of degradation kinetics, microbial tolerance thresholds, and system robustness, providing mechanistic insight and proof-of-concept data relevant for future scale-up, shock-load scenarios, and engineered treatment applications. Environmental relevance was addressed through system design and comparative analysis rather than by matching absolute concentrations.

4.2 Lab-scale Biodegradation and Adaptation Experiments

The lab-scale biodegradation experiments were designed to evaluate microbial adaptation, growth behaviour, and pollutant degradation performance under controlled laboratory conditions. This section describes the experimental methodologies applied to fungal and bacterial systems, which were intentionally structured differently to reflect fundamental differences in microbial physiology and growth requirements. For fungal systems, preliminary adaptation and growth assessments were conducted to verify viability in aqueous media containing pollutants prior to degradation experiments. In contrast, bacterial degradation experiments were conducted directly, as bacterial growth in liquid media is well established. Together, these experiments provided the mechanistic and operational foundation for subsequent pilot-scale integration into constructed wetland systems.

4.2.1 Fungal Adaptation and Growth in Natural Pollutant Media

The fungal strain *Trametes versicolor* was selected as the model organism for fungal adaptation and biodegradation experiments. The strain was identified and sourced from the Department of Air Protection Library at the Silesian University of Technology, Gliwice, Poland, as previously reported by [143]. *T. versicolor* was chosen due to its well-documented extracellular enzymatic system and its reported capability to transform structurally diverse organic pollutants.

The fungus was maintained and propagated using the dilution-plating method on Potato Dextrose Agar (PDA). PDA is a conventional, nutrient-rich medium widely employed in mycological studies to support rapid mycelial growth and physiological stability of filamentous fungi [144,145]. Agar functions as the solidifying agent in PDA, whereas its absence in Potato Dextrose Broth (PDB) enables cultivation under liquid conditions. The detailed composition of PDA and PDB media is presented in (Table 6).

PDA plates (Petri dishes) were prepared under aseptic conditions, and all standard microbiological protocols were followed throughout the experiment. Inoculated plates were incubated at 25 °C for 7 days to obtain actively growing fungal cultures prior to adaptation and biodegradation experiments.

Table 6. Composition of Potato Dextrose Agar (PDA) and Potato Dextrose Broth (PDB)

Ingredient / Parameter	PDA (Agar)	PDB (Broth)	Explanation
Potato, infusion from	200 g	200 g	Raw potato material used for extract preparation
Potato extract (approx.)	~ 4.0 g	~ 4.0 g	Dried solids retained after boiling potatoes
Dextrose (glucose)	20.0 g	20.0 g	Primary carbon and energy source
Agar	15.0 g	—	Solidifying agent (absent in PDB)

Synthetic wastewater (SWW) was used as a controlled model system to simulate contaminated surface-water and wastewater conditions. The composition of SWW was adapted from established formulations reported in the literature [146] and is presented in (Table 7).

Peptone and broth were obtained from BTL, Poland. Potassium hydrogen phosphate (K_2HPO_4) and sodium chloride (NaCl) were supplied by Chempur, Poland. Calcium chloride dihydrate ($CaCl_2 \cdot 2H_2O$), magnesium sulphate heptahydrate ($MgSO_4 \cdot 7H_2O$), and urea were obtained from POCH, Poland. All chemicals were of analytical grade and were used without further purification. For all experiments, all components were autoclaved and then mixed together to avoid contamination.

Table 7. Composition of synthetic wastewater (SWW)

No.	Component	Concentration (g/L)
1	Peptone	0.16
2	Broth	0.11
3	Urea	0.03
4	K_2HPO_4	0.028
5	NaCl	0.007
6	$CaCl_2 \cdot 2H_2O$	0.004
7	$MgSO_4 \cdot 7H_2O$	0.002

SWW was selected to provide a simplified yet representative aqueous matrix that supports microbial metabolism while minimizing the compositional variability associated with real wastewater. Although SWW does not fully replicate the biological complexity of domestic wastewater, it provides a reproducible, safe experimental environment that enables systematic evaluation of fungal adaptation and growth under nutrient-limited, pollutant-containing conditions. This controlled approach allowed a reliable comparison between conventional nutrient-rich media and aqueous systems relevant to biodegradation applications.

4.2.1.1 Fungal mycelium growth and adaptation under pollutant stress

To evaluate the feasibility of fungal growth in the presence of natural pollutants, preliminary adaptation experiments were conducted with caffeine and nicotine at varying concentrations. These experiments were designed to assess fungal tolerance, viability, and growth behaviour prior to biodegradation studies, as the ability of filamentous fungi to grow and remain metabolically active in liquid aqueous systems cannot be assumed without experimental verification.

PDA plates (Petri dishes) were prepared aseptically and amended with defined concentrations of caffeine or nicotine (0, 1, or 2 mg per 10 mL of medium). Plates without added pollutants served as controls. Actively growing fungal plugs were placed at the center of each plate, and the plates were incubated at 25 °C and 37 °C for a period of 7 days. Fungal growth was monitored by measuring radial hyphal extension from the center of the colony to the plate edge at 24-hour intervals, following procedures adapted from [147].

This concentration-dependent screening enabled the identification of pollutant levels that supported sustained fungal growth and informed the selection of working concentrations for subsequent biodegradation experiments.

4.2.1.2 Fungal biomass quantification during biodegradation experiments

Fungal biomass quantification was employed as an indicator of fungal adaptation and viability in liquid SWW. Biomass measurements were performed during lab-scale biodegradation experiments to monitor sustained fungal growth under pollutant-stress

conditions and confirm that fungal activity was maintained throughout the experimental period.

Sterile flasks containing SWW and the selected pollutant concentration were inoculated with actively growing fungal biomass. Prior to inoculation, the total mass of each flask containing the medium was recorded. During incubation, flasks were weighed at five-day intervals using an analytical balance. The increase in flask mass over time was primarily due to the growth of fungal biomass within the system, as evaporation losses were minimized and control flasks without fungal inoculation were maintained in parallel.

This gravimetric approach provided a simple, non-destructive, and reproducible method for monitoring fungal growth dynamics during biodegradation experiments and enabled verification that *T. versicolor* remained metabolically active under nutrient-limited, pollutant-containing conditions.

The fungal adaptation and growth experiments were conducted to establish the feasibility of applying *Trametes versicolor* for the biodegradation of caffeine and nicotine in aqueous systems. By systematically evaluating fungal tolerance, growth behaviour, and biomass development across different pollutant concentrations and media types, these experiments ensured that subsequent biodegradation results could be attributed to active fungal metabolism rather than incidental or stress-induced effects. This stepwise validation formed the methodological basis for fungal biodegradation experiments and for subsequent integration into the pilot-scale constructed wetland system described in Section 4.3.

4.2.2 Fungal degradation experiments of caffeine and nicotine

Lab-scale biodegradation experiments were conducted to evaluate the capacity of *Trametes versicolor* to degrade caffeine and nicotine under controlled laboratory conditions following confirmation of fungal adaptation and growth feasibility. The experiments were designed to investigate the influence of key environmental parameters, namely temperature, pH, and aqueous matrix composition, on fungal biodegradation performance. A constant pollutant concentration of 100mg/L was maintained across all experiments. This elevated concentration was intentionally selected to assess the fungal

system's degradation potential, stress tolerance, and robustness under conditions relevant to future scalability and application.

All biodegradation experiments were performed in 250 mL conical flasks containing 100 mL of the respective liquid medium. Flasks were closed with sterile cotton plugs, and all experiments were conducted under aerobic conditions. Incubation was carried out under static conditions, without agitation, to avoid mechanical disruption of fungal mycelia and better reflect conditions relevant to passive treatment systems. Flasks were incubated at 25 °C and 37 °C, depending on the experimental condition.

Fungal biodegradation experiments were conducted using different liquid media to evaluate fungal performance across increasing levels of environmental complexity. Potato Dextrose Broth (PDB) was used as a nutrient-rich reference medium, while synthetic wastewater (SWW) was employed as a nutrient-limited aqueous matrix representative of contaminated surface water conditions. In addition, natural extract-based media were used to simulate more realistic substrates. The coffee extract medium was prepared by adding 10 g of coffee to 100 mL of SWW, thereby retaining naturally occurring carbohydrates, proteins, and oils that may influence fungal growth and enzymatic activity. Similarly, a tobacco extract medium was prepared by adding 15 g of tobacco to 100 mL of SWW to evaluate the performance of fungal degradation in a complex, alkaloid-containing matrix.

To investigate the effect of pH on biodegradation, experiments were conducted in PDB at its native (pH 5.18), SWW at its native (pH 6.4), and under acidic conditions adjusted to pH 2.5 using hydrochloric acid. Temperature effects were evaluated by incubating parallel sets of flasks at 25 °C and 37 °C. For comparison, control experiments were conducted using Milli-Q water (pH 6) containing the same concentration of caffeine or nicotine. These control flasks were not inoculated with fungi and were used to assess non-biological changes in pollutant concentration.

Each flask was inoculated with actively growing fungal biomass obtained from PDA cultures, following the fungal inoculation procedure described in Section 4.2.4. Following inoculation, flasks were incubated for the designated experimental period. Samples were withdrawn from each flask at five-day intervals for subsequent extraction and analytical evaluation, as described in later sections.

A summary of the experimental conditions employed for fungal biodegradation of caffeine and nicotine is provided in (Table 8).

Table 8. Experimental matrix for fungal biodegradation of caffeine and nicotine under varying environmental conditions

No.	Caffeine biodegradation medium condition	Nicotine biodegradation medium condition	Incubation temperature
1	Caffeine + PDB	Nicotine + PDB	25 °C
2	Caffeine + PDB	Nicotine + PDB	37 °C
3	Caffeine + PDB (pH 5.18)	Nicotine + PDB (pH 5.18)	25 °C
4	Caffeine + PDB (pH 5.18)	Nicotine + PDB (pH 5.18)	37 °C
5	Caffeine + PDB (pH 2.5)	Nicotine + PDB (pH 2.5)	25 °C
6	Caffeine + PDB (pH 2.5)	Nicotine + PDB (pH 2.5)	37 °C
7	Caffeine + SWW (pH 6.4)	Nicotine + SWW (pH 6.4)	25 °C
8	Caffeine + SWW (pH 6.4)	Nicotine + SWW (pH 6.4)	37 °C
9	Coffee extract (10 g) + SWW (100 mL)	Tobacco extract (15 g) + SWW (100 mL)	25 °C
10	Coffee extract (10 g) + SWW (100 mL)	Tobacco extract (15 g) + SWW (100 mL)	37 °C
11	Control (Milli-Q water, no fungus)	Control (Milli-Q water, no fungus)	25 °C
12	Control (Milli-Q water, no fungus)	Control (Milli-Q water, no fungus)	37 °C

4.2.3 Bacterial Degradation Experiments of Methylparaben (MeP) and Trichlorocarbanilide (TCC)

Lab-scale bacterial biodegradation experiments were conducted to evaluate the degradation efficiency of a selected bacterial consortium toward the anthropogenic pollutants methylparaben (MeP) and trichlorocarbanilide (TCC). The experiments were designed to compare bacterial degradation performance in a nutrient-rich medium (Nutrient Broth, NB) and a nutrient-limited aqueous matrix (synthetic wastewater, SWW), thereby assessing the feasibility of pollutant removal under conditions representative of contaminated surface water systems. In contrast to fungal systems, bacteria readily proliferate in liquid media such as NB; therefore, preliminary growth or adaptation experiments were not required prior to biodegradation studies.

The bacterial consortium used in this study consisted of *Rhodococcus* sp. strain PK06 (GenBank accession no. PV549916.1) and *Alcaligenes* sp. strain PK5 (GenBank accession no. PV544804.1). The consortium was obtained from the Department of Biochemistry and Forensic Science, Gujarat University, Ahmedabad, India [148,149]. Their demonstrated ability to degrade structurally complex organic substrates motivated their selection for investigating the biodegradation of anthropogenic contaminants in aqueous systems.

In the present study, the consortium was employed without further genetic or physiological modification and was maintained in Nutrient Broth (NB) prior to biodegradation experiments. Synthetic wastewater (SWW), prepared as described in Section 4.2.1, was used as a nutrient-limited aqueous matrix to evaluate bacterial degradation performance under environmentally relevant conditions.

Nutrient Broth (NB) was used as the nutrient-rich reference medium for bacterial biodegradation experiments. NB is a conventional, non-selective growth medium widely employed for the cultivation and maintenance of heterotrophic bacteria, providing readily available carbon, nitrogen, and growth factors that support rapid bacterial proliferation.

In the present study, NB served as a benchmark medium to establish baseline biodegradation performance under optimal growth conditions. A detailed composition of NB, along with a Comparison of bacterial degradation efficiency in NB and synthetic wastewater (SWW), enabled evaluation of microbial performance under nutrient-rich versus nutrient-limited aqueous environments, thereby supporting assessment of environmental applicability.

Table 9. Composition of Nutrient Broth (NB) and Nutrient Agar (NA)

Component	**NB (g/L)**	**NA (g/L)**	**Functional role**
Peptone	5.0	5.0	Source of organic nitrogen, peptides, and amino acids supporting bacterial growth
Beef extract	3.0	3.0	Provides vitamins, carbohydrates, and growth factors
Sodium chloride (NaCl)	5.0	5.0	Maintains osmotic balance in the medium
Agar	-	15.0	Solidifying agent (present only in NA)

Nutrient Agar (NA) is included for reference as the solid analogue of Nutrient Broth (NB) and is commonly used for bacterial maintenance and enumeration; however, all biodegradation experiments in this study were conducted exclusively in liquid Nutrient Broth (NB). NB was employed as a nutrient-rich reference medium to establish baseline bacterial degradation performance under optimal growth conditions, against which results obtained in synthetic wastewater were compared (Table 9).

Biodegradation experiments were performed in batch mode using conical flasks under aerobic conditions. For each experimental condition, bulk solutions (250 mL) of NB or SWW were prepared and spiked with stock solutions of MeP or TCC to obtain a final pollutant concentration of 100 mg L^{-1}. The prepared solutions were then divided into 25 mL aliquots and transferred to sterile 50 mL conical flasks, allowing multiple time-point sampling without disturbing ongoing reactions. Flasks were incubated at 37 °C in a rotary shaker incubator operated at 120 rpm to ensure homogeneous mixing and sufficient oxygen transfer. All experiments were conducted under aerobic conditions throughout the incubation period (Table 10).

Separate sets of experiments were conducted for MeP and TCC. Each flask was inoculated with the bacterial consortium following the procedure described in Section 4.2.4. Control flasks containing the same media and pollutant concentrations but without bacterial inoculation were included as abiotic controls to account for non-biological losses. Additional controls containing media with bacterial culture but without added pollutants were prepared to assess background microbial activity. Samples were collected at defined time intervals (0, 48, 72, 96, and 120 h) for subsequent extraction and analytical evaluation, as described in Section 4.2.5.

Table 10. Experimental matrix for bacterial biodegradation of methylparaben (MeP) and trichlorocarbanilide (TCC)

No.	Pollutant	NB based setup	SWW based setup	Incubation conditions
1	MeP / TCC	Analytical standard	-	-
2	MeP / TCC	NB medium (media-only control)	SWW medium (media-only control)	37 °C, 120 rpm
3	MeP / TCC	NB + bacterial culture (media + bacteria control)	SWW + bacterial culture (media + bacteria control)	37 °C, 120 rpm
4	MeP / TCC	Pollutant + NB + bacterial culture (0 h)	Pollutant + SWW + bacterial culture (0 h)	37 °C, 120 rpm
5	MeP / TCC	Pollutant + NB + bacterial culture (48 h)	Pollutant + SWW + bacterial culture (48 h)	37 °C, 120 rpm
6	MeP / TCC	Pollutant + NB + bacterial culture (72 h)	Pollutant + SWW + bacterial culture (72 h)	37 °C, 120 rpm
7	MeP / TCC	Pollutant + NB + bacterial culture (96 h)	Pollutant + SWW + bacterial culture (96 h)	37 °C, 120 rpm

8	MeP / TCC	Pollutant + NB + bacterial culture (120 h)	Pollutant + SWW + bacterial culture (120 h)	37 °C, 120 rpm

4.2.4 Microbial Inoculation Procedures

Microbial inoculation strategies were deliberately designed to ensure rapid establishment of active biomass, enhanced growth stability, and reproducible biodegradation performance under conditions of elevated pollutant stress. In this study, relatively high initial pollutant concentrations were used in lab-scale experiments to challenge the degradative capacity of the selected microorganisms and to assess their potential for future scalability. Under such conditions, microbial survival and sustained metabolic activity cannot be assumed, particularly in nutrient-limited aqueous media. Therefore, inoculation procedures were optimized to maximize initial microbial viability and to increase the likelihood of successful adaptation and degradation. Distinct inoculation approaches were adopted for fungi and bacteria based on their biological characteristics. For filamentous fungi, liquid-phase inoculation was employed to promote uniform dispersion of spores and mycelial fragments, facilitating rapid colonization and resilience under static aerobic conditions. For bacterial systems, actively growing liquid cultures standardized by optical density were used to ensure controlled biomass input and consistent degradation kinetics. These tailored inoculation strategies were essential for maintaining microbial activity and enabling meaningful evaluation of biodegradation performance under high-pollutant-loading conditions.

4.2.4.1 Fungal Inoculation for Lab-Scale Biodegradation Experiments

Fungal inoculation for lab-scale biodegradation experiments was performed using a liquid inoculum of *Trametes versicolor* prepared in Potato Dextrose Broth (PDB). The fungal strain was cultivated and maintained as described in Section 4.2.1. Actively growing liquid cultures were used to ensure metabolic activity and to rapidly establish fungal biomass in aqueous degradation systems.

For inoculation, a homogeneous fungal suspension was obtained from a pure liquid PDB culture of *T. versicolor*. Prior to transfer, the culture was gently mixed under sterile laminar airflow conditions using a vortex to ensure uniform distribution of fungal mycelia and spores. Quantitative spore enumeration was not performed because the inoculum was a mixed suspension of spores and fragmented mycelia, a common approach in fungal biodegradation studies where filamentous growth is the dominant mode of colonization.

Each experimental flask (250 mL conical flask containing 100 mL of degradation medium) was inoculated once with 1 mL of the prepared fungal suspension. Inoculation was performed only at the start of the experiment, and no further additions were made during the incubation period. Following inoculation, flasks were sealed with sterile cotton plugs to maintain aerobic conditions and incubated under the same environmental conditions as defined for the corresponding biodegradation experiments (Section 4.2.2).

This liquid inoculation strategy was selected to facilitate rapid fungal dispersion and colonization within water-based media, including synthetic wastewater, where direct transfer of solid agar plugs may limit uniform fungal distribution. The approach enabled consistent fungal establishment across experimental replicates and ensured that subsequent biodegradation could be attributed to active fungal metabolism within the aqueous phase. A representative illustration of the fungal spore-based inoculation procedure and subsequent mycelial establishment in synthetic wastewater is shown in (Figure 5).

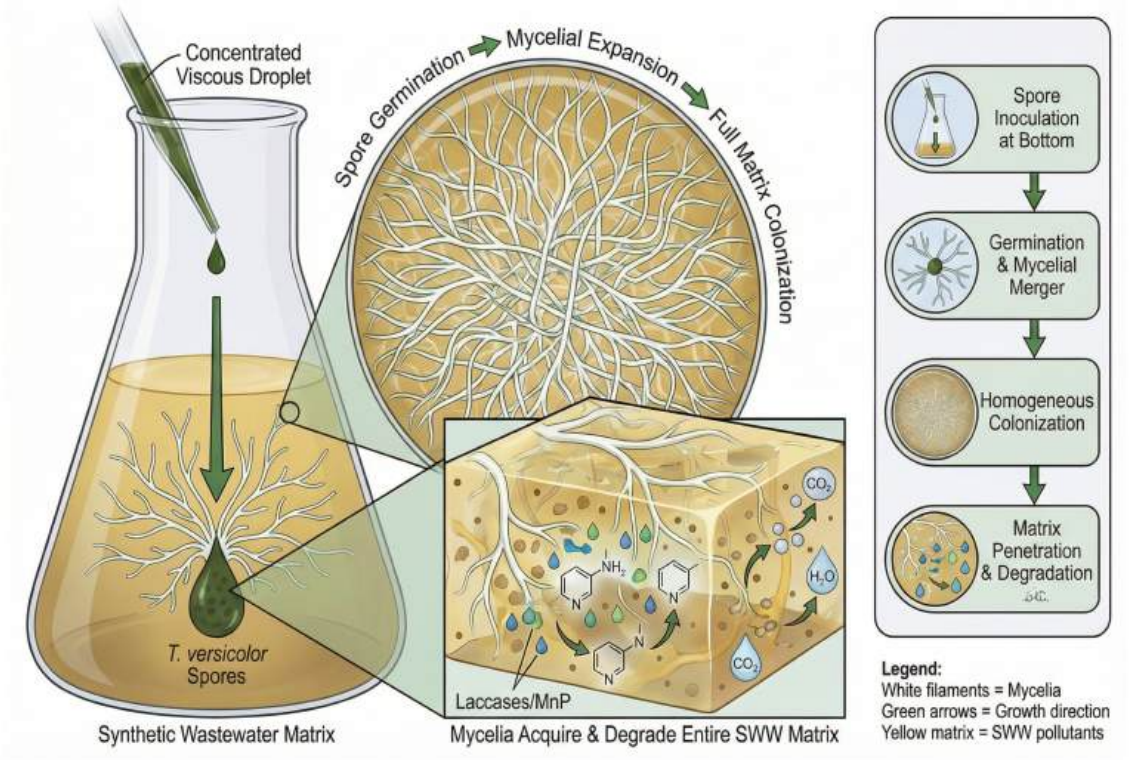

Figure 5. Liquid spore-mycelium inoculation of *Trametes versicolor* and representative mycelial growth observed in synthetic wastewater during lab-scale biodegradation experiments

4.2.4.2 Bacterial Inoculation for Lab-Scale Biodegradation Experiments

Bacterial inoculum for lab-scale biodegradation experiments was prepared from an actively growing liquid culture of the bacterial consortium described in Section 4.2.3. The consortium consisted of *Rhodococcus* sp. strain PK06 (GenBank accession no. PV549916.1) and *Alcaligenes* sp. strain PK5 (GenBank accession no. PV544804.1).

For inoculum preparation, bacterial cultures maintained on slants were transferred into sterile Nutrient Broth (NB) and incubated at 30 °C for 24 h to obtain active biomass. Following incubation, bacterial cells were harvested by centrifugation at 5000 rpm for 10 min, and the supernatant was discarded. The resulting cell pellet was resuspended in sterile normal saline solution to obtain a homogeneous bacterial suspension.

The prepared bacterial suspension was used as the inoculum for biodegradation experiments. Inoculation was performed by adding a loopful of a 1.0% (v/v) bacterial

suspension to each experimental flask containing the respective degradation medium and target pollutant. Inoculation was performed once at the start of the experiment, and no additional bacterial supplementation was applied during incubation. All inoculated flasks were incubated under aerobic conditions, as described in Section 4.2.3.

This inoculation approach ensured consistent and reproducible introduction of metabolically active bacterial biomass across all experimental conditions, enabling reliable evaluation of bacterial degradation performance toward methylparaben and trichlorocarbanilide.

4.2.5 Sampling, Extraction, and Purification

Sampling, extraction, and purification procedures were designed based on the physicochemical properties of the target pollutants, the requirements of downstream analytical techniques, and the biological characteristics of the degradation systems. While sampling from lab-scale experiments followed a unified protocol, distinct extraction and purification strategies were applied for fungal and bacterial biodegradation experiments. This differentiation was necessary because quantitative nuclear magnetic resonance (qNMR) was used for caffeine and nicotine analysis, and high-performance thin-layer chromatography (HPTLC) for methylparaben and trichlorocarbanilide analysis, as well as because of differences in biomass characteristics between fungal and bacterial systems. Fungal biodegradation experiments required effective separation of mycelial biomass and spores from the liquid phase prior to extraction, whereas bacterial biodegradation samples necessitated removal of suspended cells to prevent analytical interference. Accordingly, extraction and purification workflows were optimized to ensure analytical compatibility, recovery efficiency, and reproducibility for each pollutant group [150,151].

Sampling from all lab-scale biodegradation experiments was performed at predefined time intervals, as specified in the experimental design. Samples were collected every five days for fungal biodegradation experiments and at defined kinetic time points (0, 48, 72, 96, and 120 hours) for bacterial biodegradation experiments. Sampling was initiated at 48 h to focus on effective biodegradation performance following initial microbial acclimation, rather than short-term adsorption effects or early

lag-phase behaviour. All sampling procedures were carried out under aseptic conditions to prevent external contamination and to preserve the integrity of microbial systems. At each sampling point, the required volume of liquid medium was withdrawn using sterile syringes and transferred into sterile centrifuge tubes. Care was taken to avoid disturbing settled biomass or surface growth, particularly in fungal systems with mycelial mats. Sampling instruments and containers were sterilized prior to use, and all handling was performed in a laminar airflow cabinet wherever applicable.

4.2.5.1 Extraction and Purification of Fungal Biodegradation Samples (Caffeine and Nicotine)

Extraction and purification of fungal biodegradation samples were designed to ensure effective removal of fungal biomass, spores, and extracellular debris prior to quantitative nuclear magnetic resonance (qNMR) analysis. The presence of filamentous mycelia and spores introduces significant matrix complexity and can interfere with spectroscopic measurements if not adequately removed. Therefore, a multistep purification strategy was adopted, combining physical separation and filtration techniques commonly reported in fungal biodegradation studies [147,152].

First, 5mL of the culture medium was withdrawn from each flask using sterile syringes under aseptic conditions and transferred into sterile centrifuge tubes. The samples were centrifuged at 7000 rpm for 20 minutes to separate fungal biomass, spores, and suspended solids from the liquid phase. After centrifugation, the supernatant was carefully collected using new sterile syringes to avoid resuspension of the pellet. The collected supernatant was subsequently filtered through nylon syringe filters (0.45 µm pore size) to ensure complete removal of residual fungal fragments and spores. Filtration was performed using gentle thumb pressure, and approximately 1-2 mL of clarified filtrate was collected into sterile glass vials. To prepare samples for NMR analysis, the filtered solutions were dried in a hot air oven at 40 °C to remove residual water. Drying at moderate temperature was selected to prevent thermal degradation of caffeine and nicotine and to ensure compatibility with deuterated solvents used during qNMR analysis. The resulting dried residues were subsequently reconstituted as required for spectroscopic analysis, as described in Chapter 5.

This purification protocol ensured that the NMR spectra reflected dissolved chemical species resulting from biodegradation processes rather than interference from biological material, enabling reliable identification and quantification of caffeine and nicotine degradation products [138,147,152].

4.2.5.2 Extraction and Purification of Bacterial Biodegradation Samples (MeP and TCC)

Extraction and purification of bacterial biodegradation samples were designed to meet the requirements of high-performance thin-layer chromatography (HPTLC) analysis and the biological characteristics of bacterial systems. Unlike fungal cultures, bacterial systems primarily consist of suspended cells rather than filamentous biomass; therefore, solvent-based extraction, followed by centrifugation and filtration, was employed to efficiently separate the target analytes from the aqueous matrix.

Following completion of the incubation period, equal volumes of acetonitrile were added directly to each bacterial degradation flask to extract methylparaben (MeP) and trichlorocarbanilide (TCC) from the aqueous phase. The flasks were sealed and agitated at 180 rpm for 2 h using a rotary shaker to enhance solvent-solute interaction and analyte recovery. The extracts were then transferred to centrifuge tubes and centrifuged at 7000 rpm for 15 min (Neuation iFUGE UC02R) to remove bacterial cells and particulate matter. The resulting supernatant was collected using sterile syringes and filtered through nylon syringe filters (0.45 μm pore size) to eliminate residual suspended debris. Approximately 1-2 mL of the clarified extract was collected into sterile glass vials.

To improve detection sensitivity and ensure compatibility with HPTLC analysis, the filtered extracts were subjected to vacuum evaporation (BioChromato Inc., Smart Evaporator C1, Japan) to remove the solvent and concentrate the analytes under controlled conditions, thereby minimizing the risk of thermal degradation. The dried residues were subsequently reconstituted in methanol to obtain a ten-fold concentrated solution. For HPTLC analysis, fixed and analyte-specific aliquots of the reconstituted extracts were applied to the TLC plates. For methylparaben (MeP), 5 μL was applied per track, corresponding to an initial applied mass of 5000 ng at time zero, whereas for trichlorocarbanilide (TCC), 4 μL was applied per track, corresponding to 4000 ng. For each compound, the spotting volume and applied mass were maintained constant across

all sampling time points, while the original bulk concentration in the biodegradation system was 100 mg L^{-1}.

This extraction, concentration, and purification protocol has been widely applied in studies involving paraben and triclocarban analysis and provides reliable recovery and reproducibility for chromatographic evaluation [150,151,153]. The standardized processing of all samples ensured that densitometric responses and degradation percentages obtained by HPTLC accurately reflected temporal changes in MeP and TCC concentrations during bacterial biodegradation under both nutrient-rich and nutrient-limited conditions.

4.3 Pilot-Scale Biomimetic Constructed Wetland Experiments

The pilot-scale biomimetic constructed wetland experiments were designed to translate lab-scale biodegradation findings into a controlled ecological system that more closely represents surface water treatment conditions. While laboratory experiments enabled mechanistic evaluation of microbial degradation under defined conditions, they do not account for spatial heterogeneity, hydraulic retention, plant-microbe interactions, or long-term operational stability. Therefore, a laboratory-scale constructed wetland was developed to assess microbial self-cleaning performance under mixed-contaminant loading and continuous aqueous exposure.

To mimic environmentally relevant surface water contamination characterized by the simultaneous presence of multiple pollutants, the constructed wetland system was operated under mixed-contaminant loading conditions. Caffeine, methylparaben, and trichlorocarbanilide were selected as representative target compounds, reflecting both natural and anthropogenic contaminant classes commonly detected in wastewater-impacted surface waters. The selected pollutants exhibit contrasting physicochemical properties and biodegradation behaviours, enabling evaluation of microbial adaptation, functional complementarity, and overall system performance under realistic multi-pollutant exposure rather than isolated compound conditions.

Microbial selection for the constructed wetland emphasized ecological suitability and long-term operational stability. The fungal species *Trametes versicolor* was employed due to its strong colonization capacity, extracellular enzymatic activity, and

compatibility with solid substrates and plant-associated niches. For bacterial degradation, *Pseudomonas aeruginosa* was selected owing to its metabolic versatility, resilience in aqueous environments, and well-established role in wastewater and wetland systems [154–156]. This microbial configuration enabled evaluation of functional complementarity and sustained biodegradation under environmentally relevant conditions.

4.3.1 Design and Configuration of the Constructed Wetland System

This section describes the physical design, structural components, and baseline operational configuration of the laboratory-scale constructed wetland units used in the pilot-scale experiments. The wetland system was designed to ensure identical hydraulic and structural conditions across all units, allowing subsequent evaluation of biological and operational variables without confounding effects from reactor design.

Four identical horizontal subsurface flow (HSSF) constructed wetland units were established using rectangular glass tanks with a total capacity of 30 L each (40 cm × 25 cm × 30 cm). The horizontal subsurface configuration was selected to simulate the longitudinal hydraulic flow path and aeration flow typical of full-scale subsurface wetlands while maintaining experimental control at laboratory scale. The use of transparent glass reactors provided an additional experimental advantage by allowing non-invasive visual observation of plant root development and biofilm distribution within the porous media throughout the experimental period.

Each wetland unit was equipped with silicon tubing installed at the reactor base, serving as a contamination-free sampling port. This configuration enabled periodic collection of liquid samples without disturbing the substrate structure, plant roots, or microbial biofilms, ensuring representative monitoring of system performance over time.

Each wetland unit was operated as an identical system with a defined working volume and a consistent physical configuration, ensuring that observed performance differences could be attributed to operational and biological variables rather than to reactor design (Table 11).

To ensure adequate hydraulic conductivity, prevent clogging, and provide sufficient surface area for microbial colonization, a stratified dual-layer substrate system was employed in all wetland units. The bottom layer consisted of uncoloured cobbles with a particle size range of 7-100 mm and a thickness of approximately 20 cm. This layer functioned as the primary hydraulic channel, facilitating uniform subsurface flow and minimizing resistance to water movement.

The top layer consisted of medium gravel with a particle size range of 5-10 mm and a thickness of approximately 5 cm. This layer provided mechanical support for macrophyte anchorage and contributed additional surface area for biofilm formation while reducing evaporative losses. The combined substrate configuration enabled stable hydraulic operation and supported simultaneous microbial attachment and plant root development.

All wetland units were planted with *Phragmites australis* (common reed), a macrophyte widely used in constructed wetland systems due to its extensive root network, high tolerance to pollutant stress, and ability to transport oxygen to the rhizosphere. Prior to planting, plant specimens were surface-sterilized using isopropanol to minimize the introduction of external epiphytic microorganisms and to ensure greater experimental control over microbial colonization within the wetland system. Plants were established in the upper substrate layer and allowed to acclimatize prior to experimental operation to promote root penetration and stabilize the porous media.

To maintain stable environmental conditions and support microbial metabolic activity, each wetland unit was equipped with a 25 W submersible heater coupled with a precision thermostat (Kruger Meier Reglerheizer, Germany). This configuration allowed controlled temperature regulation and flexibility in operating the wetland units under different thermal regimes, as required by specific experimental conditions.

The wetland system was designed to accommodate both aerated and non-aerated operation. Bottom-up aeration capability was provided through a pair of 30 cm aerator strips installed at the base of selected units, enabling uniform oxygen distribution within the subsurface media. This design allowed adjustment of oxygen availability and media movement for bacterial growth to accommodate different microbial growth requirements while preserving identical physical reactor configurations (Figure 6).

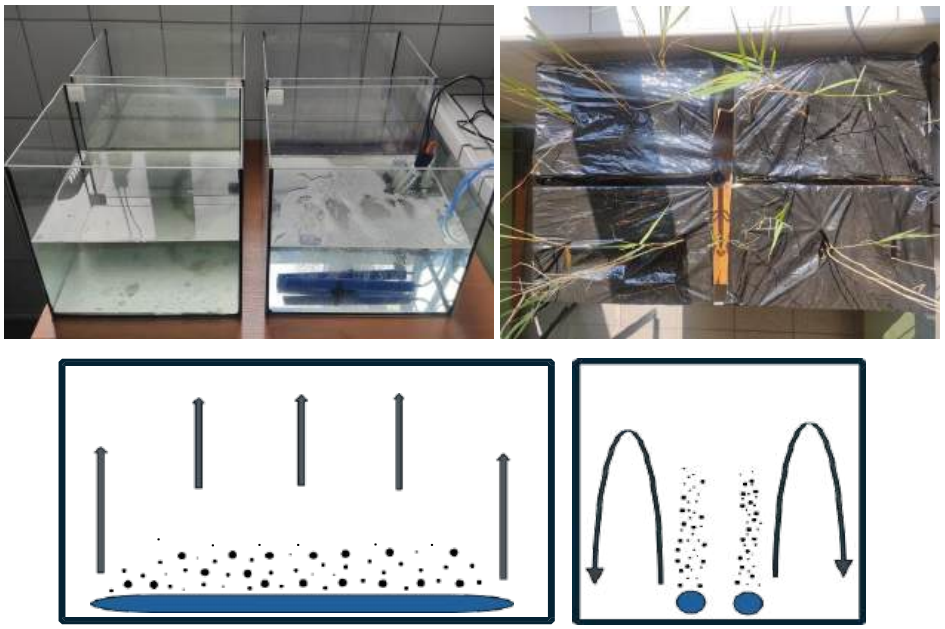

Figure 6. Wetland setup formation and aeration mechanism [157]

All wetland units were operated using synthetic wastewater (SWW) as the aqueous matrix, prepared according to the composition described in section 4.2.1. SWW was selected to provide a reproducible and controlled representation of wastewater-impacted surface water while minimizing variability associated with real influent matrices.

The influent was amended with a mixed-contaminant cocktail consisting of pure caffeine, methylparaben (MeP), and trichlorocarbanilide (TCC) (Sigma-Aldrich, Poland), each at a concentration of 100 mg L^{-1}. The relatively high pollutant loading was intentionally selected to challenge microbial survival and degradation capacity and to evaluate the wetland system's robustness under stress conditions. This mixed-contaminant configuration enabled assessment of microbial adaptation and system-level self-cleaning performance under conditions representative of complex environmental contamination rather than single-compound exposure.

Table 11. Operational configuration of identical laboratory-scale constructed wetland units

Parameter	Wetland Unit A	Wetland Unit B	Wetland Unit C	Wetland Unit D
System type	Horizontal subsurface flow CW	Horizontal subsurface flow CW	Horizontal subsurface flow CW	Horizontal subsurface flow CW
Reactor material	Glass tank	Glass tank	Glass tank	Glass tank
Total capacity	30 L	30 L	30 L	30 L
Working volume (SWW)	15 L	15 L	15 L	15 L
Substrate configuration	Dual-layer (cobbles + gravel)	Dual-layer (cobbles + gravel)	Dual-layer (cobbles + gravel)	Dual-layer (cobbles + gravel)
Plant species	Phragmites australis	Phragmites australis	Phragmites australis	Phragmites australis
Pollutant mixture	Caffeine + MeP + TCC	Caffeine + MeP + TCC	Caffeine + MeP + TCC	Caffeine + MeP + TCC
Pollutant concentration	100 mg L^{-1} (each)	100 mg L^{-1} (each)	100 mg L^{-1} (each)	100 mg L^{-1} (each)
Aqueous matrix	Synthetic wastewater (SWW)	Synthetic wastewater (SWW)	Synthetic wastewater (SWW)	Synthetic wastewater (SWW)
Microbial configuration	Pseudomonas aeruginosa	Trametes versicolor	P. aeruginosa + T. versicolor	None (abiotic control)
Temperature	37 °C	25 °C	30 °C	Room temperature

Aeration	Yes (bottom-up aeration)	No (static)	Yes (bottom-up aeration)	Yes
Operational condition	Bacterial system	Fungal system	Consortium system	Abiotic control
Porosity (%)	40-45	40-43	50-52	50-55

The porosity of the constructed wetland substrate was determined using the water displacement method. First, the internal volume of the aquarium reactor (V_{total}) was measured. The reactor was then filled with substrate stones arranged under the same conditions as during wetland operation. Water was slowly added until all void spaces between the stones were completely filled, and the volume of water required to achieve saturation was recorded as the void volume (V_{voids}). Porosity (n) was calculated as the ratio of the void volume to the total internal volume of the reactor according to Equation:

$$n = \frac{V_{\text{voids}}}{V_{\text{total}}}$$

This method provides a reliable estimate of the effective pore space available for hydraulic flow, microbial colonization, and mass transfer within the constructed wetland system [158].

4.3.2 Microbial Adaptation and Growth Dynamics in Mixed-Pollutant Medium

Prior to inoculation of the constructed wetland system, preliminary microbial adaptation experiments were conducted to assess the tolerance and growth behaviour of both fungal and bacterial strains under combined pollutant stress. This step was designed to verify microbial viability and compatibility with mixed-contaminant exposure conditions representative of the wetland influent. A mixed pollutant cocktail containing caffeine, methylparaben (MeP), and trichlorocarbanilide (TCC) was prepared and incorporated into solid growth media at increasing concentrations of 0, 1, 2, and 3 mg per 10 mL of medium. Identical pollutant concentrations were applied for both microbial groups to enable consistent evaluation of tolerance under uniform chemical stress

conditions. Potato Dextrose Agar (PDA) was used for fungal adaptation studies, while Nutrient Agar (NA) was used for bacterial adaptation studies.

For fungal adaptation assessment, *Trametes versicolor* was inoculated at the center of PDA plates amended with the pollutant cocktail and incubated at 25 °C. Plates without added pollutants served as controls. Fungal growth was monitored by measuring radial hyphal extension from the point of inoculation to the colony edge at 24-hour intervals. Growth inhibition was evaluated by comparing radial expansion rates in pollutant-amended plates with those in control conditions.

For bacterial adaptation assessment, *Pseudomonas aeruginosa* was inoculated onto NA plates containing the same pollutant cocktail concentrations and incubated at 37 °C. Inoculation was performed using a drop streak plating approach, in which 1 mL of actively growing pure bacterial culture was aseptically deposited onto the agar surface and evenly distributed using sterile streaking to promote uniform colony development. Plates without added pollutants served as controls. Bacterial tolerance and proliferation potential were evaluated by recording colony-forming units (CFU) at 24-hour intervals and comparing growth patterns across pollutant concentrations.

The purpose of this adaptation assay was to confirm microbial survival and growth compatibility under mixed-pollutant exposure prior to wetland-scale application. The results of this screening informed the selection of pollutant loading levels and microbial configurations employed in subsequent constructed wetland experiments.

4.3.3 Microbial Inoculation and System Operation

Microbial inoculation strategies were specifically designed to ensure rapid establishment, sustained activity, and spatial stability of selected degraders under high pollutant loading conditions. Given the elevated contaminant concentrations employed in the wetland system and the absence of natural microbial flora, targeted bioaugmentation approaches were implemented to maximize microbial survival and degradation efficiency. Distinct inoculation strategies were applied for bacterial, fungal, and combined systems to reflect their fundamentally different growth modes and ecological requirements.

Pseudomonas aeruginosa was selected as the bacterial degrader for the constructed wetland - A system due to its documented capacity to mineralize aromatic and antimicrobial compounds under aerobic conditions. This metabolic versatility makes the species particularly suitable for degrading anthropogenic contaminants such as methylparaben and trichlorocarbanilide in aqueous environments. Prior to wetland inoculation, the bacterium was cultivated in nutrient broth at 37 °C to obtain an actively growing culture. A defined volume (5 mL) of this liquid culture was then directly introduced into the aqueous phase of the constructed wetland unit (Wetland A). This liquid-phase inoculation strategy enabled rapid dispersion of bacterial cells throughout the pore water and facilitated early-stage colonization of the gravel substrate, promoting biofilm establishment within the wetland matrix.

To support aerobic bacterial activity and enhance microbial distribution, Wetland A was equipped with a centrally positioned, bottom-mounted aerator strip (30 cm length) installed along the reactor base. This aeration configuration generated upward-directed airflow, inducing gentle circular movement of the liquid phase from the bottom toward the upper regions of the wetland. The resulting hydraulic circulation improved oxygen availability within the porous medium and ensured effective contact among bacterial cells, dissolved pollutants, and substrate surfaces, thereby sustaining bacterial metabolic activity and uniform biofilm development. Importantly, this aeration-induced circulation was intentionally designed to reproduce the hydrodynamic and oxygen-transfer conditions used during lab-scale bacterial biodegradation experiments (Section 4.2.3), where continuous mixing was required to maintain aerobic conditions and support bacterial degradation. By aligning physical operating conditions across experimental scales, the wetland configuration ensured methodological continuity between batch experiments and system-level biodegradation, strengthening the interpretation of scale-up performance.

To establish a stable and vertically propagating fungal network within the constructed wetland - B system, a solid-state inoculation strategy was developed for *Trametes versicolor*. Following sterilization of the reactor, 100 mL of autoclaved Potato Dextrose Agar (PDA) was evenly poured onto the aquarium bottom to form a uniform basal layer. After solidification, fungal spores were aseptically distributed across the agar surface. The reactor was incubated under static conditions for 7 days,

allowing the development of a continuous and uniform fungal mycelial mat approximately 1 cm thick. Once the fungal mat was established, sterilized porous gravel layers were carefully placed above the fungal base, followed by the introduction of synthetic wastewater containing the defined pollutant load and the planting of *Phragmites australis*. This configuration enabled upward fungal colonization through the substrate profile while minimizing mechanical disturbance of the hyphal network. In contrast to conventional liquid-phase fungal inoculation methods, this approach provided a physically anchored fungal biomass, enhancing resistance to hydraulic washout and supporting long-term metabolic stability under continuous-flow conditions.

In the hybrid wetland C, both inoculation strategies were applied simultaneously. The basal fungal mat was established as described for Wetland B, followed by liquid-phase inoculation of *Pseudomonas aeruginosa* into the aqueous phase. This configuration was designed to exploit functional complementarity between microbial groups, whereby fungal extracellular oxidative enzymes initiate transformation of structurally complex compounds, and bacterial metabolism facilitates downstream degradation and mineralization of transformation products.

Wetland D served as a control unit and received no deliberate microbial inoculation. This configuration was used to quantify pollutant attenuation arising from non-biological and background processes, including adsorption onto the substrate, plant uptake, and activity of indigenous microbial populations.

All wetland units were planted with three evenly spaced *Phragmites australis* individuals rooted within the gravel layer. To minimize evaporative losses and reduce external microbial intrusion, reactors were covered with a thin plastic sheet containing openings for plant stems. While this configuration did not provide fully aseptic conditions due to the presence of plants and gas-exchange openings, it reflects realistic operating conditions of constructed wetlands, where complete sterility is neither achievable nor environmentally representative.

Measures were implemented to minimize external microbial contamination during system establishment, thereby promoting rapid colonization and dominance of the deliberately inoculated microbial species. Once established, these targeted microbial communities were expected to competitively occupy available ecological niches within

the wetland matrix, reducing susceptibility to invasion by external microorganisms. This design balances experimental control with ecological relevance and reflects conditions encountered in practical wetland-based treatment systems [159–161].

4.3.4 Monitoring of Operational Parameters (pH, Plant Growth)

To evaluate the stability of the wetland environment and to indirectly assess microbial metabolic activity, the pH of the aqueous phase was monitored throughout the experimental period. pH is a critical operational parameter in constructed wetland systems, as it influences microbial enzyme activity, pollutant speciation, nutrient availability, and overall biodegradation efficiency. Significant pH fluctuations may indicate microbial stress, accumulation of acidic or alkaline transformation products, or shifts in dominant biochemical processes.

In the present study, pH measurements were performed weekly in all four wetland units (Wetlands A, B, C, and D) using a calibrated pH meter. Measurements were taken directly from the aqueous phase to ensure a representative assessment of system-wide conditions. Monitoring pH across different microbial configurations enabled comparison of system stability under bacterial-only, fungal-only, combined microbial, and control conditions.

Plant growth was monitored to assess vegetation tolerance, system stability, and physical support functions within the constructed wetland, rather than to assess direct pollutant degradation. *Phragmites australis* (common reed) was selected due to its robustness, well-developed root system, and widespread use in constructed wetland systems, where plants primarily contribute to structural stability, rhizosphere development, and facilitation of microbial colonization [162].

Shoot height was measured weekly to monitor above-ground plant development and overall vitality during exposure to the mixed-pollutant influent. At the end of the 7-week experimental period, plants were carefully removed from the gravel substrate to allow visual inspection and measurement of below-ground biomass, including rhizome development and root penetration within the porous media. Evaluation of plant growth ensured that vegetation remained physiologically stable under high pollutant loading and supported interpretation of wetland performance by confirming the presence of an intact

plant-substrate framework conducive to microbial activity. This approach allowed pollutant removal to be attributed primarily to microbial processes while recognizing the indirect structural and ecological role of vegetation within the wetland system.

4.3.5 Sample Extraction and Purification of Wetland Samples

To enable reliable identification and characterization of biodegradation products while minimizing interference from microbial biomass, plant-derived material, and wetland particulates, a dedicated extraction and purification protocol was applied to wetland samples intended for Nuclear Magnetic Resonance (NMR) analysis.

Liquid samples (50 mL) were collected from each wetland unit using sterile syringes connected to the silicon sampling ports installed at the base of the reactors. Samples were collected at week 4 and week 7 of operation, corresponding to intermediate and advanced stages of system operation under stabilized conditions. All sampling procedures were conducted under aseptic conditions to minimize external contamination. Collected samples were transferred to sterile centrifuge tubes and centrifuged at 7000 rpm for 20 min to sediment fungal hyphae, bacterial cells, and suspended solids originating from the wetland matrix. The clarified supernatant was carefully recovered using sterile syringes and subsequently filtered through 0.45 µm nylon syringe filters to ensure complete removal of residual particulate matter. To eliminate water content, which interferes with NMR signal acquisition, 1-2 mL aliquots of the filtered samples were evaporated to complete dryness in a hot-air oven maintained at 40 °C. The resulting dry residues were reconstituted in 0.7 mL of deuterated chloroform ($CDCl_3$) containing 0.03% tetramethylsilane (TMS) as an internal chemical shift reference. The prepared samples were transferred to NMR tubes and analyzed using an Agilent Magnet 400 MHz spectrometer at 25 °C to characterize transformation products formed during wetland-scale biodegradation [147,163–165].

Although operational parameters such as pH and plant growth were monitored weekly, chemical analysis of degradation products was intentionally limited to weeks 4 and 7. Preliminary observations indicated that early operational phases were dominated by microbial acclimation, biofilm establishment, and system stabilization. Consequently, analysis at later time points allowed discrimination between transient effects (e.g., adsorption or initial adaptation) and sustained biodegradation activity, ensuring that

detected transformation products reflected established microbial processes within the wetland system.

Chapter 5: Analytical Methods and Data Validation

5.1 Overview of Analytical Strategy and Method Selection

The analytical strategy adopted in this study was designed to address the chemical diversity of the target pollutants, the varying complexity of sample matrices, and the different experimental scales investigated, ranging from lab-scale biodegradation systems to an pilot scale biomimetic constructed wetland. Rather than relying on a single analytical technique, a multi-technique framework was implemented to ensure reliable compound identification, accurate quantification, and mechanistic interpretation of biodegradation processes.

Analytical methods were selected based on three primary criteria: (i) chemical properties of the target pollutants, (ii) matrix complexity and biological interference, and (iii) analytical purpose, distinguishing between qualitative confirmation, quantitative determination, and semi- quantitative performance assessment.

The studied pollutants were divided into two distinct classes: naturally derived alkaloids (caffeine and nicotine) and anthropogenic contaminants (methylparaben and trichlorocarbanilide). This classification directly informed the analytical approach. Caffeine and nicotine, extracted from natural sources, required structural confirmation and absolute concentration determination prior to biodegradation experiments. For this purpose, Fourier Transform Infrared Spectroscopy (FT-IR) and Nuclear Magnetic Resonance (NMR) spectroscopy were employed. FT-IR served as a rapid qualitative tool to verify functional group integrity and confirm successful extraction, while NMR provided definitive structural identification and quantitative concentration determination.

In contrast, methylparaben and trichlorocarbanilide were used as analytical-grade standards and monitored during bacterial biodegradation experiments conducted in complex biological liquid matrices. For these compounds, High-Performance Thin-Layer Chromatography (HPTLC) was selected as the primary analytical tool due to its

robustness, matrix tolerance, and suitability for time-resolved monitoring of concentration changes in nutrient-rich and synthetic wastewater media.

For the constructed wetland system, which contained suspended solids, microbial biomass, plant-derived materials, and heterogeneous degradation products, high-resolution NMR spectroscopy was selectively employed to analyze compounds soluble in deuterated organic solvents. This enabled qualitative tracking of transformation processes under stabilized wetland operating conditions. Structural limitations encountered for trichlorocarbanilide under these conditions were analytically addressed and are discussed in subsequent chapters.

Finally, Scanning Electron Microscopy (SEM) was used as a complementary structural tool to visualize microbial colonization and biofilm development on wetland porous media. SEM was not used for chemical quantification, but it provided critical physical evidence supporting biological activity and system functionality.

Due to the specialized nature of certain analytical techniques, this study employed collaborative laboratory facilities for selected measurements. HPTLC method development, validation, and densitometric analysis were conducted in collaboration with an external research laboratory equipped with advanced CAMAG instrumentation. NMR analyses were performed using high-field spectrometers available through institutional research facilities.

The use of collaborative infrastructure enabled access to validated analytical platforms while maintaining methodological consistency and reproducibility. All analytical procedures were conducted in accordance with standardized protocols, and method validation parameters were explicitly documented to ensure transparency and compliance with accepted analytical guidelines.

Overall, the integrated analytical strategy adopted in this study ensured that each pollutant, experimental scale, and sample matrix was evaluated using the most appropriate and defensible technique.

5.2 Fourier Transform Infrared Spectroscopy (FT-IR)

Fourier Transform Infrared Spectroscopy (FT-IR) was employed as a qualitative analytical technique to confirm the molecular identity and functional group integrity of caffeine and nicotine extracted from natural sources. FT-IR analysis was intentionally restricted to extracted parent compounds and was not applied to biodegradation samples. This methodological decision was based on the inherent limitations of FT-IR in complex matrices, where the presence of microbial biomass, water, and transformation products reduces spectral selectivity and interpretability.

The primary purpose of FT-IR analysis in this study was to verify that the extraction procedures yielded chemically intact caffeine and nicotine prior to their use in biodegradation experiments. Structural confirmation at this stage was essential to ensure that any subsequent concentration changes observed during microbial degradation could be attributed to biological activity rather than impurities or extraction-induced chemical alterations.

FT-IR measurements were performed using a Thermo Scientific Nicolet 6700 FT-IR spectrometer equipped with an attenuated total reflectance (ATR) accessory. Extracted samples were analyzed in solid or semi-solid form after removal of residual moisture by drying at 40 °C for 24 h in a hot-air oven, thereby minimizing interference from water absorption bands. Infrared spectra were recorded over the mid-infrared range (4000-400 cm^{-1}). The obtained spectra were compared with reference spectra reported in the literature and spectral databases to confirm compound identity [134,135,139].

FT-IR was not used to monitor biodegradation progress or identify transformation products. Such analyses require higher chemical specificity and tolerance to aqueous and biological matrices, which were addressed using Nuclear Magnetic Resonance (NMR) spectroscopy and High-Performance Thin-Layer Chromatography (HPTLC), as described in subsequent sections.

5.2.1 Qualitative Identification of Extracted Natural Pollutants

Qualitative identification of the extracted caffeine and nicotine was performed by examining characteristic infrared absorption bands associated with their known

molecular structures. FT-IR analysis focused on functional group regions commonly used for compound verification rather than quantitative assessment.

For caffeine, spectral evaluation targeted absorption bands corresponding to carbonyl stretching vibrations, imide functionalities, and aromatic ring structures. For nicotine, characteristic absorption features related to heterocyclic ring systems, tertiary amine groups, and aliphatic C-H stretching vibrations were examined. These spectral features were selected based on established reference spectra in the library. The obtained FT-IR spectra were compared with reference spectra available in the NIST IR spectral library, Sigma-Aldrich (Merck) reference spectra, and published literature data to verify compound identity.

Compound identity was considered confirmed when the observed absorption bands matched the expected functional group signatures reported for analytical-grade caffeine and nicotine. This qualitative verification step served as a validation criterion, ensuring that the extraction process yielded chemically intact parent compounds suitable for subsequent quantitative NMR analysis and for use in biodegradation experiments. No FT-IR analysis was conducted on biodegradation samples, as such matrices exceed the selectivity limits of infrared spectroscopy.

5.3 Nuclear Magnetic Resonance (NMR) Spectroscopy

Nuclear Magnetic Resonance (NMR) spectroscopy was employed as a core analytical technique for both the quantitative determination of extracted natural pollutants and the qualitative characterization of biodegradation processes at the flask and wetland scales. Owing to its high chemical specificity, non-destructive nature, and tolerance to complex matrices, NMR was selected to confirm compound identity, establish initial pollutant concentrations, and assess structural transformation during microbial degradation.

All NMR measurements were performed using a Varian 400 spectrometer operating at 400 MHz for proton (^{1}H) and 100 MHz for carbon (^{13}C) nuclei. Deuterated chloroform ($CDCl_3$) was used as the solvent for all analyses. Proton chemical shifts were referenced to tetramethylsilane (TMS) at 0.00 ppm, while carbon chemical shifts were referenced to the solvent resonance of $CDCl_3$ at 77.16 ppm. Chemical shifts (δ) are

reported in parts per million (ppm), and coupling constants (J) in hertz (Hz), following standard conventions [140–142]. All spectra were acquired at ambient temperature (25 °C).

The application of NMR spectroscopy in this study was divided into two methodological categories: (i) quantitative NMR (qNMR) for determining concentrations of extracted caffeine and nicotine, and (ii) qualitative NMR analysis for monitoring biodegradation-induced structural changes at flask and wetland scales.

5.3.1 Determination of Caffeine and Nicotine by ^{1}H NMR Spectroscopy

Quantitative nuclear magnetic resonance (qNMR) spectroscopy was used to determine the concentrations and purities of caffeine and nicotine extracted from natural sources prior to their application in biodegradation experiments. qNMR enables absolute quantification without the need for compound-specific calibration curves, as signal integrals are directly proportional to the number of contributing nuclei. This approach provides high analytical accuracy for relatively pure analytes and ensures reliable mass determination.

For quantitative analysis, extracted samples were dissolved in deuterated chloroform ($CDCl_3$) containing a known mass of dimethyldiphenylsilane ($C_{14}H_{16}Si$; MW = 212.36 g·mol^{-1}) as an internal standard. Proton (^{1}H) NMR spectra were acquired under identical instrumental and acquisition parameters for all samples. Quantification was based on the comparison of integrated signal areas of selected, non-overlapping proton resonances of the analyte with those of the internal standard, taking into account the number of equivalent protons contributing to each signal.

Dimethyldiphenylsilane was selected as the internal standard due to its chemical stability, solubility in $CDCl_3$, and the presence of a sharp, well-resolved singlet corresponding to six equivalent methyl protons bonded to silicon. Although the molecule also contains 10 aromatic protons, only the silicon-bound methyl protons (6H) were used for quantitative integration to avoid potential issues.

5.3.2 NMR Analysis of Biodegradation Products

Qualitative NMR analysis was employed to investigate structural changes and transformation pathways of caffeine and nicotine during microbial biodegradation at both lab-scale and caffeine, methylparaben (MeP), and trichlorocarbanilide (TCC) at wetland-scale systems. In these applications, NMR was used to monitor the disappearance of characteristic parent-compound signals and the emergence of new resonances corresponding to transformation products.

For lab-scale fungal biodegradation experiments, samples were subjected to extraction and purification procedures as described in Section 4.2.5 prior to NMR analysis. Similarly, wetland-scale samples collected at selected operational time points were processed according to the protocol outlined in Section 4.3.5.

Trichlorocarbanilide (TCC) could not be reliably analyzed by NMR under the experimental conditions employed due to its limited solubility in deuterated chloroform ($CDCl_3$) at the concentrations required for spectral acquisition. This solvent-analyte incompatibility limited meaningful detection of NMR signals. Consequently, chromatographic techniques were selected as the primary analytical approach for monitoring TCC biodegradation, as described in Section 5.4.

5.4 High Performance Thin Layer Chromatography (HPTLC)

High-Performance Thin-Layer Chromatography (HPTLC) was employed for the qualitative and quantitative analysis of anthropogenic pollutants, specifically methylparaben (MeP) and trichlorocarbanilide (TCC), during lab-scale bacterial biodegradation experiments. HPTLC was selected as the primary analytical technique for these compounds due to its robustness, suitability for hydrophobic and poorly NMR-soluble analytes, and its ability to provide reliable quantification in biologically complex matrices.

Unlike Nuclear Magnetic Resonance (NMR) spectroscopy, which requires high analyte solubility in deuterated solvents, HPTLC allows direct analysis of compounds such as TCC that exhibit limited solubility under conventional NMR conditions. Additionally, HPTLC enables simultaneous sample processing, visual confirmation of compound migration, and densitometric quantification, making it particularly suitable

for time-resolved degradation studies conducted under collaborative laboratory conditions. In this study, HPTLC analysis was applied exclusively to bacterial biodegradation experiments of MeP and TCC conducted at the lab scale.

5.4.1 Method Development for Anthropogenic Pollutants

HPTLC was employed for the qualitative and quantitative analysis of bacterial biodegradation of the anthropogenic pollutants methylparaben (MeP) and trichlorocarbanilide (TCC) at the lab scale. HPTLC was selected as the most appropriate analytical technique for this phase of the study due to its robustness, cost-effectiveness, and suitability for complex aqueous matrices containing bacterial biomass and residual media components. Unlike spectroscopic methods, HPTLC enables simultaneous multi-sample analysis, clear visualization of degradation progress, and reliable quantification of hydrophobic and semi-polar compounds such as MeP and TCC (Figure 7).

All analyses were performed using a CAMAG HPTLC system (Muttenz, Switzerland) equipped with a semi-automated sample applicator, plate visualizer, and densitometric scanner controlled by winCATS software. A sample application was carried out using a CAMAG Linomat 5 applicator fitted with a 100 µL Hamilton syringe, ensuring precise, reproducible band application. Samples were applied as bands on aluminium-backed silica gel 60 F_{254} HPTLC plates (E. Merck, India), with controlled band dimensions and inter-track spacing to avoid cross-contamination and ensure optimal resolution.

Chromatographic development was conducted in a twin-trough glass chamber using a mobile phase consisting of toluene and ethyl acetate in a 9:1 (v/v) ratio. Prior to development, the chamber was saturated for 20 minutes using saturation pads to ensure reproducible solvent migration. Plates were developed up to a solvent front distance of 80 mm and subsequently air-dried at room temperature. This mobile phase composition provided effective separation of MeP and TCC from potential matrix interferences and degradation by-products.

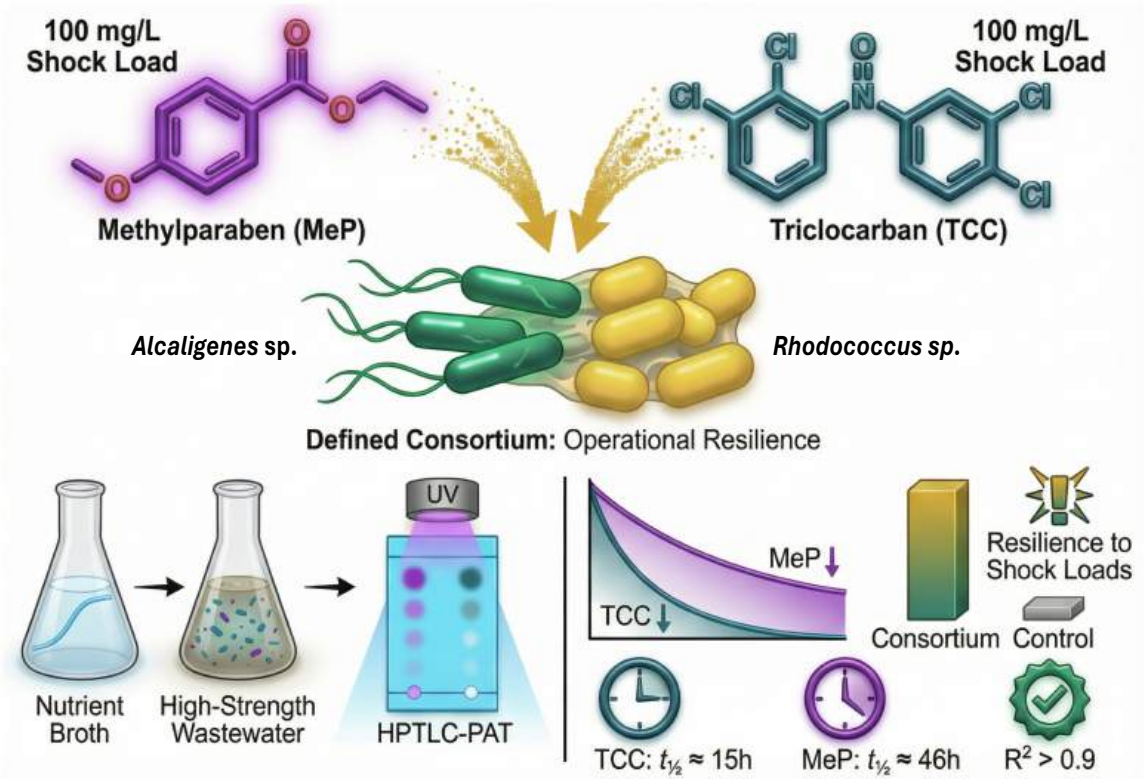

Figure 7. Schematic diagram of the bacterial degradation methodology using HPTLC

Developed plates were visualized under white light and ultraviolet illumination at 254 nm and 366 nm using a CAMAG Visualizer 3 to document chromatographic profiles and assess qualitative changes during biodegradation. Quantitative analysis was performed using a CAMAG TLC Scanner 4 operated in absorbance mode at 254 nm, employing a deuterium lamp as the radiation source. Densitometric scanning was conducted under optimized conditions to maximize sensitivity and reproducibility. Spectral scanning across the range of 190-450 nm was additionally performed to confirm peak identity and assess spectral purity (Figure 8).

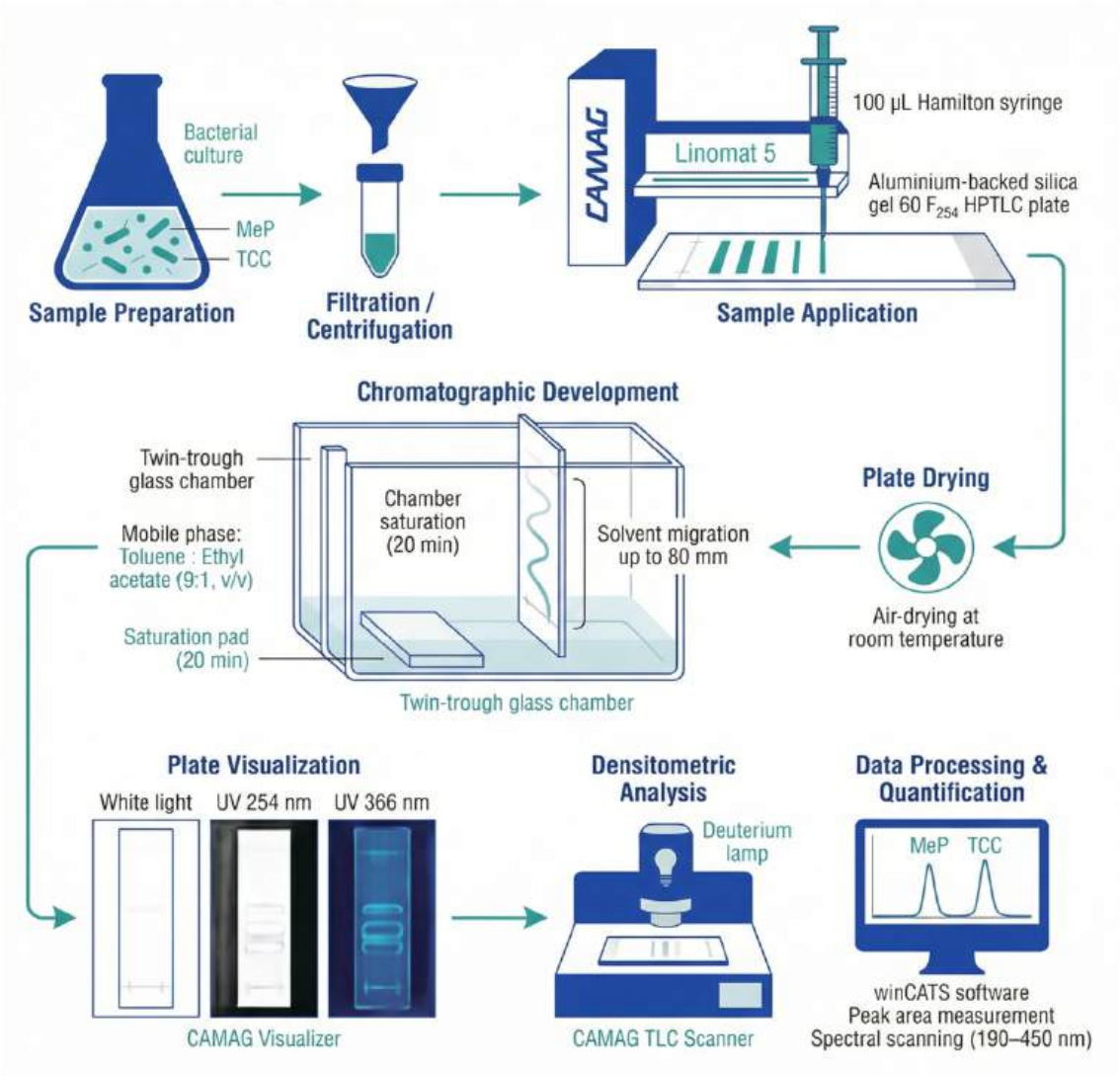

Figure 8. Schematic overview of the HPTLC workflow used to monitor bacterial biodegradation, including sample application, chromatographic development, plate visualization, densitometric scanning, and data analysis.

The combination of controlled sample application, optimized mobile phase selection, and densitometric detection enabled reliable monitoring of bacterial degradation of MeP and TCC over time. Detailed instrumental parameters and operating conditions are summarized in (Table 12). This analytical framework provided both visual and quantitative confirmation of pollutant removal and was subsequently used to validate the method and assess degradation in the bacterial biodegradation experiments.

Table 12. HPTLC instrumentation and analytical conditions used for MeP and TCC analysis

Category	Parameter	Specification
HPTLC system	Manufacturer	CAMAG, Muttenz, Switzerland
	Software	winCATS (version 3.2.2.23346.3)
Sample application	Applicator	CAMAG Linomat 5 (S/N: 180344)
	Syringe	100 µL Hamilton syringe
	Application mode	Band
	Band length	8.0 mm
	Application rate	50 nL s^{-1}
	Pre-dosage volume	0.20 µL
	First track position (X)	20.0 mm
	Distance between tracks	11.4 mm
Stationary phase	Plate type	HPTLC Silica gel 60 F_{254}
	Plate backing	Aluminium
	Plate dimensions	200 × 100 mm
	Layer thickness	0.2 mm
	Supplier	E. Merck, India
Development chamber	Chamber type	Twin-trough glass chamber
	Chamber size	20 × 10 cm
	Supplier	CAMAG, Switzerland
Mobile phase	Composition	Toluene : Ethyl acetate (9:1, v/v)
Chamber conditions	Saturation time	20 min
	Saturation pad	Used
	Solvent volume (front trough)	10 mL
	Solvent volume (rear trough)	10 mL
	Migration distance	80 mm

	Development temperature	Room temperature
	Drying time	5 min
Plate visualization	Instrument	CAMAG Visualizer 3 (S/N: 300884)
	Modes	White light, UV 254 nm, UV 366 nm
	Exposure	Automatic (85% level)
Densitometric scanning	Scanner	CAMAG TLC Scanner 4 (S/N: 180404)
	Measurement mode	Absorbance
	Scanner type	Single wavelength (λ)
	Detection wavelength	254 nm
	Light source	Deuterium lamp
	Scanning speed	20 mm s^{-1}
	Data resolution	100 µm $step^{-1}$
	Slit dimensions	6 × 0.45 mm (micro)
Spectral scanning	Mode	Spectrum scan
	Wavelength range	190-450 nm
	Scan speed	20 nm s^{-1}
	Spectral resolution	1 nm
	Reference spectrum	Per plate (X = 10.0 mm, Y = 10.0 mm)

To ensure accurate, reliable, and reproducible quantification of methylparaben (MeP) during bacterial biodegradation experiments, the developed High-Performance Thin-Layer Chromatography (HPTLC) method was systematically validated in accordance with the International Council for Harmonisation (ICH) guideline Q2(R1) for analytical method validation [166].

Initial validation focused on confirming the identity and chromatographic behaviour of MeP by comparing the retention factor (Rf) values and densitometric responses of standard solutions with those obtained from bacterial degradation samples

and corresponding controls. The presence of MeP in test samples was verified through consistent Rf values and spectral matching, establishing method specificity.

During preliminary method development, simultaneous separation of methylparaben and trichlorocarbanilide (TCC) was evaluated to enable combined analysis. However, chromatographic trials using the optimized mobile phase (toluene: ethyl acetate, 9:1 v/v) revealed significant overlap in Rf values for MeP and TCC within the range of 0.30-0.40 (Figure 9a). Furthermore, UV spectral overlay analysis demonstrated that both compounds exhibited a single absorption maximum in the 200-300 nm range, resulting in indistinguishable densitometric signals at 254 nm (Figure 9b).

Although simultaneous analysis was initially explored to maximize throughput, overlapping Rf values and UV absorption profiles precluded compound-specific quantification. Separate chromatographic runs were therefore established to ensure analytical specificity and compliance with ICH validation criteria.

5.4.2 Method Validation for Methylparaben (MeP)

Method validation for methylparaben followed the same ICH-compliant framework, including assessment of specificity, linearity, sensitivity, and precision, with compound-specific chromatographic optimization.

Chromatographic separation of methylparaben was optimized using aluminium-backed silica gel 60 F_{254} plates (20 × 10 cm, 0.2 mm thickness). Multiple mobile phase systems were evaluated, and a toluene: ethyl acetate (9:1 v/v) mixture provided well-defined, compact, and symmetrical MeP spots with reproducible migration behaviour.

Plates were developed in a pre-saturated twin-trough chamber with a saturation time of 20 min. The solvent front was allowed to migrate 90 mm from the application origin. Following development, plates were air-dried at room temperature and visualized under UV light at 254 nm and 366 nm. Densitometric scanning was performed at 254 nm in absorbance mode.

The optimized chromatographic conditions and instrumental parameters for MeP analysis are summarized in (Table 13).

Table 13. Optimized chromatographic conditions for methylparaben analysis

Chromatographic Conditions	Paraben
Stationary phase	Aluminium-backed TLC silica gel 60 F254 plates (20 × 10cm, 0.2mm thick),
Mobile phase	Toluene: Ethyl acetate (9:1 v/v)
Volume of standard	5 µL
Volume of sample	5 µL
Saturation time	20min
Development distance	90mm (90%)
Room temperature	25 ± 2oC
Relative humidity	40%
Wavelength	254nm
Scanning mode	Absorption
Lamp	Deuterium & Tungsten
Rf (retention factor)	0.33

Method specificity was further confirmed through spectral correlation analysis. The UV absorption spectrum of MeP showed a distinct maximum at 254 nm (Figure 10a). Spectral purity assessment across multiple tracks demonstrated high correlation coefficients ($r > 0.99$) between standard and sample peaks, confirming peak homogeneity and absence of co-eluting interferences. High correlation values observed in Tracks 6-13 indicate excellent spectral matching with the reference standard, confirming the specificity of the developed method for MeP quantification.

Linearity of the method was established by analyzing standard MeP solutions over the concentration range of 100-600 ng per band. Calibration curves were constructed by plotting applied concentration against the corresponding peak area. The method demonstrated good linearity with a correlation coefficient (R^2) of 0.9974, indicating proportional response across the studied range (Figure 10c).

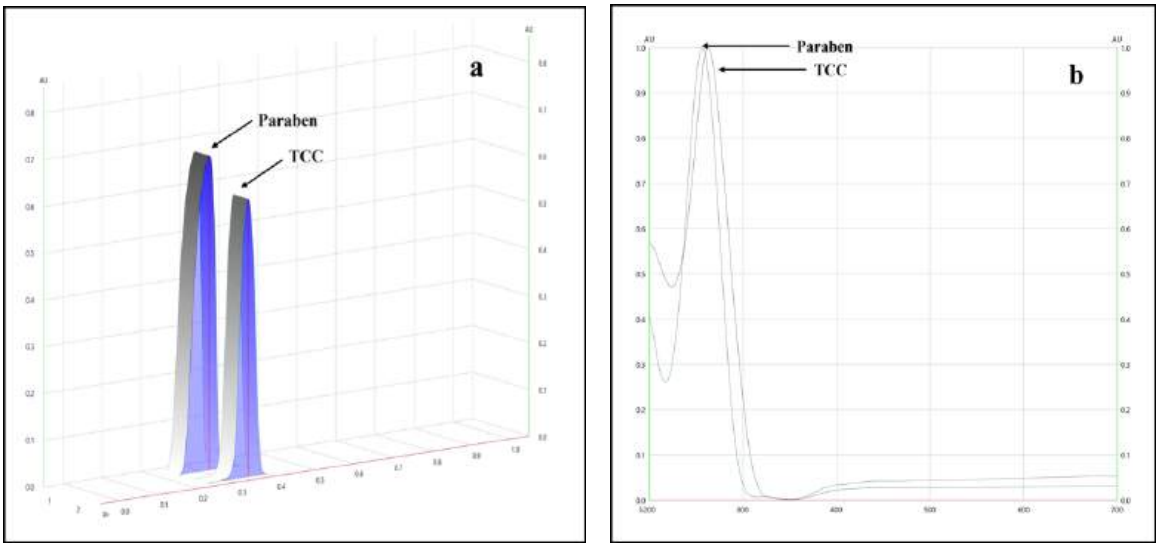

Figure 9. (a) Densitogram of Paraben and TCC at 254nm, (b) Spectra overlay of Paraben and TCC

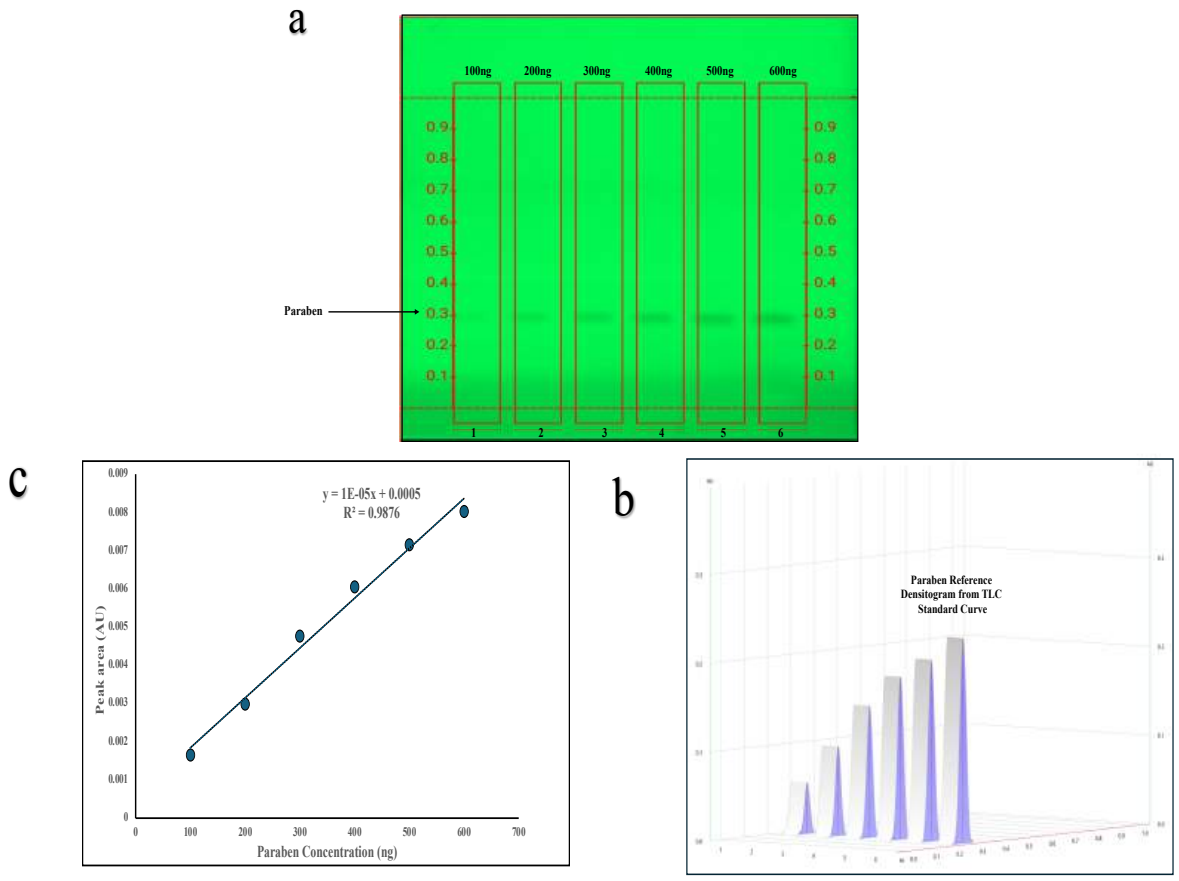

Figure 10. (a) Paraben standard on TLC plate under 256 nm UV light image, (b) 3D densitogram of paraben TLC plate, and (c) Standard linear curve of Paraben concentration with peak area.

Method sensitivity was assessed by calculating the limit of detection (LOD) and the limit of quantification (LOQ) using signal-to-noise criteria. The LOD and LOQ for methylparaben were determined as 108.13 ng/band and 327.67 ng/band, respectively. Repeatability and system precision were evaluated by applying standard MeP solutions across seven replicate tracks within the validated range. The method demonstrated excellent repeatability with a relative standard deviation (RSD) of 0.942%, confirming suitability for time-resolved biodegradation studies (Table 14).

Table 14. Summary of validation parameters for methylparaben

Parameters	**Paraben**
Wavelength, nm	254
Linearity range, ng/band	100-600
Regression equation	y = 1E-05x + 0.0005
Correlation coefficient (r2)	0.9974
Limit of detection (LOD)	108.13 ng/band
Limit of quantification (LOQ)	327.67 ng/band
Specificity	Specific
Repeatability (%RSD)	0.942%

Densitometric scanning enabled precise quantification of methylparaben by correlating peak area with standard calibration data. This validated approach provided the analytical basis for calculating relative concentration changes in biodegradation samples collected at defined time intervals. The method enabled reliable comparison of MeP levels across different media conditions and experimental setups, forming the foundation for the evaluation of degradation efficiency presented in Chapter 6 (Figure 10b).

The validated HPTLC method for methylparaben provided a reliable, high-throughput analytical basis for time-resolved biodegradation assessment, supporting quantitative interpretation of bacterial degradation kinetics presented in Chapter 6.

5.4.3 Method Validation for Trichlorocarbanilide (TCC)

Method validation for trichlorocarbanilide was conducted using the same ICH-compliant framework as methylparaben, with adjustments made to mobile phase composition to accommodate the compound's higher hydrophobicity.

To enable accurate, selective, and reproducible quantification of trichlorocarbanilide (TCC) during lab-scale bacterial biodegradation experiments, a High-Performance Thin-Layer Chromatography (HPTLC) method was systematically developed and validated in accordance with the International Council for Harmonisation guideline Q2(R1) for analytical method validation [166]. Method validation focused on establishing chromatographic specificity, linearity, sensitivity, and precision for TCC in bacterial degradation matrices. The identity of TCC in experimental samples was confirmed through consistent retention factor (Rf) values and UV spectral matching with analytical standards.

Multiple mobile phase compositions were evaluated to achieve optimal chromatographic resolution and spot symmetry for TCC. The mobile phase consisting of toluene: ethyl acetate (8:2 v/v) provided well-defined, compact spots with stable migration behaviour and minimal tailing. Chromatographic development was carried out in a pre-saturated twin-trough chamber with a saturation time of 20 min. The solvent front was allowed to migrate 90 mm from the application origin. After development, plates were air-dried and analyzed densitometrically using absorbance mode at 254 nm. Under optimized conditions, TCC exhibited a consistent mean Rf value of approximately 0.33, demonstrating reproducible chromatographic performance across analytical runs (Table 15).

Table 15. Optimized chromatographic conditions for trichlorocarbanilide analysis

Chromatographic Conditions	Trichlorocarbanilide (TCC)
Stationary phase	Aluminium-backed TLC silica gel 60 F254 plates (20 × 10cm, 0.2mm thick),
Mobile phase	Toluene: Ethyl acetate (8:2 v/v)
Volume of standard	4 µL
Volume of sample	4 µL
Saturation time	20min
Development distance	90mm (90%)
Room temperature	25 ± 20C
Relative humidity	40%
Wavelength	254nm
Scanning mode	Absorption
Lamp	Deuterium & Tungsten
Rf (retention factor)	0.33

Method specificity was evaluated by comparing the chromatographic behaviour and UV absorption spectra of TCC standards, media blanks, bacterial controls, and degradation samples collected at different time points. TCC exhibited a characteristic absorption maximum (λmax) at 254 nm, with emission observed at 264 nm. Densitometric spectral analysis confirmed consistent peak profiles across degradation samples, indicating peak purity and absence of co-eluting interferences (Figure 11a).

Retention factor values for degradation samples remained within a narrow range throughout the experimental period, further confirming chromatographic specificity. Spectral overlay analysis confirmed consistent UV absorbance profiles between the TCC standard and degradation samples, indicating peak purity throughout the kinetic study. The consistency of Rf values across Tracks 6-13 confirms reliable identification of TCC during time-resolved analysis. Linearity of the developed HPTLC method was established over a concentration range of 100-600 ng per band. Calibration curves were constructed by plotting applied concentration against corresponding peak area, yielding a strong linear relationship with a correlation coefficient (R^2) of 0.991 (Figure 11c).

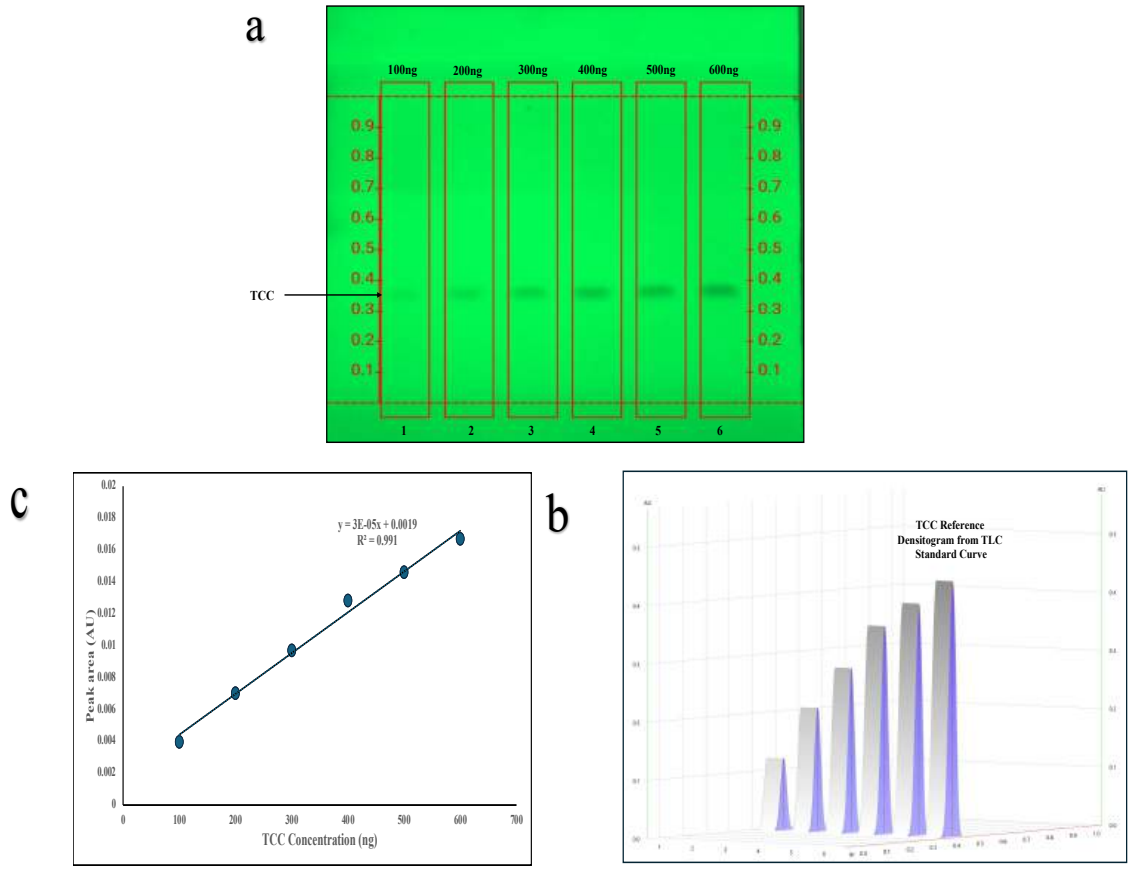

Figure 11. (a) TCC standard on TLC plate under 256 nm UV light, (b) 3D densitogram of TCC TLC plate, and (c) Standard linear curve of trichlorocarbanilide (TCC) concentration with peak area

Method sensitivity was assessed by calculating the limit of detection (LOD) and limit of quantification (LOQ) from the calibration data. The LOD and LOQ for TCC were determined as 127.57 ng/band and 386.59 ng/band, respectively. System precision and repeatability were evaluated by applying TCC standards across seven replicate tracks, yielding a relative standard deviation (RSD) of 1.2%, indicating satisfactory analytical precision (Table 16).

Table 16. Summary of validation parameters for trichlorocarbanilide

Parameters	**TCC**
Wavelength, nm	254
Linearity range, ng/band	100-600
Regression equation	y = 3E-05x + 0.0019
Correlation coefficient (r2)	0.991
Limit of detection, ng/band	127.57
Limit of quantification, ng/band	386.58
Specificity	Specific
Repeatability (%RSD)	1.2

Densitometric scanning enabled quantitative assessment of TCC by correlating peak areas with validated calibration data. This analytical framework provided the basis for calculating relative concentration changes in degradation samples collected at defined time intervals. The validated method enabled a comparative evaluation of TCC levels under different media conditions (nutrient broth and synthetic wastewater) and incubation times, supporting the kinetic interpretation of the biodegradation performance presented in Chapter 6 (Figure 11b).

Despite the hydrophobic and structurally recalcitrant nature of TCC, the validated HPTLC method enabled reproducible quantification under biologically complex conditions, forming the analytical foundation for evaluating bacterial degradation performance under nutrient broth and synthetic wastewater matrices.

5.5 Scanning Electron Microscopy (SEM)

Scanning Electron Microscopy (SEM) was employed as a complementary characterization technique to support the interpretation of wetland-scale biodegradation performance. While chemical transformation and pollutant removal were quantified using spectroscopic and chromatographic methods, SEM analysis was used exclusively to examine the physical structure of the wetland porous media and the extent of microbial

attachment and biofilm development. This approach enabled visual confirmation of substrate suitability and microbial colonization within the constructed wetland system, without implying direct chemical degradation mechanisms. SEM therefore served as a structural validation tool, linking wetland design, microbial inoculation strategy, and long-term system stability.

5.5.1 Morphological Analysis of Wetland Porous Media and Microbial Attachment Patterns

Scanning Electron Microscopy (SEM) was employed to qualitatively examine the surface morphology of the wetland porous media and to visualize microbial colonization and biofilm development within the constructed wetland systems. SEM analysis was used exclusively as a structural and morphological characterization tool and was not intended for quantitative assessment of microbial abundance or activity.

At the conclusion of the wetland experiment, representative cobbles were carefully retrieved from the porous media of the wetland units under aseptic handling conditions to minimize disturbance of surface-attached biomass. The collected samples were gently rinsed with distilled water to remove loosely attached debris while preserving firmly adhered microbial structures. The samples were then air-dried prior to further preparation.

To prevent charging effects and enhance surface conductivity during electron beam exposure, the dried samples were sputter-coated with a thin layer of gold. SEM analysis was performed using a Zeiss EVO MA 15 Scanning Electron Microscope (ZEISS, Jena, Germany). Imaging was conducted under high-vacuum conditions using a secondary electron (SE) detector, which enabled high-resolution visualization of surface topography and microstructural features. Micrographs were acquired at multiple magnifications to capture both the overall texture of the porous media and localized regions of microbial attachment.

The resulting SEM images provided detailed insight into the surface roughness, porosity, and microstructural integrity of the cobbles used as wetland substrate. In inoculated wetland units, SEM observations revealed microbial biofilms and filamentous structures attached to the stone surfaces, indicating successful colonization of the porous

media. These structural features support the substrate's role as a physical scaffold for microbial retention and biofilm formation within the wetland system.

SEM analysis thus served as a complementary validation technique, confirming effective microbial attachment and spatial distribution within the constructed wetland matrix. The observations provided structural context for the biodegradation performance discussed in Chapter 6, while avoiding overinterpretation of biological activity beyond the scope of morphological evidence.

Chapter 6: Results and Discussion

This chapter presents and critically interprets experimental results obtained at both laboratory (lab) and system (constructed wetland) scales to evaluate the feasibility, robustness, and scalability of engineered microbial self-cleaning processes for the removal of emerging contaminants from wastewater-impacted surface waters. In alignment with the research aims and hypotheses defined in Chapter 3, the results are structured to first establish mechanistic biodegradation performance under controlled conditions (Section 6.1), followed by validation of these processes within a biomimetic constructed wetland system that incorporates spatial structure, plant-microbe interactions, and wastewater-based growth conditions (Section 6.2).

Section 6.1 focuses on pollutant-specific degradation behaviour, microbial adaptation, and analytical confirmation of transformation processes using compound-appropriate techniques, thereby providing mechanistic insight into fungal and bacterial degradation pathways at the lab scale. Section 6.2 subsequently evaluates whether these laboratory-scale self-cleaning mechanisms persist under pilot-scale, ecologically structured conditions, emphasizing system stability, mixed-pollutant removal, microbial attachment, and integrated wetland performance. Together, these results establish a continuous experimental progression from controlled biodegradation experiments to an engineered wetland platform, enabling a rigorous assessment of microbial self-cleaning as a scalable strategy for surface water remediation.

6.1 Lab-scale Biodegradation and Microbial Adaptation

This section presents the results and discussion of lab-scale biodegradation experiments conducted to evaluate microbial adaptation, survival, and pollutant transformation under controlled laboratory conditions. These experiments were intentionally designed as simplified, reductionist systems to isolate biological effects from the hydraulic, plant-mediated, and physicochemical complexities inherent to constructed wetlands.

Lab-scale studies served three primary objectives: (i) to verify the identity and concentration of naturally extracted pollutants prior to biological treatment, (ii) to assess the capacity of selected fungal and bacterial systems to tolerate and metabolize target

compounds at elevated concentrations, and (iii) to identify system-level limitations that inform the transition from laboratory-scale experiments to an integrated wetland-based treatment approach.

Natural pollutants (caffeine and nicotine) were investigated using a fungal model system, with particular emphasis on microbial adaptation and growth behaviour in aqueous media. Anthropogenic pollutants (methylparaben and trichlorocarbanilide) were examined using a bacterial consortium under nutrient-rich and nutrient-limited conditions to evaluate degradation performance and matrix effects. The applied pollutant concentrations were intentionally higher than those typically reported in environmental matrices, reflecting a stress-testing strategy to assess microbial robustness and degradation potential under conservative conditions.

The results presented in this section are organized sequentially, beginning with quantitative verification of extracted compounds, followed by microbial adaptation responses, degradation performance of individual pollutant classes, and a comparative evaluation of system efficiency and constraints. Together, these findings establish the scientific and methodological foundation for the pilot-scale biomimetic constructed wetland experiments discussed in Section 6.2.

6.1.1 Quantification and Validation of Extracted Caffeine and Nicotine by qNMR

6.1.1.1 Extracted Caffeine: Structural Confirmation and Quantitative Determination

Before initiating biodegradation experiments, the presence, structural integrity, and purity of the extracted caffeine were rigorously verified using Fourier Transform Infrared (FT-IR) spectroscopy and Nuclear Magnetic Resonance (NMR) spectroscopy. This step was essential to ensure that subsequent biodegradation results reflected true microbial transformation rather than variability arising from extraction artifacts or impurities.

The FTIR spectra provided initial insights into the chemical composition, showcasing characteristic peaks corresponding to caffeine and confirming its presence by comparison with standard reference spectra available in the Spectral Database for

Organic Compounds (SDBS) (Figure 12). Notably, the absence of impurity peaks underscored the high purity of caffeine in the extract. With the IR spectrum of a caffeine-containing extract, the spectral library was searched to check the degree of match to the standard reference spectra available in the database.

The following characteristic signals of functional groups or other elements of the molecular backbone were detected to confirm the presence of caffeine in the obtained extract:

- **Band at 2956 cm^{-1} :** C-H stretching.
- **Bands at 1694 and 1645 cm^{-1} :** C=O stretching.
- **Bands at 1599 and 1547 cm^{-1}:** C=N double-bond stretching in the amidine moiety.
- **Band at approx. 1590 cm^{-1} :** This overlapped with the band at 1599 cm^{-1}, derived from the C=C double bond stretching conjugated to the nitrogen atom.
- **Bands at 1455 and 1403 cm^{-1} :** C-H bending of the methyl group at the nitrogen atom [167,168].

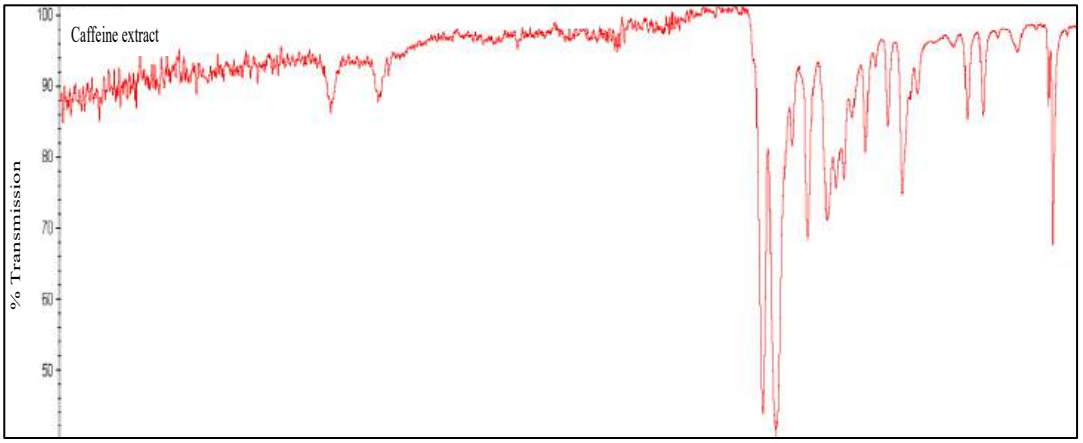

Figure 12. FT-IR spectrum of extracted caffeine [138]

The caffeine extract was analyzed by nuclear magnetic resonance (NMR) spectroscopy to confirm its structure and purity and enable quantitative determination. The ^{1}H NMR spectrum (Figure 13) was recorded at 400 MHz using deuterated chloroform ($CDCl_3$) as the solvent, with chemical shifts (δ) reported in parts per million

(ppm) relative to tetramethylsilane (TMS). The spectrum displayed a singlet at δ 7.51 ppm corresponding to one proton, and three singlets at δ 4.00, 3.59, and 3.41 ppm, each integrating for three protons. These signals are characteristics of caffeine structure.

The ^{13}C NMR spectrum (Figure 14) was recorded at 100 MHz using $CDCl_3$, with chemical shifts referenced to the central solvent peak (δ = 77.0 ppm). The spectrum exhibited signals at δ 155.59, 151.88, 148.88, 141.52, 107.77, 33.73, 29.89, and 28.07 ppm, corresponding to the carbonyl, quaternary, and methyl carbons of caffeine. These ^{1}H and ^{13}C NMR data are consistent with reported literature values and confirm the successful extraction and high purity of the caffeine sample [169–171].

Quantitative determination of caffeine was carried out using ^{1}H NMR spectroscopy (Figure 15) with dimethyldiphenylsilane as an internal standard. A precisely weighed amount of the internal standard was added to the NMR sample, and quantification was based on comparison of the integrated areas of selected caffeine signals with that of the internal standard signal appearing at approximately δ 0.55 ppm. The calculation relied on the principle that the integral area per proton of a given compound in the mixture is proportional to its molar amount.

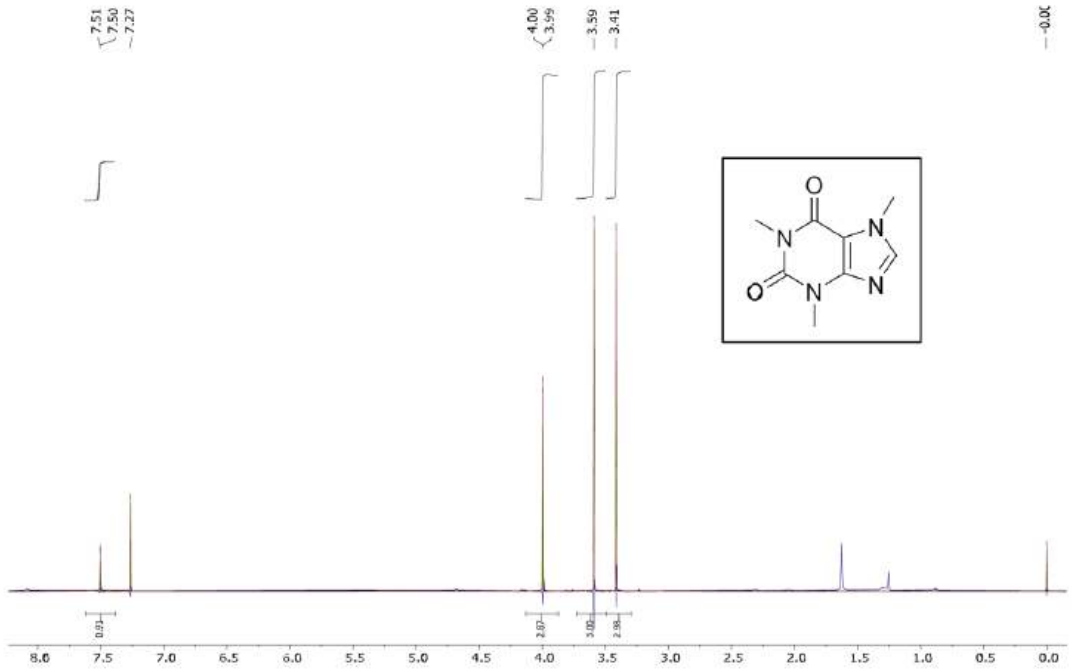

Figure 13. ^{1}H NMR spectrum of extracted caffeine recorded in $CDCl_3$ at 400 MHz [138]

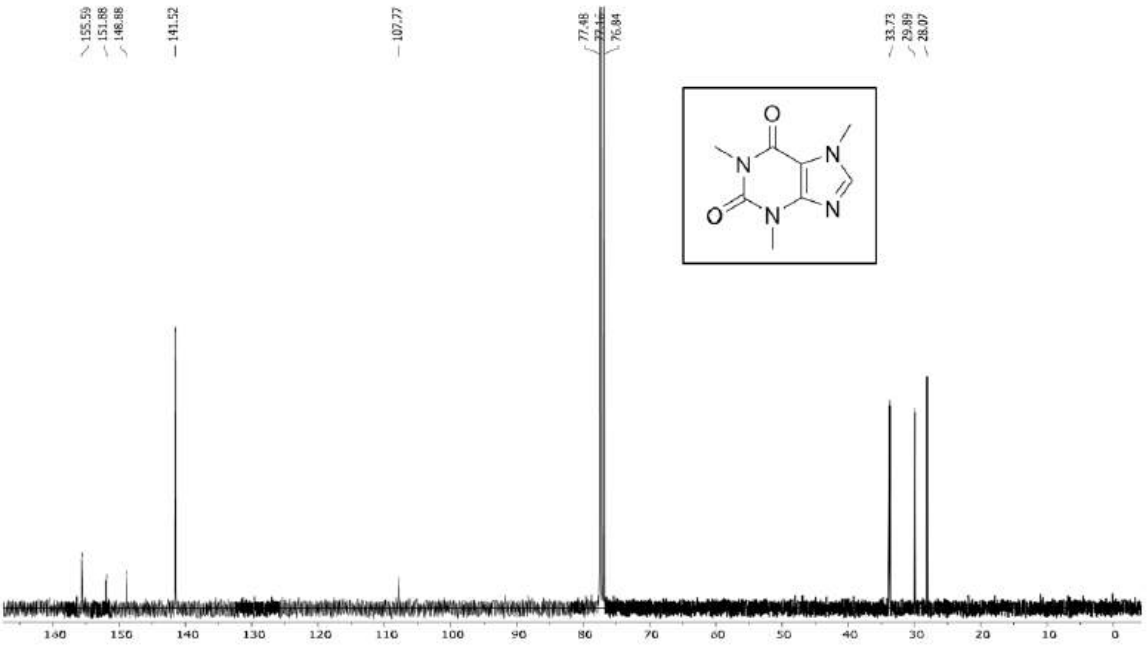

Figure 14. ^{13}C NMR spectrum of extracted caffeine recorded in $CDCl_3$ at 100 MHz [138]

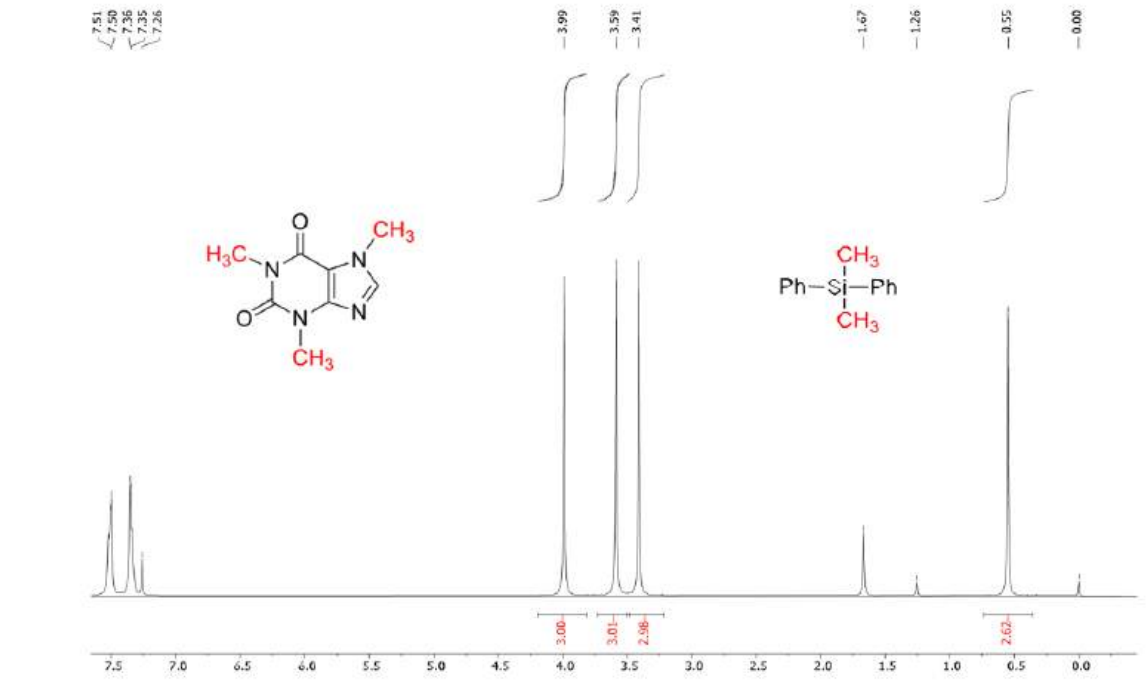

Figure 15. ^{1}H NMR spectrum of extracted caffeine with the addition of a known mass of dimethyldiphenylsilane used as an internal standard for qNMR analysis [138]

A known mass (4.6 mg) of dimethyldiphenylsilane was added to the NMR sample prior to analysis. Quantitative integration was performed on the silicon-bound methyl signal of dimethyldiphenylsilane (6 protons) and the combined N-methyl signals of caffeine (9 protons). The integral values obtained were 2.40 for the internal standard and 5.56 for caffeine.

The mass of caffeine was calculated using the standard qNMR relationship:

$$m_{\text{caf}} = \frac{I_{\text{caf}}}{I_{\text{std}}} \times \frac{H_{\text{std}}}{H_{\text{caf}}} \times \frac{MW_{\text{caf}}}{MW_{\text{std}}} \times m_{\text{std}}$$

where

I = integrated peak area,

H = number of contributing protons,

MW = molecular weight,

m = mass.

Substitution of experimental values:

$$\mathrm{m}_{\text{caf}} = \frac{5.56}{2.40} \times \frac{6}{9} \times \frac{194.19}{212.36} \times 4.6$$

Stepwise evaluation:

- Integral ratio = 5.56 / 2.40 = 2.317
- Proton correction factor = 6 / 9 = 0.667
- Molecular weight ratio = 194.19 / 212.36 = 0.914

$$m_{\text{caf}} = 2.317 \times 0.667 \times 0.914 \times 4.6 \approx 6.5 \text{ mg}$$

Stepwise evaluation yielded an integral ratio of 2.317, a proton correction factor of 0.667, and a molecular weight ratio of 0.914. Accordingly, the mass of caffeine present in the analyzed NMR sample was calculated to be approximately 6.5 mg.

The presence and purity of caffeine in the obtained extract were further confirmed by FT-IR spectroscopy. The FT-IR spectrum exhibited characteristic absorption bands

corresponding to caffeine, including C-H stretching at 2956 cm^{-1}, strong carbonyl (C=O) stretching bands at 1694 and 1645 cm^{-1}, C=N stretching vibrations at 1599 and 1547 cm^{-1}, and N-methyl C-H bending vibrations at 1455 and 1403 cm^{-1}. The absence of extraneous absorption bands indicated a high degree of purity in the extracted compound. Comparison with reference spectra from the SDBS database further confirmed the successful extraction of caffeine.

From the above results, the structure of caffeine is spectroscopically confirmed, and its mass was determined using q^1H NMR, indicating that the extract consists predominantly of caffeine. Similarly, an appropriate amount of caffeine was collected for the laboratory-scale biodegradation study. The combined application of FT-IR and $^1H/^{13}C$ NMR spectroscopy thus provided a rapid and reliable approach for confirming both the identity and relative purity of caffeine in the extract.

6.1.1.2 Extracted Nicotine: Structural Confirmation and Quantitative Determination

Similarly to caffeine, the presence, structural integrity, and purity of the extracted nicotine were rigorously verified using Fourier Transform Infrared (FT-IR) spectroscopy and Nuclear Magnetic Resonance (NMR) spectroscopy.

FT-IR spectroscopy was employed to confirm the presence of nicotine in the extracted samples. The FT-IR spectrum provided initial insight into the chemical composition of the extract and was compared with standard reference spectra available in the Spectral Database for Organic Compounds (SDBS). A high degree of spectral similarity was observed between the experimental spectrum and the reference nicotine spectrum, confirming successful extraction. The absence of additional or unexpected absorption bands further indicated the high purity of nicotine in the extract.

The following characteristic absorption bands (Figure 16) corresponding to nicotine were identified in the FT-IR spectrum:

- **Bands between 2966 and 2776 cm^{-1}:** C-H stretching vibrations of aliphatic groups.
- **Band at 1577 cm^{-1}:** aromatic C=C and C=N double-bond stretching vibrations associated with the pyridinic ring.

- **Bands at 1458, 1428, and 1363 cm⁻¹:** C-H bending vibrations of aliphatic groups.
- **Bands at 903, 806, and 716 cm⁻¹:** out-of-plane C-H bending vibrations characteristic of a monosubstituted pyridinic ring.

The presence of these characteristic bands is consistent with reported FT-IR spectra of nicotine and confirms the structural integrity of the extracted compound [172,173].

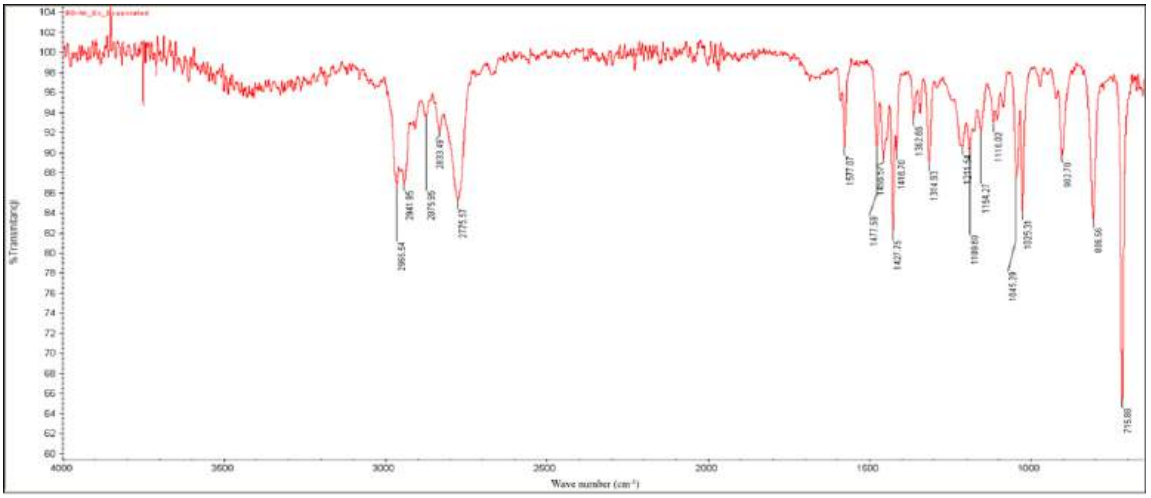

Figure 16. FT-IR spectrum of extracted nicotine [165]

The structure and purity of the nicotine extract were further examined using ^{1}H (Figure 17) and ^{13}C (Figure 18) NMR spectroscopy. The ^{1}H NMR spectrum, recorded at 400 MHz in $CDCl_3$, displayed well-resolved chemical shifts and coupling patterns characteristic of nicotine. Four distinct aromatic protons of the pyridine ring are observed in the range of 8.53 to 7.24 δ ppm. All the aliphatic protons of the pyrrolidine ring are observed as multiplets in the range from 3.10 - 3.06, 2.34 - 2.28, and 1.90 - 1.60 δ ppm. A singlet at δ 2.17 ppm integrating for three protons confirmed the presence of an N-methyl group. These spectral features closely matched those of reference nicotine in terms of chemical shift values, multiplicities, and integration patterns, confirming the identity and purity of the extracted compound [174–176]. The ^{13}C NMR spectrum, in $CDCl_3$ solvent, further supported structural confirmation by exhibiting peaks corresponding to the expected aliphatic and heterocyclic carbon environments of

nicotine. The absence of extraneous signals in both ^{1}H and ^{13}C NMR spectra indicated minimal impurity content.

Quantitative determination of nicotine was performed using ^{1}H NMR spectroscopy with dimethyldiphenylsilane ($C_{14}H_{16}Si$) as an internal standard (Figure 19). A precisely weighed mass of the internal standard was added to the nicotine extract prior to analysis. Quantification was based on comparison of the integrated area of a single, well-resolved N-methyl signal of nicotine (3 protons) with the silicon-bound methyl signal of dimethyldiphenylsilane (6 protons) appearing at approximately 0.55 ppm. This approach relies on the principle that the integral area per proton is proportional to the molar amount of the compound present in the analyzed mixture.

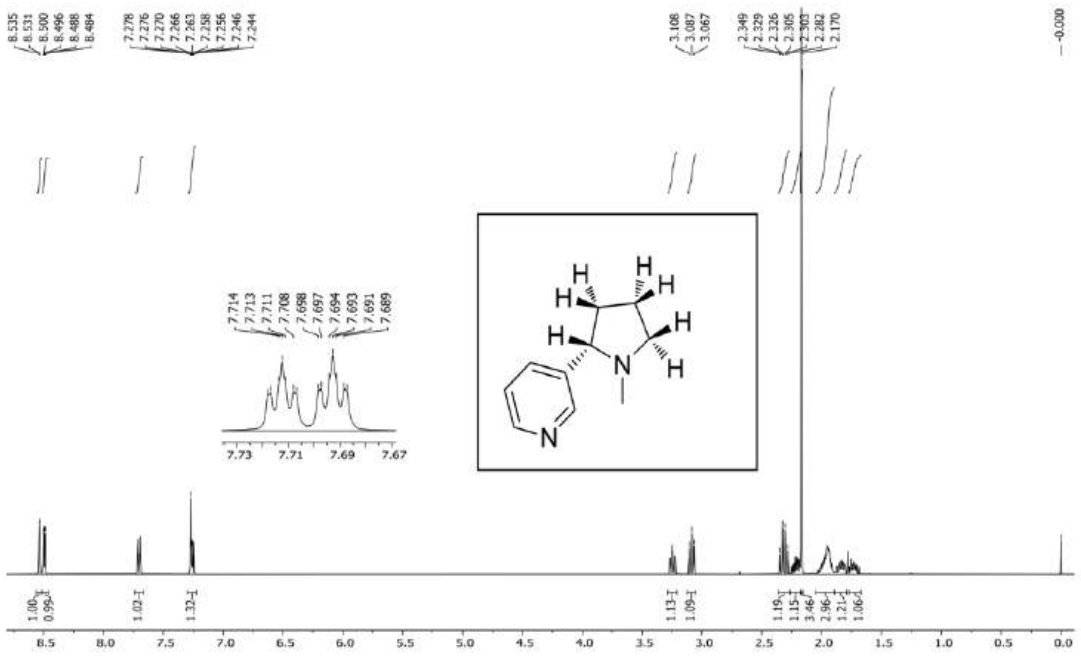

Figure 17. ^{1}H NMR spectrum of the extracted nicotine [165]

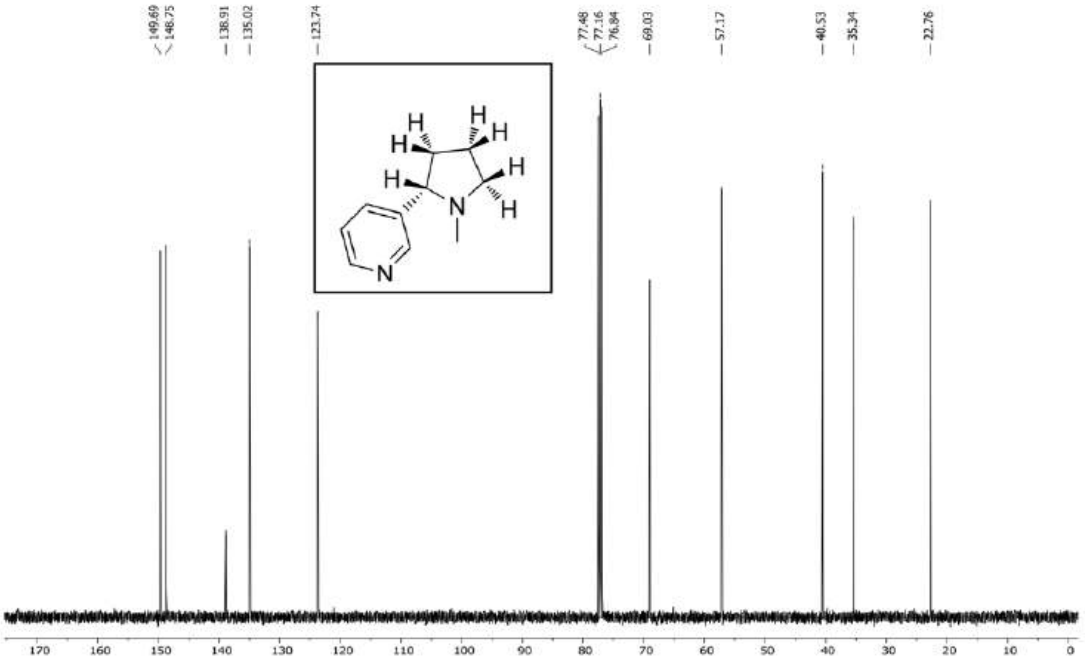

Figure 18. ^{13}C NMR spectrum of the extracted nicotine [165]

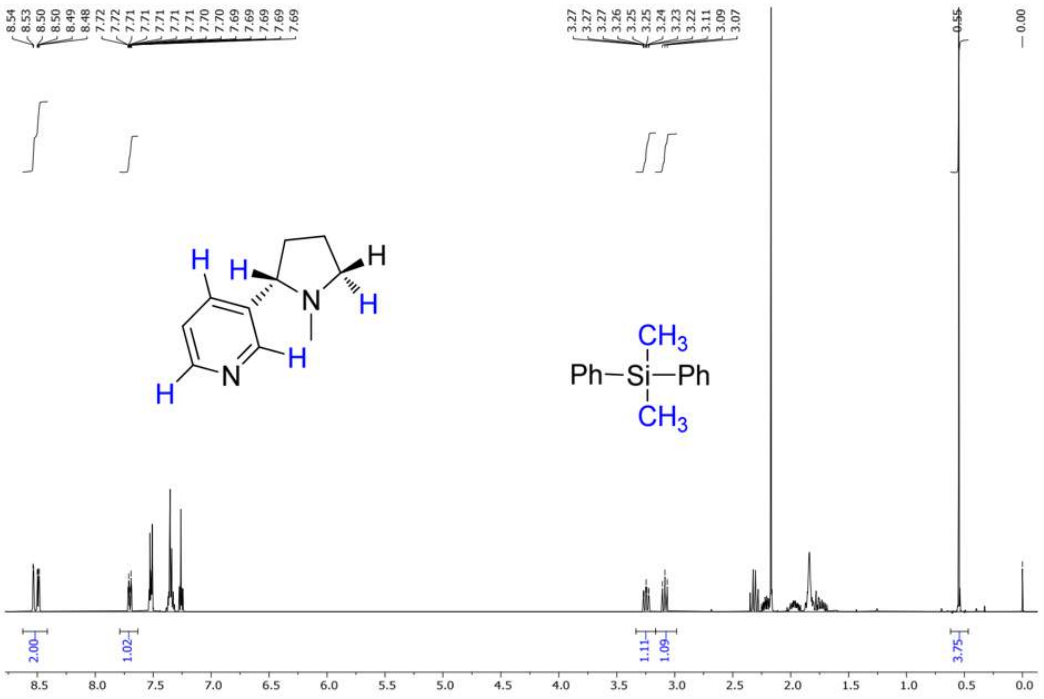

Figure 19. ^{1}H NMR spectrum of the nicotine extract with the addition of a known mass of dimethyldiphenylsilane used for qNMR analysis [165]

A known mass (5.2 mg) of dimethyldiphenylsilane was added to the NMR sample prior to analysis. Quantitative integration was performed on the silicon-bound methyl signal of dimethyldiphenylsilane (6 protons) and a single, well-resolved N-methyl signal of nicotine (3 protons). The integral values obtained were 2.26 for the internal standard and 3.59 for nicotine.

The mass of nicotine was calculated using the standard q^{1}H NMR relationship:

$$m_{\text{nic}} = \frac{I_{\text{nic}}}{I_{\text{std}}} \times \frac{H_{\text{std}}}{H_{\text{nic}}} \times \frac{MW_{\text{nic}}}{MW_{\text{std}}} \times m_{\text{std}}$$

where

I = integrated peak area,

H = number of contributing protons,

MW = molecular weight,

m = mass.

Substitution of experimental values

$$m_{\text{nic}} = \frac{3.59}{2.26} \times \frac{6}{3} \times \frac{162.23}{212.36} \times 5.2$$

Stepwise evaluation:

- Integral ratio = 3.59 / 2.26 = 1.58
- Proton correction factor = 6 / 3 = 2
- Molecular weight ratio = 162.23 / 212.36 = 0.76

$$= 1.58 \times 2 \times 0.76 \times 5.2 \approx 12.62 \text{ mg}$$

- Integral ratio = 1.589
- Proton correction factor = 2.000
- Molecular weight ratio = 0.764

Accordingly, the mass of nicotine present in the analyzed NMR sample was calculated to be approximately 12.6 mg.

Based on q^{1}H NMR analysis, approximately 12.6 mg of nicotine was determined to be present in the analyzed NMR sample. This value corresponds specifically to the purified extract aliquot analyzed by NMR. The agreement between the NMR-confirmed structure, the absence of impurity signals, and the quantitative result indicates that the analyzed extract consisted predominantly of nicotine. The use of a single, well-resolved methyl signal for quantification ensured reliable integration and minimized uncertainty arising from signal overlap.

The combined application of FT-IR and ^{1}H/^{13}C NMR spectroscopy, together with q^{1}H NMR quantification, provided a rapid and reliable approach for confirming both the identity and relative purity of nicotine in the extract.

6.1.2 Fungal Adaptation and Growth on Natural Pollutants (Caffeine and Nicotine)

6.1.2.1 Fungal Mycelial Growth and Biomass Response to Caffeine

The influence of caffeine on fungal growth dynamics and biomass accumulation was systematically evaluated to establish tolerance limits and identify conditions suitable for subsequent biodegradation experiments. The assessment considered multiple environmental variables, including caffeine concentration, temperature, pH, and growth medium, allowing integrated interpretation of fungal adaptation behaviour.

The effects of caffeine concentration and incubation temperature on the growth of *Trametes versicolor* were evaluated by measuring daily mycelial growth rates, calculated as the incremental increase in radial extension between consecutive days. This representation allowed assessment of temporal changes in growth dynamics rather than cumulative growth alone.

At 25 °C, daily growth rates under caffeine concentrations of 1 mg/10 mL and 2 mg/10 mL were comparable to those observed in the control throughout the incubation period (Figure 20). Growth rate was calculated as the difference in mycelial extension between consecutive days. The grouped bar representation highlights temporal variations in growth dynamics under different caffeine concentrations. Minor fluctuations in growth rate were observed across individual time intervals; however, no consistent or concentration-dependent reduction in growth rate was detected. The

similarity in daily growth patterns across treatments indicates that, within the tested concentration range, caffeine did not exert a measurable inhibitory effect on mycelial extension under optimal temperature conditions. These results demonstrate a clear tolerance of *T. versicolor* to caffeine at environmentally relevant concentrations and suggest the absence of acute fungistatic or fungicidal effects at 25 °C.

In contrast, incubation at 37 °C resulted in a pronounced reduction in daily mycelial growth rates across all treatments, including the control (Figure 21). Growth rates were markedly lower during the early and mid-incubation phases than at 25 °C, indicating a temperature-induced suppression of fungal growth. Although caffeine-treated cultures exhibited temporal growth-rate patterns similar to those of the control, overall growth dynamics were constrained under elevated-temperature conditions. This finding indicates that temperature, rather than caffeine concentration, was the dominant factor limiting mycelial expansion at 37 °C.

Collectively, the growth-rate analysis confirms that *T. versicolor* exhibits optimal growth dynamics at 25 °C, while exposure to 37 °C imposes thermal stress that significantly suppresses mycelial extension. The absence of a clear caffeine-dependent inhibitory trend under both temperature conditions suggests that caffeine does not adversely affect fungal growth within the tested concentration range, whereas temperature plays a critical regulatory role in governing mycelial growth dynamics.

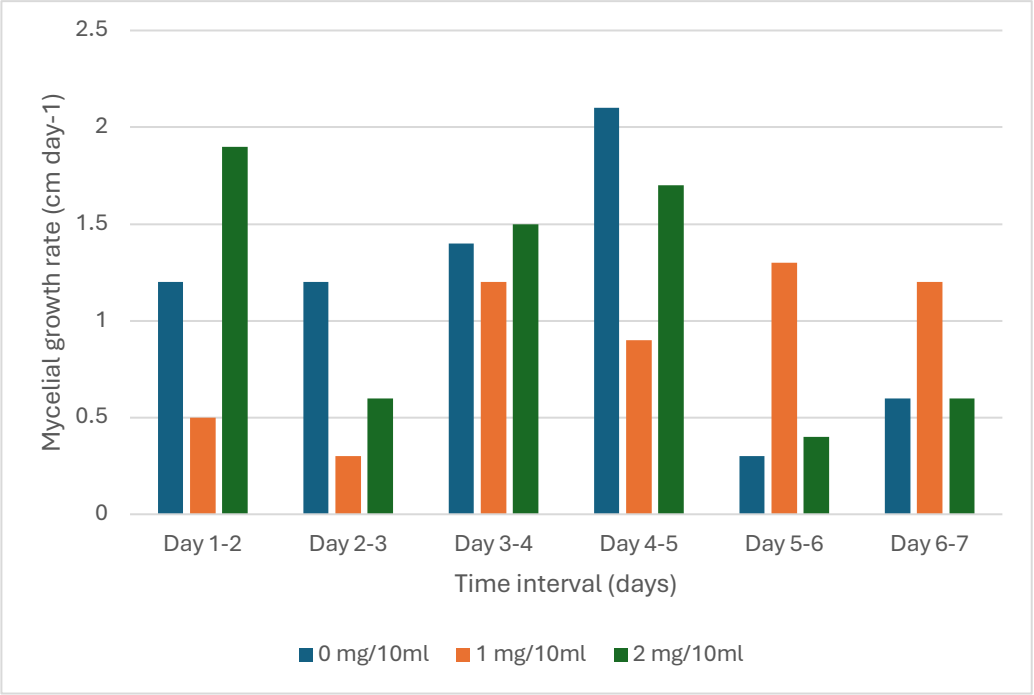

Figure 20. Daily mycelial growth rate (cm day^{-1}) of the fungal isolate exposed to different concentrations of caffeine (0, 1, and 2 mg/10 mL) at 25 °C

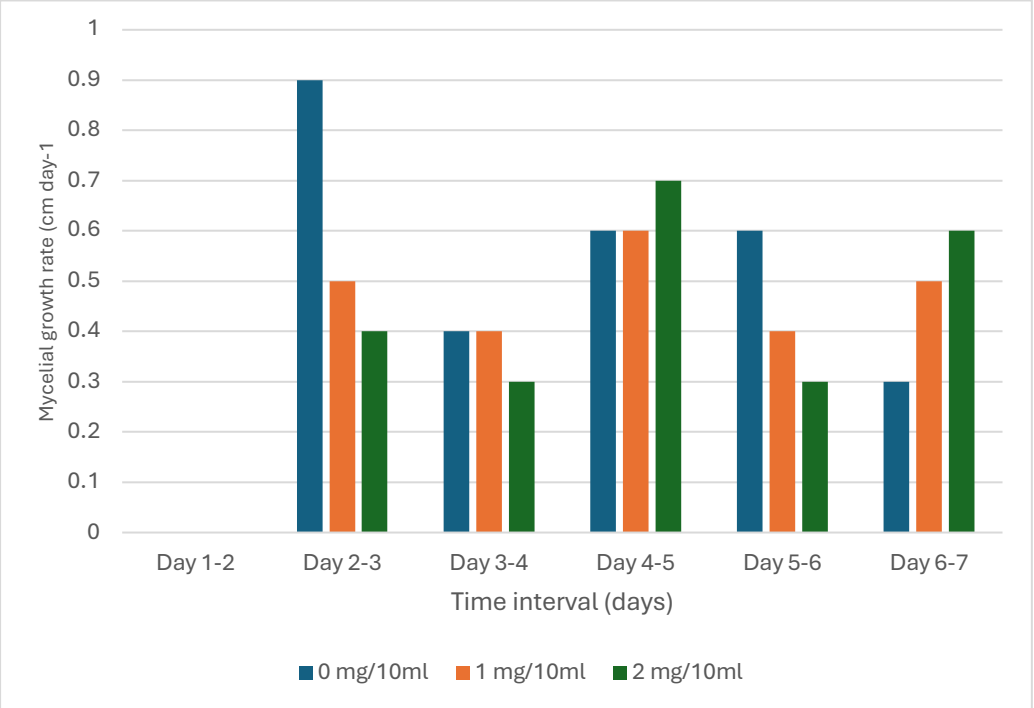

Figure 21. Daily mycelial growth rate (cm day^{-1}) of the fungal isolate exposed to different concentrations of caffeine (0, 1, and 2 mg/10 mL) at 37 °C

Quantitative biomass measurements conducted at 5-day intervals provided deeper insight into fungal adaptation beyond surface growth on solid media. The fungal inoculation methodology for lab-scale degradation experiments is described in section 4.2.4. Successful fungal growth was observed following spore inoculation. (Figure 22a) presents a graphical representation of the spore inoculation process and the development of the fungal growth matrix, while (Figure 22b) shows visible and successful fungal growth within the incubation flask.

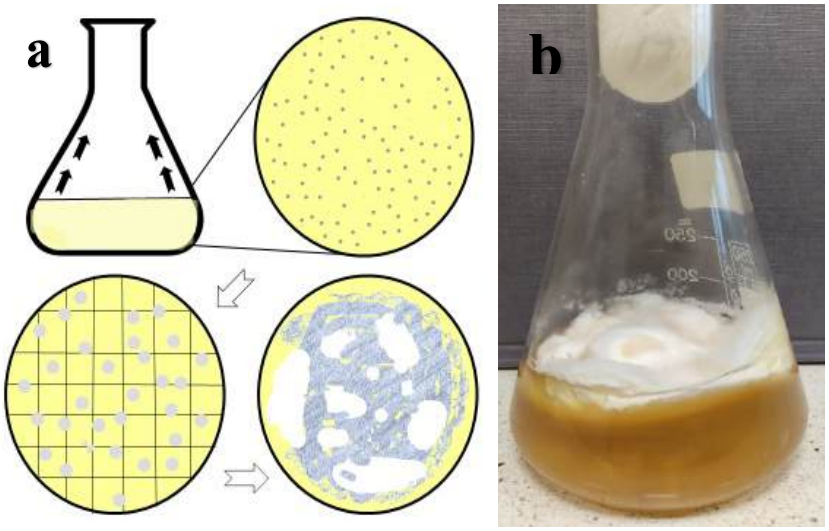

Figure 22. Fungal inoculation and growth during lab-scale degradation experiments. (a) Schematic representation of fungal spore inoculation and formation of the fungal growth matrix. (b) Visual confirmation of successful fungal growth inside the incubation lab after inoculation [138]

Biomass accumulation rates were used to assess fungal growth dynamics under caffeine exposure across varying pH, temperature, and medium conditions (Figures 23, 24, 25, 26, and 27). The rate-based representation reveals that growth kinetics, rather than final biomass alone, are strongly regulated by environmental parameters, with temperature exerting the dominant inhibitory effect, followed by pH, while medium composition modulates growth primarily under permissive temperature conditions.

Fungal growth under caffeine exposure was evaluated using biomass accumulation rates to resolve temporal growth dynamics under different environmental conditions. Across all treatments, the highest biomass accumulation rates were consistently observed

in synthetic wastewater incubated at 25 °C, indicating that this condition provided the most favourable environment for sustained fungal growth. In contrast, samples incubated at 37 °C exhibited substantially lower accumulation rates throughout the incubation period, confirming the inhibitory effect of elevated temperature on fungal metabolic activity.

Acidic conditions further constrained fungal growth dynamics. Samples maintained at pH 2.5 exhibited reduced biomass accumulation rates relative to those at pH 5.20, with the suppressive effect being most pronounced at 37 °C. Under these combined stress conditions, biomass accumulation rates approached zero during late incubation intervals, indicating limited capacity for sustained growth. This pattern reflects a synergistic inhibitory effect of low pH and elevated temperature rather than acute toxicity, as growth remained detectable during early incubation phases.

Rate-based analysis also revealed that control samples incubated at 25 °C exhibited low but persistent biomass accumulation over extended incubation periods. Visual observations indicated the presence of thin, interconnected mycelial networks rather than dense biomass formation, suggesting survival and maintenance metabolism under nutrient-limited conditions. These findings indicate that while *Trametes versicolor* can persist under suboptimal nutrient availability, active biomass accumulation requires both favourable temperature and an adequate nutrient matrix.

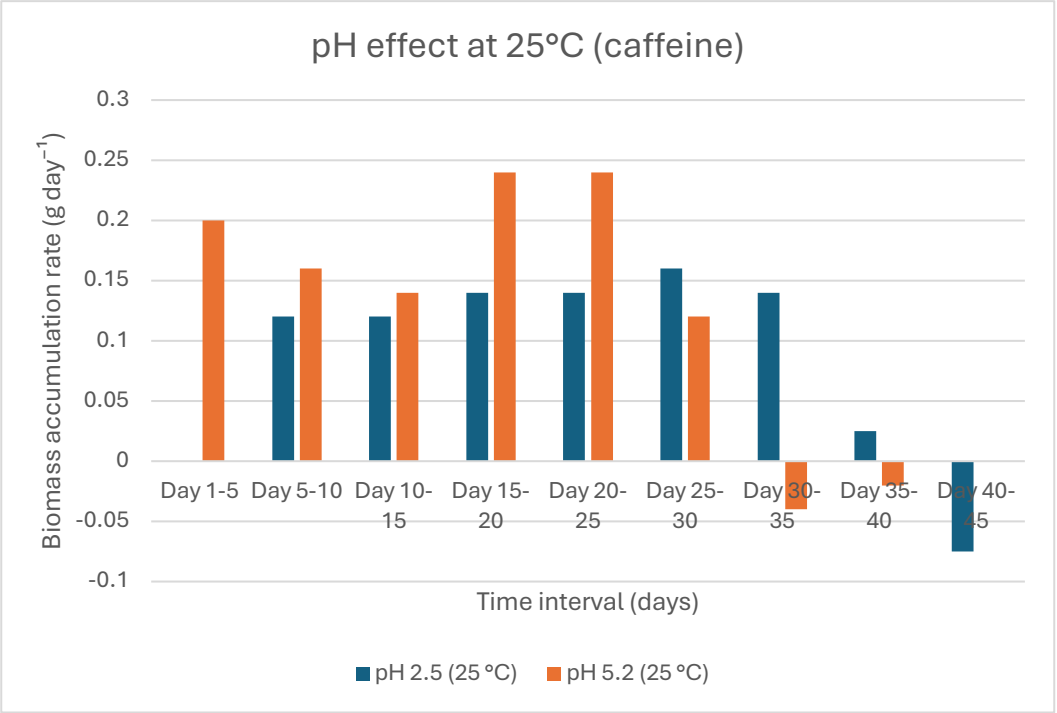

Figure 23. Biomass accumulation rate (g day^{-1}) of fungal biomass under caffeine exposure at pH 2.5 and pH 5.20 at 25 °C

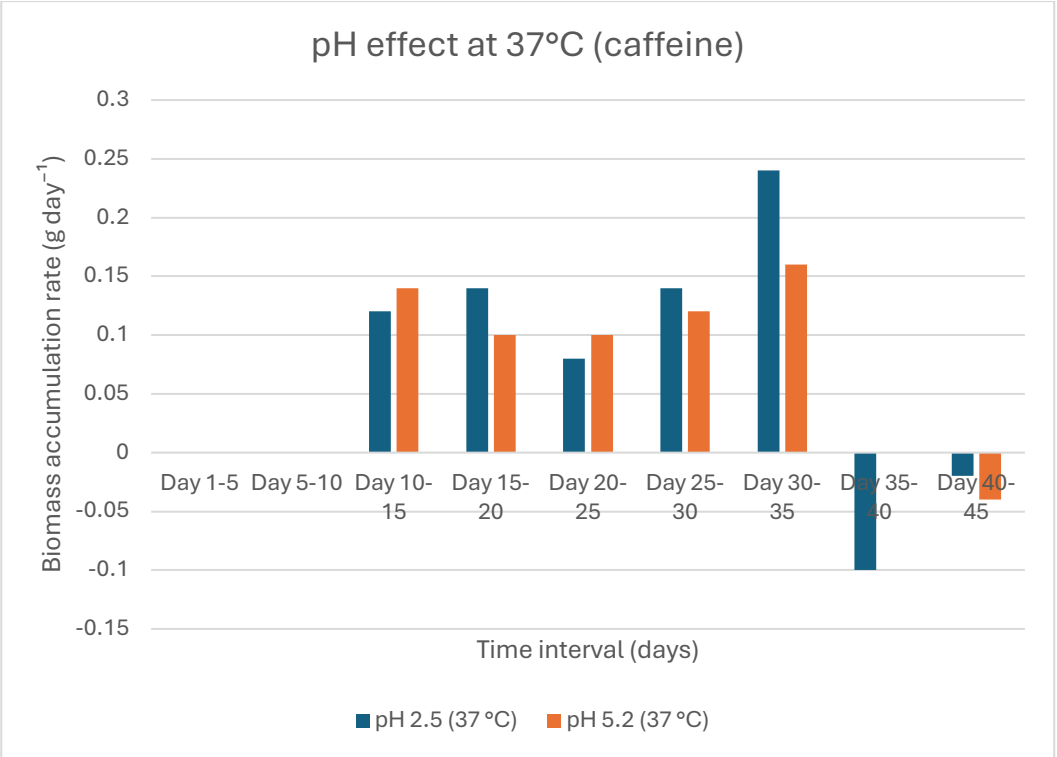

Figure 24. Biomass accumulation rate (g day^{-1}) of fungal biomass under caffeine exposure at pH 2.5 and pH 5.20 at 37 °C

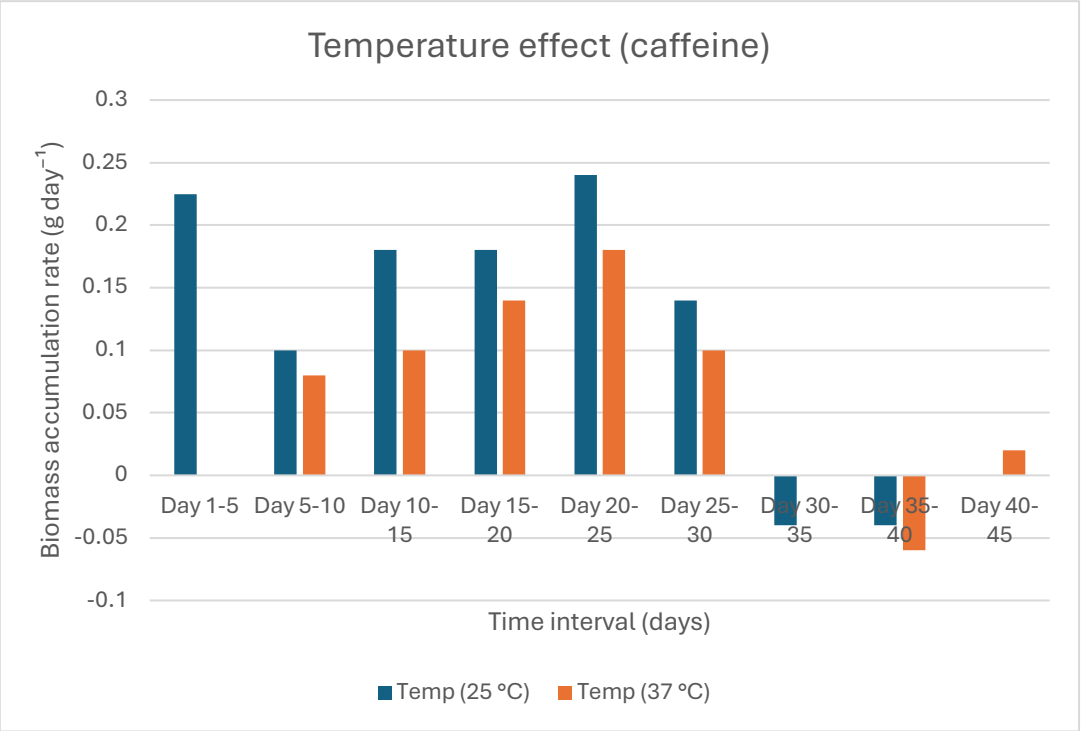

Figure 25. Effect of temperature on fungal biomass accumulation rate (g day⁻¹) under caffeine exposure at 25 °C and 37 °C

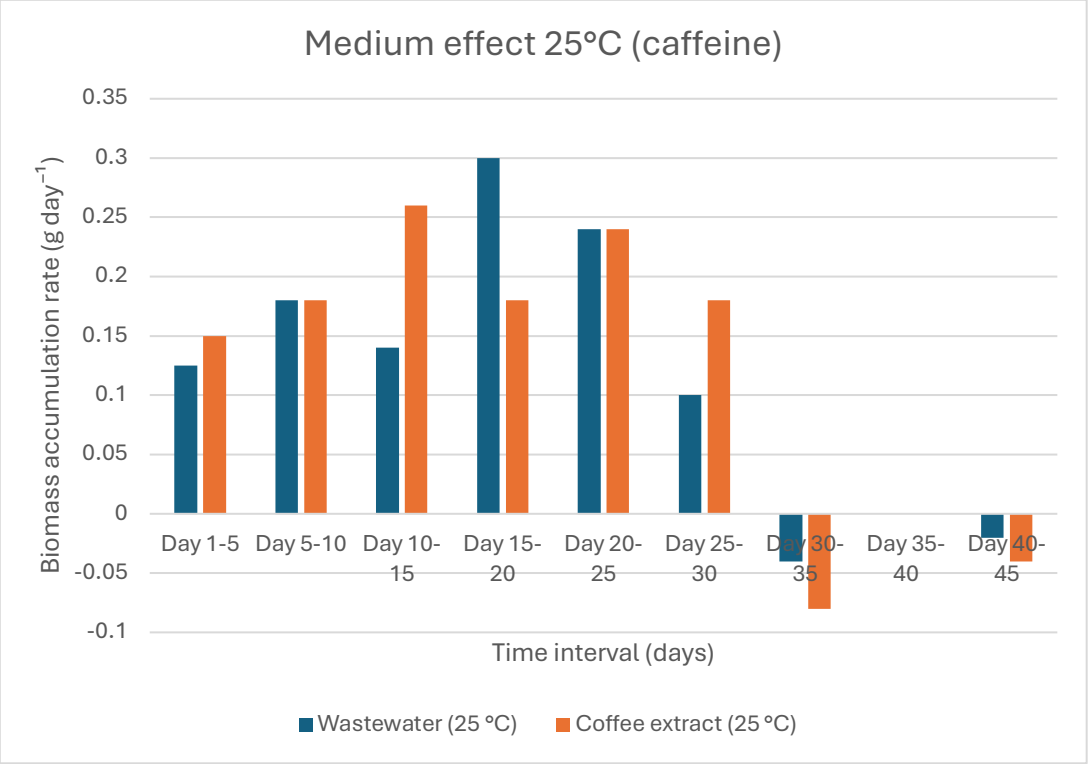

Figure 26. Biomass accumulation rate (g day⁻¹) of fungal biomass under caffeine exposure in wastewater and tobacco-based media at 25 °C

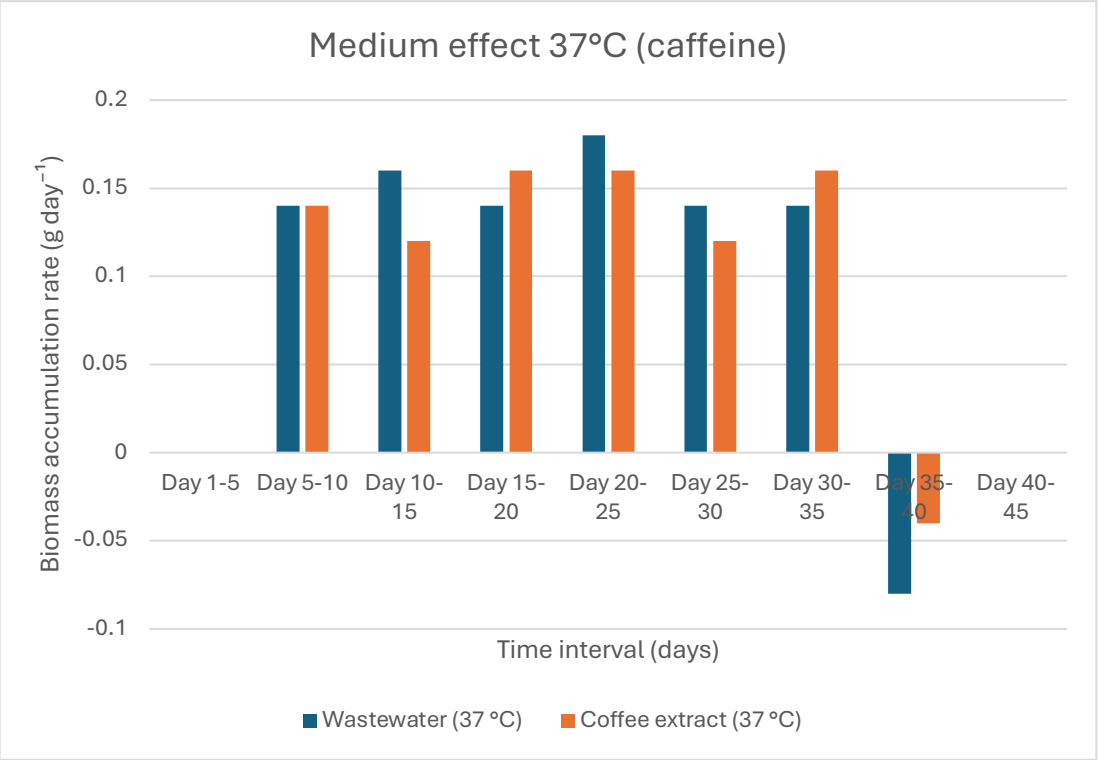

Figure 27. Biomass accumulation rate (g day^{-1}) of fungal biomass under caffeine exposure in wastewater and tobacco-based media at 37 °C

Comparison across different liquid media revealed that synthetic wastewater supported superior fungal growth relative to other matrices when incubated at 25 °C. This observation indicates that the balanced nutrient composition of synthetic wastewater provides sufficient carbon, nitrogen, and micronutrients to sustain fungal metabolism while avoiding excessive nutrient richness that could suppress adaptive enzyme expression. At 37 °C, growth in all tested media, including synthetic wastewater and coffee extract, was consistently reduced, reinforcing temperature as the primary controlling factor. These findings demonstrate that medium composition modulates fungal growth only under favourable environmental conditions. Taken together, these results demonstrate that *Trametes versicolor* exhibits substantial tolerance to caffeine at concentrations up to 2 mg/10 mL under optimal temperature conditions. Temperature emerged as the dominant factor governing both mycelial expansion and biomass accumulation, followed by pH, while caffeine concentration within the tested range exerted a comparatively minor inhibitory effect.

Based on these findings, a caffeine concentration of 1 mg/10 mL and an incubation temperature of 25 °C were selected for subsequent liquid-phase biodegradation

experiments. These conditions provided a balance between pollutant exposure and fungal viability, ensuring sustained growth, metabolic activity, and experimental reproducibility. This merged analysis confirms that fungal adaptation precedes effective biodegradation and underscores the need to evaluate growth dynamics prior to degradation studies, particularly when working with liquid media and bioactive compounds such as caffeine.

6.1.2.2 Fungal Mycelial Growth and Biomass Response to Nicotine

The resistance of *Trametes versicolor* to nicotine was systematically evaluated to understand fungal tolerance, growth dynamics, and biomass development under nicotine-induced stress. The assessment integrated solid-phase mycelial inhibition assays and liquid-phase biomass quantification to assess the combined influence of nicotine concentration, temperature, pH, and growth medium.

The influence of nicotine concentration and incubation temperature on the growth of *Trametes versicolor* was evaluated using daily mycelial growth rates, calculated as the incremental increase in radial extension between consecutive days. This approach enabled assessment of temporal growth dynamics and phase-specific responses to nicotine exposure.

At 25 °C, daily growth rates observed in the presence of nicotine at 1 mg/10 mL and 3 mg/10 mL were broadly comparable to those of the control throughout the incubation period (Figure 28). Growth rate was calculated as the difference in mycelial extension between consecutive days. The grouped bar representation highlights temperature-dependent suppression of mycelial growth under nicotine exposure. Although minor fluctuations in growth rate were observed across individual time intervals, no sustained or concentration-dependent inhibition of mycelial extension was detected. The maintenance of positive growth rates across all treatments indicates that nicotine did not exert a strong inhibitory effect on fungal growth under optimal temperature conditions. These results suggest that *T. versicolor* tolerates nicotine within the tested concentration range, and that nicotine does not act as an acute fungistatic agent at 25 °C.

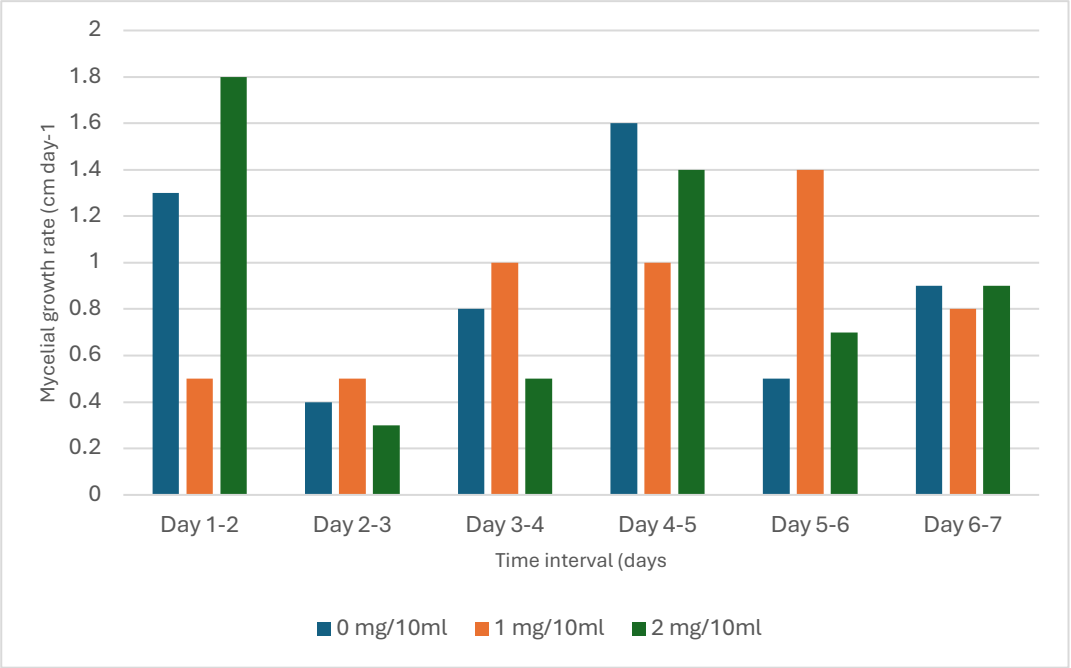

Figure 28. Daily mycelial growth rate (cm day^{-1}) of *Trametes versicolor* exposed to different concentrations of nicotine (0, 1, and 3 mg/10 mL) at 25 °C

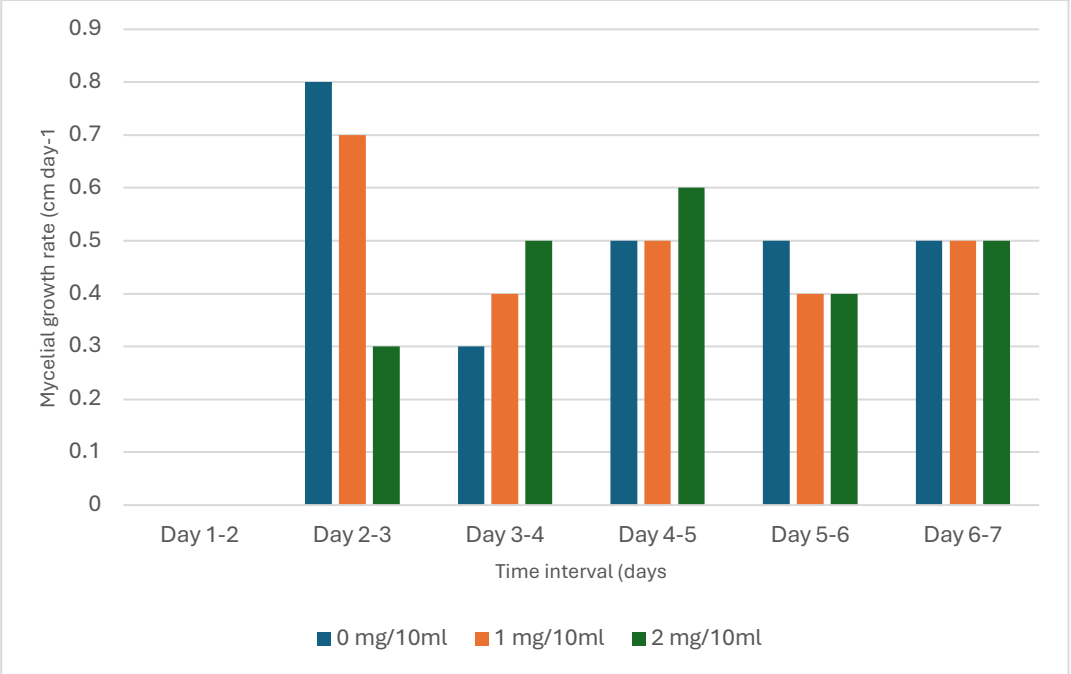

Figure 29. Daily mycelial growth rate (cm day^{-1}) of *Trametes versicolor* exposed to different concentrations of nicotine (0, 1, and 3 mg/10 mL) at 37 °C

In contrast, incubation at 37 °C resulted in a marked reduction in daily mycelial growth rates across all treatments, including the control (Figure 29). Growth rates were consistently lower during the early and mid-incubation phases than at 25 °C, reflecting temperature-induced physiological stress. While nicotine-amended cultures exhibited growth-rate patterns similar to those of the control, overall mycelial expansion was substantially constrained under elevated-temperature conditions. This indicates that temperature, rather than nicotine concentration, was the dominant factor limiting fungal growth at 37 °C.

Qualitative observations further revealed that, despite continued surface hyphal extension on PDA plates, internal mycelial penetration and biomass development were slower at higher nicotine concentrations, particularly under elevated temperature conditions. Based on the combined quantitative growth-rate analysis and qualitative growth characteristics, a nicotine concentration of 1 mg/10 mL was selected as the optimal working concentration for subsequent liquid-phase degradation experiments, as it allowed sustained fungal growth while maintaining pollutant exposure.

Fungal growth during nicotine biodegradation was evaluated using biomass accumulation rates to resolve growth dynamics under varying environmental conditions (Figures 30 to 34). Rate-based analysis revealed a clear hierarchy in fungal performance across temperature, pH, and medium conditions.

The highest biomass accumulation rates were consistently observed in synthetic wastewater at 25 °C and in samples maintained at pH 5.20 at 25 °C, indicating that moderate acidity combined with optimal temperature provides favourable conditions for fungal adaptation in nicotine-containing systems (Figure 30). Under these conditions, biomass accumulation remained positive across successive sampling intervals, reflecting sustained metabolic activity and effective growth.

Intermediate biomass accumulation rates were observed in samples incubated at 37 °C, under acidic conditions at pH 2.5 and 25 °C, and in coffee-extract medium incubated at 37 °C (Figures 31, 32, and 33). These patterns indicate that *Trametes versicolor* can tolerate nicotine under suboptimal environmental conditions; however, additional stressors such as elevated temperature or increased acidity reduce growth efficiency and limit sustained biomass accumulation.

The lowest biomass accumulation rates were consistently recorded under combined low pH (pH 2.5) and elevated temperature (37 °C), where rates approached zero or became negative during late incubation intervals (Figure 34). This pattern reflects a synergistic inhibitory effect of acidity and thermal stress, demonstrating that environmental parameters can amplify nicotine-induced growth suppression even at concentrations otherwise tolerated.

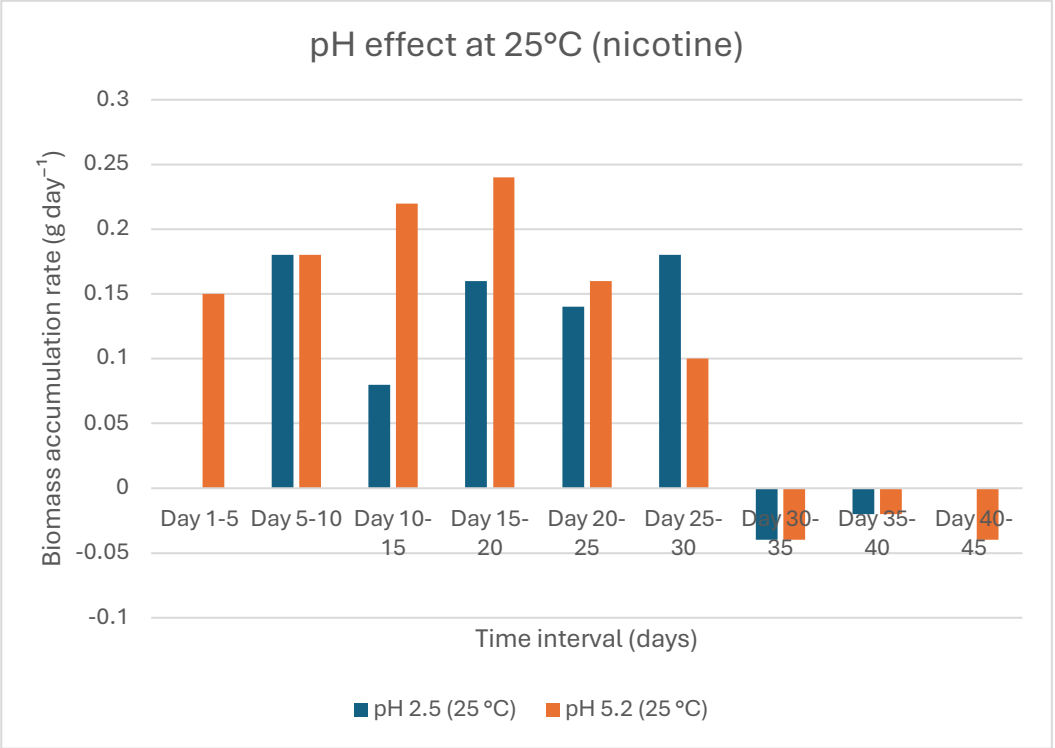

Figure 30. Biomass accumulation rate (g day^{-1}) of fungal biomass under nicotine exposure at pH 2.5 and pH 5.20 at 25 °C

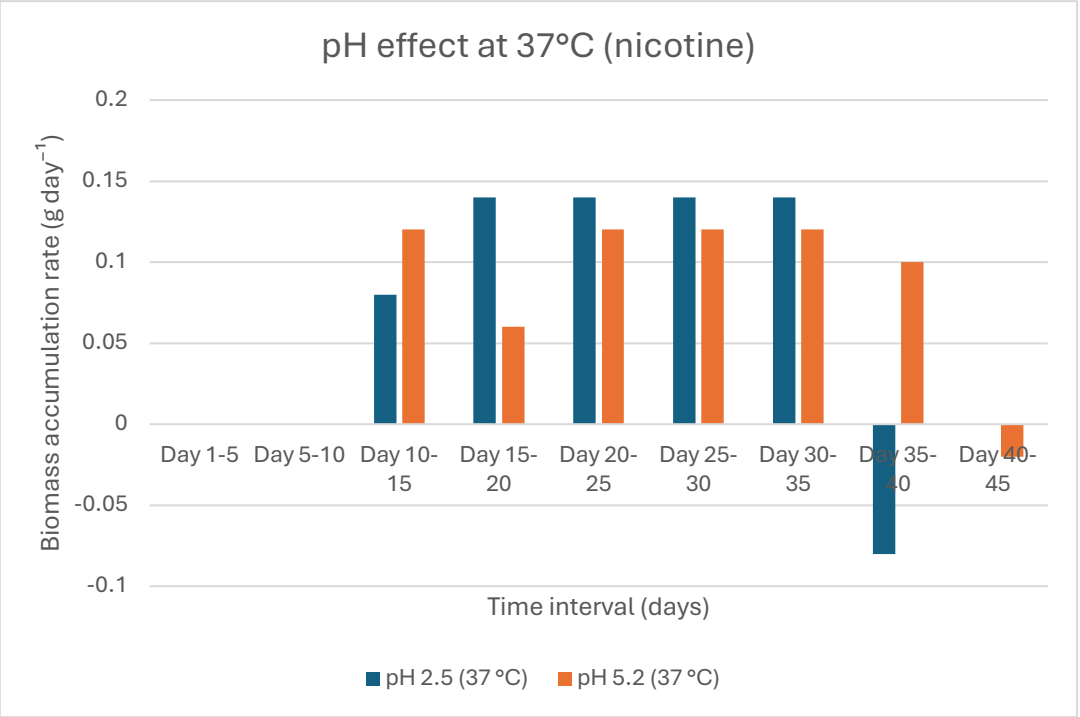

Figure 31. Biomass accumulation rate (g day^{-1}) of fungal biomass under nicotine exposure at pH 2.5 and pH 5.20 at 37 °C

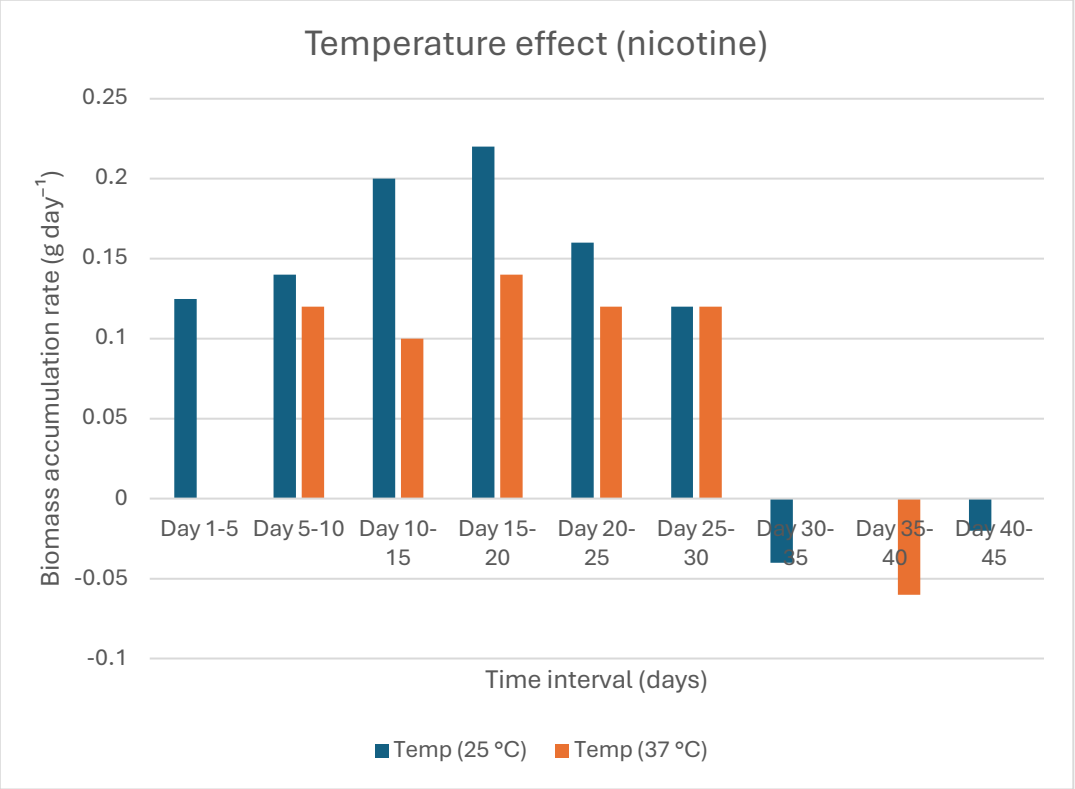

Figure 32. Effect of temperature on fungal biomass accumulation rate (g day^{-1}) under nicotine exposure at 25 °C and 37 °C

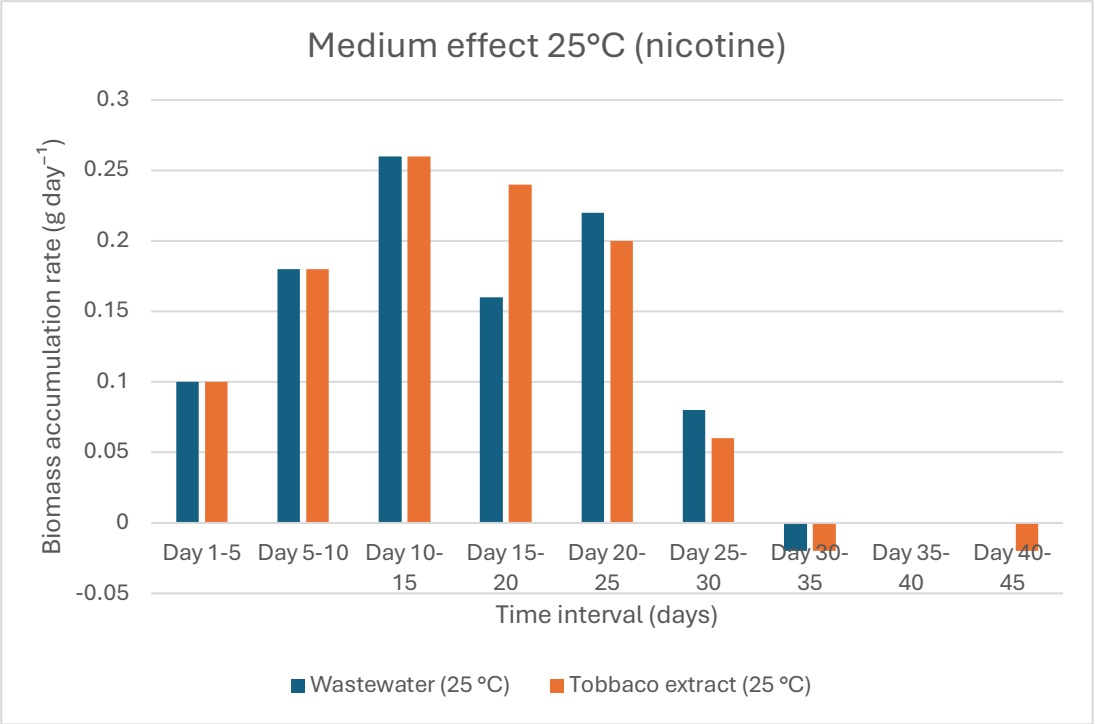

Figure 33. Effect of temperature on fungal biomass accumulation rate (g day⁻¹) under nicotine exposure at 25 °C and 37 °C

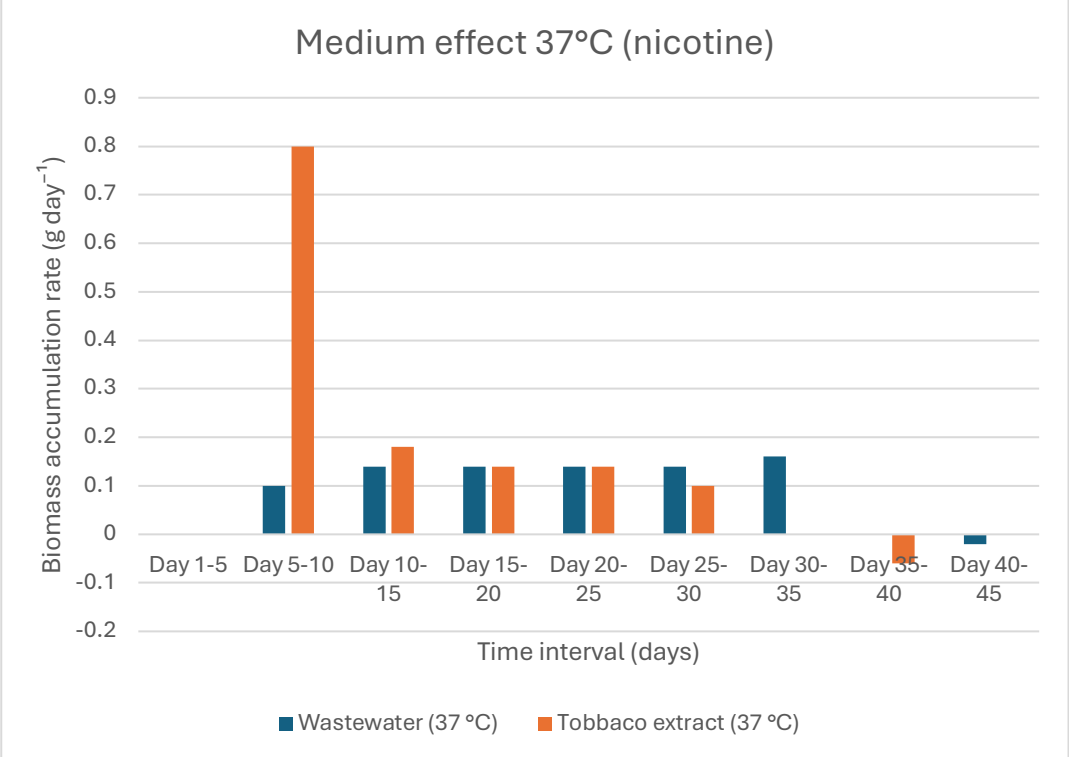

Figure 34. Biomass accumulation rate (g day⁻¹) of fungal biomass under nicotine exposure in wastewater and coffee-extract media at 37 °C

Qualitative observations of fungal development in liquid media supported the quantitative rate-based trends, with continued formation of internal mycelial networks despite reduced accumulation rates under stress conditions. The persistence of growth across most treatments indicates that nicotine exposure imposed metabolic stress rather than complete toxicity. Collectively, these results demonstrate that *Trametes versicolor* exhibits substantial tolerance to nicotine at concentrations up to 2 mg/10 mL under favourable environmental conditions. Temperature emerged as the dominant factor governing biomass accumulation dynamics, followed by pH, while nicotine concentration within the tested range exerted a secondary but measurable inhibitory effect.

Based on the combined growth-rate analysis, a nicotine concentration of 1 mg/10 mL and an incubation temperature of 25 °C were selected for subsequent liquid-phase biodegradation experiments. These conditions ensured sustained fungal viability and active biomass accumulation while minimizing confounding stress effects, thereby enabling reliable assessment of nicotine degradation performance in later experimental stages [177–181].

A direct comparison of fungal adaptation responses to caffeine and nicotine reveals both shared trends and compound-specific differences in growth inhibition patterns, biomass development, and environmental sensitivity. Because both alkaloids were evaluated at identical concentrations (1 and 2 mg/10 mL) under comparable experimental conditions, the observed differences can be attributed primarily to their intrinsic chemical properties and biological interactions rather than methodological variability.

At 25 °C, *Trametes versicolor* exhibited robust tolerance toward both caffeine and nicotine. Inhibition assays on PDA plates showed no statistically meaningful suppression of radial mycelial extension at 1 mg/10 mL for either compound, indicating that both pollutants fall within the fungal tolerance threshold under optimal temperature conditions. However, nicotine displayed a slightly stronger concentration-dependent inhibitory tendency than caffeine, particularly at 2 mg/10 mL, where delayed internal mycelial penetration was more pronounced. This suggests a higher intrinsic bioactivity of nicotine against fungal cellular processes, consistent with its documented fungicidal and neuroactive properties.

Temperature emerged as the dominant controlling factor for fungal adaptation in both systems. Incubation at 37 °C resulted in a marked reduction in mycelial growth rates for both caffeine- and nicotine-exposed samples, with comparable developmental delays. In nicotine-containing media, this delay was more pronounced, with growth trajectories lagging approximately 21 days behind those observed at 25 °C, whereas caffeine-exposed cultures exhibited slower but more continuous development. This indicates that nicotine imposes a higher combined thermal and chemical stress burden on fungal metabolism than caffeine.

Biomass quantification further highlighted differential adaptation strategies. In liquid-phase experiments, maximum biomass accumulation for both compounds occurred in synthetic wastewater at 25 °C, confirming that moderate nutrient availability combined with optimal temperature supports fungal resilience. However, nicotine-exposed cultures demonstrated greater sensitivity to acidic conditions (pH 2.5), with a sharper decline in biomass compared to caffeine-exposed samples. This suggests that nicotine toxicity is amplified under acidic stress, potentially due to increased protonation and enhanced cellular uptake.

Despite these differences, sustained mycelial growth in liquid media was observed for both compounds beyond the surface colonization stage. This indicates active metabolic engagement rather than passive survival, supporting the hypothesis that *T. versicolor* employs adaptive detoxification mechanisms such as enzymatic transformation or cellular efflux systems to cope with alkaloid stress. The persistence of internal biomass development in nicotine-containing systems, despite delayed kinetics, is particularly significant given nicotine's known antimicrobial properties.

Overall, the comparative analysis demonstrates that while *T. versicolor* can tolerate and adapt to both caffeine and nicotine at environmentally relevant concentrations, nicotine represents a higher physiological stressor, especially under elevated temperature and acidic conditions. These findings justified selecting 1 mg/10 mL as the working concentration for both pollutants in subsequent degradation experiments and underscore the importance of controlling environmental parameters when evaluating fungal biodegradation performance.

6.1.3 Fungal Biodegradation Performance of Natural Pollutants

This section evaluates the biodegradation performance of the selected fungal system toward representative natural pollutants under controlled laboratory conditions. Caffeine and nicotine were investigated as model compounds due to their frequent occurrence in surface waters and their contrasting physicochemical and biological behaviours. The following subsection first presents the degradation results for caffeine, supported by spectroscopic evidence, before addressing nicotine biodegradation under comparable experimental conditions.

6.1.3.1 Fungal Degradation: Caffeine

The biodegradation performance of caffeine by the white-rot basidiomycete *Trametes versicolor* was evaluated under controlled lab-scale conditions to determine the influence of temperature, pH, and medium composition on cumulative pollutant removal. All experiments were conducted using an initial caffeine concentration of 100 mg L^{-1} (1 mg per 10 mL), selected based on prior adaptation and growth inhibition experiments (Section 6.1.2), which confirmed sustained mycelial growth and metabolic activity at this concentration without observable inhibitory effects. Because fungal systems exhibit prolonged adaptation phases under nutrient-limited aqueous conditions, biodegradation performance was assessed using an endpoint-based quantitative approach. Samples were collected after 40 - 45 days of incubation, corresponding to stabilized biomass formation and sustained metabolic activity. This strategy was intentionally selected to evaluate cumulative removal capacity rather than short-term degradation kinetics. Endpoint quantification was performed using ^{1}H NMR spectroscopy with dimethyldiphenylsilane as an internal standard. Signal integration values were normalized to the internal standard to ensure quantitative comparability across experimental conditions. Abiotic controls were maintained under identical conditions for the full incubation period.

Prior to biodegradation experiments, the chemical identity and structural integrity of extracted caffeine were confirmed using FT-IR and $^{1}H/^{13}C$ NMR spectroscopy. Spectral features were consistent with the reference data, with no evidence of structural modification or contamination. The abiotic control system yielded a consistent caffeine integration value ($I_0 = 30.50$), which served as the quantitative baseline for all removal calculations. Importantly, no measurable change in integration was observed in abiotic

controls over the incubation period, excluding spontaneous hydrolysis, volatilization, or analytical drift as contributors to signal loss. Thus, reductions in integration values observed in inoculated systems are attributable to biologically mediated processes (Table 17).

Table 17. Endpoint quantitative ^{1}H NMR integration and caffeine removal

Condition / Medium	**Temp (°C)**	**Biomass (gram)**	**NMR Residual Integration (I_t)**	**Removal (%)**
Abiotic control	25 / 37	-	30.50 (I_0)	-
Caffeine - pH 2.5	25	3.9	2.56	91.6
Caffeine - pH 2.5	37	3.0	1.76	94.2
Caffeine - pH 5.18	25	5.0	0.68	97.8
Caffeine - pH 5.18	37	2.9	1.55	94.9
Caffeine - wastewater (pH 7.1)	25	5.0	0.71	97.7
Caffeine - wastewater (pH 7.1)	37	4.1	0.64	97.9
Coffee extract	25	5.2	Not quantifiable	-
Coffee extract	37	4.1	Not quantifiable	-

Cumulative caffeine removal (%) was calculated using normalized integration values:

$$\text{Removal (\%)} = \frac{I_0 - I_t}{I_0} \times 100$$

Where:

- I_0 = baseline integration from abiotic control (30.50)
- I_t = residual integration after incubation

Representative endpoint ^{1}H NMR spectra from synthetic wastewater and coffee extract media at 25 °C are shown in Figures 35 and 36. These spectra illustrate pronounced attenuation of characteristic caffeine methyl and aromatic proton signals relative to the internal standard. Due to the consistency of spectral attenuation patterns

across experimental conditions and the quantitative focus of this study, full spectral datasets are not presented for every system. Instead, complete numerical integration data are summarized in (Table 17). This approach prioritizes quantitative comparability over repetitive spectral presentation. In coffee extract media, extensive signal overlap from co-extracted organic constituents precluded reliable quantitative integration. However, qualitative attenuation of caffeine-associated resonances, combined with substantial formation of fungal biomass, indicates effective transformation in chemically complex matrices.

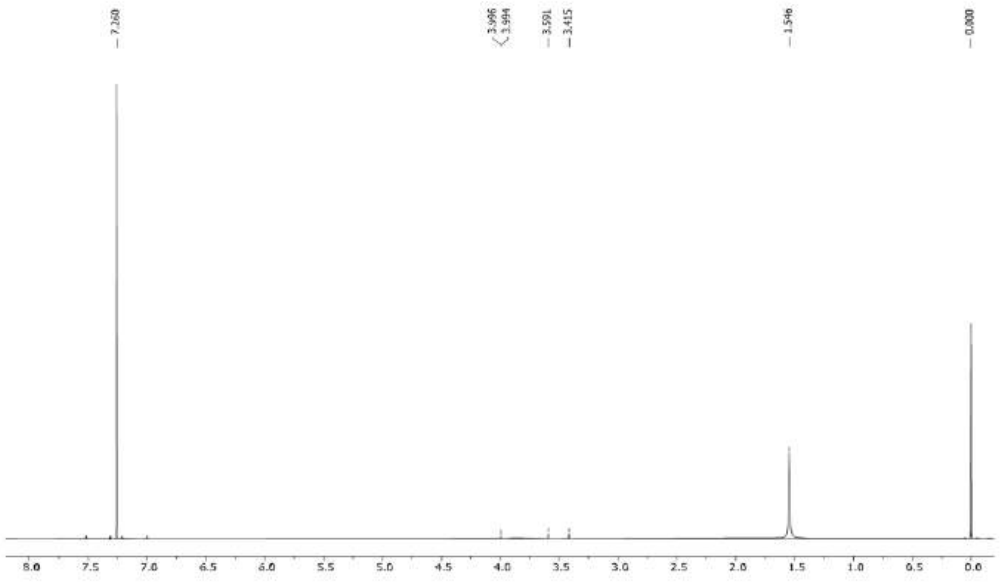

Figure 35. ^{1}H NMR spectrum of caffeine in synthetic wastewater (pH 7.1) after 45 days of fungal treatment at 25 °C, demonstrating 97.7% removal [138]

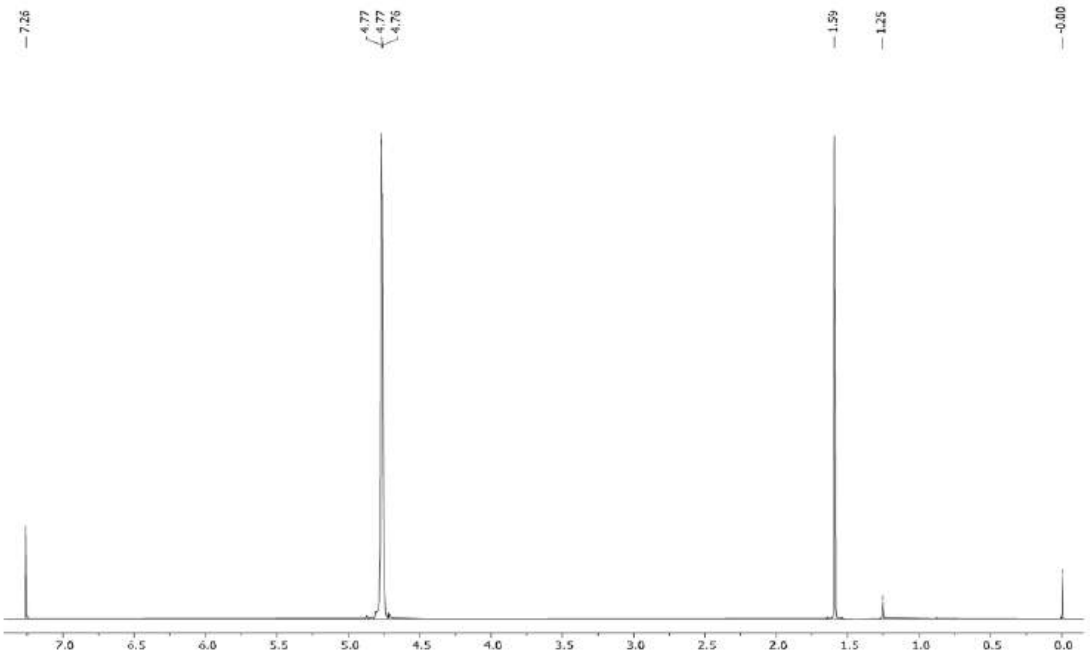

Figure 36. ^{1}H NMR spectrum of coffee extract after 45 days of fungal treatment at 25 °C, illustrating qualitative attenuation of caffeine signals [138]

Temperature exerted a measurable effect on cumulative removal performance. At 25 °C, removal efficiencies reached 97-98% in pH-adjusted aqueous systems and synthetic wastewater, coinciding with maximal biomass accumulation (approximately 5.0-5.2 g). These data indicate that 25 °C provided physiologically favourable conditions for sustained enzymatic and metabolic activity during prolonged incubation. At 37 °C, removal efficiencies in acidic media decreased to approximately 94-95%, accompanied by reduced biomass formation. This decline suggests that prolonged exposure to elevated temperature imposed metabolic stress, limiting long-term degradation capacity. The effect is consistent with the known thermal sensitivity of white-rot fungal enzymatic systems during extended cultivation. Notably, wastewater at 37 °C maintained high removal rates (~98%), suggesting that nutrient availability may partially mitigate the effects of thermal stress.

pH significantly influenced endpoint removal performance. At pH 5.18, removal reached 97-98% at 25 °C, corresponding to maximal biomass accumulation. This moderately acidic range aligns with documented optimal conditions for white-rot fungal growth and extracellular oxidative enzyme activity. At pH 2.5, removal decreased to 91-94%, despite measurable biomass formation. Strongly acidic conditions likely constrained metabolic efficiency over prolonged incubation. These findings indicate

that *T. versicolor* tolerates acidic stress but achieves optimal cumulative removal under moderately acidic conditions.

Synthetic wastewater supported high biomass accumulation and efficient caffeine removal, demonstrating that *T. versicolor* can utilize wastewater-derived nutrients without additional supplementation. In coffee extract media, biomass formation was particularly pronounced at 25 °C, indicating successful adaptation to complex organic matrices. Although quantitative NMR was not feasible, qualitative spectral attenuation and fungal growth strongly support substantial caffeine transformation under matrix-rich conditions resembling real effluents. A clear positive relationship was observed between fungal biomass accumulation and cumulative caffeine removal. Conditions that consistently supported greater biomass formation yielded higher removal efficiencies, whereas thermal or pH stress reduced both biomass and removal performance. Abiotic controls confirmed that integration values remained stable in the absence of fungal inoculation, excluding passive loss mechanisms.

This study evaluated endpoint cumulative removal under controlled lab-scale conditions using disappearance-based quantitative ^{1}H NMR analysis. The approach provides robust evidence of substantial caffeine depletion but does not resolve the formation of intermediate transformation products, degradation kinetics, or mineralization pathways. Therefore, the findings establish a validated experimental foundation for fungal-mediated caffeine removal under environmentally relevant conditions rather than a complete mechanistic description of the biodegradation pathway.

6.1.3.2 Fungal Degradation: Nicotine

The biodegradation performance of nicotine by the white-rot basidiomycete *Trametes versicolor* was investigated under controlled lab-scale conditions to evaluate cumulative pollutant removal and fungal tolerance under varying environmental parameters. All experiments were conducted using a defined nicotine concentration of 100 mg L^{-1} (1 mg per 10 mL), selected based on preliminary tolerance studies demonstrating sustained fungal viability and metabolic activity across the tested conditions. Given the toxic nature of nicotine and the extended adaptation phase commonly observed in fungal systems exposed to alkaloids, removal performance was

assessed using an endpoint-based quantitative strategy. Samples were collected after 40 days of incubation, corresponding to stabilized fungal biomass and prolonged metabolic exposure. The results, therefore, reflect cumulative removal capacity rather than degradation kinetics.

Prior to biodegradation experiments, nicotine identity and structural integrity were confirmed using FT-IR spectroscopy and $^{1}H/^{13}C$ NMR spectroscopy. The ^{1}H NMR spectrum displayed characteristic resonances corresponding to pyridine and pyrrolidine moieties, while ^{13}C NMR confirmed the expected carbon framework. Quantitative analysis was performed using ^{1}H NMR spectroscopy with dimethyldiphenylsilane as an internal standard (0.55 ppm). Baseline integration from abiotic controls yielded a stable value of 32.56 (I_0). No measurable change in nicotine integration was observed in abiotic controls over 40 days, confirming that spontaneous degradation, volatilization, or analytical drift did not contribute to signal attenuation.

Table 18. Endpoint ^{1}H NMR integration and cumulative nicotine removal

Experimental Condition / Medium	**Biomass (gram)**	**NMR Residual Integration (I_t)**	**Removal (%)**
Nicotine - Abiotic control	-	32.56 (I_0)	-
Nicotine - PDA medium, 25 °C	4.6	0.62	98.1
Nicotine - PDA medium, 37 °C	2.8	2.31	92.9
Nicotine - pH 2.5, 25 °C	3.4	2.42	92.6
Nicotine - pH 5.20, 25 °C	4.6	0.61	98.1
Nicotine - pH 2.5, 37 °C	2.8	1.58	95.1
Nicotine - pH 5.20, 37 °C	3.1	1.47	95.5
Nicotine - wastewater (pH 7.1), 25 °C	4.8	0.63	98.1
Nicotine - wastewater (pH 7.1), 37 °C	4.0	1.36	95.8
Tobacco medium, 25 °C	4.9	Not quantifiable	-
Tobacco medium, 37 °C	2.9	Not quantifiable	-

Cumulative nicotine removal (%) was calculated using:

$$\text{Removal (\%)} = \frac{I_0 - I_t}{I_0} \times 100$$

Where:

- $I_0 = 32.56$ (abiotic control baseline)
- I_t = residual nicotine integration

Representative endpoint ^{1}H NMR spectra from synthetic wastewater and tobacco media at 25 °C are shown in Figures 37 to 38. These spectra demonstrate pronounced attenuation of characteristic nicotine resonances relative to the internal standard. Because spectral attenuation patterns were consistent across quantitative systems, full spectral datasets are not shown for every condition. Instead, complete normalized integration values are summarized in (Table 18), allowing direct numerical comparison of removal performance. In tobacco-based media, extensive signal overlap from co-extracted organic constituents precluded reliable quantitative integration. However, substantial formation of fungal biomass and qualitative attenuation of nicotine-associated resonances indicate effective transformation in chemically complex matrices.

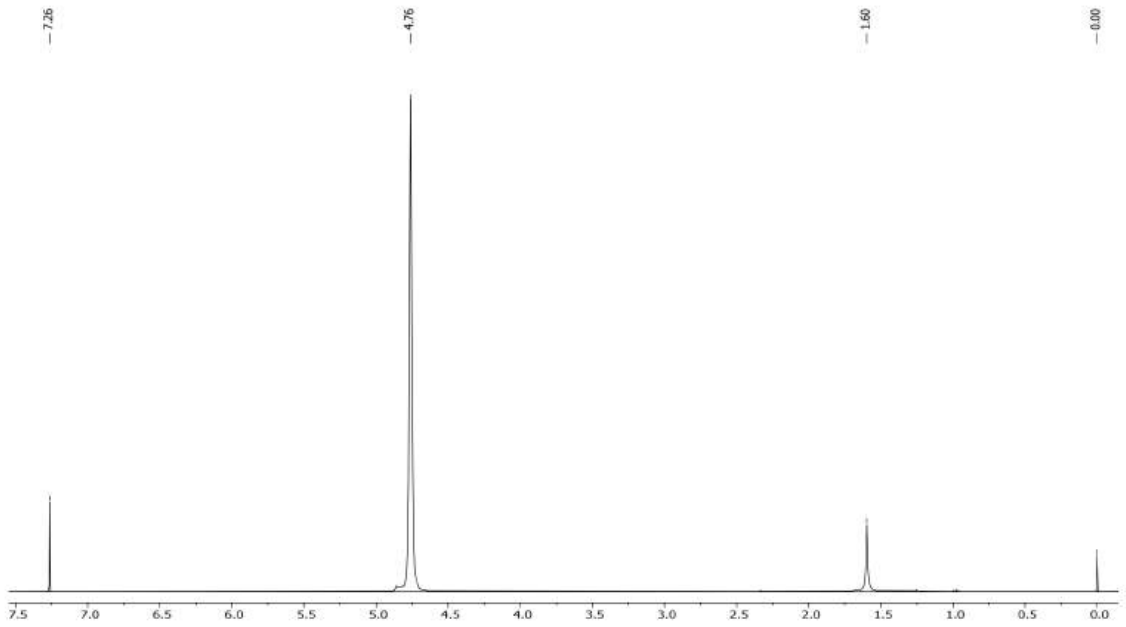

Figure 37. ^{1}H NMR spectrum of nicotine in synthetic wastewater (pH 7.1) after 45 days of fungal treatment at 25 °C, demonstrating 98.1% removal [165]

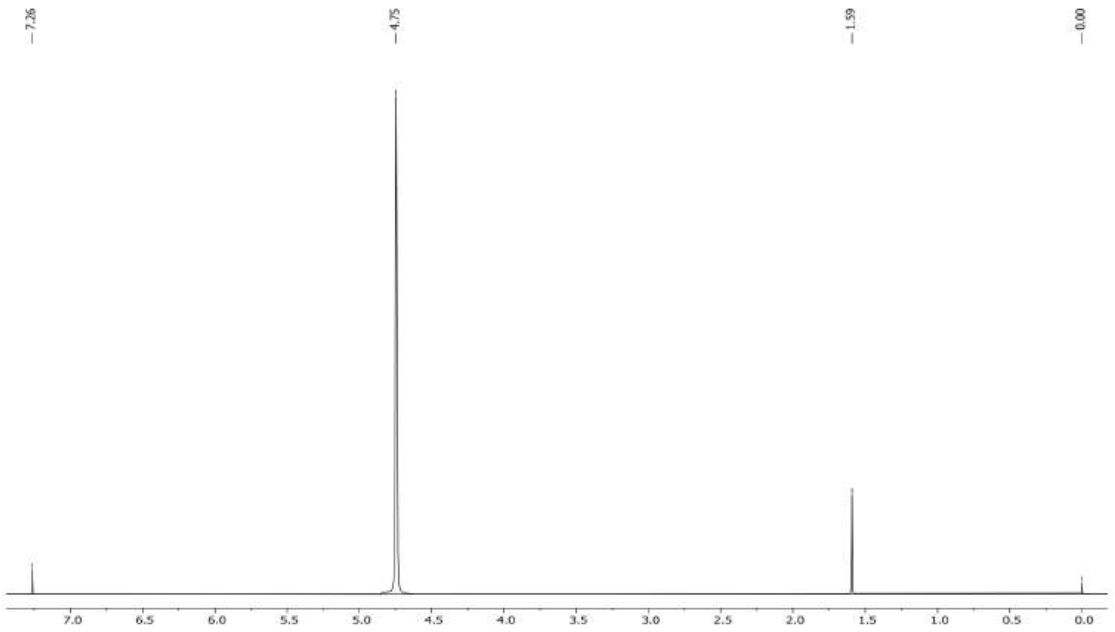

Figure 38. ^{1}H NMR spectrum of tobacco medium after 45 days of fungal treatment at 25 °C, illustrating qualitative attenuation of caffeine signals [165]

Temperature significantly influenced cumulative nicotine removal. At 25 °C, removal efficiencies were approximately 98% under standard conditions (pH 5.20) and synthetic wastewater, coinciding with maximal fungal biomass accumulation (4.6-4.8 g). These results indicate that 25 °C provided optimal physiological conditions for sustained nicotine transformation. At 37 °C, removal efficiencies decreased to 92-96%, accompanied by reduced biomass formation. This trend suggests that prolonged exposure to elevated temperature imposed metabolic constraints, limiting long-term removal capacity. The effect was particularly pronounced in acidic systems.

pH exerted a measurable influence on removal performance. At pH 5.20 and 25 °C, cumulative nicotine removal reached ~98%, corresponding to maximal biomass formation. Moderately acidic conditions are widely reported as optimal for white-rot fungal enzymatic systems. At pH 2.5, removal decreased to ~92-95%, particularly under elevated temperature. Reduced biomass accumulation under strongly acidic conditions indicates constrained metabolic performance during prolonged exposure.

Synthetic wastewater supported both substantial biomass accumulation and high cumulative removal, demonstrating fungal adaptability to nutrient-limited aqueous matrices without external supplementation. In tobacco-based media, biomass accumulation was highest at 25 °C (4.9 g), indicating successful adaptation to chemically

complex substrates. Although quantitative NMR was not feasible due to signal overlap, qualitative spectral attenuation supports substantial nicotine transformation under matrix-rich conditions representative of real waste environments.

A consistent positive correlation was observed between fungal biomass accumulation and cumulative nicotine removal. Systems exhibiting reduced biomass due to combined thermal and pH stress showed intermediate levels of nicotine attenuation. Under suboptimal conditions, partial adsorption to fungal biomass may have contributed to apparent removal; however, unchanged integration values in abiotic controls confirm that the dominant removal mechanism was biologically mediated.

Numerous studies have demonstrated the capacity of fungal species to degrade nicotine under controlled conditions. [182] reported effective nicotine degradation by white-rot fungi, including *Trametes versicolor*, attributing detoxification to ligninolytic enzyme systems. Transcriptomic studies by [181] identified oxidative enzymes, including cytochrome P450 monooxygenases and FAD-dependent oxidases, as key components of fungal nicotine metabolism. It should be noted, however, that many reported studies focus on short-term kinetics or detailed pathway elucidation under optimized laboratory conditions. In contrast, the present study evaluates cumulative nicotine removal under long-term, low-energy incubation using adapted fungal systems. While mechanistic pathways were not resolved here, the observed endpoint-removal performance is consistent with reported fungal nicotine-degradation capabilities.

In summary, endpoint analysis demonstrated that *Trametes versicolor* can achieve substantial cumulative nicotine removal under controlled lab-scale conditions, with optimal performance observed at 25 °C, pH 5.20, and in synthetic wastewater and tobacco-based media. Quantitative ^{1}H NMR analysis, supported by appropriate controls, provided reliable evidence of nicotine attenuation, while fungal biomass measurements highlighted the importance of sustained growth for effective removal. This investigation was limited to endpoint-based assessment and relied on evidence of disappearance. Degradation kinetics, intermediate metabolites, and complete transformation pathways were not evaluated. Accordingly, the results establish the feasibility of fungal-mediated nicotine removal under environmentally relevant conditions and provide a foundation for subsequent scale-up and system-level investigations.

6.1.4 Bacterial Biodegradation Performance of Anthropogenic Pollutants

This section investigates the biodegradation performance of the selected bacterial consortium toward representative anthropogenic pollutants under controlled laboratory conditions. Methylparaben (MeP) and trichlorocarbanilide (TCC) were selected for their widespread use, persistence in wastewater-impacted surface waters, and contrasting structural complexities. The following subsection first presents the biodegradation behaviour of methylparaben, serving as a model antimicrobial preservative, and then evaluates TCC degradation under comparable experimental conditions.

6.1.4.1 Bacterial Consortium Biodegradation: Methylparaben (MeP)

The biodegradation of methylparaben (MeP) by a bacterial consortium was evaluated using time-resolved High-Performance Thin-Layer Chromatography (HPTLC) analysis over a 120-hour incubation period. Degradation performance was assessed in two contrasting media, nutrient broth (NB) and synthetic wastewater (SWW), to examine the adaptability of the consortium under nutrient-rich and nutrient-limited conditions relevant to environmental engineering applications.

The degradation was performed using bacterial consortia isolated from a polluted industrial area, selected for their high tolerance characteristics. A "media replacement hypothesis" was employed to enhance bacterial degradation in Synthetic Wastewater (SWW). Consequently, the degradation performance was compared between the standard Nutrient Broth (NB) and SWW from 0 to 120 hours to evaluate the consortia's adaptability and efficiency in two distinct nutritional environments. A key aspect of our study was the successful application of HPTLC to detect and quantify Paraben degradation. The method proved invaluable due to its high sensitivity, resolution, and reproducibility, which are essential for tracking progressive degradation. The high resolution and compact spot formation facilitated by the optimized mobile phases provided reliable data, allowing for the effective monitoring of decreasing Paraben concentrations in both media types. This methodology underscores the utility of HPTLC in pollutant degradation studies, providing a clear means to track biodegradation even within complex sample matrices like synthetic wastewater.

To ensure robust kinetic interpretation and appropriate control correction, a total of fifteen discrete sample tracks were applied to the HPTLC plate for methylparaben analysis. The track layout was designed to simultaneously capture reference standards, abiotic and biotic controls, initial concentrations, and time-resolved degradation samples within a single analytical run, thereby minimizing inter-plate variability.

Track 1 contained the methylparaben reference standard and served as the basis for compound identification and densitometric quantification. Tracks 2 and 3 were loaded with sterile nutrient broth (NB) and synthetic wastewater (SWW), respectively, to establish baseline matrix behaviour and exclude interference from media constituents. Tracks 4 and 5 contained NB and SWW inoculated with the bacterial consortia but without methylparaben, functioning as biotic controls to evaluate microbial effects on the matrix in the absence of the target compound.

Initial methylparaben concentrations (100 mg/L) at 0 h were represented by Tracks 6 and 7 for NB and SWW, respectively. Time-resolved biodegradation was monitored by loading samples collected at 48, 72, 96, and 120 h in Tracks 8-15, with parallel NB and SWW samples at each time point. This layout enabled direct comparison of degradation progression in nutrient-rich and nutrient-limited media across the full incubation period. A summary of track assignments and sampling points is provided in (Table 19) (Figure 39).

Table 19. HPTLC sample tracks and experimental design for methylparaben biodegradation

Track	Vial ID	Description	Type	Time Point
1	1	Methylparaben (MeP) Standard	Reference	-
2	2	NB media (Blank)	Blank	-
3	3	SWW media (Blank)	Blank	-
4	4	Bacterial consortia + NB (Biotic Control)	Blank	-
5	5	Bacterial consortia + SWW (Biotic Control)	Blank	-
6	6	MeP + Bacterial consortia + NB	Sample	0 Hours

7	7	MeP + Bacterial consortia + SWW	Sample	0 Hours
8	8	NB_48hrs	Sample	48 Hours
9	9	SWW_48 hrs	Sample	48 Hours
10	10	NB_72 hrs	Sample	72 Hours
11	11	SWW_72 hrs	Sample	72 Hours
12	12	NB_96 hrs	Sample	96 Hours
13	13	SWW_96 hrs	Sample	96 Hours
14	14	NB_120 hrs	Sample	120 Hours
15	15	SWW_120 hrs	Sample	120 Hours

HPTLC plates were visualized under visible light and UV illumination at 254 nm and 366 nm to evaluate the suitability of each mode for monitoring methylparaben degradation. Comparative inspection of plate images demonstrated that visualization at 254 nm provided the clearest and most consistent representation of methylparaben bands, with well-defined spot boundaries and minimal background interference. In contrast, visible light imaging primarily served to confirm plate uniformity and sample application quality, while imaging at 366 nm offered limited additional contrast for methylparaben and was mainly useful for detecting potential fluorescent impurities.

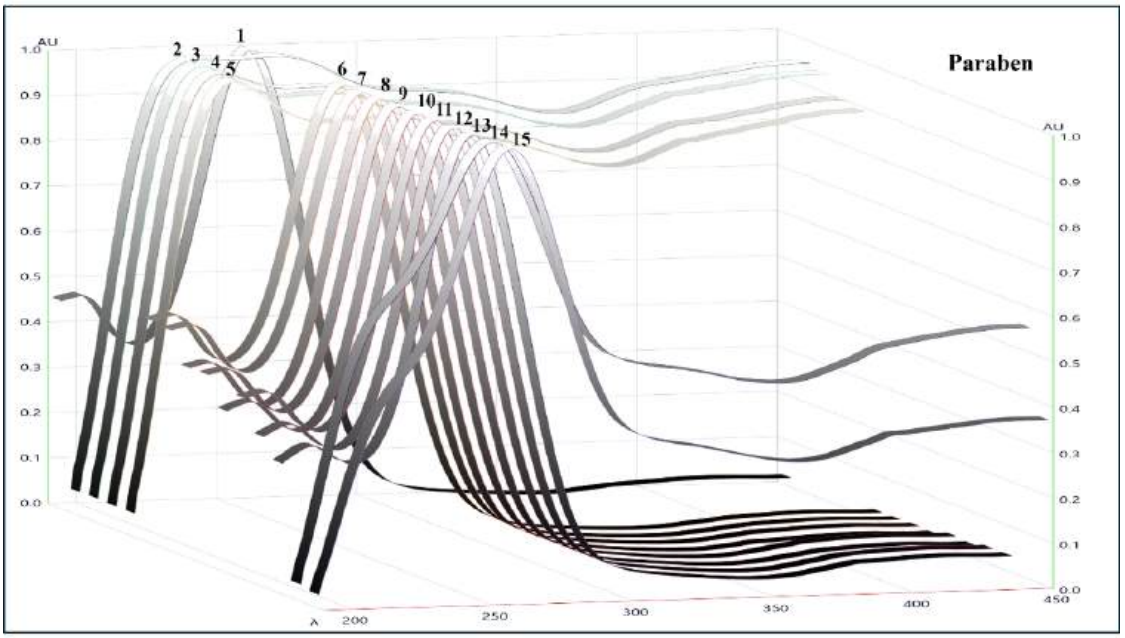

Figure 39. D Overlain UV spectra of standard Paraben and corresponding band in the sample for peak purity, AU denotes absorbance units

Based on this comparative evaluation, UV visualization at 254 nm was selected as the optimal wavelength for quantitative densitometric analysis and for presentation of all subsequent degradation images. The superior signal clarity at this wavelength ensured reliable tracking of methylparaben attenuation over time and supported consistent interpretation of degradation kinetics across different media (Table 20) (Figure 40).

HPTLC analysis enabled clear detection and quantification of MeP throughout the incubation period. Overlain UV spectra of the MeP standard and corresponding sample bands confirmed peak purity and consistent compound identification across all sampling points (Figure 41). Corresponding densitometric analysis further illustrated this trend, with a marked reduction in peak area over time (Figure 42) (Table 21).

Table 20. Imaging and detection parameters for MeP plate visualization

Parameter	**Visible Light (White)**	**UV 254 nm**	**UV 366 nm**
Exposure Time	0.035 s	0.083 s	0.638 s
Contrast	1.0	1.0	1.0
Normalized Exposure	Disabled	Disabled	Disabled
Clarify	Disabled	Disabled	Disabled
White Balance	1.00, 1.00, 1.00	1.00, 1.00, 1.00	1.00, 1.00, 1.00

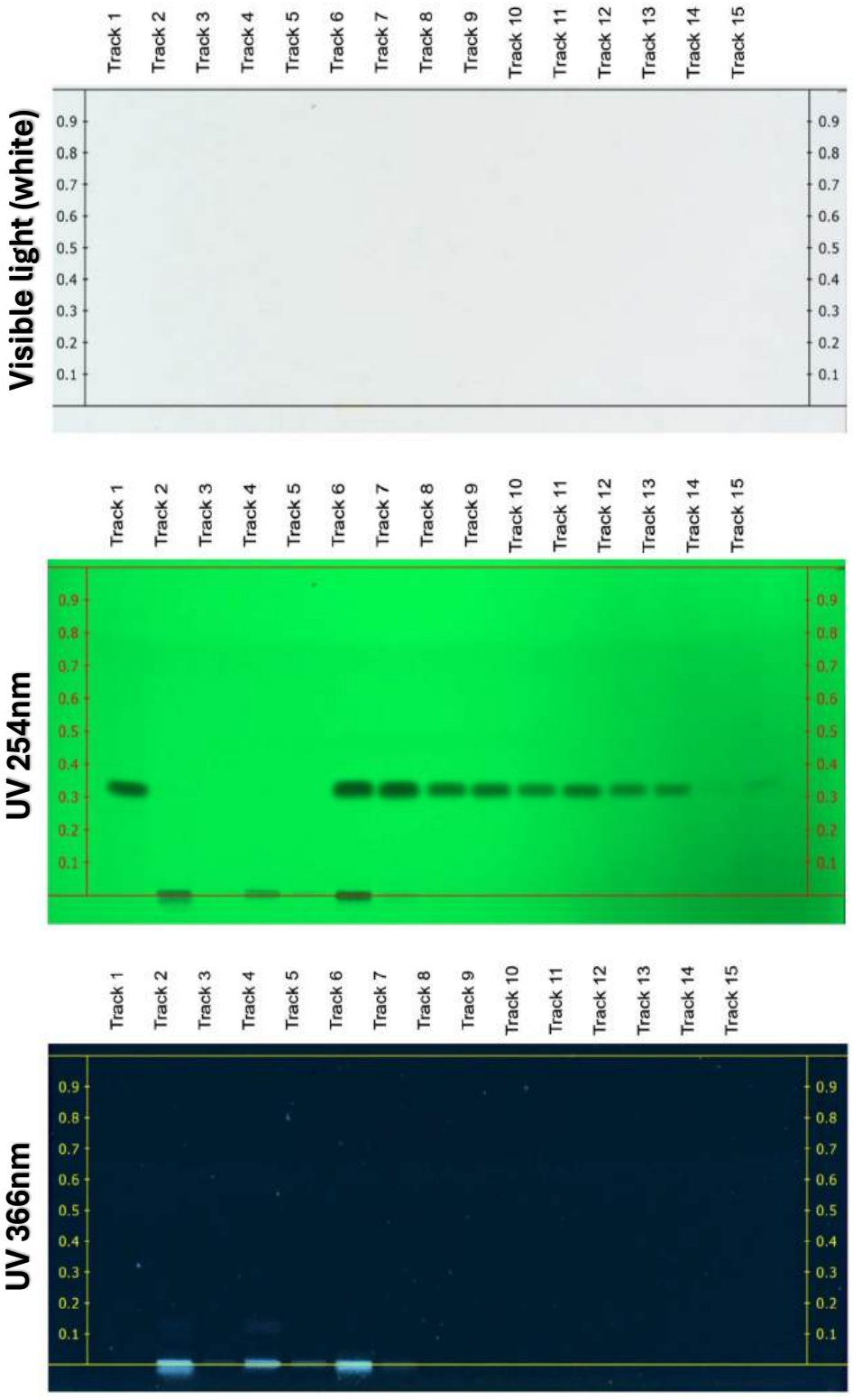

Figure 40. Comparison of HPTLC visualization modes (visible light, UV 254 nm, and UV 366 nm) for methylparaben analysis, demonstrating superior band clarity and contrast at 254 nm, which was therefore selected for all subsequent degradation profiling

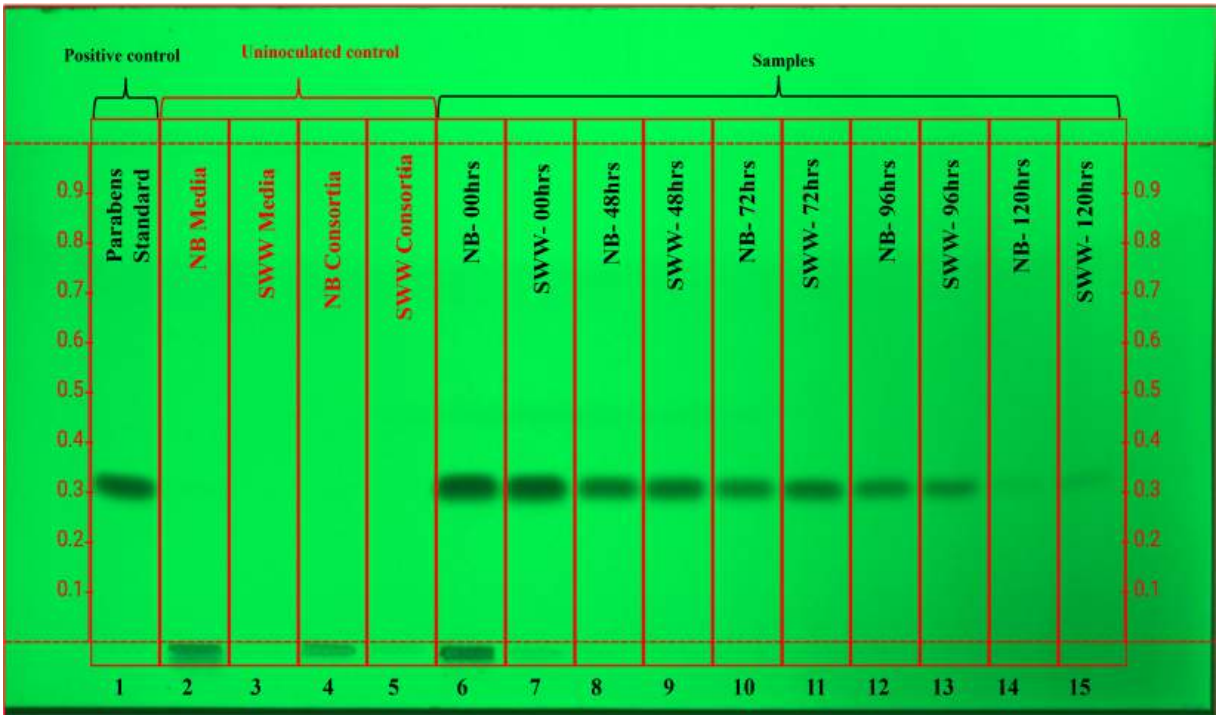

Figure 41. MeP TLC plate under 254nm UV light with standard, controls, and degradation results

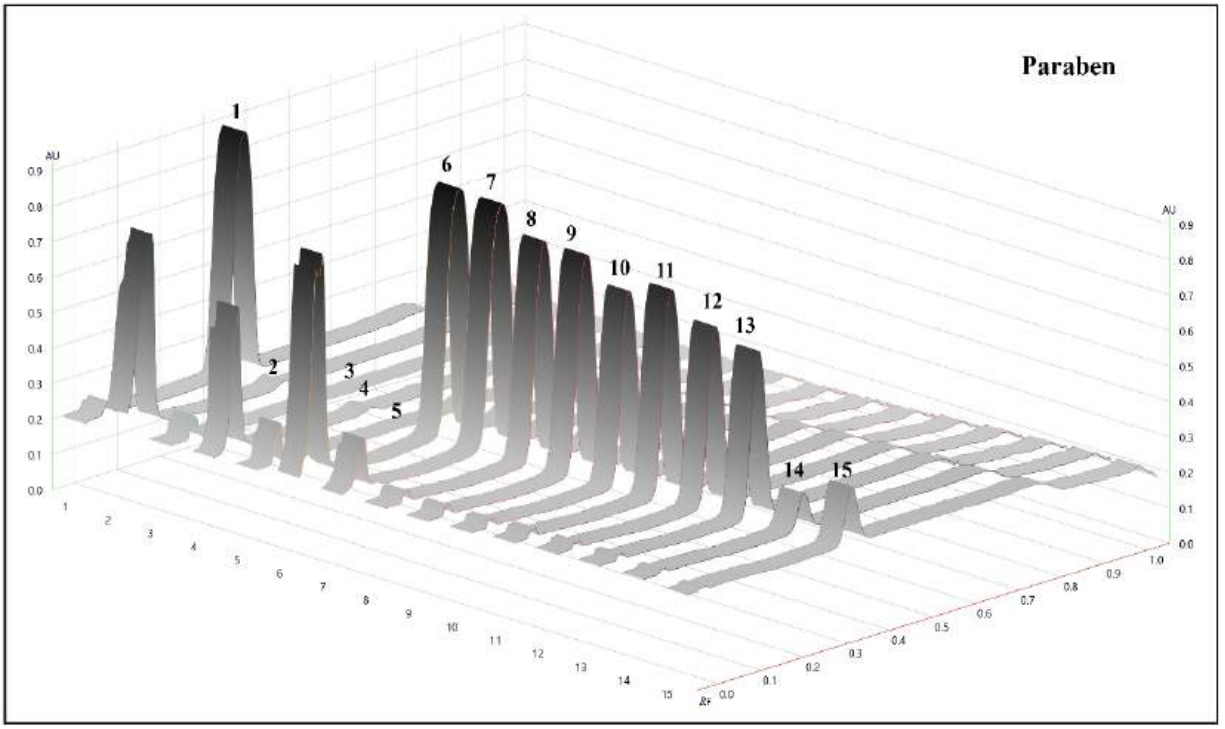

Figure 42. Densitogram of the MeP TLC plate including standard, controls, and degradation results. AU denotes absorbance units, and *R*f represents the retention factor

Table 21. Time-resolved degradation of methylparaben by bacterial consortium determined by HPTLC densitometry

Sample	Track	Densitometric area (A_t)	Degradation (%)	Remaining (%)	Equivalent amount (ng)
Methylparaben (MeP) Standard	1	0.03204	0.00	100.00	5000
NB media (Blank)	2	-	-	-	-
SWW media (Blank)	3	-	-	-	-
Bacterial consortia + NB (Biotic Control)	4	-	-	-	-
Bacterial consortia + SWW (Biotic Control)	5	-	-	-	-
MeP + Bacterial consortia + NB	6	0.03108	0.22	99.78	4989.18
MeP + Bacterial consortia + SWW	7	0.03100	0.09	99.91	4995.70
NB_48hrs	8	0.02840	11.36	88.63	4431.96
SWW_48 hrs	9	0.02873	10.33	89.66	4483.45
NB_72 hrs	10	0.02325	27.43	72.56	3628.27
SWW_72 hrs	11	0.02570	19.78	80.21	4010.61
NB_96 hrs	12	0.02067	35.48	64.51	2891.69
SWW_96 hrs	13	0.01853	42.15	57.83	2891.69
NB_120 hrs	14	0.00349	89.10	10.89	544.63
SWW_120 hrs	15	0.00549	82.86	17.13	856.74

Equivalent amount (ng) represents the mass of MeP applied per HPTLC track (5 µL aliquot) after ten-fold concentration of samples by vacuum evaporation. Degradation percentages were calculated relative to the initial applied mass and reflect degradation from the original bulk concentration of 100 mg L^{-1}.

The percentage degradation of methylparaben was calculated based on the relative reduction in densitometric peak area with respect to the methylparaben reference standard, according to the following equations:

$$\text{Degradation (\%)} = \left(\frac{A_{\text{std}} - A_t}{A_{\text{std}}}\right) \times 100$$

$$\text{Remaining (\%)} = \left(\frac{A_t}{A_{\text{std}}}\right) \times 100$$

where:

- A_{std} is the densitometric peak area of the methylparaben reference standard (Track 1),
- A_t is the densitometric peak area of the sample at time t.

Normalization to the reference standard was applied to ensure consistent comparison across different media and sampling points and to minimize variability associated with sample loading and matrix effects.

The quantitative degradation data obtained from densitometric scanning are summarized in (Table 21) Initial measurements at 0 h showed negligible MeP loss in both NB and SWW (0.22% and 0.09%, respectively), indicating minimal abiotic loss or immediate adsorption and validating the experimental controls. This confirmed that subsequent reductions in MeP concentration were attributable to biological activity rather than analytical artefacts.

At 48 h, MeP degradation reached 11.36% in NB and 10.33% in SWW. This modest early-stage removal suggests that the bacterial consortium required an acclimation period before initiating effective degradation. The slightly higher degradation observed in NB at this stage can be attributed to its nutrient-rich composition, which likely supported more rapid bacterial metabolic activation compared to the comparatively nutrient-limited SWW [183,184]. A pronounced shift in degradation behaviour was observed during the mid-incubation phase. By 72 h, MeP degradation increased to 27.43% in NB and 19.78% in SWW. Notably, by 96 h, SWW surpassed NB in degradation efficiency, achieving 42.15% removal compared to 35.48% in NB. This crossover suggests that the bacterial consortium adapted progressively to the SWW matrix,

enhancing degradation efficiency once acclimatization was achieved. Similar delayed-onset degradation patterns have been reported for methylparaben-degrading bacterial systems following initial lag phases associated with metabolic adaptation [185].

At the final incubation stage (120 h), cumulative MeP degradation reached 89.1% in NB and 82.86% in SWW. Although NB ultimately supported slightly higher total degradation, the strong performance in SWW demonstrates that effective MeP removal can be achieved under nutrient-limited conditions representative of real wastewater environments. The degradation trends observed across both media are further illustrated by concentration-normalized plots (C/C_0 versus time), comparative degradation profiles between NB and SWW, and semi-logarithmic $\ln(C/C_0)$ plots, which collectively confirm sustained biological removal over time (Figure 43 a, b, and c).

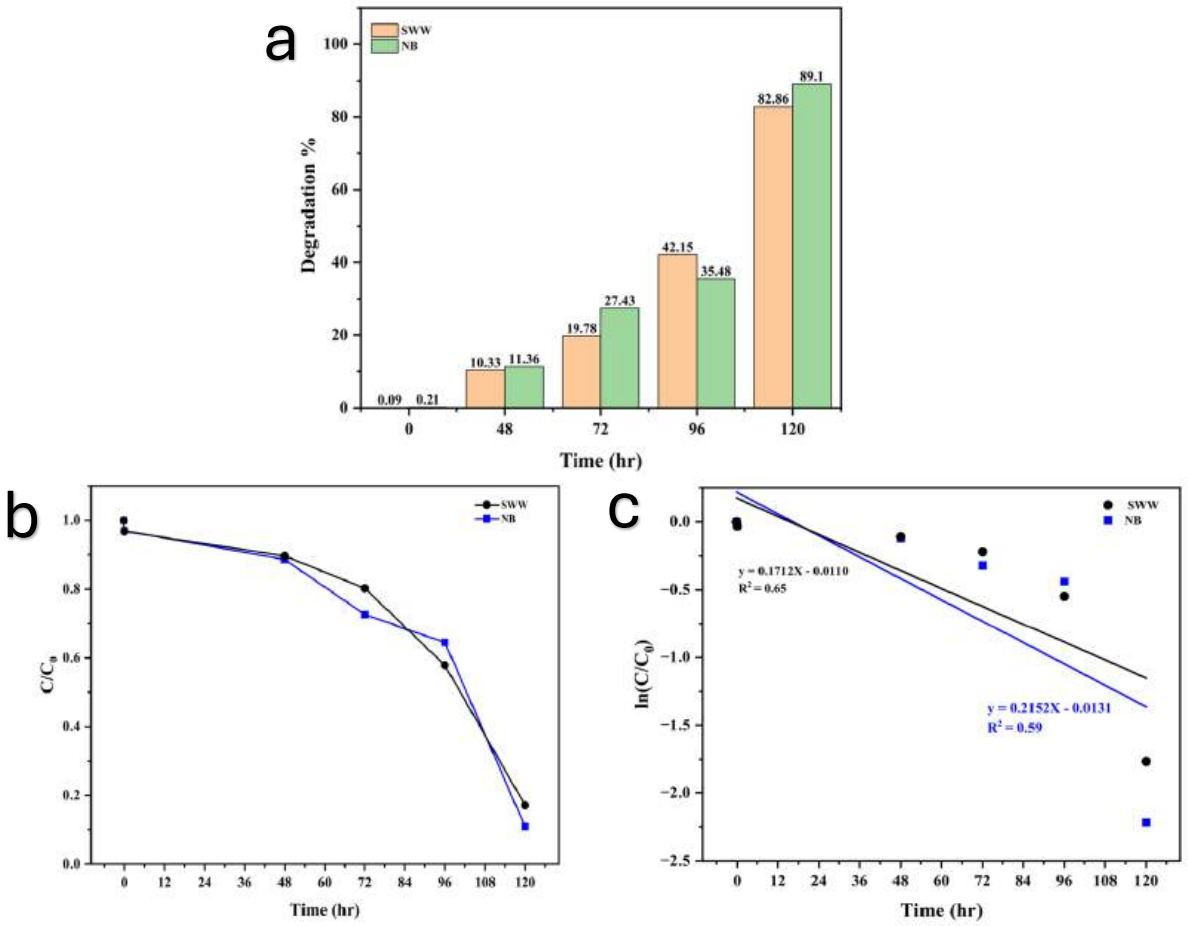

Figure 43. (a) C/C_0 vs. time plots for paraben degradation, (b) Degradation comparison between SWW and NB, (c) $\ln(C/C_0)$ vs. time plots for paraben degradation

The time-resolved degradation profiles reveal distinct kinetic behaviours in NB and SWW. In NB, the degradation trend reflects rapid initial microbial activation followed by steady MeP removal, consistent with the availability of readily metabolizable nutrients supporting bacterial growth. In contrast, SWW exhibited a longer adaptation phase but showed accelerated degradation during the mid-incubation period, highlighting the consortium's capacity to adjust its metabolic activity in response to complex, nutrient-limited matrices.

These findings underscore the importance of medium composition in governing bacterial degradation kinetics. While nutrient-rich conditions promote early-stage activity, nutrient-limited systems such as SWW may favour more efficient pollutant-targeted metabolism following adaptation. This behaviour is particularly relevant for wastewater treatment applications, where rapid intermediate pollutant reduction may be more critical than marginal differences in final removal efficiency. The bacterial consortium used in this study, comprising *Alcaligenes* sp. strain PK5 (GenBank: PV544804.1) and *Rhodococcus* sp. strain PK06 (GenBank: PV549916.1), demonstrated substantial MeP degradation capacity under both tested conditions. Degradation efficiencies of 82.86-89.1% at an initial concentration of 100 mg L^{-1} indicate robust performance under pollutant loads significantly higher than typical environmental concentrations [84]. This elevated concentration was deliberately selected to assess system resilience under stressed conditions relevant to industrial and pharmaceutical wastewater scenarios.

The high degradation efficiency observed in SWW highlights the practical relevance of the consortium for engineered treatment systems. Compared to single-strain bacterial systems, which often achieve only 50-60% degradation at lower pollutant concentrations [111,186], the consortium’s performance underscores the advantage of synergistic metabolic interactions. *Alcaligenes* species are known for their hydrolytic versatility, while *Rhodococcus* species exhibit strong capabilities for degrading complex aromatic compounds, together enabling enhanced pollutant transformation. The use of HPTLC proved particularly advantageous for monitoring MeP degradation kinetics, offering a cost-effective and reliable alternative to more resource-intensive analytical techniques [151,187]. Given the insolubility constraints of trichlorocarbanilide in NMR solvents, the successful application of HPTLC in this study further establishes its suitability for tracking biodegradation of structurally diverse anthropogenic pollutants.

In summary, time-resolved HPTLC analysis demonstrated effective bacterial degradation of methylparaben in both nutrient broth and synthetic wastewater. While nutrient broth supported slightly higher cumulative removal, synthetic wastewater exhibited strong intermediate-stage degradation following microbial adaptation, underscoring its relevance for real-world wastewater treatment applications. The results confirm that bacterial consortia can sustain high degradation performance under nutrient-limited conditions, supporting their potential integration into engineered self-cleaning systems. This study focused on concentration-based degradation kinetics and did not identify transformation products or intermediate metabolites. As degradation byproducts may exhibit residual toxicity, future work should include comprehensive byproduct characterization and pilot-scale validation to fully assess environmental safety and scalability [188–190].

6.1.4.2 Bacterial Consortium Biodegradation: Trichlorocarbanilide (TCC)

The biodegradation of trichlorocarbanilide (TCC) by a bacterial consortium was evaluated using time-resolved High-Performance Thin-Layer Chromatography (HPTLC) over a 120-hour incubation period. As with methylparaben, degradation performance was assessed in nutrient broth (NB) and synthetic wastewater (SWW) to compare removal efficiency under nutrient-rich and nutrient-limited conditions representative of engineered wastewater systems.

HPTLC analysis enabled the reliable detection and quantification of TCC throughout the experiment. The optimized mobile phase (toluene: ethyl acetate, 8:2 v/v) produced sharp, well-resolved TCC bands with a consistent Rf value of approximately 0.33, allowing accurate densitometric evaluation of residual TCC concentrations. Overlain UV spectra of the TCC standard and corresponding sample bands confirmed peak purity and compound identity throughout the incubation period (Figure 44) (Table 22).

Table 22. HPTLC sample tracks and experimental design for TCC

Track	Vial ID	Description	Type	Time Point
1	1	Trichlorocarbanilide (TCC) Standard	Reference	-
2	2	NB Media (Blank)	Blank	-

3	3	SWW media (Blank)	Blank	-
4	4	Bacterial consortia + NB (Biotic Control)	Blank	-
5	5	Bacterial consortia + SWW (Biotic Control)	Blank	-
6	6	TCC + Bacterial consortia + NB	Sample	0 Hours
7	7	TCC + Bacterial consortia + SWW	Sample	0 Hours
8	8	NB_48	Sample	48 Hours
9	9	WW_48	Sample	48 Hours
10	10	NB_72	Sample	72 Hours
11	11	WW_72	Sample	72 Hours
12	12	NB_96	Sample	96 Hours
13	13	WW_96	Sample	96 Hours
14	14	NB_120	Sample	120 Hours
15	15	WW_120	Sample	120 Hours

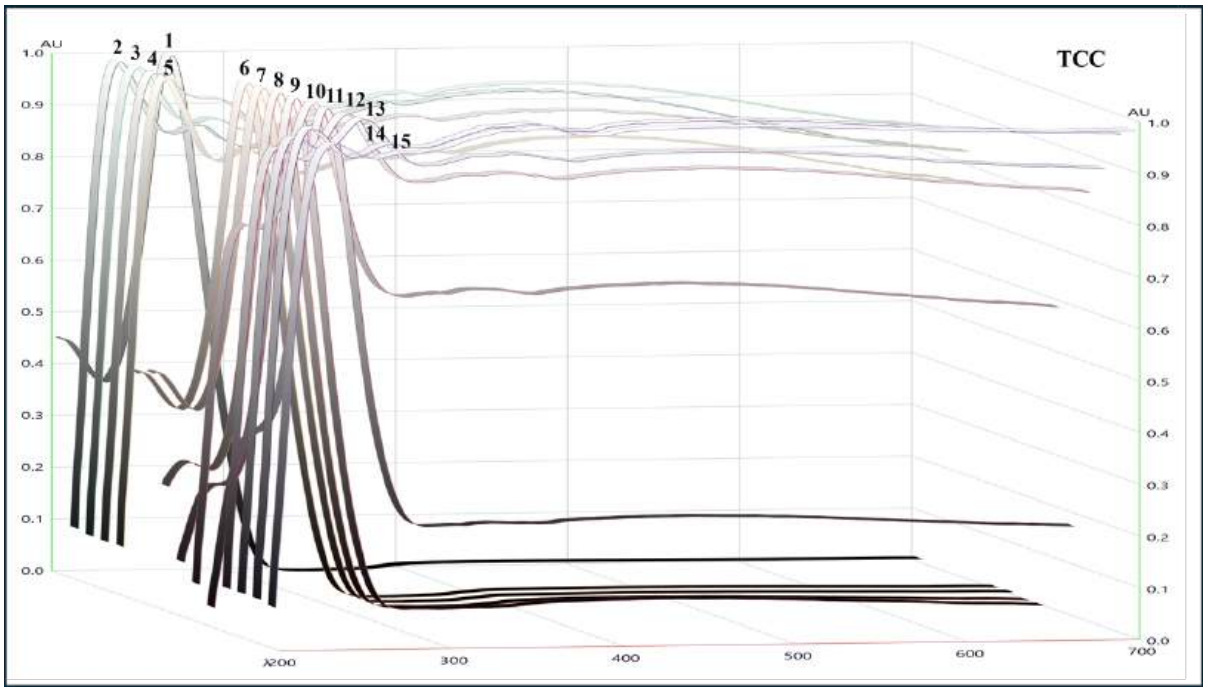

Figure 44. Overlain UV spectra of standard TCC and the corresponding band in the sample for peak purity, AU denotes absorbance units

To ensure robust kinetic interpretation and appropriate control correction, fifteen discrete sample tracks were applied to the HPTLC plate. Track 1 contained the TCC reference standard and served as the basis for compound identification and densitometric normalization. Tracks 2 and 3 consisted of sterile NB and SWW, respectively, to confirm the absence of matrix interference. Tracks 4 and 5 contained NB and SWW inoculated with the bacterial consortia without TCC, serving as biotic controls.

Initial TCC concentrations (100 mg/L) at 0 h were represented by Tracks 6 (NB) and 7 (SWW). Time-resolved degradation was monitored by loading samples collected at 48, 72, 96, and 120 h in Tracks 8-15, with parallel NB and SWW samples at each time point. This layout enabled direct comparison of degradation progression between media under identical analytical conditions. Track assignments and sampling points are summarized in (Table 22).

TCC plates were visualized under visible light and UV illumination at 254 nm and 366 nm to assess the suitability of each mode for monitoring degradation. Comparative evaluation demonstrated that UV visualization at 254 nm provided the highest contrast and clearest definition of TCC bands, with minimal background interference. Visualization under visible light primarily confirmed plate uniformity, while 366 nm imaging aided impurity screening but offered limited quantitative advantage. Consequently, all degradation results and densitometric analyses presented for TCC are based on UV imaging at 254 nm (Table 23) (Figure 45).

Table 23. Imaging and detection parameters for TCC plate visualization

Parameter	**Visible Light (White)**	**UV 254 nm**	**UV 366 nm**
Exposure Time	0.032 s	0.093 s	0.482 s
Contrast	1.0	1.1	1.0
Normalized Exposure	Disabled	Disabled	Disabled
Clarify	Disabled	Disabled	Disabled
White Balance	1.00, 1.00, 1.00	1.00, 1.00, 1.00	1.00, 1.00, 1.00

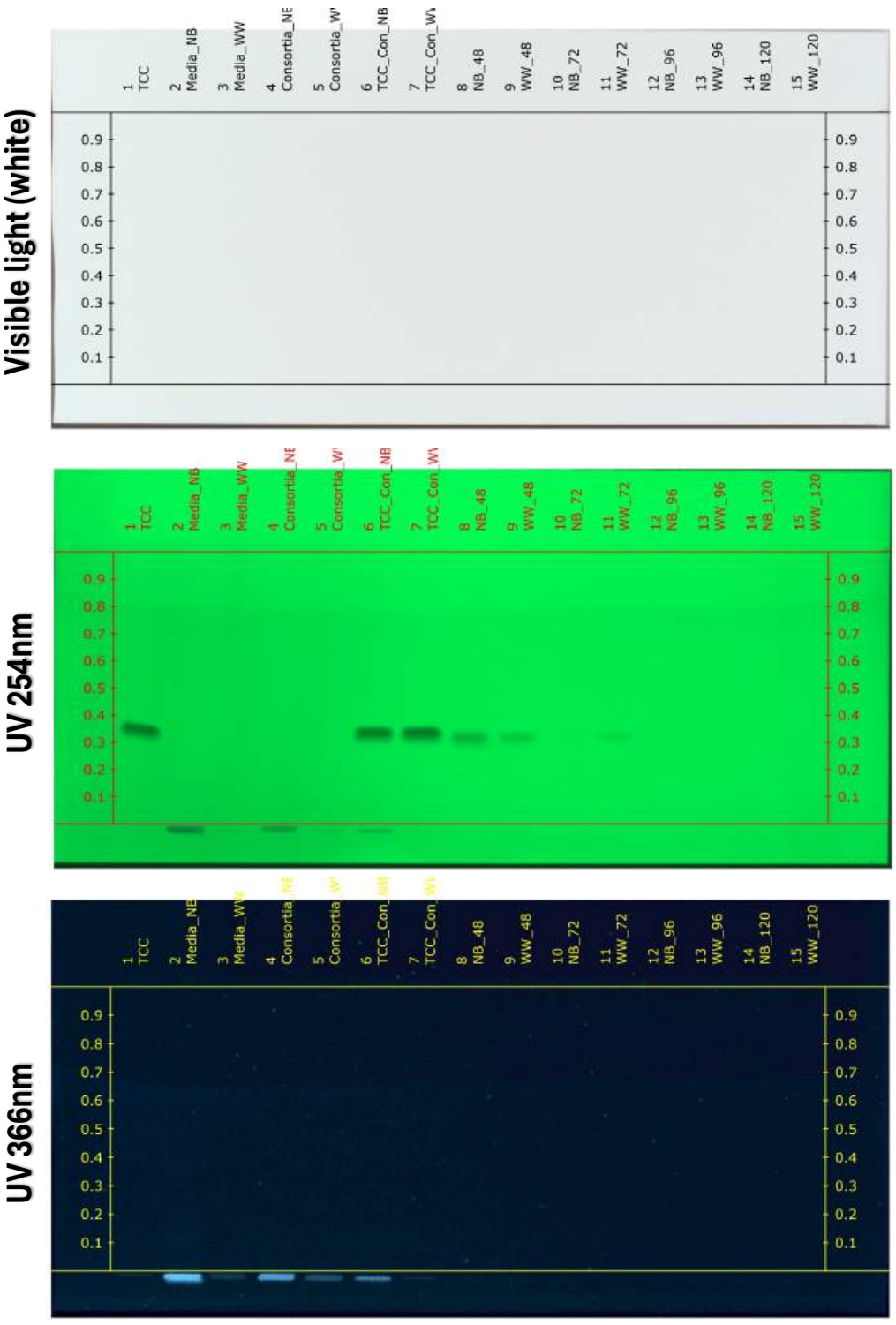

Figure 45. Comparison of HPTLC visualization modes (visible light, UV 254 nm, and UV 366 nm) for trichlorocarbanilide (TCC) analysis, demonstrating superior band clarity and contrast at 254 nm, which was therefore selected for all subsequent degradation profiling

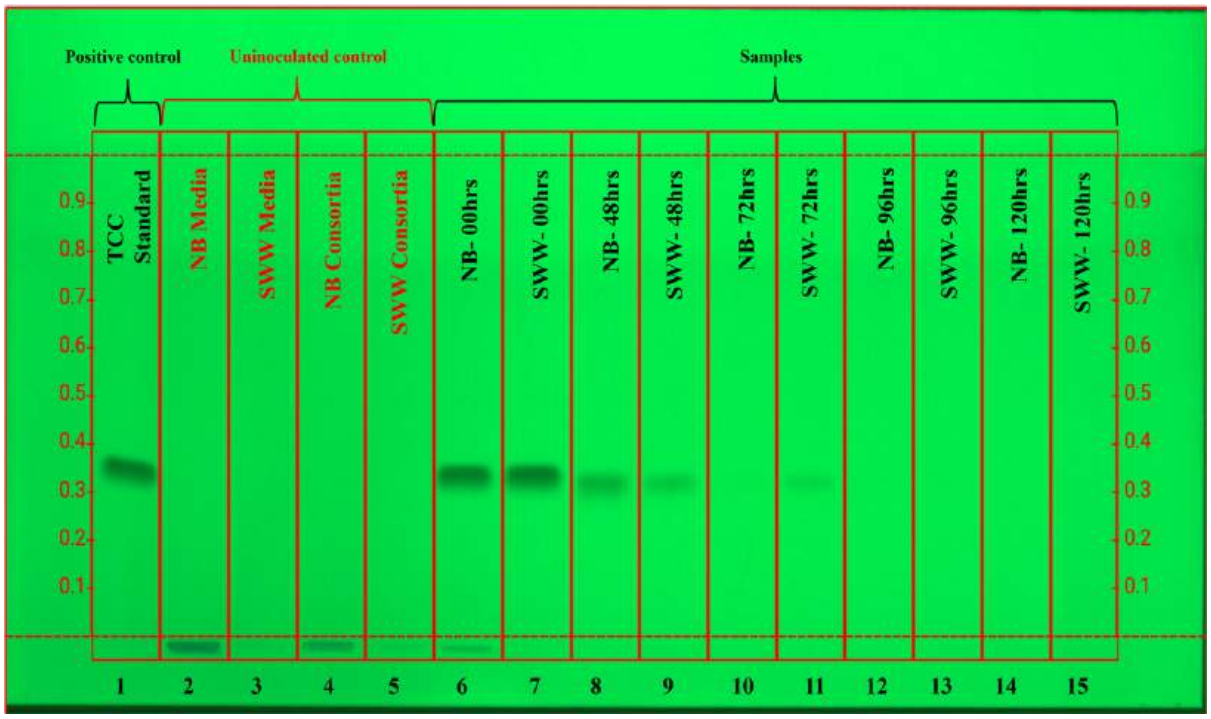

Figure 46. TCC TLC plate under 254nm UV light with standard, controls, and degradation results

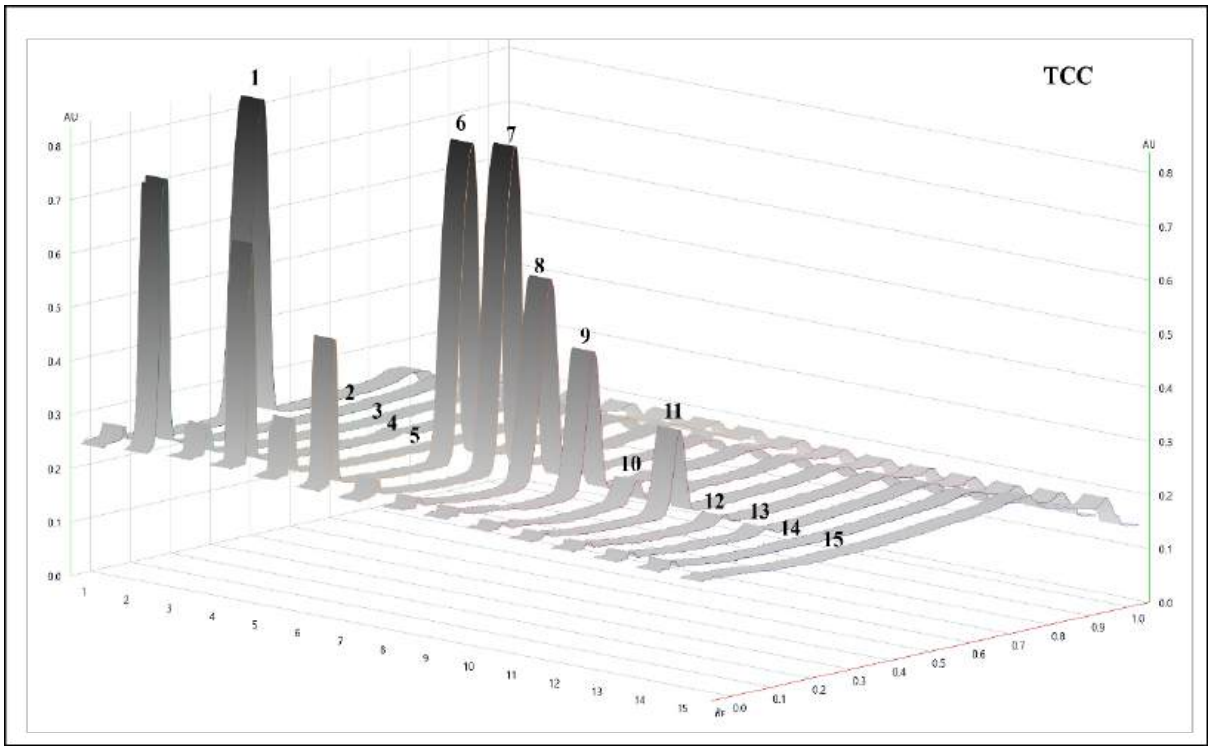

Figure 47. Densitogram of the TCC TLC plate, including standard, controls, and degradation results, AU denotes absorbance units, and *Rf* represents the retention factor

Visual inspection of the TLC plates under UV illumination confirmed progressive attenuation and eventual disappearance of the TCC band over the 120-hour incubation period (Figure 46). Corresponding densitometric scans showed a continuous decline in peak area, consistent with cumulative TCC removal (Figure 47).

Quantitative densitometric results are summarized in (Table 24). Initial measurements at 0 h showed negligible TCC loss in both NB and SWW (0.15% and 1.00%, respectively), indicating minimal abiotic loss and confirming the validity of the control systems. At 48 h, marked degradation was observed, particularly in SWW, where TCC removal reached 63.37%, substantially exceeding the 37.29% observed in NB. This pronounced early-stage removal in SWW indicates rapid bacterial adaptation under nutrient-limited conditions.

By 72 h, TCC degradation in NB accelerated sharply to 94.81%, while SWW maintained a high removal efficiency of 80.80%. At 96 h, near-complete degradation was observed in both media, with 97.98% removal in NB and 98.65% in SWW. By the final incubation stage (120 h), TCC was no longer detectable in either medium, indicating complete disappearance of the parent compound within the method's detection limits (Table 24).

Degradation and remaining percentages were calculated based on the relative reduction in densitometric peak area relative to the TCC reference standard, using the same normalization and calculation approach as for methylparaben (Section 6.1.4). ND indicates concentrations below the detection limit of the HPTLC method.

Table 24. Time-resolved degradation of trichlorocarbanilide (TCC) by bacterial consortium determined by HPTLC densitometry

Sample	Track	Densitometric peak area (A_t)	Degradation (%)	Remaining (%)	Equivalent amount (ng)
Trichlorocarbanilide (TCC) Standard	1	0.02834	0.00	100.00	4000.00
NB Media (Blank)	2	-	-	-	-
SWW media (Blank)	3	-	-	-	-

Bacterial consortia + NB (Biotic Control)	4	-	-	-	-
Bacterial consortia + SWW (Biotic Control)	5	-	-	-	-
TCC + Bacterial consortia + NB	6	0.02830	0.15	99.85	3994.35
TCC + Bacterial consortia + SWW	7	0.02825	1.00	99.00	3960.29
NB_48	8	0.01777	37.29	62.70	2508.11
WW_48	9	0.01038	63.37	36.62	1465.06
NB_72	10	0.00147	94.81	5.19	207.48
WW_72	11	0.00544	80.80	19.19	767.81
NB_96	12	0.00057	97.98	2.01	80.45
WW_96	13	0.00038	98.65	1.34	53.63
NB_120	14	ND	100.00	0.00	-
WW_120	15	ND	100.00	0.00	-

Equivalent amount (ng) represents the mass of trichlorocarbanilide (TCC) applied per HPTLC track (4 µL aliquot) after ten-fold concentration of samples by vacuum evaporation. Degradation percentages were calculated relative to the initial applied mass and reflect degradation from the original bulk concentration of 100 mg L^{-1}.

Degradation (%) = ((A_std − A_t)/A_std) × 100; Remaining (%) = (A_t/A_std) × 100, where A_std is the densitometric peak area of the TCC reference standard and A_t is the peak area at time t. ND indicates concentrations below the detection limit of the HPTLC method.

Normalized concentration profiles (C/C_0 versus time) and semi-logarithmic $\ln(C/C_0)$ plots further illustrate the rapid degradation kinetics of TCC and the convergence of removal performance between NB and SWW at later stages (Figure 48 a, b, and c).

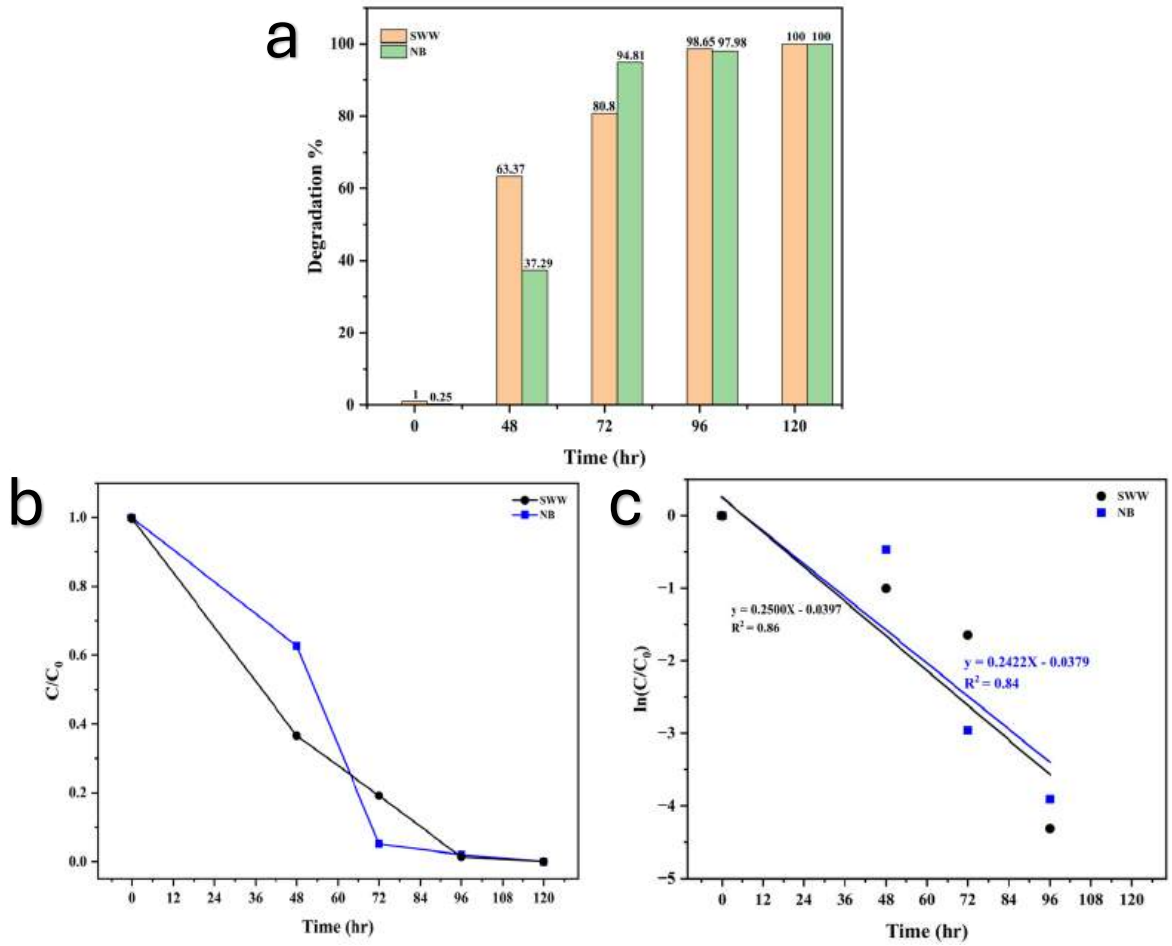

Figure 48. (a) C/C_0 vs. time plots for TCC degradation, (b) Degradation comparison between SWW and NB, (c) $In(C/C_0)$ vs. time plots for TCC degradation

In contrast to methylparaben, TCC exhibited faster and more complete degradation under the same experimental conditions. The rapid initial removal observed in SWW suggests that nutrient limitation promoted early induction of TCC-degrading pathways. In NB, the presence of readily assimilable carbon sources likely delayed expression of enzymes involved in TCC transformation, resulting in slower initial degradation followed by rapid removal once preferential substrates were depleted. This behaviour is consistent with catabolite repression phenomena reported for xenobiotic degradation in nutrient-rich environments.

The superior mid-stage performance in SWW highlights the relevance of oligotrophic conditions for targeting recalcitrant compounds such as TCC. These results demonstrate that synthetic wastewater not only supports bacterial survival but can actively enhance the

degradation of chlorinated pollutants by forcing metabolic prioritization of the target compound.

The higher degradation efficiency observed for TCC relative to methylparaben suggests a strong affinity of the bacterial consortium for chlorinated urea compounds. TCC possesses a stable urea linkage flanked by chlorinated aromatic rings, rendering it resistant to non-specific hydrolysis. Its effective removal indicates the presence of specialized enzymatic systems within the consortium, likely involving amide hydrolysis followed by oxidative or dechlorination reactions [191].

Literature reports indicate that *Alcaligenes* species frequently dominate TCC-enriched communities and can initiate degradation via amidase-mediated cleavage of the urea bond [192]. Subsequent transformation of chlorinated aromatic intermediates may be facilitated by *Rhodococcus* species, which are known to express monooxygenases capable of dechlorination and hydroxylation of halogenated phenolics [193]. The observed degradation behaviour is therefore consistent with a synergistic metabolic sequence within the consortium.

Although a complete disappearance of the parent TCC peak was achieved, HPTLC analysis alone cannot confirm full mineralization. Previous studies have reported the formation of intermediates such as 4-chloroaniline and dichlorocarbanilide during partial TCC degradation, which may exhibit higher toxicity than the parent compound [194]. The slowing of degradation observed prior to complete removal suggests potential transient product inhibition, as also reported in the literature.

In summary, time-resolved HPTLC analysis demonstrated rapid and complete disappearance of trichlorocarbanilide in both nutrient broth and synthetic wastewater, with degradation occurring more efficiently and rapidly than for methylparaben. The results highlight the strong capability of *Alcaligenes*- and *Rhodococcus*-dominated consortia to transform recalcitrant chlorinated pollutants under environmentally relevant conditions.

This study focused on the disappearance of the parent compound and did not identify transformation products or assess the toxicity of intermediates. Future work should incorporate targeted analysis of chloroaniline derivatives and evaluate potential impacts on nitrogen-cycling microorganisms to ensure that effective removal corresponds to true detoxification [195].

6.1.5 Comparative Degradation Efficiency and System-Level Interpretation of Fungal and Bacterial Systems

This section integrates the lab-scale biodegradation results obtained for natural pollutants (caffeine and nicotine) using fungal systems and anthropogenic pollutants (methylparaben and trichlorocarbanilide) using bacterial consortia. The objective of this comparative analysis is not to rank individual removal efficiencies, but to critically evaluate how pollutant class, microbial strategy, analytical resolution, and growth environment collectively determine biodegradation performance (Figure 49). This synthesis directly addresses the research aim and objectives defined in Chapter 3 and establishes the scientific rationale for subsequent scale-up to constructed wetland systems.

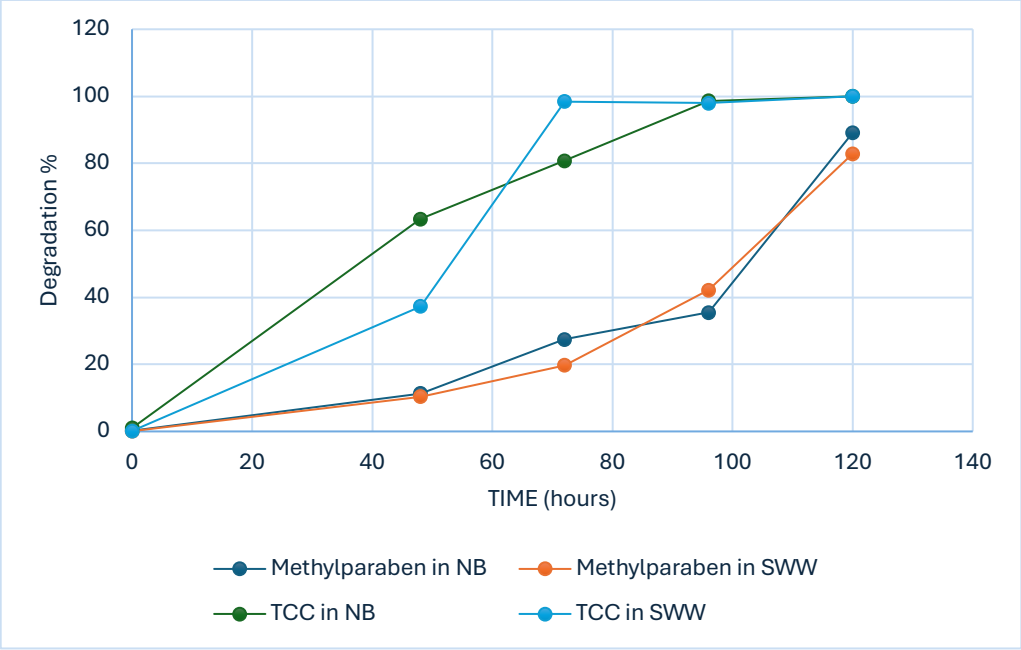

Figure 49. Degradation of paraben and TCC in NB and SWW over time

The deliberate separation of pollutants into natural (caffeine, nicotine) and anthropogenic (methylparaben, trichlorocarbanilide) categories was a foundational design choice in this study, rather than a consequence of experimental convenience. These two pollutant classes differ fundamentally in origin, structural complexity, environmental familiarity, and expected biodegradation behaviour, and therefore demand distinct microbial and analytical approaches.

Caffeine and nicotine are naturally occurring or lifestyle-derived compounds that are continuously introduced into surface waters through diffuse sources. Their molecular structures are relatively simple and biologically familiar, and they are known to interact with oxidative

and detoxification pathways present in fungi. Consequently, fungal systems, particularly white-rot fungi such as *Trametes versicolor,* were selected to investigate their degradation under low-energy, environmentally relevant conditions that mimic natural self-cleaning processes.

In contrast, methylparaben and trichlorocarbanilide are synthetic anthropogenic compounds designed for chemical stability and antimicrobial activity. These properties confer persistence in aquatic environments and reduce susceptibility to non-specific biodegradation. For such compounds, bacterial consortia offer a more appropriate strategy due to their metabolic diversity, rapid adaptive capacity, and ability to express specialized enzymatic systems targeting ester bonds (methylparaben) or chlorinated urea structures (trichlorocarbanilide).

This intentional pairing of pollutant class and microbial system is central to the thesis hypothesis that surface water self-cleaning capacity can be intensified by deploying functionally specialized microbial degraders rather than relying on a single, universal biodegradation strategy.

A key outcome of this study is the demonstration that different microbial systems necessitate different evaluation frameworks. Fungal degradation of caffeine and nicotine was assessed using an endpoint-based approach, while bacterial degradation of methylparaben and trichlorocarbanilide was evaluated using time-resolved kinetic analysis. This distinction reflects biological reality rather than analytical limitation.

Fungal systems exhibited slow but sustained growth, long adaptation periods, and progressive biomass accumulation over extended incubation times. Under optimal conditions (25 °C, favourable pH, and nutrient-supported aqueous matrices), *Trametes versicolor* achieved endpoint removal efficiencies of approximately 97-98% for both caffeine and nicotine. These results were obtained after prolonged incubation (≈40 days), capturing cumulative biodegradation rather than short-term reaction rates. The endpoint approach is therefore appropriate for assessing the contribution of fungi to long-term pollutant attenuation in surface water systems.

By contrast, bacterial consortia demonstrated rapid and measurable degradation of anthropogenic pollutants within hours to days. Methylparaben degradation reached 82.9-89.1% within 120 hours, while trichlorocarbanilide exhibited even more rapid disappearance,

becoming non-detectable in both nutrient broth and synthetic wastewater by the end of the incubation period. Time-resolved HPTLC analysis enabled clear identification of lag phases, acceleration during microbial adaptation, and medium-dependent differences in degradation kinetics.

The coexistence of endpoint-based and kinetic datasets within the same thesis is not a weakness; rather, it reflects an adaptive analytical strategy aligned with microbial physiology. Attempting to force kinetic modelling onto fungal systems or endpoint analysis onto bacterial systems would have compromised interpretability and scientific rigor.

The separation of analytical techniques, quantitative NMR for fungal systems and HPTLC for bacterial systems, was driven by chemical and operational constraints rather than methodological inconsistency. NMR spectroscopy was selected for caffeine and nicotine due to their high solubility in deuterated solvents, structural simplicity, and suitability for internal-standard-based quantification. In fungal systems, where degradation occurred over long timescales and concentration changes were gradual, NMR provided robust endpoint confirmation of pollutant disappearance while minimizing sample handling and matrix interference.

For methylparaben and trichlorocarbanilide, HPTLC offered decisive advantages. Methylparaben required rapid, multi-sample comparison to resolve medium-dependent kinetics, while trichlorocarbanilide exhibited extremely poor solubility in standard NMR solvents and significant interference from wastewater matrices. Under these conditions, HPTLC enabled reliable separation, densitometric quantification, and visualization of degradation progression that would not have been feasible using NMR. Thus, the analytical divergence across systems reflects methodological appropriateness rather than inconsistency, reinforcing the thesis objective of designing experimentally defensible and environmentally relevant biodegradation assessments.

Across both fungal and bacterial systems, growth medium composition emerged as a decisive factor governing biodegradation performance. However, its influence manifested differently depending on microbial strategy.

In fungal systems, synthetic wastewater and complex matrices such as coffee extract and tobacco-based media supported substantial biomass accumulation and high endpoint removal

efficiencies for caffeine and nicotine. These results demonstrate that fungi can utilize intrinsic nutrients present in wastewater matrices without external supplementation, aligning with the concept of low-energy, in situ self-cleaning.

In bacterial systems, medium composition exerted a stronger influence on degradation kinetics. Nutrient broth supported rapid early growth but in some cases delayed pollutant degradation, consistent with preferential utilization of readily assimilable substrates. In contrast, synthetic wastewater characterized by limited organic carbon and higher inorganic content promoted faster adaptation and earlier initiation of pollutant degradation, particularly for trichlorocarbanilide. The observation that more than 60% of trichlorocarbanilide was removed within 48 hours in synthetic wastewater highlights the role of nutrient limitation in forcing metabolic prioritization of recalcitrant compounds.

The collective results from both fungal and bacterial degradation experiments demonstrate that the composition of the growth medium is a decisive design parameter in engineered treatment systems. Importantly, the successful growth, adaptation, and pollutant removal observed in synthetic wastewater across all investigated microbial systems confirm that external nutrient-rich media are not a prerequisite for effective biodegradation. In fungal systems, *Trametes versicolor* exhibited sustained biomass development and high endpoint removal efficiencies for caffeine and nicotine in synthetic wastewater and complex aqueous matrices, indicating that intrinsic wastewater-derived nutrients were sufficient to support metabolic activity and pollutant transformation. Similarly, bacterial consortia rapidly and efficiently degraded methylparaben and trichlorocarbanilide in synthetic wastewater, often matching or exceeding performance observed in nutrient broth after a short adaptation phase.

These findings directly fulfil the media replacement objective defined in Chapter 3 by demonstrating that both fungal and bacterial degraders can be transitioned from laboratory growth media to wastewater-based systems without loss of functional performance. The ability of microbial systems to maintain degradation efficiency under nutrient-limited conditions validates synthetic wastewater as a realistic and appropriate model for evaluating microbial self-cleaning processes. From an engineering perspective, this outcome is critical, as it supports the development of low-energy, cost-effective treatment strategies that avoid reliance on external nutrient supplementation and are therefore more compatible with scalable, nature-based wastewater treatment systems.

Comparison across pollutants reveals that biodegradation efficiency is not solely dictated by molecular complexity. Trichlorocarbanilide, despite its chlorinated and structurally rigid nature, was degraded more rapidly and completely than methylparaben under the tested conditions. This counterintuitive result reflects the bacterial consortium's specialization toward halogenated urea compounds rather than inherent compound recalcitrance.

For fungal systems, both caffeine and nicotine exhibited strong correlations between biomass accumulation and endpoint removal, indicating that sustained growth is a prerequisite for effective degradation. However, the absence of kinetic resolution and metabolite identification limits mechanistic interpretation and requires cautious framing of results as disappearance-based removal rather than confirmed mineralization.

For bacterial systems, rapid degradation and complete disappearance of parent compounds were achieved, but literature evidence indicates that intermediate transformation products, particularly during trichlorocarbanilide degradation, may exhibit residual toxicity [196–198]. The potential formation of such intermediates represents a system-level limitation that must be addressed during scale-up.

While the lab-scale results demonstrate high biodegradation potential across all systems, several limitations emerge when considering translation to engineered environments. First, the disappearance of the parent compound does not guarantee detoxification, particularly for anthropogenic pollutants with known toxic intermediates. Second, bacterial systems, while kinetically efficient, may be sensitive to fluctuating nutrient loads and microbial competition under non-sterile conditions. Third, fungal systems, although robust and low energy, operate on longer timescales that may not be compatible with short hydraulic retention times.

These limitations highlight the need for integrated treatment platforms that combine the strengths of both microbial strategies. Constructed wetlands offer such a platform by providing spatial organization, microbial diversity, extended retention, and buffering against environmental variability. The complementary performance observed here, fungal stability and bacterial kinetics, provides a strong scientific basis for their integration into engineered self-cleaning systems.

In summary, the comparative analysis demonstrates that effective enhancement of surface water self-cleaning requires pollutant-specific microbial strategies, adaptive analytical

frameworks, and careful consideration of the growth environment. Fungal systems provide sustained, low-energy removal of natural pollutants, while bacterial consortia enable rapid and efficient degradation of anthropogenic compounds with well-resolved kinetics. The intentional separation of pollutant classes, microbial systems, and analytical techniques is therefore a central strength of this thesis rather than a limitation.

These findings directly inform the design and operation of the biomimetic constructed wetland system evaluated in the following section, where microbial adaptation, system stability, and pollutant removal are examined under continuous-flow and ecologically relevant conditions.

6.2 Pilot-Scale Performance of the Biomimetic Constructed Wetland System

This section evaluates the performance of the laboratory-scale biomimetic constructed wetland system designed to translate the lab-scale biodegradation mechanisms established in Section 6.1 into an ecologically structured treatment environment. While batch experiments enabled controlled assessment of microbial adaptation and degradation kinetics, they do not capture the spatial heterogeneity, plant-microbe interactions, substrate colonization, and operational stability characteristic of surface water treatment systems. Accordingly, the constructed wetland experiments were implemented to validate whether the microbial self-cleaning processes demonstrated at laboratory scale remain effective under mixed-pollutant loading, wastewater-based growth conditions, and prolonged operation within a porous, plant-supported matrix. The results presented in this section focus on system stability and microbial adaptation (Section 6.2.1), pollutant removal performance at defined operational milestones (Section 6.2.2), structural and biological stabilization within the wetland media (Section 6.2.3), and an integrated evaluation of wetland-level self-cleaning functionality and scalability (Section 6.2.4). Collectively, these analyses establish a direct experimental bridge between lab-scale biodegradation and wetland-scale self-cleaning performance, addressing the central objective of this dissertation.

6.2.1 Microbial Adaptation and Operational Stability in the Constructed Wetland

Prior to evaluating pollutant removal at the wetland scale, it was necessary to assess whether the selected fungal and bacterial systems could tolerate simultaneous exposure to chemically diverse pollutants representative of wastewater-impacted surface waters. Accordingly, the growth responses of fungal and bacterial degraders were examined under increasing concentrations of a mixed-pollutant cocktail comprising caffeine, methylparaben, and trichlorocarbanilide.

Growth responses were evaluated using daily growth-rate and net-change analyses rather than cumulative growth alone, allowing clearer resolution of dose-dependent stress effects and population dynamics. Both fungal and bacterial systems exhibited concentration-dependent growth suppression; however, neither system showed complete growth arrest even at the highest tested pollutant loading. This finding demonstrates microbial survivability under mixed-pollutant stress conditions, rather than in optimal laboratory environments, and establishes the suitability of the selected concentrations for subsequent wetland-scale experiments.

6.2.1.1 Fungal Growth Dynamics Under Mixed Pollutant Exposure

Fungal tolerance was assessed based on daily mycelial growth rates derived from radial extension measurements on PDA plates incubated at 25 °C (Figure 50). At low pollutant loading (1 mg per 10 mL), daily growth-rate patterns were comparable to those of the control throughout the incubation period, indicating minimal interference with mycelial expansion. Growth remained progressive across all time intervals, demonstrating a high intrinsic tolerance of *Trametes versicolor* to low-level mixed-pollutant exposure. Growth rates were calculated as incremental changes in radial extension from one day to the next, highlighting concentration-dependent suppression of fungal growth dynamics under mixed-pollutant stress.

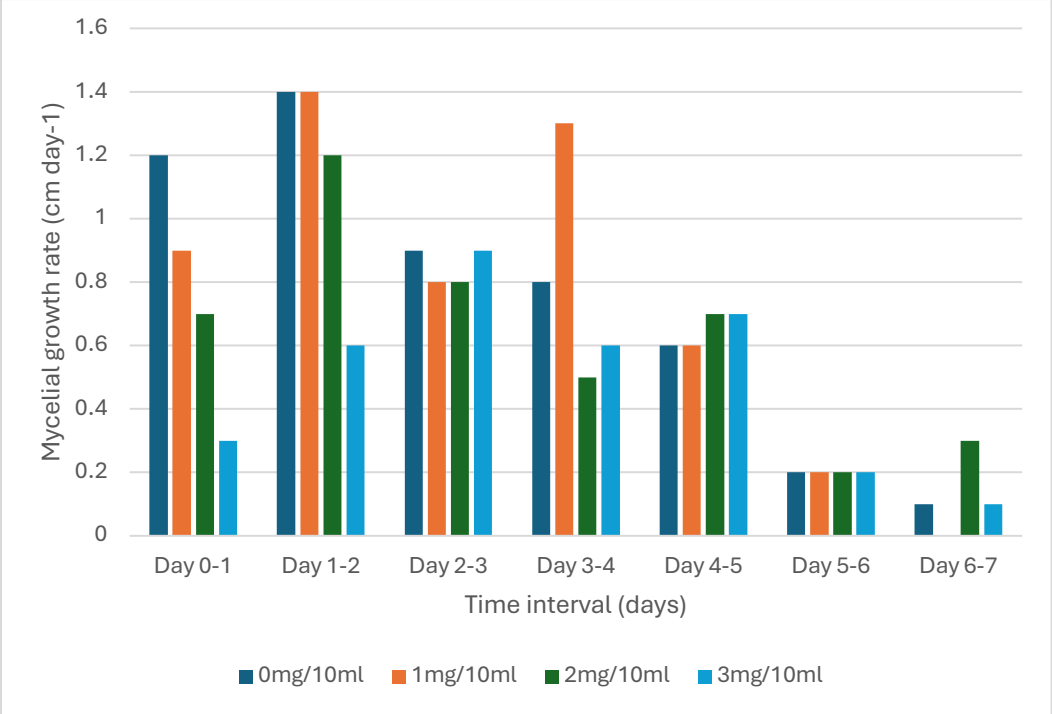

Figure 50. Daily mycelial growth rate (cm day^{-1}) of *Trametes versicolor* exposed to increasing concentrations of a mixed-pollutant cocktail (caffeine, methylparaben, and trichlorocarbanilide) at 25 °C

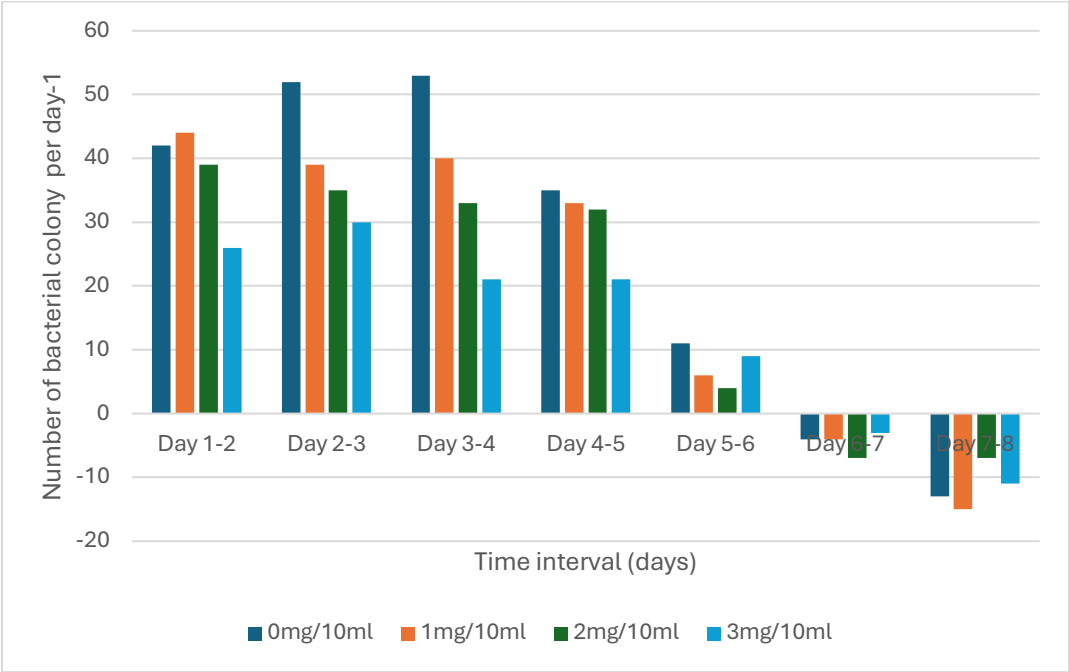

Figure 51. Daily net change in bacterial colony counts (colonies day^{-1}) under increasing concentrations of a mixed-pollutant cocktail (caffeine, methylparaben, and trichlorocarbanilide) at 37 °C

At higher pollutant concentrations, growth-rate suppression became evident. Treatments amended with 2 mg and 3 mg per 10 mL exhibited consistently lower daily growth rates than the control, particularly during the mid-incubation phase. Although mycelial expansion continued under all conditions, cumulative growth was reduced in a concentration-dependent manner, with the highest pollutant loading resulting in an overall reduction of approximately 35% relative to the control by the end of the incubation period. The absence of abrupt cessation of growth suggests that the observed inhibition reflects metabolic interference, potentially involving oxidative enzyme systems, rather than acute fungicidal toxicity.

6.2.1.2 Bacterial Population Dynamics Under Mixed-Pollutant Exposure

Bacterial tolerance was evaluated using daily net changes in colony counts on nutrient agar plates incubated at 37 °C (Figure 51). Control cultures exhibited rapid population expansion during the early incubation period, followed by a transition toward the stationary and decline phases. Increasing pollutant concentrations resulted in a pronounced reduction in net colony gain across successive time intervals, indicating progressive inhibition of bacterial proliferation. Positive and negative values represent population growth and decline phases, respectively, illustrating dose-dependent inhibition of bacterial population dynamics under mixed-pollutant exposure.

At 1 mg per 10 mL, net colony increases were reduced relative to the control but remained positive throughout most of the incubation period. Higher pollutant loadings (2 and 3 mg per 10 mL) led to substantially lower peak colony numbers and earlier onset of population decline, with the highest concentration producing an overall reduction of approximately 47% relative to the control. Negative net changes observed during late incubation reflect a transition to the decline phase rather than experimental artefacts and are consistent with pollutant-induced stress combined with nutrient limitation. The stronger inhibitory response observed in bacterial systems aligns with the known antimicrobial properties of trichlorocarbanilide and the higher susceptibility of rapidly dividing bacterial cells to membrane-active and enzyme-inhibiting compounds.

Despite measurable growth suppression at elevated pollutant concentrations, both fungal and bacterial systems maintained active growth across all tested conditions. This confirms that the mixed-pollutant cocktail imposed metabolic stress without inducing complete toxicity, validating its use as a stress-testing scenario rather than an unrealistically lethal exposure.

These findings provide a critical interpretive foundation for the constructed wetland experiments by demonstrating that both microbial groups can survive simultaneous exposure to natural and anthropogenic pollutants typical of wastewater-impacted surface waters.

Furthermore, the differential sensitivity observed between fungal and bacterial systems supports the functional separation adopted in the wetland design, wherein fungi were immobilized within solid substrates to promote long-term stability, while bacterial activity was sustained through aeration. The persistence of growth under mixed-pollutant stress indicates that subsequent removal efficiencies observed at the wetland scale reflect microbial adaptation within an operationally stable system rather than survival bias or selective toxicity.

6.2.1.3 Vegetative Stability and Plant-Substrate Compatibility

All wetland units were planted with *Phragmites australis*, a macrophyte widely used in constructed wetland systems due to its high tolerance to pollutant stress and its capacity to develop extensive root systems within porous media. Throughout the 7-week operational period, plant growth was monitored as an indicator of the wetland system's vegetative stability and structural integrity, rather than as a direct mechanism of pollutant removal.

In the biologically augmented wetlands (Wetlands A, B, and C), *P. australis* exhibited consistent vertical shoot growth, indicating successful adaptation to the synthetic wastewater matrix and tolerance to mixed-pollutant loading (Figure 52). In contrast, plant growth in the abiotic control wetland (Wetland D) was noticeably slower, suggesting that microbial activity indirectly supports vegetative performance by stabilizing rhizosphere conditions and improving nutrient availability. This observation is consistent with the concept of plant-microbe mutualism, defined as an ecological interaction in which both plants and microorganisms derive functional benefits that enhance overall system performance.

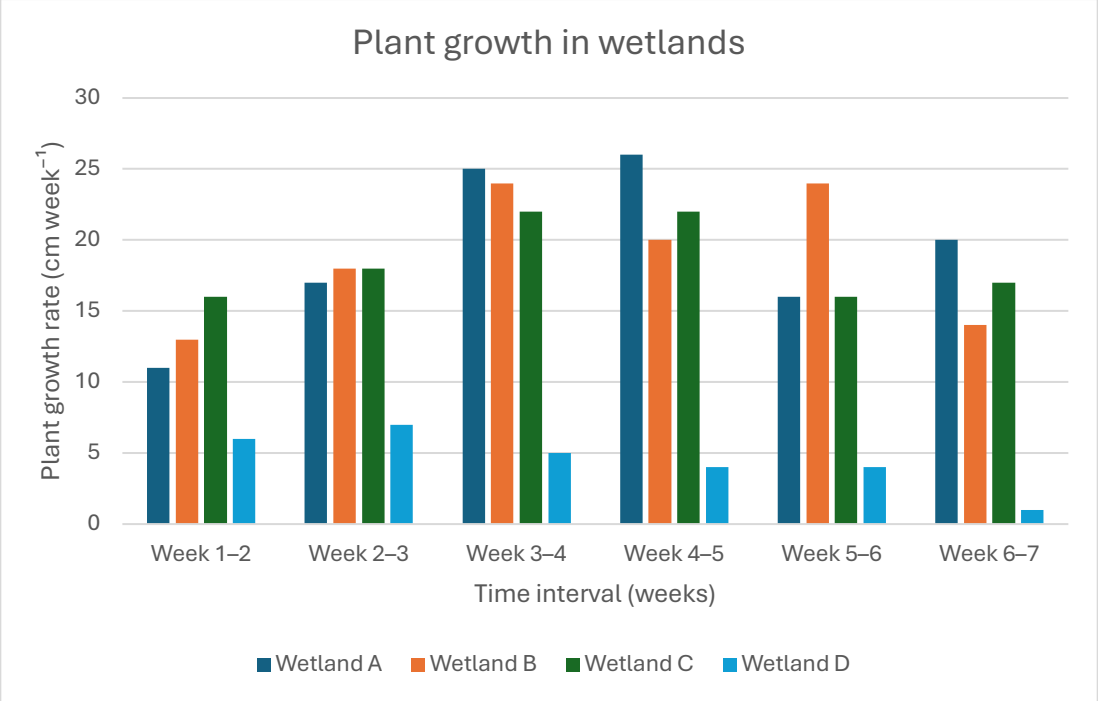

Figure 52. Weekly plant growth rate (cm week⁻¹) in Wetland A-D calculated from changes in plant height between consecutive weeks

From a structural and ecological perspective, plant roots provide microorganisms with increased surface area for attachment, biofilm formation, and spatial stabilization within the wetland matrix. The rhizosphere creates a protected microenvironment that supports microbial persistence and metabolic activity through localized nutrient availability and physicochemical gradients. In return, microbial metabolism contributes indirectly to plant growth by transforming complex organic pollutants and wastewater-derived compounds into simpler, more bioavailable forms. As biodegradation progresses, chemically complex structures are converted into low-molecular-weight metabolites and inorganic nutrients that can be more readily assimilated by plant roots, thereby supporting continued vegetative development [195,199].

Shoot elongation progressed steadily during the initial operational phase and began to plateau after approximately six weeks. This levelling-off of vertical growth is consistent with biomass redistribution rather than physiological stress. As above-ground biomass increased, some plants exhibited bending due to the limited mechanical support provided by gravel-based porous media compared to compact soil. Importantly, no symptoms of phytotoxicity, such as chlorosis or necrosis, were observed in any wetland configuration, confirming plant tolerance under high mixed-pollutant exposure.

Subsurface examination revealed extensive root development within the porous media, with roots becoming wider and thicker over time. This dense root network enhances wetland functionality by increasing physical filtration capacity, stabilizing the substrate matrix, and promoting microbial attachment. In combination with the intrinsic nutrient content of synthetic wastewater, which serves as a shared resource for both plants and microorganisms, these interactions establish a positive feedback loop in which microbial activity supports plant growth and plant development, in turn, sustains microbial colonization [200,201].

Overall, the coexistence of sustained plant growth and active microbial communities under mixed-pollutant loading demonstrates that the constructed wetland operated as an integrated, mutually supportive ecological system. While plants did not function as primary degraders of target pollutants, their structural and ecological roles amplified microbial self-cleaning processes, contributing indirectly to system-level stability and long-term treatment performance.

6.2.1.4 pH Behaviour in Wetlands

Weekly pH monitoring was conducted to assess chemical stability and, indirectly, to track microbial metabolic activity within the constructed wetland units. Across all systems, pH values remained within a moderately neutral range throughout the experimental period, indicating the absence of extreme acidification or alkalization that could compromise microbial or plant viability.

In the biologically active wetlands, pH increased gradually over time. Wetland A (bacterial system) exhibited a steady shift from mildly acidic to near-neutral conditions, consistent with sustained bacterial metabolic activity. Wetland B (fungal system) maintained a relatively stable pH during early operation, followed by a more pronounced increase toward the later stages of the experiment. Wetland C (combined fungal-bacterial system) displayed the most stable pH profile, characterized by moderate adjustment and minimal fluctuation over the full operational period. In contrast, the abiotic control wetland (Wetland D) showed a slight decline in pH over time, reflecting the absence of active microbial metabolism and the dominance of background physicochemical processes. Temporal monitoring of pH indicated that all wetland systems maintained values within a narrow, near-neutral range throughout the experimental period (Figure 53). Minor system-specific fluctuations were observed; however,

no abrupt pH shifts occurred, indicating effective buffering and overall operational stability of the wetland systems.

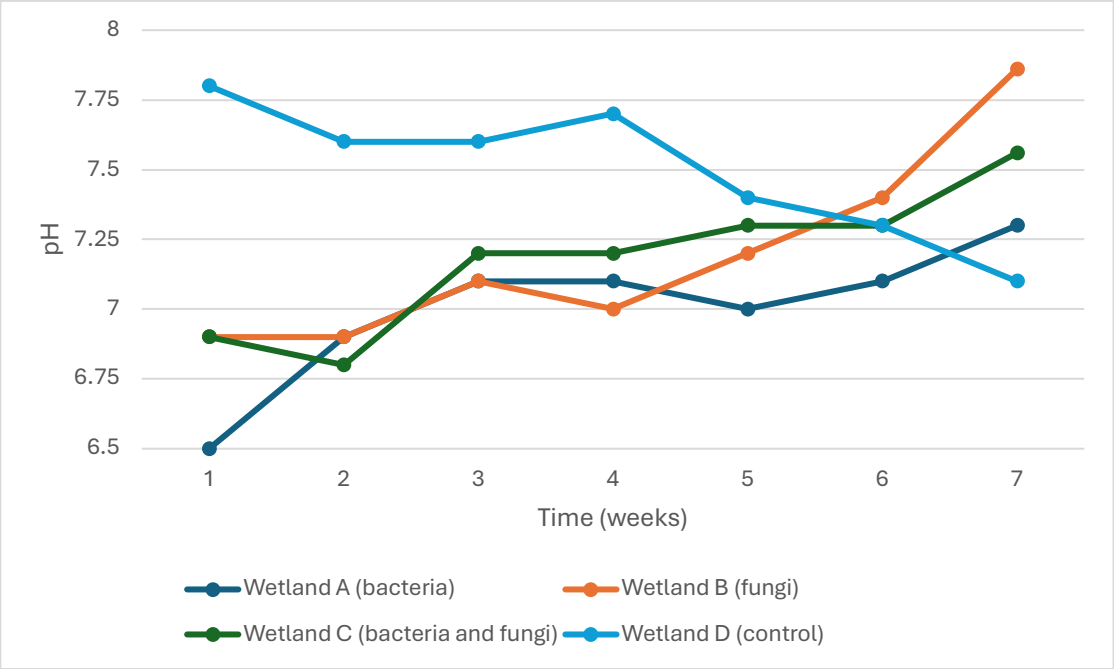

Figure 53. Temporal variation in pH across different wetland systems over the experimental period [157]

These pH trends indicate successful microbial acclimation and establishment within the wetland matrix. The absence of abrupt pH excursions suggests that metabolic by-products did not accumulate to inhibitory levels and that the combined buffering capacity of the synthetic wastewater, substrate, and plant-microbe interactions was sufficient to maintain chemical stability. Notably, the pH-modulated behaviour observed in the combined microbial system suggests functional complementarity between fungal and bacterial metabolism, thereby enhancing environmental buffering under mixed-pollutant conditions [202,203].

Taken together, plant growth patterns and pH stability provide converging evidence that the constructed wetland systems transitioned successfully from start-up to stabilized operation by Week1, 4, and remained operationally stable through Week 7. Vegetative integrity, sustained microbial viability under mixed-pollutant stress, and chemically stable conditions confirm that the wetland functioned as an integrated ecological system rather than a fragile laboratory setup. Establishing this stability is essential for interpreting pollutant removal performance, as it confirms that subsequent reductions in contaminant concentrations can be

attributed to active biological self-cleaning processes occurring within a mature and resilient system rather than transient adaptation effects or system instability.

6.2.2 Removal Efficiency of Constructed Wetland System

The removal efficiency of selected target pollutants in the laboratory-scale constructed wetland system was evaluated using Nuclear Magnetic Resonance (NMR) spectroscopy to provide both quantitative and structural confirmation of biodegradation under wetland conditions. The analysis focused on caffeine and methylparaben, which are sufficiently soluble in deuterated solvents to allow reliable NMR detection, while trichlorocarbanilide (TCC) could not be directly quantified due to intrinsic solubility constraints. Pollutant removal was assessed at two stabilized operational stages: Week 4 and Week 7, representing intermediate and advanced phases of wetland operation, respectively.

All systems were operated in batch mode; therefore, removal performance reflects time-dependent biodegradation rather than hydraulic treatment efficiency. Wetland B (fungal system) was maintained at 25 °C, Wetland A (bacterial system) at 37 °C, and Wetland C (fungal-bacterial consortium) at 30 °C. These temperature differences were assessed by comparing degradation kinetics, as microbial metabolic activity is strongly temperature-dependent.

^{1}H NMR (Figure 54) and ^{13}C NMR (Figure 55) spectra were recorded using a Varian 400 MHz spectrometer. Chemical shifts in NMR spectra were referenced to tetramethylsilane (TMS) and reported in parts per million (ppm). Samples were extracted, purified, and prepared in deuterated chloroform as described in Section 4.3.5 to minimize interference from microbial biomass, plant material, and wetland particulates.

NMR spectroscopy was selected because the relatively high influent concentrations used in this study (100 mg L^{-1}) provided sufficient signal intensity to track the disappearance of parent compounds and assess structural transformation without pre-concentration. Importantly, NMR enables direct discrimination between true biodegradation (structural loss of parent signals) and apparent removal due to physical processes such as adsorption or dilution. However, this approach is inherently unsuitable for highly hydrophobic compounds such as TCC, whose insolubility in $CDCl_3$ precludes reliable spectral detection.

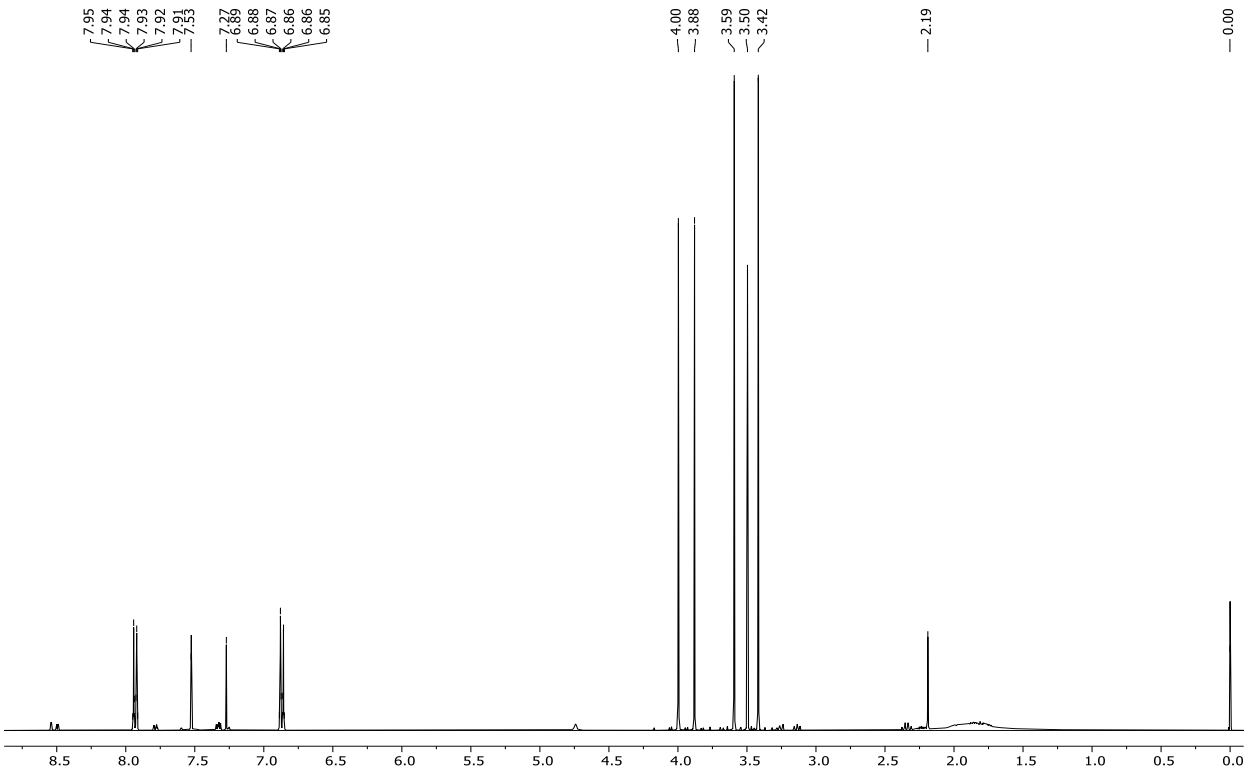

Figure 54. ^{1}H NMR spectrum of combined pollutants (wetland D, control) [157]

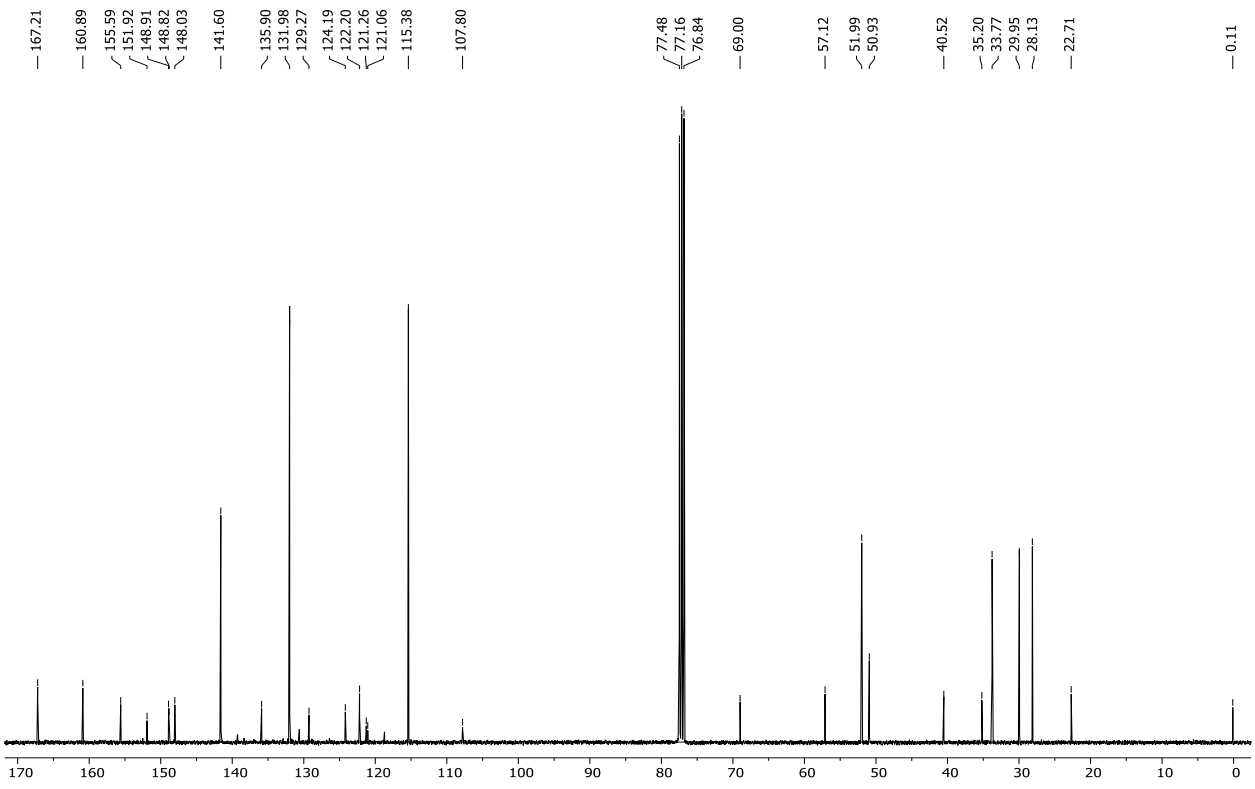

Figure 55. ^{13}C NMR spectrum of combined pollutants (wetland D, control) [157]

6.2.2.1 Performance of Wetland A (Bacterial Degradation - *Pseudomonas aeruginosa*)

Wetland A, inoculated with *Pseudomonas aeruginosa*, demonstrated compound-dependent degradation behaviour under batch operating conditions. Caffeine exhibited rapid biodegradation, with complete disappearance of the characteristic proton signal observed by week 4, indicating removal below the quantification limit of the ^{1}H NMR method. This result confirms that bacterial metabolism was highly effective for caffeine transformation within a short treatment period.

Caffeine is a small, nitrogen-containing heterocyclic compound that is readily bioavailable to bacterial cells. Its degradation by bacteria typically proceeds via N-demethylation followed by oxidative transformations that channel intermediates into central metabolic pathways [204,205]. The rapid loss of the parent caffeine signal in Wetland A indicates that these intracellular enzymatic pathways were active and did not require prolonged acclimation under the applied wetland conditions.

In contrast, methylparaben exhibited slower initial degradation in Wetland A. At week 4, removal reached 52.0%, with a residual NMR integral of 1.18. This comparatively lower early-stage removal suggests that ester-containing aromatic compounds require additional metabolic adaptation or enzymatic induction prior to efficient bacterial transformation. The presence of an aromatic ring and ester functionality in methylparaben may necessitate preliminary hydrolytic or oxidative steps before assimilation into bacterial metabolic pathways. Nevertheless, by week 7, the complete disappearance of the caffeine and methylparaben proton signals was observed, indicating removal below the analytical quantification limit (Figure 56).

The high overall degradation performance observed in Wetland A can be attributed to the applied inoculation strategy and wetland design. *Pseudomonas aeruginosa* was selected due to its documented metabolic versatility and ability to degrade aromatic and antimicrobial compounds under aerobic conditions [206]. Prior to wetland inoculation, the bacterium was cultivated in nutrient broth at 37 °C to obtain an actively growing culture.

The aerobic support for bacterial growth and metabolism enhances microbial substrate interactions. Wetland A was equipped with a centrally positioned, bottom-mounted aerator strip. This aeration configuration generated upward-directed airflow, inducing gentle

circulation of the liquid phase from the base toward the upper regions of the wetland. The resulting hydraulic movement improved oxygen availability within the porous media and ensured uniform contact between bacterial cells, dissolved pollutants, and substrate surfaces. In addition, successful adaptation to the nutrient conditions provided by synthetic wastewater supported sustained microbial growth and metabolic activity throughout the experimental period. Collectively, the combination of active inoculation, effective aeration, controlled temperature (37 °C), and nutrient availability contributed to the high caffeine removal efficiency and progressive methylparaben degradation observed in Wetland A.

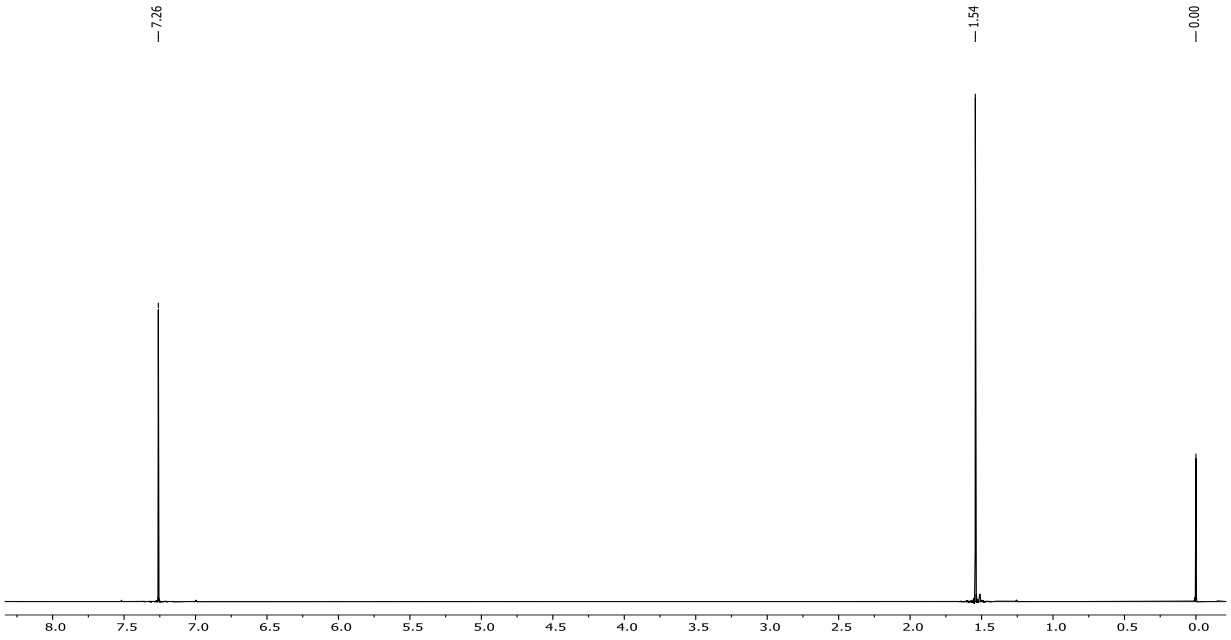

Figure 56. ^{1}H NMR spectrum of wetland A (*Pseudomonas aeruginosa*), 7 weeks [157]

6.2.2.2 Performance of Wetland B (Fungal Degradation - *Trametes versicolor*)

Wetland B, inoculated with the white-rot fungus *Trametes versicolor*, demonstrated strong removal performance for both target pollutants under batch operating conditions. At week 4, caffeine removal reached 89.7%, with the ^{1}H NMR integral decreasing from 2.52 in the abiotic control to 0.26. Methylparaben exhibited a comparable removal efficiency of 89.4%, with its integral decreasing from 2.46 to 0.26. These results indicate that the fungal wetland achieved rapid and effective attenuation of both compounds during the early treatment stage (Figure 57).

The observed degradation behaviour is consistent with the known oxidative metabolic capabilities of *Trametes versicolor*, which produces extracellular enzymes such as laccases and peroxidases capable of initiating the transformation of aromatic and heterocyclic compounds [207–209]. In particular, the efficient early-stage removal of methylparaben suggests effective oxidative activation of the aromatic ester structure. Although caffeine is a smaller and more water-soluble molecule, substantial removal was still achieved within four weeks, indicating broad substrate accessibility under the applied wetland conditions.

Importantly, the caffeine degradation behaviour observed in Wetland B is consistent with the results obtained during lab-scale fungal biodegradation experiments (Section 6.1.3), where *Trametes versicolor* demonstrated efficient caffeine transformation under aerobic conditions. The similarity in qualitative degradation outcomes across experimental scales indicates that the fungal metabolic pathways identified at the lab scale remained functional following integration into the constructed wetland system.

By week 7, the complete disappearance of both caffeine and methylparaben proton signals was observed. The absence of detectable parent resonances indicates removal below the quantification limit of the ^{1}H NMR method. No persistent intermediate signals were detected in the endpoint spectra, suggesting that transformation products did not accumulate at detectable concentrations during the batch treatment period.

Overall, the performance of Wetland B confirms that the applied fungal inoculation and wetland configuration were effective in sustaining oxidative activity and rapidly degrading both target pollutants under batch conditions.

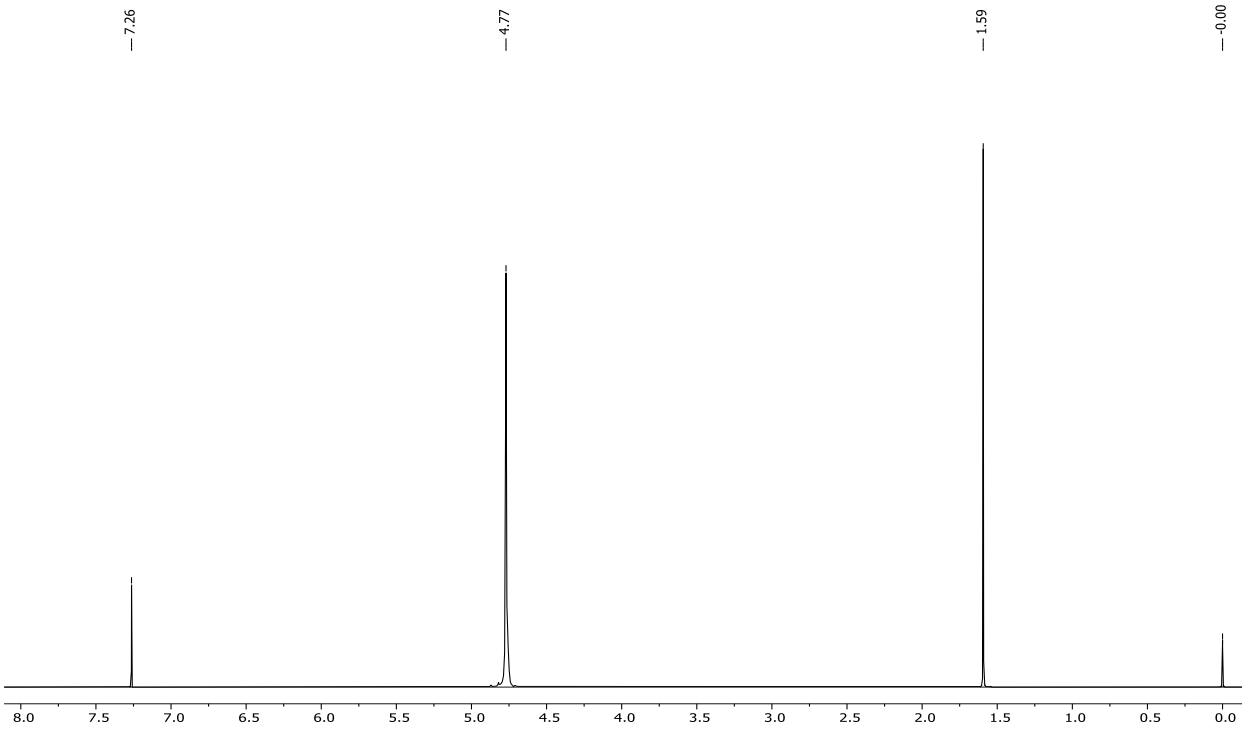

Figure 57. ^{1}H NMR spectrum of wetland B (*Trametes versicolor*) 7 weeks [157]

6.2.2.3 Performance of Wetland C (Fungal-Bacterial Consortium Degradation)

Wetland C, incorporating both fungal and bacterial components, demonstrated compound-dependent degradation behaviour under batch operating conditions. For caffeine, the characteristic proton signal disappeared completely by week 4, indicating removal below the quantification limit of the ^{1}H NMR method. This performance was comparable to that of the bacterial monoculture, indicating that bacterial metabolism alone was sufficient for rapid caffeine degradation and that the consortium provided no measurable kinetic enhancement beyond the bacterial system.

In contrast, methylparaben exhibited intermediate degradation kinetics in the consortium system. At week 4, removal reached 62.6%, exceeding the bacterial system's performance (50.0%) but remaining below that achieved in the fungal wetland (89.4%). This pattern indicates partial functional complementarity between fungal and bacterial processes rather than strong synergistic enhancement. The consortium improved early-stage methylparaben removal compared with bacteria alone, but it did not surpass the oxidative capability of the fungal system during the initial treatment phase.

By week 7, the complete disappearance of both caffeine and methylparaben proton signals was observed in Wetland C. The absence of detectable parent resonances indicates removal below the quantification limit of the ^{1}H NMR method. No persistent intermediate signals were detected in the endpoint spectra, suggesting that transformation products did not accumulate at detectable concentrations during the batch operation period (Figure 58).

The observed performance of Wetland C is consistent with the intended functional design of the hybrid system, in which fungal extracellular oxidative activity and bacterial intracellular metabolism operate in parallel. While the consortium did not accelerate caffeine degradation beyond bacterial performance, it facilitated improved methylparaben attenuation compared to the bacterial monoculture. These results demonstrate that the combined system supports complementary degradation pathways; however, the extent of enhancement is compound-specific and does not constitute universal synergistic behaviour under the tested batch conditions [210–212].

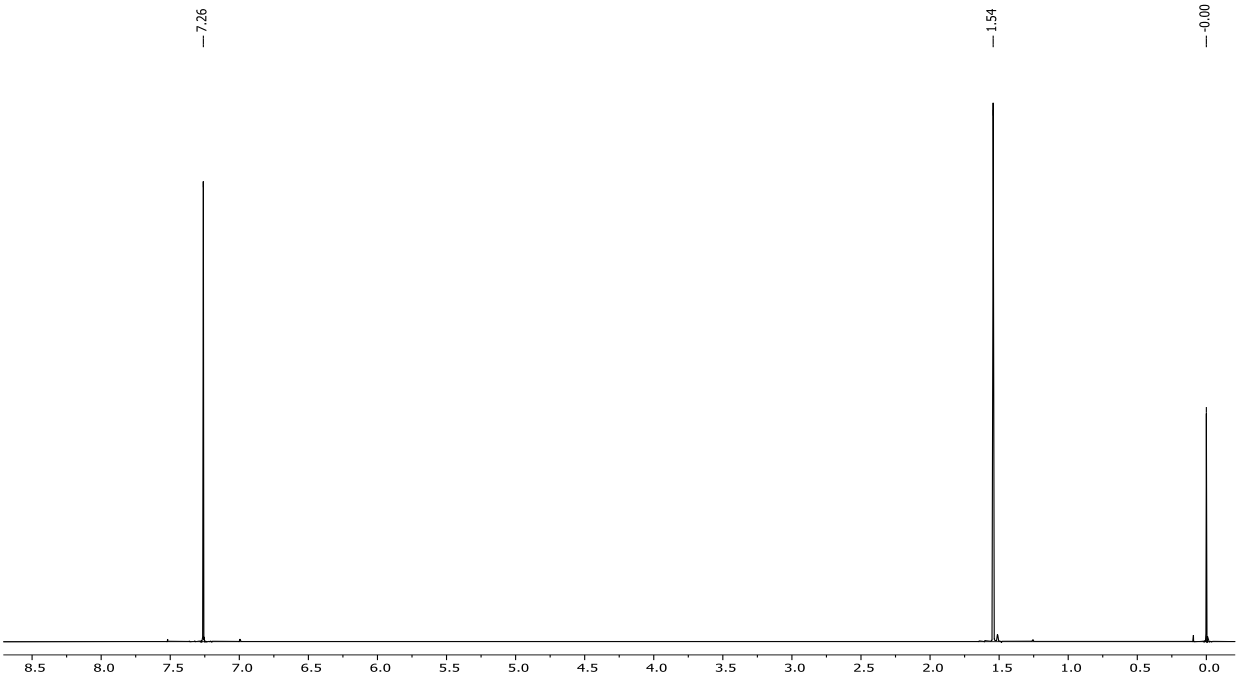

Figure 58. ^{1}H NMR spectrum of wetland C (*Pseudomonas aeruginosa* + *Trametes versicolor*) 7 weeks [157]

The removal efficiencies for caffeine and methylparaben across wetland configurations at Weeks 4 and 7 are summarized in Table 25.

Table 25. Removal efficiency of target pollutants in constructed wetlands based on ^{1}H NMR analysis

Wetland Configuration	Caffeine Integral (4W)	Caffeine Removal 4W (%)	Caffeine Integral (7W)	Caffeine Removal 7W (%)	MeP Integral (4W)	MeP Removal 4W (%)	MeP Integral (7W)	MeP Removal 7W (%)
Wetland D (Control)	2.52	—	2.52	—	2.46	—	2.46	—
Wetland A (Fungi)	0.26	89.7%	0	100*	0.26	89.4%	0	100*
Wetland B (Bacteria)	0	100*	0	100*	1.18	52.0%	0	100*
Wetland C (Fungi + Bacteria)	0	100*	0	100*	0.92	62.6%	0	100*

** Complete disappearance of the characteristic proton signal, indicating removal below the quantification limit of the ^{1}H NMR method.*

All biological wetlands exhibited complete disappearance of caffeine and methylparaben signals by week 7, indicating removal below the quantification limit of the ^{1}H NMR method. However, clear differences in degradation behaviour were observed during the earlier treatment phase (week 4). Results for trichlorocarbanilide (TCC) are not reported, as the compound was insoluble in $CDCl_3$ and could not be reliably analyzed by ^{1}H NMR under the applied analytical conditions.

For caffeine, complete signal disappearance was observed by week 4 in Wetland A (bacterial system, 37 °C) and Wetland C (consortium, 30 °C), whereas Wetland B (fungal system, 25 °C) exhibited 89.7% removal, which was completely removed by week 7. The more rapid caffeine degradation observed in the bacterial and consortium systems may reflect both efficient intracellular bacterial metabolic pathways and operation at higher temperatures, which generally enhance enzymatic reaction rates and microbial growth kinetics. Consequently, while

bacterial metabolism appears highly effective for caffeine degradation, the contribution of elevated temperature cannot be excluded.

In contrast, methylparaben degradation exhibited a different kinetic pattern. Wetland B (fungal system, 25 °C) demonstrated the highest week 4 removal (89.4%), followed by Wetland C (62.6%) and Wetland A (50.0%). The superior early-stage performance of the fungal system suggests that extracellular oxidative enzymes produced by *Trametes versicolor* effectively initiated the transformation of the aromatic ester structure. Notably, despite operating at a lower temperature, the fungal wetland achieved faster initial methylparaben degradation than the bacterial system, indicating that enzymatic capability rather than temperature alone governed degradation kinetics for this compound.

Because the systems were operated at different temperatures, the results should be interpreted as comparative performance under defined operational conditions rather than absolute biological superiority. Nonetheless, the data clearly demonstrate that caffeine is rapidly biodegradable under bacterial and consortium conditions, methylparaben exhibits faster initial transformation in the fungal system, and all biological configurations ultimately achieve complete removal within seven weeks under batch operation.

The findings of this study were interpreted in light of several limitations. First, all experiments were conducted under batch conditions; therefore, the results describe time-dependent degradation behaviour and cannot be directly extrapolated to hydraulic treatment efficiency or continuous-flow wetland performance. Second, the wetland systems were operated at different temperatures (25, 37, and 30 °C), which showed few variations when comparing degradation kinetics across configurations. As microbial activity is temperature-dependent, observed differences in removal rates reflect the combined influence of microbial metabolism and operating temperature rather than biological capability alone.

Additionally, the analytical approach was restricted to compounds soluble in $CDCl_3$; consequently, highly hydrophobic pollutants such as TCC could not be evaluated using ^1H NMR and were excluded from comparative analysis. Degradation was assessed based on the disappearance of parent compound signals.

Trichlorocarbanilide (TCC) degradation could not be directly monitored using NMR spectroscopy due to its extremely low solubility in deuterated chloroform, resulting in the

absence of detectable ^{1}H or ^{13}C NMR signals across all wetland configurations and sampling time points. This analytical limitation arises from the intrinsic chemical structure of TCC, which comprises two chlorinated phenyl rings linked by a urea bridge, conferring high hydrophobicity and poor compatibility with commonly used NMR solvents.

NMR spectroscopy is inherently better suited to relatively polar, structurally simple compounds such as caffeine and methylparaben, whereas hydrophobic antimicrobial agents such as TCC generally require chromatographic or mass-spectrometric techniques for reliable detection and quantification. Consequently, TCC was excluded from NMR-based kinetic evaluation in this study. This limitation underscores the necessity of a multi-analytical approach for comprehensive assessment of pollutant fate in constructed wetlands, as implemented elsewhere in this dissertation through the application of HPTLC for bacterial degradation studies.

Although direct NMR-based evaluation of TCC was not possible, the rapid and effective degradation of caffeine and methylparaben within the same wetland systems indicates favourable conditions for microbial activity and organic pollutant transformation. Such conditions are also relevant to the biodegradation of more persistent compounds such as TCC. Previous studies have reported microbial transformation of TCC by both fungal and bacterial communities under controlled and engineered conditions [168,213,214].

In constructed wetland environments, reported TCC removal efficiencies typically range from 60 to 65%, with sorption to organic matter and porous media contributing substantially to attenuation. However, reliance on sorption alone raises environmental concerns, as transformation products such as carbanilide and dichlorocarbanilide have been detected in surface waters at concentrations up to 615 ng L^{-1}. These products are commonly formed via reductive dechlorination pathways and have been associated with endocrine-disrupting effects, highlighting the importance of distinguishing between physical removal and true biochemical transformation [215–217].

Within the context of this study, the absence of NMR-detectable TCC does not imply a lack of removal; rather, it defines the analytical boundary conditions governing compound-specific evaluation. The deliberate pairing of NMR spectroscopy for soluble pollutants with chromatographic techniques for hydrophobic compounds strengthens the overall

methodological framework of this thesis and ensures that conclusions regarding wetland self-cleaning processes are grounded in chemical realism rather than analytical convenience.

6.2.3 Structural and Biological Insights from Wetland Porous Media

Scanning Electron Microscopy (SEM) was employed to qualitatively assess the surface morphology of the wetland porous media and to examine microbial attachment following system operation. The objective of this analysis was not to quantify microbial biomass, but to evaluate whether the physical properties of the substrate supported stable microbial colonization under mixed-pollutant wetland conditions.

SEM analysis was conducted using a Zeiss EVO MA 15 scanning electron microscope operated under high-vacuum conditions with secondary electron detection. Prior to imaging, samples were sputter-coated with a thin gold layer to enhance surface conductivity and image resolution. Representative micrographs were acquired at multiple magnifications to capture both overall surface texture and localized microbial accumulation.

SEM micrographs of the unused porous substrate (Figure 59a) revealed an irregular, heterogeneous surface morphology characterized by microscale pores, crevices, cracks, and angular edges. Such intrinsic surface roughness and porosity are advantageous in constructed wetland systems, as they increase the available surface area for microbial attachment and create protected micro-niches that can reduce microbial detachment due to hydraulic shear.

In contrast, SEM images obtained after wetland operation (Figure 59b, c, and d) showed pronounced microbial colonization of the substrate surface. These images display extensive coverage of pore walls and surface depressions by dense microbial aggregates, consistent with the establishment of bacterial biofilms. Accumulation of extracellular polymeric substances and clustered biomass within pore spaces indicates stable microbial attachment and retention within the porous matrix.

Higher-magnification micrographs (Figure 59e and 59f) further revealed compact microbial structures occupying intergranular regions and rough surface features. The preferential localization of biomass at highly irregular regions of the substrate suggests that surface roughness promotes physical anchoring and enhances access to nutrients transported through the pore network. Together, these observations confirm that the porous media

effectively support microbial growth by providing structurally favourable sites for biofilm and fungal biomass development within the wetland system.

Although SEM does not distinguish between bacterial and fungal cells at this resolution, the observed surface coverage is consistent with the bio-augmentation strategy employed in the constructed wetlands. The images confirm that the porous media provided a stable physical scaffold for microbial attachment, supporting sustained biological activity throughout the experimental period.

Importantly, these structural observations align with the degradation results presented in Section 6.2.2. The formation of stable biofilms on the wetland media likely contributed to the enhanced and sustained removal efficiencies observed, particularly in the combined fungal-bacterial system. By facilitating close contact between microorganisms, pollutants, and the aqueous phase, the porous substrate plays a critical enabling role in the engineered self-cleaning process.

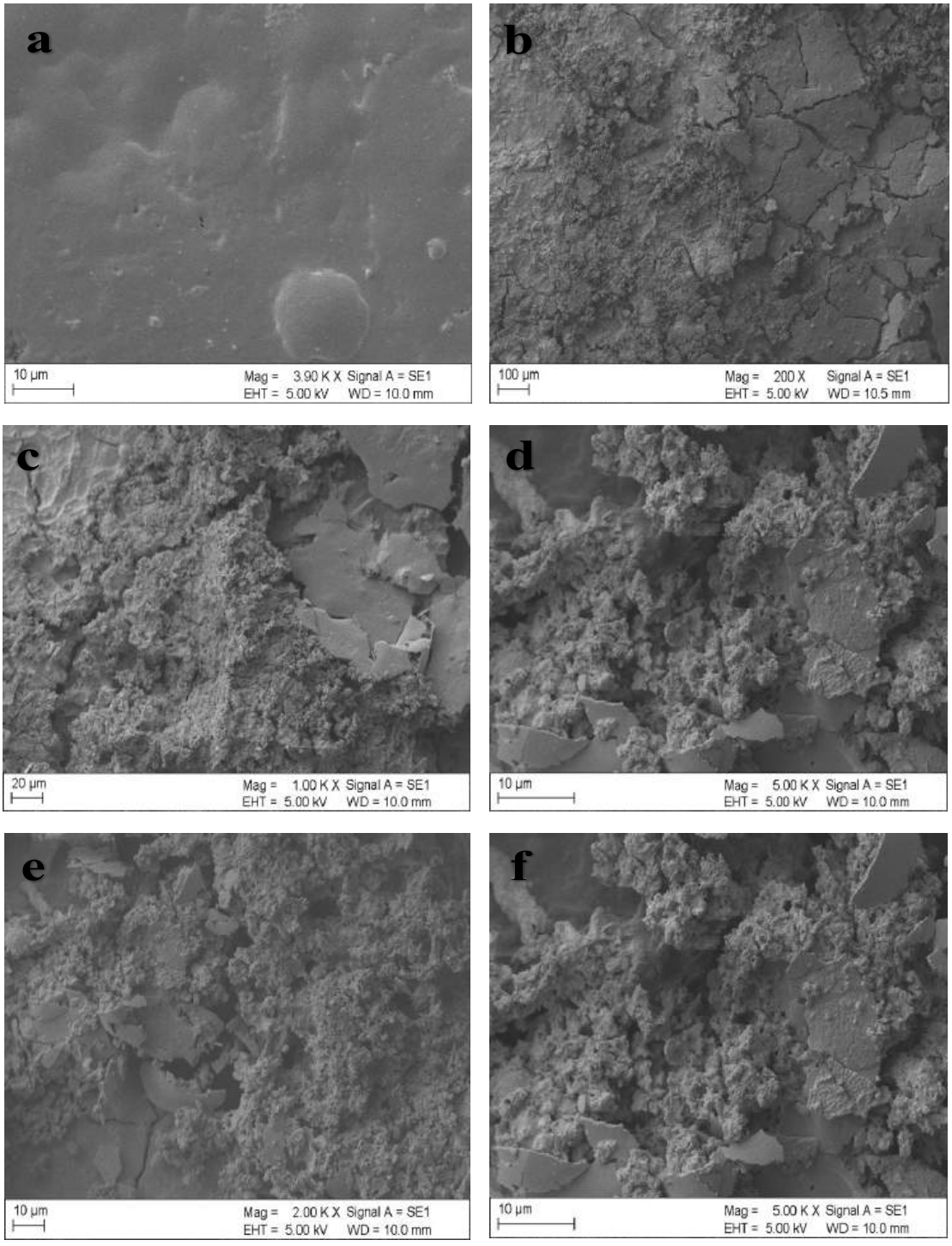

Figure 59. SEM images illustrating microbial colonization of porous media used in the constructed wetland system [157]

Overall, SEM analysis provides direct visual confirmation that the wetland media supported durable microbial colonization under high pollutant loading. While not a quantitative measure of activity, this structural evidence strengthens the mechanistic interpretation of wetland performance by demonstrating that the system architecture was suitable for long-term microbial stabilization rather than transient pollutant attenuation.

6.2.4 Evaluation of Pilot-Scale Wetland Self-Cleaning Performance

The pilot-scale constructed wetland experiments were designed to evaluate whether the microbial self-cleaning mechanisms identified under controlled laboratory conditions remain functional within a spatially structured, ecologically realistic treatment system. By integrating biological stability indicators (Section 6.2.1), pollutant removal performance (Section 6.2.2), and microstructural evidence of microbial attachment and stabilization within the wetland matrix (Section 6.2.3), this section assesses the engineered wetland's effectiveness, robustness, and operational constraints as a self-cleaning platform.

Across all configurations, effective pollutant removal was not attributable to any single system component, but instead emerged from the interaction between microorganisms, porous support media, vegetation, and the aqueous matrix. Biologically compatible porous media enabled microbial attachment and biofilm development, synthetic wastewater provided basal nutrient availability, and plant-microbe interactions within the rhizosphere contributed to a chemically and physically stable environment. This integrated system supported sustained biodegradation under mixed-pollutant loading rather than short-term attenuation driven by adsorption or dilution effects.

Operational stability indicators further confirm that the wetland systems transitioned from initial acclimation to stabilized operation. Controlled pH evolution, consistent plant growth, and microbial tolerance to combined pollutant stress were observed across bio-augmented wetlands, indicating that biological activity remained resilient once establishment was achieved. This stabilization was a prerequisite for reliable pollutant removal and distinguishes sustained self-cleaning from transient degradation during start-up phases.

Among the evaluated configurations, wetlands inoculated with a fungal-bacterial consortium consistently exhibited faster pollutant removal and greater operational stability than monoculture systems. While fungal-only and bacterial-only wetlands ultimately achieved high

removal efficiencies, they required longer adaptation periods and were more sensitive to operational fluctuations. These results indicate that microbial composition influences not only removal efficiency but also system robustness under stress conditions.

The enhanced performance of the consortium wetlands reflects functional complementarity between microbial groups. Fungal communities contributed strong extracellular oxidative activity, facilitating the initial transformation of structurally complex compounds, while bacterial metabolism supported downstream degradation and mineralization of transformation products. This functional partitioning reduced the accumulation of potentially inhibitory intermediates and accelerated overall pollutant turnover at the system level.

Microstructural analysis using scanning electron microscopy provided direct physical evidence supporting these observations. Extensive microbial colonization within surface pores and crevices of the wetland media confirmed that the porous matrix functioned as a stable scaffold for long-term microbial attachment rather than a transient adsorption surface. The persistence of biofilm structures is consistent with the sustained removal performance observed over extended experimental periods.

Synthetic wastewater successfully supported microbial survival, adaptation, and pollutant degradation across all bio-augmented wetlands, despite the absence of nutrient-rich laboratory growth media. Stable performance under these conditions indicates that the microbial communities were able to exploit the intrinsic nutrient content of the wastewater matrix to maintain functional activity throughout the experimental timeframe.

Compound-specific analytical constraints were encountered during wetland-scale evaluation. While caffeine and methylparaben were effectively monitored using solution-state NMR, trichlorocarbanilide (TCC) could not be reliably tracked due to its hydrophobicity and limited solubility in NMR-compatible solvents. This limitation reflects analytical constraints rather than biological inefficacy and underscores the importance of aligning analytical techniques with contaminant chemistry when evaluating wetland systems.

The use of complementary analytical approaches—NMR for soluble compounds and chromatographic techniques for hydrophobic pollutants—represents a methodological strength

of the study. The inability to monitor TCC by NMR at the wetland scale underscores the need for multi-technique frameworks for comprehensive assessment of self-cleaning performance.

Complete exclusion of external microbial inputs was not feasible due to the inherently open nature of wetland systems. Airborne and waterborne microbial ingress occurred despite precautionary measures; however, this did not compromise system performance. Consistently high removal efficiencies across bio-augmented wetlands indicate that the introduced microbial communities established and maintained functional dominance within the wetland matrix, even under ecologically realistic conditions.

The wetland experiments were conducted under batch operation with extended hydraulic retention times, which differs from the continuous-flow operation typically employed in constructed wetlands for wastewater treatment. While this operational mode enabled evaluation of maximum degradation potential under controlled conditions, future studies must address hydraulic optimization to balance treatment efficiency with throughput under continuous-flow regimes. Nevertheless, the accelerated kinetics observed in consortium systems suggest that effective self-cleaning may be achievable at reduced retention times relative to monoculture wetlands.

Overall, the pilot-scale wetland experiments demonstrate that bio-augmented systems can achieve stable, sustained removal of structurally diverse emerging contaminants under mixed-pollutant loading. The observed performance reflects genuine biological self-cleaning supported by microbial stabilization, functional complementarity, and appropriate system architecture, rather than transient physicochemical processes.

6.3 Overall Synthesis and Scale-up Implications

This dissertation investigated whether microbial self-cleaning processes can be deliberately engineered through the rational selection of microorganisms, growth media, and analytical strategies, and whether these processes remain effective when translated from controlled laboratory systems to an ecologically structured constructed wetland. The integrated findings across fungal, bacterial, and consortium-based configurations demonstrate that this objective has been met, establishing a coherent framework linking microbial adaptation, pollutant chemistry, analytical constraints, and system-level performance.

6.3.1 Functional Differentiation Between Natural and Anthropogenic Pollutants

A central outcome of this work is the clear functional differentiation observed between natural pollutants (caffeine and nicotine) and anthropogenic pollutants (methylparaben and trichlorocarbanilide). Natural compounds were preferentially transformed by fungal systems characterized by extracellular oxidative metabolism, whereas anthropogenic contaminants required bacterial or consortium-based pathways capable of targeting ester linkages, urea bonds, and halogenated aromatic structures.

These results demonstrate that pollutant origin alone does not determine biodegradation behaviour. Instead, molecular structure, functional groups, and bioavailability dictate the biological strategy required for effective removal. This distinction provides a chemically grounded basis for microbial selection in engineered self-cleaning systems.

The analytical framework employed in this study was therefore a necessary design decision rather than a methodological convenience. Solution-state NMR proved effective for monitoring soluble natural compounds at elevated concentrations, while HPTLC enabled kinetic resolution of poorly soluble anthropogenic pollutants. The inability to track TCC using NMR further reinforces the principle that analytical selection must follow contaminant chemistry, with direct implications for future wetland monitoring and design.

6.3.2 Microbial Adaptation as the Foundation of Self-Cleaning Performance

Across all experimental scales, microbial adaptation emerged as the primary determinant of degradation efficiency. Both fungi and bacteria exhibited defined tolerance thresholds under mixed-pollutant exposure, yet retained functional activity following acclimation. Once

adapted, microbial performance proved robust to moderate environmental variability, indicating that adaptation outweighed individual physicochemical parameters such as pH or temperature when considered in isolation.

Synthetic wastewater consistently supported microbial survival, growth, and pollutant transformation across laboratory and wetland systems. This confirms that nutrient-rich laboratory media are not a prerequisite for effective biodegradation and that microorganisms can exploit simplified wastewater matrices without loss of function. This finding directly fulfils the media-replacement objective defined in Chapter 3 and has practical implications for engineered treatment systems where nutrient minimization is desirable.

6.3.3 Synergistic Microbial Interactions and Accelerated Degradation Kinetics

The most significant functional advance demonstrated by this work is the kinetic advantage of fungal-bacterial consortia over monoculture systems. While individual fungi or bacteria ultimately achieved high removal efficiencies, consortium systems consistently compressed degradation timescales, achieving near-complete removal of caffeine and methylparaben substantially earlier than single-organism treatments.

This behaviour is mechanistically consistent with a metabolic hand-off model, in which fungal oxidative enzymes initiate transformation of complex molecules, and bacterial metabolism completes downstream degradation and mineralization. Importantly, this synergistic interaction was preserved during scale-up to the constructed wetland system, indicating that microbial self-cleaning is not confined to highly controlled batch environments but can persist within spatially heterogeneous, plant-supported systems.

6.3.4 Translation from Laboratory Systems to Constructed Wetlands

The constructed wetland experiments establish that microbial self-cleaning mechanisms remain operational under increased ecological and structural complexity. Despite the presence of porous media, vegetation, hydraulic gradients, and unavoidable external microbial inputs, bio-augmented wetlands consistently outperformed abiotic controls and monoculture configurations.

Indicators of system stabilization, including pH regulation, sustained plant growth, and SEM-verified microbial attachment, confirm that the wetlands transitioned from acclimation

to stable operation within the experimental timeframe. Although batch operation and elevated pollutant concentrations represent a stress-testing scenario rather than a direct simulation of full-scale wetlands, the results demonstrate proof-of-concept scalability of engineered microbial self-cleaning.

6.3.5 Implications for Engineered Wetland Design and Future Application

Collectively, the findings of this dissertation support a shift from passive contaminant attenuation toward actively engineered microbial self-cleaning wetlands. Key design implications include:
(i) prioritizing functional microbial complementarity over taxonomic diversity,
(ii) employing simplified or synthetic wastewater matrices during system optimization,
(iii) aligning analytical techniques with pollutant chemistry at the design stage, and
(iv) Integrating fungi and bacteria as structurally stabilizing and enzymatically versatile components of wetland systems.

While further research is required to assess long-term performance under continuous-flow conditions and real wastewater matrices, this study provides a robust scientific foundation for such investigations. By demonstrating controlled, scalable, and chemically informed microbial self-cleaning, this work establishes a transferable framework for treating emerging contaminants in surface waters.

The integrated outcomes presented in this chapter define both the capabilities and limitations of bio-augmented constructed wetlands and provide the basis for the conclusions and future research directions presented in Chapter 7.

Chapter 7: General Conclusions and Future Perspectives

This doctoral thesis addressed the critical limitation of degrading and removing recalcitrant emerging contaminants (ECs). Guided by the research objectives defined in Chapter 3, the study systematically developed and validated a biomimetic constructed wetland strategy capable of intensifying microbial self-cleaning processes under environmentally relevant conditions.

The research progressed logically from controlled lab-scale biodegradation experiments to a laboratory-scale engineered wetland system. Across these scales, the work demonstrated that intentional integration of functionally complementary microbial systems, rather than reliance on undefined native communities, provides a robust framework for enhanced pollutant removal. Specifically, the enzymatic versatility of the white-rot fungus *Trametes versicolor* and the metabolic resilience of specialized bacterial degraders (*Alcaligenes-Rhodococcus* consortia at lab scale and *Pseudomonas aeruginosa* at wetland scale) were shown to collectively enable efficient treatment of both natural and anthropogenic pollutants.

The principal scientific achievements of the thesis are summarized below.

7.1 Experimental Conclusions

7.1.1 Lab-Scale Evaluation of Microbial Biodegradation

Lab-scale experiments demonstrated that the white-rot fungus *Trametes versicolor* is highly effective in degrading natural alkaloids under nutrient-limited aqueous conditions. Caffeine and nicotine removal exceeded 97-98% under optimal conditions (25 °C, moderately acidic pH), with effective degradation also maintained in synthetic wastewater and chemically complex natural matrices. These results confirm that fungal systems can successfully adapt from nutrient-rich laboratory media to wastewater-based environments and sustain biodegradation using wastewater-derived nutrients alone.

Bacterial degradation studies using *Alcaligenes-Rhodococcus* consortia confirmed strong tolerance to high concentrations of anthropogenic pollutants. Trichlorocarbanilide was completely removed within 120 h, while methylparaben achieved up to 89.1% removal. Importantly, degradation performance in synthetic wastewater equalled or exceeded that observed in nutrient-rich media at later stages, demonstrating that nutrient limitation can enhance pollutant utilization following microbial adaptation.

Together, these findings validate synthetic wastewater as an active biodegradation matrix that supports microbial growth and enhances contaminant degradation without external nutrient supplementation.

7.1.2 Pilot-scale Evaluation of Microbial Biodegradation Performance

Laboratory-scale constructed wetlands planted with *Phragmites australis* successfully supported wastewater-adapted fungal, bacterial, and combined microbial systems under mixed-pollutant loading. All biological wetlands remained operationally stable for seven weeks, maintaining near-neutral pH and sustained plant growth, confirming successful ecological integration and system acclimation.

Pollutant removal exhibited compound-specific behaviour. Caffeine was rapidly degraded in bacterial and combined systems, while fungal systems achieved complete removal at later stages. In contrast, methylparaben degraded more rapidly in the early stages of the fungal wetland, with the combined system displaying intermediate performance. All biological configurations achieved complete removal of caffeine and methylparaben by Week 7. These results demonstrate functional complementarity, with different microbial groups contributing distinct advantages depending on compound structure.

7.2 Key Conclusions

Based on the integrated experimental evidence generated across lab-scale and wetland-scale investigations, the following conclusions are drawn:

1. **Microbial synergy and adaptation are essential for treating chemically complex wastewater.**

   Fungal and bacterial systems perform distinct yet complementary roles in biodegradation. Even more, a single microbial group alone was sufficient to achieve

rapid and complete removal of chemically diverse contaminant mixtures. The combined fungal-bacterial system consistently demonstrated superior performance, confirming that engineered microbial synergy is a prerequisite for effective self-cleaning of mixed-pollutant wastewater.

2. **Environmental parameters critically govern system efficiency.** Temperature emerged as a dominant control variable, particularly for fungal activity. The pronounced reduction in fungal performance at elevated temperatures demonstrates that effective application of fungal-based systems requires operation within mesophilic ranges or the incorporation of thermal management strategies in engineered treatment units.

3. **Microbial degradation can be stimulated under realistic conditions.** Contrary to the assumption that clean nutrient media inherently promote superior biodegradation, synthetic wastewater matrices often enhanced specific degradation rates. This effect is attributed to nutrient limitation, which forces microorganisms to use target pollutants as primary or secondary substrates for survival. These findings validate the use of synthetic wastewater as a realistic and informative model for evaluating biodegradation performance under environmentally relevant conditions.

4. **Biomimetic constructed wetlands represent scalable treatment platforms** The successful transition from 250 mL lab-scale systems to 30 L laboratory-scale constructed wetlands demonstrates the scalability of the proposed biomimetic approach. The engineered wetland configuration effectively stabilized microbial communities, prevented biomass washout, and sustained biodegradation under high contaminant loading, indicating its suitability as a foundation for low-energy-input, scalable wastewater treatment applications.

7.3 Contribution to Knowledge and Significance of the Study

This doctoral research makes several original and significant contributions to the fields of environmental biotechnology and constructed wetland engineering, particularly regarding the degradation of emerging contaminants in polluted surface waters.

First, this study demonstrates that microbial self-cleaning can be intentionally engineered and intensified by integrating functionally complementary fungal and bacterial degraders.

While previous studies have reported isolated biodegradation by either fungi or bacteria, this work provides systematic, multi-scale evidence that functional complementarity between microbial groups enhances treatment robustness and contaminant coverage under mixed-pollutant conditions. The integration of *Trametes versicolor* and *Pseudomonas aeruginosa* established a reproducible framework in which fungal extracellular oxidative processes facilitate initial transformation of complex compounds, while bacterial metabolism supports further degradation under wastewater-relevant conditions.

Second, this research advances conceptual understanding of wastewater as an active biodegradation matrix rather than a passive pollutant carrier. The use of synthetic wastewater was not limited to experimental convenience; rather, it served as a realistic and mechanistically informative model of polluted surface water. The observed enhancement of pollutant removal in synthetic wastewater compared to clean nutrient media demonstrates that nutrient-complex wastewater environments can actively stimulate microbial degradation by forcing microorganisms to utilize target pollutants within a competitive matrix, rather than relying on simplified laboratory substrates.

This finding represents a key conceptual contribution: polluted wastewater can simultaneously serve as both a nutrient source and a driver of degradation. By exploiting the intrinsic nutrient content of wastewater, microbial systems can be designed to support both microbial growth and pollutant removal without reliance on external nutrient supplementation. This approach directly supports the development of cost-effective, energy-efficient, and environmentally sustainable treatment strategies for wastewater streams contaminated with high concentrations of multiple pollutants.

Third, this study provides a validated scale-up pathway from lab-scale biodegradation experiments to a laboratory-scale biomimetic constructed wetland. The successful transition from batch experiments to an engineered wetland ecosystem demonstrates that enhanced microbial self-cleaning is not limited to controlled laboratory systems but can be stabilized within porous media, plant-associated environments, and mixed-pollutant conditions. This establishes a defensible bridge between mechanistic biodegradation studies and practical wetland-based treatment systems.

Finally, the analytical framework developed in this work constitutes an additional methodological contribution. The combined use of FT-IR for qualitative confirmation, qNMR

and NMR spectroscopy for quantification and removal assessment, and HPTLC for time-resolved biodegradation analysis enabled reliable monitoring under high pollutant loading and clearly defined compound-specific analytical limitations.

Overall, this thesis contributes both mechanistic insight and applied relevance, establishing wastewater-adapted microbial self-cleaning as a scalable, low-input, and biologically driven treatment strategy. The findings provide a strong scientific foundation for future implementation of bio-augmented constructed wetlands in the treatment of polluted surface waters and high-strength wastewater systems.

Chapter 8: Conclusions

Based on the laboratory studies and experiments conducted in the constructed wetland system, the following conclusions can be drawn:

It is possible to develop and validate a strategy for enhancing the self-purification of surface waters based on the deliberate selection, adaptation, and integration of microorganisms capable of degrading caffeine, nicotine, methylparaben, and triclocarban.

1. The targeted enhancement of microbial self-purification processes leads to more efficient removal of selected contaminants compared to natural attenuation processes.
2. The white-rot fungus *Trametes versicolor* demonstrated high efficiency in the biodegradation of natural alkaloids under nutrient-limited conditions, achieving more than 97–98% removal of caffeine and nicotine under optimal environmental conditions.
3. Bacterial consortia (*Alcaligenes–Rhodococcus* and *Pseudomonas aeruginosa*) exhibited high tolerance to anthropogenic contaminants and the ability to effectively degrade compounds such as triclocarban and methylparaben.
4. The integration of fungal and bacterial systems within a single treatment system resulted in complementary metabolic activity, enabling more effective removal of contaminant mixtures with different chemical structures.
5. The composition and availability of nutrients in synthetic wastewater can stimulate biodegradation processes, as the limitation of easily assimilable carbon sources promotes the utilization of contaminants as metabolic substrates.
6. Temperature and other environmental parameters significantly influence biodegradation efficiency, with fungal activity being particularly sensitive to increases in temperature above the mesophilic range.
7. Biomimetic constructed wetland systems planted with *Phragmites australis* enable stable functioning of contaminant-degrading microorganisms and effective removal of the studied compounds under environmentally relevant conditions.
8. Scaling the system from laboratory experiments to a wetland configuration confirmed the feasibility of practical implementation of the proposed strategy for microbial enhancement of self-purification processes.

9. The developed concept of bioaugmented biomimetic wetlands represents a promising, low-energy and scalable solution for supporting the treatment of contaminated surface waters and wastewater containing mixtures of anthropogenic pollutants.

References

1. Rathi, B.S.; Kumar, P.S.; Show, P.-L. A Review on Effective Removal of Emerging Contaminants from Aquatic Systems: Current Trends and Scope for Further Research. *Journal of Hazardous Materials* **2021**, *409*, 124413, doi:10.1016/j.jhazmat.2020.124413.
2. Lavudya, S.; Kalyan, Ch.P.; Sindhu, A.; Shankaraiah, G.; Himabindu, V. Current Challenges and Future Directions of Emerging Contaminants in the Environment. In *Emerging Contaminants in the Environment*; Reddy, K.V., Maddela, N.R., Reddy, A.V.K., Eds.; Emerging Contaminants and Associated Treatment Technologies; Springer Nature Switzerland: Cham, 2026; pp. 455–483 ISBN 978-3-032-10431-1.
3. Chen, Y.; Vymazal, J.; Březinová, T.; Koželuh, M.; Kule, L.; Huang, J.; Chen, Z. Occurrence, Removal and Environmental Risk Assessment of Pharmaceuticals and Personal Care Products in Rural Wastewater Treatment Wetlands. *Science of The Total Environment* **2016**, *566–567*, 1660–1669, doi:10.1016/j.scitotenv.2016.06.069.
4. Akhiladas, E.K.; Chakraborty, S. Bioremediation of Petroleum Refinery Wastewater Using Constructed Wetlands: A Focus on Microbial Diversity and Pollutant Degradation. *International Biodeterioration & Biodegradation* **2025**, *204*, 106152, doi:10.1016/j.ibiod.2025.106152.
5. Annamalai, J.; Ummalyma, S.B.; Pandey, A. Recent Trends in the Microbial Degradation and Bioremediation of Emerging Pollutants in Wastewater Treatment System. In *Development in Wastewater Treatment Research and Processes*; Elsevier, 2022; pp. 99–125 ISBN 978-0-323-85657-7.
6. Ali, M.; Rousseau, D.P.L.; Ahmed, S. A Full-Scale Comparison of Two Hybrid Constructed Wetlands Treating Domestic Wastewater in Pakistan. *Journal of Environmental Management* **2018**, *210*, 349–358, doi:10.1016/j.jenvman.2018.01.040.
7. Van Vliet, M.T.H.; Flörke, M.; Wada, Y. Quality Matters for Water Scarcity. *Nature Geosci* **2017**, *10*, 800–802, doi:10.1038/ngeo3047.
8. Yap, H.C.; Pang, Y.L.; Lim, S.; Abdullah, A.Z.; Ong, H.C.; Wu, C.-H. A Comprehensive Review on State-of-the-Art Photo-, Sono-, and Sonophotocatalytic Treatments to Degrade Emerging Contaminants. *Int. J. Environ. Sci. Technol.* **2019**, *16*, 601–628, doi:10.1007/s13762-018-1961-y.
9. Higgins, T.E.; Sachdev, J.A.; Engleman, S.A. *Toxic Chemicals: Risk Prevention through Use Reduction*; 1st ed.; CRC Press: Boca Raton, 2016; ISBN 978-0-429-10623-1.
10. Butarewicz, A. THE TOXICITY OF SEWAGE FROM SELECTED MUNICIPAL SEWAGE TREATMENT PLANTS. *Inż. Ekolog.* **2015**, *43*, 30–34, doi:10.12912/23920629/58899.
11. Patel, M.; Kumar, R.; Kishor, K.; Mlsna, T.; Pittman, C.U.; Mohan, D. Pharmaceuticals of Emerging Concern in Aquatic Systems: Chemistry, Occurrence, Effects, and Removal Methods. *Chem. Rev.* **2019**, *119*, 3510–3673, doi:10.1021/acs.chemrev.8b00299.
12. Tran, T.M.; Tran-Lam, T.-T.; Mai, H.H.T.; Bach, L.H.T.; Nguyen, H.M.N.; Trinh, H.T.; Dang, L.T.; Minh, T.B.; Quan, T.C.; Hoang, A.Q. Parabens in Personal Care Products and Indoor Dust from Hanoi, Vietnam: Temporal Trends, Emission Sources, and Non-Dietary Exposure through Dust Ingestion. *Science of The Total Environment* **2021**, *761*, 143274, doi:10.1016/j.scitotenv.2020.143274.
13. Barbosa, M.O.; Moreira, N.F.F.; Ribeiro, A.R.; Pereira, M.F.R.; Silva, A.M.T. Occurrence and Removal of Organic Micropollutants: An Overview of the Watch List

of EU Decision 2015/495. *Water Research* **2016**, *94*, 257–279, doi:10.1016/j.watres.2016.02.047.
14. Lutterbeck, C.A.; Colares, G.S.; Dell'Osbel, N.; Da Silva, F.P.; Kist, L.T.; Machado, Ê.L. Hospital Laundry Wastewaters: A Review on Treatment Alternatives, Life Cycle Assessment and Prognosis Scenarios. *Journal of Cleaner Production* **2020**, *273*, 122851, doi:10.1016/j.jclepro.2020.122851.
15. Xiang, Y.; Wu, H.; Li, L.; Ren, M.; Qie, H.; Lin, A. A Review of Distribution and Risk of Pharmaceuticals and Personal Care Products in the Aquatic Environment in China. *Ecotoxicology and Environmental Safety* **2021**, *213*, 112044, doi:10.1016/j.ecoenv.2021.112044.
16. Al-Qaim, F.F.; Mussa, Z.H.; Othman, M.R.; Abdullah, M.P. Removal of Caffeine from Aqueous Solution by Indirect Electrochemical Oxidation Using a Graphite-PVC Composite Electrode: A Role of Hypochlorite Ion as an Oxidising Agent. *Journal of Hazardous Materials* **2015**, *300*, 387–397, doi:10.1016/j.jhazmat.2015.07.007.
17. Nanjundaiah, S.; Mutturi, S.; Bhatt, P. Modeling of Caffeine Degradation Kinetics during Cultivation of Fusarium Solani Using Sucrose as Co-Substrate. *Biochemical Engineering Journal* **2017**, *125*, 73–80, doi:10.1016/j.bej.2017.05.018.
18. Daneshvar, A.; Aboulfadl, K.; Viglino, L.; Broséus, R.; Sauvé, S.; Madoux-Humery, A.-S.; Weyhenmeyer, G.A.; Prévost, M. Evaluating Pharmaceuticals and Caffeine as Indicators of Fecal Contamination in Drinking Water Sources of the Greater Montreal Region. *Chemosphere* **2012**, *88*, 131–139, doi:10.1016/j.chemosphere.2012.03.016.
19. Zucconi, S.; Volpato, C.; Adinolfi, F.; Gandini, E.; Gentile, E.; Loi, A.; Fioriti, L. Gathering Consumption Data on Specific Consumer Groups of Energy Drinks. *EFS3* **2013**, *10*, doi:10.2903/sp.efsa.2013.EN-394.
20. Rudolph, E.; Faerbinger, A.; Koenig, J. Caffeine Intake from All Sources in Adolescents and Young Adults in Austria. *Eur J Clin Nutr* **2014**, *68*, 793–798, doi:10.1038/ejcn.2014.50.
21. Lim, H.S.; Hwang, J.Y.; Choi, J.C.; Kim, M. Assessment of Caffeine Intake in the Korean Population. *Food Additives & Contaminants: Part A* **2015**, *32*, 1786–1798, doi:10.1080/19440049.2015.1077396.
22. Jagoda, A.; Żukowski, W.; Dąbrowska, B. Investigations of the Presence of Caffeine in the Rudawa River, Kraków, Poland. *Environ Monit Assess* **2015**, *187*, 566, doi:10.1007/s10661-015-4760-7.
23. Gardinali, P.R.; Zhao, X. Trace Determination of Caffeine in Surface Water Samples by Liquid Chromatography–Atmospheric Pressure Chemical Ionization–Mass Spectrometry (LC–APCI–MS). *Environment International* **2002**, *28*, 521–528, doi:10.1016/S0160-4120(02)00080-6.
24. Siegener, R.; Chen, R.F. Caffeine in Boston Harbor Seawater. *Marine Pollution Bulletin* **2002**, *44*, 383–387, doi:10.1016/S0025-326X(00)00176-4.
25. Benotti, M.J.; Brownawell, B.J. Microbial Degradation of Pharmaceuticals in Estuarine and Coastal Seawater. *Environmental Pollution* **2009**, *157*, 994–1002, doi:10.1016/j.envpol.2008.10.009.
26. Knee, K.L.; Gossett, R.; Boehm, A.B.; Paytan, A. Caffeine and Agricultural Pesticide Concentrations in Surface Water and Groundwater on the North Shore of Kauai (Hawaii, USA). *Marine Pollution Bulletin* **2010**, *60*, 1376–1382, doi:10.1016/j.marpolbul.2010.04.019.
27. Singh, S.P.; Azua, A.; Chaudhary, A.; Khan, S.; Willett, K.L.; Gardinali, P.R. Occurrence and Distribution of Steroids, Hormones and Selected Pharmaceuticals in South Florida Coastal Environments. *Ecotoxicology* **2010**, *19*, 338–350, doi:10.1007/s10646-009-0416-0.

28. Gonzalez-Rey, M.; Tapie, N.; Le Menach, K.; Dévier, M.-H.; Budzinski, H.; Bebianno, M.J. Occurrence of Pharmaceutical Compounds and Pesticides in Aquatic Systems. *Marine Pollution Bulletin* **2015**, *96*, 384–400, doi:10.1016/j.marpolbul.2015.04.029.
29. Sun, Q.; Li, M.; Ma, C.; Chen, X.; Xie, X.; Yu, C.-P. Seasonal and Spatial Variations of PPCP Occurrence, Removal and Mass Loading in Three Wastewater Treatment Plants Located in Different Urbanization Areas in Xiamen, China. *Environmental Pollution* **2016**, *208*, 371–381, doi:10.1016/j.envpol.2015.10.003.
30. González-Alonso, S.; Merino, L.M.; Esteban, S.; López De Alda, M.; Barceló, D.; Durán, J.J.; López-Martínez, J.; Aceña, J.; Pérez, S.; Mastroianni, N.; et al. Occurrence of Pharmaceutical, Recreational and Psychotropic Drug Residues in Surface Water on the Northern Antarctic Peninsula Region. *Environmental Pollution* **2017**, *229*, 241–254, doi:10.1016/j.envpol.2017.05.060.
31. Rodriguez Del Rey, Z.; Granek, E.F.; Sylvester, S. Occurrence and Concentration of Caffeine in Oregon Coastal Waters. *Marine Pollution Bulletin* **2012**, *64*, 1417–1424, doi:10.1016/j.marpolbul.2012.04.015.
32. Biel-Maeso, M.; Baena-Nogueras, R.M.; Corada-Fernández, C.; Lara-Martín, P.A. Occurrence, Distribution and Environmental Risk of Pharmaceutically Active Compounds (PhACs) in Coastal and Ocean Waters from the Gulf of Cadiz (SW Spain). *Science of The Total Environment* **2018**, *612*, 649–659, doi:10.1016/j.scitotenv.2017.08.279.
33. Mendoza, A.; Zonja, B.; Mastroianni, N.; Negreira, N.; López De Alda, M.; Pérez, S.; Barceló, D.; Gil, A.; Valcárcel, Y. Drugs of Abuse, Cytostatic Drugs and Iodinated Contrast Media in Tap Water from the Madrid Region (Central Spain):A Case Study to Analyse Their Occurrence and Human Health Risk Characterization. *Environment International* **2016**, *86*, 107–118, doi:10.1016/j.envint.2015.11.001.
34. Jagoda, A.; Żukowski, W.; Dąbrowska, B. Investigations of the Presence of Caffeine in the Rudawa River, Kraków, Poland. *Environ Monit Assess* **2015**, *187*, 566, doi:10.1007/s10661-015-4760-7.
35. Loos, R.; Locoro, G.; Contini, S. Occurrence of Polar Organic Contaminants in the Dissolved Water Phase of the Danube River and Its Major Tributaries Using SPE-LC-MS2 Analysis. *Water Research* **2010**, *44*, 2325–2335, doi:10.1016/j.watres.2009.12.035.
36. Dsikowitzky, L.; Schwarzbauer, J.; Littke, R. The Anthropogenic Contribution to the Organic Load of the Lippe River (Germany). Part II: Quantification of Specific Organic Contaminants. *Chemosphere* **2004**, *57*, 1289–1300, doi:10.1016/j.chemosphere.2004.08.053.
37. Togola, A.; Budzinski, H. Analytical Development for Analysis of Pharmaceuticals in Water Samples by SPE and GC–MS. *Anal Bioanal Chem* **2007**, *388*, 627–635, doi:10.1007/s00216-007-1251-x.
38. Froehner, S.; Machado, K.S.; Falcão, F.; Monnich, C.; Bessa, M. Inputs of Domestic and Industrial Sewage in Upper Iguassu, Brazil Identified by Emerging Compounds. *Water Air Soil Pollut* **2011**, *215*, 251–259, doi:10.1007/s11270-010-0475-0.
39. Civilini, M. NICOTINE DECONTAMINATION OF TOBACCO AGRO-INDUSTRIAL WASTE AND ITS DEGRADATION BY MICRO-ORGANISMS. *Waste Management & Research* **1997**, *15*, 349–358, doi:10.1006/wmre.1997.0091.
40. Stanisavljević, I.T.; Lazić, M.L.; Veljković, V.B. Ultrasonic Extraction of Oil from Tobacco (Nicotiana Tabacum L.) Seeds. *Ultrasonics Sonochemistry* **2007**, *14*, 646–652, doi:10.1016/j.ultsonch.2006.10.003.
41. Kondo, T.; Nakano, Y.; Adachi, S.; Murohara, T. Effects of Tobacco Smoking on Cardiovascular Disease. *Circ J* **2019**, *83*, 1980–1985, doi:10.1253/circj.CJ-19-0323.

42. Al-Tamrah, S.A. Spectrophotometric Determination of Nicotine. *Analytica Chimica Acta* **1999**, *379*, 75–80, doi:10.1016/S0003-2670(98)00517-0.
43. Bush, D.; Goniewicz, M.L. A Pilot Study on Nicotine Residues in Houses of Electronic Cigarette Users, Tobacco Smokers, and Non-Users of Nicotine-Containing Products. *International Journal of Drug Policy* **2015**, *26*, 609–611, doi:10.1016/j.drugpo.2015.03.003.
44. Padhiary, S.; Samal, D.; Khandayataray, P.; Murthy, M.K. A Systematic Review Report on Tobacco Products and Its Health Issues in India. *Reviews on Environmental Health* **2021**, *36*, 367–389, doi:10.1515/reveh-2020-0037.
45. Kumar, R.; Tscharke, B.; O'Brien, J.; Mueller, J.F.; Wilkins, C.; Padhye, L.P. Assessment of Drugs of Abuse in a Wastewater Treatment Plant with Parallel Secondary Wastewater Treatment Train. *Science of The Total Environment* **2019**, *658*, 947–957, doi:10.1016/j.scitotenv.2018.12.167.
46. Venohr, M.; Beusch, C.; Goldhammer, T.; Nguyen, H.H.; Podschun, S.; Schmalsch, C.; Wolter, C. Spatial Distribution of Nicotine Concentrations in Berlin's Surface Waters and Their Potential Sources. *Environ Sci Pollut Res* **2025**, *32*, 6784–6803, doi:10.1007/s11356-025-36124-w.
47. Urbaniak, M.; Chinthakindi, S.; Martinez, A.; Hornbuckle, K.C.; Kannan, K. Occurrence of Primary Aromatic Amines and Nicotine in Sediments Collected from the United States. *Science of The Total Environment* **2022**, *851*, 158102, doi:10.1016/j.scitotenv.2022.158102.
48. Hedgespeth, M.L.; Sapozhnikova, Y.; Pennington, P.; Clum, A.; Fairey, A.; Wirth, E. Pharmaceuticals and Personal Care Products (PPCPs) in Treated Wastewater Discharges into Charleston Harbor, South Carolina. *Science of The Total Environment* **2012**, *437*, 1–9, doi:10.1016/j.scitotenv.2012.07.076.
49. Baker, D.R.; Kasprzyk-Hordern, B. Spatial and Temporal Occurrence of Pharmaceuticals and Illicit Drugs in the Aqueous Environment and during Wastewater Treatment: New Developments. *Science of The Total Environment* **2013**, *454–455*, 442–456, doi:10.1016/j.scitotenv.2013.03.043.
50. Evgenidou, E.N.; Konstantinou, I.K.; Lambropoulou, D.A. Occurrence and Removal of Transformation Products of PPCPs and Illicit Drugs in Wastewaters: A Review. *Science of The Total Environment* **2015**, *505*, 905–926, doi:10.1016/j.scitotenv.2014.10.021.
51. Estévez, E.; Cabrera, M.D.C.; Molina-Díaz, A.; Robles-Molina, J.; Palacios-Díaz, M.D.P. Screening of Emerging Contaminants and Priority Substances (2008/105/EC) in Reclaimed Water for Irrigation and Groundwater in a Volcanic Aquifer (Gran Canaria, Canary Islands, Spain). *Science of The Total Environment* **2012**, *433*, 538–546, doi:10.1016/j.scitotenv.2012.06.031.
52. Verovšek, T.; Heath, D.; Heath, E. Occurrence, Fate and Determination of Tobacco (Nicotine) and Alcohol (Ethanol) Residues in Waste- and Environmental Waters. *Trends in Environmental Analytical Chemistry* **2022**, *34*, e00164, doi:10.1016/j.teac.2022.e00164.
53. Albero, B.; Pérez, R.A.; Sánchez-Brunete, C.; Tadeo, J.L. Occurrence and Analysis of Parabens in Municipal Sewage Sludge from Wastewater Treatment Plants in Madrid (Spain). *Journal of Hazardous Materials* **2012**, *239–240*, 48–55, doi:10.1016/j.jhazmat.2012.05.017.
54. Molins-Delgado, D.; Díaz-Cruz, M.S.; Barceló, D. Ecological Risk Assessment Associated to the Removal of Endocrine-Disrupting Parabens and Benzophenone-4 in Wastewater Treatment. *Journal of Hazardous Materials* **2016**, *310*, 143–151, doi:10.1016/j.jhazmat.2016.02.030.

55. Bolujoko, N.B.; Unuabonah, E.I.; Alfred, M.O.; Ogunlaja, A.; Ogunlaja, O.O.; Omorogie, M.O.; Olukanni, O.D. Toxicity and Removal of Parabens from Water: A Critical Review. *Science of The Total Environment* **2021**, *792*, 148092, doi:10.1016/j.scitotenv.2021.148092.
56. Błędzka, D.; Gromadzińska, J.; Wąsowicz, W. Parabens. From Environmental Studies to Human Health. *Environment International* **2014**, *67*, 27–42, doi:10.1016/j.envint.2014.02.007.
57. Mitra, P.; Chatterjee, S.; Paul, N.; Ghosh, S.; Das, M. An Overview of Endocrine Disrupting Chemical Paraben and Search for An Alternative – A Review. *Proc Zool Soc* **2021**, *74*, 479–493, doi:10.1007/s12595-021-00418-x.
58. Hager, E.; Chen, J.; Zhao, L. Minireview: Parabens Exposure and Breast Cancer. *IJERPH* **2022**, *19*, 1873, doi:10.3390/ijerph19031873.
59. Downs, C.A.; Amin, M.M.; Tabatabaeian, M.; Chavoshani, A.; Amjadi, E.; Afshari, A.; Kelishadi, R. Parabens Preferentially Accumulate in Metastatic Breast Tumors Compared to Benign Breast Tumors and the Association of Breast Cancer Risk Factors with Paraben Accumulation. *Environmental Advances* **2023**, *11*, 100325, doi:10.1016/j.envadv.2022.100325.
60. Kasprzyk-Hordern, B.; Dinsdale, R.M.; Guwy, A.J. The Occurrence of Pharmaceuticals, Personal Care Products, Endocrine Disruptors and Illicit Drugs in Surface Water in South Wales, UK. *Water Research* **2008**, *42*, 3498–3518, doi:10.1016/j.watres.2008.04.026.
61. González-Mariño, I.; Quintana, J.B.; Rodríguez, I.; Cela, R. Simultaneous Determination of Parabens, Triclosan and Triclocarban in Water by Liquid Chromatography/Electrospray Ionisation Tandem Mass Spectrometry. *Rapid Comm Mass Spectrometry* **2009**, *23*, 1756–1766, doi:10.1002/rcm.4069.
62. Kimura, K.; Kameda, Y.; Yamamoto, H.; Nakada, N.; Tamura, I.; Miyazaki, M.; Masunaga, S. Occurrence of Preservatives and Antimicrobials in Japanese Rivers. *Chemosphere* **2014**, *107*, 393–399, doi:10.1016/j.chemosphere.2014.01.008.
63. Li, W.; Gao, L.; Shi, Y.; Wang, Y.; Liu, J.; Cai, Y. Spatial Distribution, Temporal Variation and Risks of Parabens and Their Chlorinated Derivatives in Urban Surface Water in Beijing, China. *Science of The Total Environment* **2016**, *539*, 262–270, doi:10.1016/j.scitotenv.2015.08.150.
64. Evans, W.A.; Davies, P.J.; McRae, C. The Occurrence of Methyl, Ethyl, Propyl, and Butyl Parabens in the Urban Rivers and Stormwaters of Sydney, Australia. *Environ. Sci.: Water Res. Technol.* **2016**, *2*, 733–742, doi:10.1039/C5EW00240K.
65. Xue, J.; Kannan, K. Accumulation Profiles of Parabens and Their Metabolites in Fish, Black Bear, and Birds, Including Bald Eagles and Albatrosses. *Environment International* **2016**, *94*, 546–553, doi:10.1016/j.envint.2016.06.015.
66. Kung, T.A.; Lee, S.H.; Yang, T.C.; Wang, W.H. Survey of Selected Personal Care Products in Surface Water of Coral Reefs in Kenting National Park, Taiwan. *Science of The Total Environment* **2018**, *635*, 1302–1307, doi:10.1016/j.scitotenv.2018.04.115.
67. Zhao, X.; Qiu, W.; Zheng, Y.; Xiong, J.; Gao, C.; Hu, S. Occurrence, Distribution, Bioaccumulation, and Ecological Risk of Bisphenol Analogues, Parabens and Their Metabolites in the Pearl River Estuary, South China. *Ecotoxicology and Environmental Safety* **2019**, *180*, 43–52, doi:10.1016/j.ecoenv.2019.04.083.
68. Lincho, J.; Martins, R.C.; Gomes, J. Paraben Compounds—Part I: An Overview of Their Characteristics, Detection, and Impacts. *Applied Sciences* **2021**, *11*, 2307, doi:10.3390/app11052307.

69. Gao, C.-J.; Kannan, K. Phthalates, Bisphenols, Parabens, and Triclocarban in Feminine Hygiene Products from the United States and Their Implications for Human Exposure. *Environment International* **2020**, *136*, 105465, doi:10.1016/j.envint.2020.105465.
70. Styszko, K.; Proctor, K.; Castrignanò, E.; Kasprzyk-Hordern, B. Occurrence of Pharmaceutical Residues, Personal Care Products, Lifestyle Chemicals, Illicit Drugs and Metabolites in Wastewater and Receiving Surface Waters of Krakow Agglomeration in South Poland. *Science of The Total Environment* **2021**, *768*, 144360, doi:10.1016/j.scitotenv.2020.144360.
71. Senta, I.; Rodríguez-Mozaz, S.; Corominas, L.; Covaci, A.; Petrovic, M. Applicability of an On-Line Solid-Phase Extraction Liquid Chromatography – Tandem Mass Spectrometry for the Wastewater-Based Assessment of Human Exposure to Chemicals from Personal Care and Household Products. *Science of The Total Environment* **2022**, *845*, 157309, doi:10.1016/j.scitotenv.2022.157309.
72. Evans, W.A.; Davies, P.J.; McRae, C. The Occurrence of Methyl, Ethyl, Propyl, and Butyl Parabens in the Urban Rivers and Stormwaters of Sydney, Australia. *Environ. Sci.: Water Res. Technol.* **2016**, *2*, 733–742, doi:10.1039/C5EW00240K.
73. Wang, C.-F.; Tian, Y. Reproductive Endocrine-Disrupting Effects of Triclosan: Population Exposure, Present Evidence and Potential Mechanisms. *Environmental Pollution* **2015**, *206*, 195–201, doi:10.1016/j.envpol.2015.07.001.
74. Gautam, P.; Carsella, J.S.; Kinney, C.A. Presence and Transport of the Antimicrobials Triclocarban and Triclosan in a Wastewater-Dominated Stream and Freshwater Environment. *Water Research* **2014**, *48*, 247–256, doi:10.1016/j.watres.2013.09.032.
75. Mulla, S.I.; Hu, A.; Wang, Y.; Sun, Q.; Huang, S.-L.; Wang, H.; Yu, C.-P. Degradation of Triclocarban by a Triclosan-Degrading Sphingomonas Sp. Strain YL-JM2C. *Chemosphere* **2016**, *144*, 292–296, doi:10.1016/j.chemosphere.2015.08.034.
76. Liang, J.; Zhang, L.; Li, C.; Mo, Z.; Ye, M.; Zhu, Z.; Sun, S.; Wong, J.W.C. Triclocarban Transformation and Removal in Sludge Conditioning Using Chalcopyrite–Triggered Percarbonate Treatment. *Journal of Hazardous Materials* **2024**, *463*, 132944, doi:10.1016/j.jhazmat.2023.132944.
77. Heidler, J.; Sapkota, A.; Halden, R.U. Partitioning, Persistence, and Accumulation in Digested Sludge of the Topical Antiseptic Triclocarban during Wastewater Treatment. *Environ. Sci. Technol.* **2006**, *40*, 3634–3639, doi:10.1021/es052245n.
78. Bedoux, G.; Roig, B.; Thomas, O.; Dupont, V.; Le Bot, B. Occurrence and Toxicity of Antimicrobial Triclosan and By-Products in the Environment. *Environ Sci Pollut Res* **2012**, *19*, 1044–1065, doi:10.1007/s11356-011-0632-z.
79. Lozano, N.; Rice, C.P.; Ramirez, M.; Torrents, A. Fate of Triclocarban, Triclosan and Methyltriclosan during Wastewater and Biosolids Treatment Processes. *Water Research* **2013**, *47*, 4519–4527, doi:10.1016/j.watres.2013.05.015.
80. Lapen, D.R.; Topp, E.; Metcalfe, C.D.; Li, H.; Edwards, M.; Gottschall, N.; Bolton, P.; Curnoe, W.; Payne, M.; Beck, A. Pharmaceutical and Personal Care Products in Tile Drainage Following Land Application of Municipal Biosolids. *Science of The Total Environment* **2008**, *399*, 50–65, doi:10.1016/j.scitotenv.2008.02.025.
81. Wei, L.; Qiao, P.; Shi, Y.; Ruan, Y.; Yin, J.; Wu, Q.; Shao, B. Triclosan/Triclocarban Levels in Maternal and Umbilical Blood Samples and Their Association with Fetal Malformation. *Clinica Chimica Acta* **2017**, *466*, 133–137, doi:10.1016/j.cca.2016.12.024.
82. McAvoy, D.C.; Schatowitz, B.; Jacob, M.; Hauk, A.; Eckhoff, W.S. Measurement of Triclosan in Wastewater Treatment Systems. *Enviro Toxic and Chemistry* **2002**, *21*, 1323–1329, doi:10.1002/etc.5620210701.

83. Li, N.; Li, J.; Zhang, Q.; Gao, S.; Quan, X.; Liu, P.; Xu, C. Effects of Endocrine Disrupting Chemicals in Host Health: Three-Way Interactions between Environmental Exposure, Host Phenotypic Responses, and Gut Microbiota. *Environmental Pollution* **2021**, *271*, 116387, doi:10.1016/j.envpol.2020.116387.
84. Lee, J.-W.; Lee, H.-K.; Moon, H.-B. Contamination and Spatial Distribution of Parabens, Their Metabolites and Antimicrobials in Sediment from Korean Coastal Waters. *Ecotoxicology and Environmental Safety* **2019**, *180*, 185–191, doi:10.1016/j.ecoenv.2019.05.012.
85. Halden, R.U.; Paull, D.H. Co-Occurrence of Triclocarban and Triclosan in U.S. Water Resources. *Environ. Sci. Technol.* **2005**, *39*, 1420–1426, doi:10.1021/es049071e.
86. Halden, R.U.; Paull, D.H. Co-Occurrence of Triclocarban and Triclosan in U.S. Water Resources. *Environ. Sci. Technol.* **2005**, *39*, 1420–1426, doi:10.1021/es049071e.
87. Chen, Z.-F.; Wen, H.-B.; Dai, X.; Yan, S.-C.; Zhang, H.; Chen, Y.-Y.; Du, Z.; Liu, G.; Cai, Z. Contamination and Risk Profiles of Triclosan and Triclocarban in Sediments from a Less Urbanized Region in China. *Journal of Hazardous Materials* **2018**, *357*, 376–383, doi:10.1016/j.jhazmat.2018.06.020.
88. Chen, J.; Meng, X.; Bergman, A.; Halden, R.U. Nationwide Reconnaissance of Five Parabens, Triclosan, Triclocarban and Its Transformation Products in Sewage Sludge from China. *Journal of Hazardous Materials* **2019**, *365*, 502–510, doi:10.1016/j.jhazmat.2018.11.021.
89. Wang, Z.; Li, X.; Liu, H.; Zhou, T.; Li, J.; Li, Y.; Lin, C.S.K.; Wang, Q. Triclosan in Sludge: Exploring Its Journey from the Sewage Treatment Plants to Land Application and Potential Impacts on the Environment. *Critical Reviews in Environmental Science and Technology* **2024**, *54*, 1340–1363, doi:10.1080/10643389.2024.2309846.
90. Schwarzenbach, R.P.; Escher, B.I.; Fenner, K.; Hofstetter, T.B.; Johnson, C.A.; Von Gunten, U.; Wehrli, B. The Challenge of Micropollutants in Aquatic Systems. *Science* **2006**, *313*, 1072–1077, doi:10.1126/science.1127291.
91. Fenner, K.; Canonica, S.; Wackett, L.P.; Elsner, M. Evaluating Pesticide Degradation in the Environment: Blind Spots and Emerging Opportunities. *Science* **2013**, *341*, 752–758, doi:10.1126/science.1236281.
92. Barnes, K.K.; Christenson, S.C.; Kolpin, D.W.; Focazio, M.J.; Furlong, E.T.; Zaugg, S.D.; Meyer, M.T.; Barber, L.B. Pharmaceuticals and Other Organic Waste Water Contaminants Within a Leachate Plume Downgradient of a Municipal Landfill. *Groundwater Monitoring & Remediation* **2004**, *24*, 119–126, doi:10.1111/j.1745-6592.2004.tb00720.x.
93. Luo, Y.; Guo, W.; Ngo, H.H.; Nghiem, L.D.; Hai, F.I.; Zhang, J.; Liang, S.; Wang, X.C. A Review on the Occurrence of Micropollutants in the Aquatic Environment and Their Fate and Removal during Wastewater Treatment. *Science of The Total Environment* **2014**, *473–474*, 619–641, doi:10.1016/j.scitotenv.2013.12.065.
94. Aus Der Beek, T.; Weber, F.-A.; Bergmann, A.; Hickmann, S.; Ebert, I.; Hein, A.; Küster, A. Pharmaceuticals in the Environment—Global Occurrences and Perspectives. *Environmental Toxicology and Chemistry* **2015**, *35*, 823–835, doi:10.1002/etc.3339.
95. Kozuch, O.; Mayer, V. Pig Kidney Epithelial (PS) Cells: A Perfect Tool for the Study of Flaviviruses and Some Other Arboviruses. *Acta Virol* **1975**, *19*, 498.
96. Helbling, D.E.; Johnson, D.R.; Honti, M.; Fenner, K. Micropollutant Biotransformation Kinetics Associate with WWTP Process Parameters and Microbial Community Characteristics. *Environ. Sci. Technol.* **2012**, *46*, 10579–10588, doi:10.1021/es3019012.

97. Onesios, K.M.; Yu, J.T.; Bouwer, E.J. Biodegradation and Removal of Pharmaceuticals and Personal Care Products in Treatment Systems: A Review. *Biodegradation* **2009**, *20*, 441–466, doi:10.1007/s10532-008-9237-8.
98. Sun, B.; Wang, Y.; Xiang, Y.; Shang, C. Influence of Pre-Ozonation of DOM on Micropollutant Abatement by UV-Based Advanced Oxidation Processes. *Journal of Hazardous Materials* **2020**, *391*, 122201, doi:10.1016/j.jhazmat.2020.122201.
99. Ateş, H.; Argun, M.E. Advanced Oxidation of Landfill Leachate: Removal of Micropollutants and Identification of by-Products. *Journal of Hazardous Materials* **2021**, *413*, 125326, doi:10.1016/j.jhazmat.2021.125326.
100. Yang, Y.; Chen, Z.; Zhang, J.; Wu, S.; Yang, L.; Chen, L.; Shao, Y. The Challenge of Micropollutants in Surface Water of the Yangtze River. *Science of The Total Environment* **2021**, *780*, 146537, doi:10.1016/j.scitotenv.2021.146537.
101. Benotti, M.J.; Brownawell, B.J. Microbial Degradation of Pharmaceuticals in Estuarine and Coastal Seawater. *Environmental Pollution* **2009**, *157*, 994–1002, doi:10.1016/j.envpol.2008.10.009.
102. Head, I.M.; Jones, D.M.; Röling, W.F.M. Marine Microorganisms Make a Meal of Oil. *Nat Rev Microbiol* **2006**, *4*, 173–182, doi:10.1038/nrmicro1348.
103. Helbling, D.E.; Johnson, D.R.; Honti, M.; Fenner, K. Micropollutant Biotransformation Kinetics Associate with WWTP Process Parameters and Microbial Community Characteristics. *Environ. Sci. Technol.* **2012**, *46*, 10579–10588, doi:10.1021/es3019012.
104. Van Der Meer, J.R. Environmental Pollution Promotes Selection of Microbial Degradation Pathways. *Frontiers in Ecology and the Environment* **2006**, *4*, 35–42, doi:10.1890/1540-9295(2006)004%5B0035:EPPSOM%5D2.0.CO;2.
105. Johnson, D.R.; Helbling, D.E.; Lee, T.K.; Park, J.; Fenner, K.; Kohler, H.-P.E.; Ackermann, M. Association of Biodiversity with the Rates of Micropollutant Biotransformations among Full-Scale Wastewater Treatment Plant Communities. *Appl Environ Microbiol* **2015**, *81*, 666–675, doi:10.1128/AEM.03286-14.
106. Verlicchi, P.; Al Aukidy, M.; Zambello, E. Occurrence of Pharmaceutical Compounds in Urban Wastewater: Removal, Mass Load and Environmental Risk after a Secondary Treatment—A Review. *Science of The Total Environment* **2012**, *429*, 123–155, doi:10.1016/j.scitotenv.2012.04.028.
107. Nika, C.E.; Gusmaroli, L.; Ghafourian, M.; Atanasova, N.; Buttiglieri, G.; Katsou, E. Nature-Based Solutions as Enablers of Circularity in Water Systems: A Review on Assessment Methodologies, Tools and Indicators. *Water Research* **2020**, *183*, 115988, doi:10.1016/j.watres.2020.115988.
108. Jain, R.; Gaur, A.; Suravajhala, R.; Chauhan, U.; Pant, M.; Tripathi, V.; Pant, G. Microplastic Pollution: Understanding Microbial Degradation and Strategies for Pollutant Reduction. *Science of The Total Environment* **2023**, *905*, 167098, doi:10.1016/j.scitotenv.2023.167098.
109. Blanco, P.; Hernando-Amado, S.; Reales-Calderon, J.; Corona, F.; Lira, F.; Alcalde-Rico, M.; Bernardini, A.; Sanchez, M.; Martinez, J. Bacterial Multidrug Efflux Pumps: Much More Than Antibiotic Resistance Determinants. *Microorganisms* **2016**, *4*, 14, doi:10.3390/microorganisms4010014.
110. Zahmatkesh, S.; Bokhari, A.; Karimian, M.; Zahra, M.M.A.; Sillanpää, M.; Panchal, H.; Alrubaie, A.J.; Rezakhani, Y. A Comprehensive Review of Various Approaches for Treatment of Tertiary Wastewater with Emerging Contaminants: What Do We Know? *Environ Monit Assess* **2022**, *194*, 884, doi:10.1007/s10661-022-10503-z.
111. De Marines, F.; Cruciata, I.; Di Bella, G.; Di Trapani, D.; Giustra, M.G.; Scirè Calabrisotto, L.; Greco Lucchina, P.; Quatrini, P.; Viviani, G. Degradation of 1,2-

Dichloroethane in Real Polluted Groundwater by Using Enriched Bacterial Consortia in Aerobic and Anaerobic Laboratory-Scale Conditions. *International Biodeterioration & Biodegradation* **2023**, *183*, 105644, doi:10.1016/j.ibiod.2023.105644.
112. Azubuike, C.C.; Chikere, C.B.; Okpokwasili, G.C. Bioremediation Techniques–Classification Based on Site of Application: Principles, Advantages, Limitations and Prospects. *World J Microbiol Biotechnol* **2016**, *32*, 180, doi:10.1007/s11274-016-2137-x.
113. Dvořák, L.; Gómez, M.; Dolina, J.; Černín, A. Anaerobic Membrane Bioreactors—a Mini Review with Emphasis on Industrial Wastewater Treatment: Applications, Limitations and Perspectives. *Desalination and Water Treatment* **2016**, *57*, 19062–19076, doi:10.1080/19443994.2015.1100879.
114. Kadlec, R.H.; Wallace, S. *Treatment Wetlands*; 0 ed.; CRC Press, 2008; ISBN 978-0-429-13795-2.
115. Vymazal, J.; Zhao, Y.; Mander, Ü. Recent Research Challenges in Constructed Wetlands for Wastewater Treatment: A Review. *Ecological Engineering* **2021**, *169*, 106318, doi:10.1016/j.ecoleng.2021.106318.
116. Brix, H. Functions of Macrophytes in Constructed Wetlands. *Water Science and Technology* **1994**, *29*, 71–78, doi:10.2166/wst.1994.0160.
117. Hijosa-Valsero, M.; Fink, G.; Schlüsener, M.P.; Sidrach-Cardona, R.; Martín-Villacorta, J.; Ternes, T.; Bécares, E. Removal of Antibiotics from Urban Wastewater by Constructed Wetland Optimization. *Chemosphere* **2011**, *83*, 713–719, doi:10.1016/j.chemosphere.2011.02.004.
118. Gargallo, S.; Martín, M.; Oliver, N.; Hernández-Crespo, C. Sedimentation and Resuspension Modelling in Free Water Surface Constructed Wetlands. *Ecological Engineering* **2017**, *98*, 318–329, doi:10.1016/j.ecoleng.2016.09.014.
119. Solano, M.L.; Soriano, P.; Ciria, M.P. Constructed Wetlands as a Sustainable Solution for Wastewater Treatment in Small Villages. *Biosystems Engineering* **2004**, *87*, 109–118, doi:10.1016/j.biosystemseng.2003.10.005.
120. Liang, Y.; Zhu, H.; Bañuelos, G.; Yan, B.; Zhou, Q.; Yu, X.; Cheng, X. Constructed Wetlands for Saline Wastewater Treatment: A Review. *Ecological Engineering* **2017**, *98*, 275–285, doi:10.1016/j.ecoleng.2016.11.005.
121. Arden, S.; Ma, X. Constructed Wetlands for Greywater Recycle and Reuse: A Review. *Science of The Total Environment* **2018**, *630*, 587–599, doi:10.1016/j.scitotenv.2018.02.218.
122. Fletcher, D.E.; Lindell, A.H.; Stankus, P.T.; Fletcher, N.D.; Lindell, B.E.; McArthur, J.V. Metal Accumulation in Dragonfly Nymphs and Crayfish as Indicators of Constructed Wetland Effectiveness. *Environmental Pollution* **2020**, *256*, 113387, doi:10.1016/j.envpol.2019.113387.
123. Dotro, G.; Langergraber, G.; Molle, P.; Nivala, J.; Puigagut, J.; Stein, O.; Von Sperling, M. उपचार आर्द्रभूमियाँ; IWA Publishing, 2021; ISBN 978-1-78040-877-4.
124. Ji, J.; Kakade, A.; Yu, Z.; Khan, A.; Liu, P.; Li, X. Anaerobic Membrane Bioreactors for Treatment of Emerging Contaminants: A Review. *Journal of Environmental Management* **2020**, *270*, 110913, doi:10.1016/j.jenvman.2020.110913.
125. Nuamah, L.A.; Li, Y.; Pu, Y.; Nwankwegu, A.S.; Haikuo, Z.; Norgbey, E.; Banahene, P.; Bofah-Buoh, R. Constructed Wetlands, Status, Progress, and Challenges. The Need for Critical Operational Reassessment for a Cleaner Productive Ecosystem. *Journal of Cleaner Production* **2020**, *269*, 122340, doi:10.1016/j.jclepro.2020.122340.
126. Verlicchi, P.; Al Aukidy, M.; Zambello, E. Occurrence of Pharmaceutical Compounds in Urban Wastewater: Removal, Mass Load and Environmental Risk after a Secondary

Treatment—A Review. *Science of The Total Environment* **2012**, *429*, 123–155, doi:10.1016/j.scitotenv.2012.04.028.
127. Horemans, B.; Bers, K.; Ruiz Romero, E.; Pose Juan, E.; Dunon, V.; De Mot, R.; Springael, D. Functional Redundancy of Linuron Degradation in Microbial Communities in Agricultural Soil and Biopurification Systems. *Appl Environ Microbiol* **2016**, *82*, 2843–2853, doi:10.1128/AEM.04018-15.
128. Philippot, L.; Griffiths, B.S.; Langenheder, S. Microbial Community Resilience across Ecosystems and Multiple Disturbances. *Microbiol Mol Biol Rev* **2021**, *85*, e00026-20, doi:10.1128/MMBR.00026-20.
129. Schwarzenbach, R.P.; Egli, T.; Hofstetter, T.B.; Von Gunten, U.; Wehrli, B. Global Water Pollution and Human Health. *Annu. Rev. Environ. Resour.* **2010**, *35*, 109–136, doi:10.1146/annurev-environ-100809-125342.
130. Introduction to Membrane Biological Reactors. In *Membrane Biological Reactors*; Hai, F.I., Yamamoto, K., Lee, C.-H., Eds.; IWA Publishing, 2019; pp. 1–34 ISBN 978-1-78040-917-7.
131. Vymazal, J. Constructed Wetlands for Wastewater Treatment: Five Decades of Experience. *Environ. Sci. Technol.* **2011**, *45*, 61–69, doi:10.1021/es101403q.
132. Matamoros, V.; Arias, C.; Brix, H.; Bayona, J.M. Removal of Pharmaceuticals and Personal Care Products (PPCPs) from Urban Wastewater in a Pilot Vertical Flow Constructed Wetland and a Sand Filter. *Environ. Sci. Technol.* **2007**, *41*, 8171–8177, doi:10.1021/es071594+.
133. Zhang, Y.; Shen, M.; Tian, Y.; Zeng, G. Cyclic Volatile Methylsiloxanes in Sediment, Soil, and Surface Water from Dongting Lake, China. *J Soils Sediments* **2018**, *18*, 2063–2071, doi:10.1007/s11368-018-1948-9.
134. Oral, H.V.; Carvalho, P.; Gajewska, M.; Ursino, N.; Masi, F.; Hullebusch, E.D.V.; Kazak, J.K.; Exposito, A.; Cipolletta, G.; Andersen, T.R.; et al. A Review of Nature-Based Solutions for Urban Water Management in European Circular Cities: A Critical Assessment Based on Case Studies and Literature. *Blue-Green Systems* **2020**, *2*, 112–136, doi:10.2166/bgs.2020.932.
135. Abdulwahid, R.T.; Aziz, S.B.; Kadir, M.F.Z. Insights into Ion Transport in Biodegradable Solid Polymer Blend Electrolyte Based on FTIR Analysis and Circuit Design. *Journal of Physics and Chemistry of Solids* **2022**, *167*, 110774, doi:10.1016/j.jpcs.2022.110774.
136. Caracostea, L.-M.; Sîrbu, R.; Buşuricu, F. Determination of Caffeine Content in Arabica and Robusta Green Coffee of Indian Origin. *European Journal of Natural Sciences and Medicine* **2021**, *4*, 67–77, doi:10.26417/425qba31z.
137. Hossain, A.M.; Salehuddin, S.M. Analytical Determination of Nicotine in Tobacco Leaves by Gas Chromatography–Mass Spectrometry. *Arabian Journal of Chemistry* **2013**, *6*, 275–278, doi:10.1016/j.arabjc.2010.10.006.
138. Dave, B.; Moysa, E.L.; Kuźnik, A. Enhancing Fungal Adaptation for Efficient Caffeine Degradation in Wastewater: Biomimetic Approach and Environmental Optimization. *Desalination and Water Treatment* **2025**, *321*, 100938, doi:10.1016/j.dwt.2024.100938.
139. Zyoud, S.; Zyoud, A.H. Revealing Global Trends on Nature-Based Solutions: Mapping and Visualizing Research Landscapes. *Nature-Based Solutions* **2025**, *7*, 100229, doi:10.1016/j.nbsj.2025.100229.
140. Jang, S.; Kim, H. Direct Chiral^{19} F NMR Analysis of Fluorine-Containing Analytes and Its Application to Simultaneous Chiral Analysis. *Org. Lett.* **2020**, *22*, 7804–7808, doi:10.1021/acs.orglett.0c02620.

141. Lv, T.-M.; Chen, D.-L.; Liang, J.-J.; Bai, M.; Lin, B.; Huang, X.-X.; Ma, G.-X.; Song, S.-J. Structural Revisions of Two Highly Aromatic Naphthoquinone-Derived Dimers Based on NMR Analysis, Computer-Assisted Structure Elucidation Methods, and Computations. *Org. Lett.* **2021**, *23*, 7231–7235, doi:10.1021/acs.orglett.1c02626.
142. Yao, H.-Y.-Y.; Wang, J.-Q.; Yin, J.-Y.; Nie, S.-P.; Xie, M.-Y. A Review of NMR Analysis in Polysaccharide Structure and Conformation: Progress, Challenge and Perspective. *Food Research International* **2021**, *143*, 110290, doi:10.1016/j.foodres.2021.110290.
143. Jureczko, M.; Przystaś, W.; Krawczyk, T.; Gonciarz, W.; Rudnicka, K. White-Rot Fungi-Mediated Biodegradation of Cytostatic Drugs - Bleomycin and Vincristine. *Journal of Hazardous Materials* **2021**, *407*, 124632, doi:10.1016/j.jhazmat.2020.124632.
144. Veresoglou, S.D.; Wang, D.; Andrade-Linares, D.R.; Hempel, S.; Rillig, M.C. Fungal Decision to Exploit or Explore Depends on Growth Rate. *Microb Ecol* **2018**, *75*, 289–292, doi:10.1007/s00248-017-1053-4.
145. Syamsia, S.; Idhan, A.; Latifah, H.; Noerfityani, N.; Akbar, A. Alternative Medium for the Growth of Endophytic Fungi. *IOP Conf. Ser.: Earth Environ. Sci.* **2021**, *886*, 012045, doi:10.1088/1755-1315/886/1/012045.
146. Łobos-Moysa, E.; Bodzek, M. Application of Hybrid Biological Techniques to the Treatment of Municipal Wastewater Containing Oils and Fats. *Desalination and Water Treatment* **2012**, *46*, 32–37, doi:10.1080/19443994.2012.677451.
147. Rodarte-Morales, A.I.; Feijoo, G.; Moreira, M.T.; Lema, J.M. Degradation of Selected Pharmaceutical and Personal Care Products (PPCPs) by White-Rot Fungi. *World J Microbiol Biotechnol* **2011**, *27*, 1839–1846, doi:10.1007/s11274-010-0642-x.
148. Patel, D.; Pardhi, D.; Rathod, T.; Solanki, A.; Raval, V.; Panchal, R.; Joshi, R.; Rajput, K. Unveiling the Potential of Bacillus Safensis PG-54 Isolated from Fermented Panchagavya on Sorghum Bicolor under Salinity Stress. *Discov. Plants* **2025**, *2*, 87, doi:10.1007/s44372-025-00164-w.
149. Vaghela, B.; Vashi, R.; Rajput, K.; Joshi, R. Plant Chitinases and Their Role in Plant Defense: A Comprehensive Review. *Enzyme and Microbial Technology* **2022**, *159*, 110055, doi:10.1016/j.enzmictec.2022.110055.
150. Abdelwahab, N.S.; Abdelaleem, E.A.; Abdelrahman, M.M. HPTLC-Densitometric Method for Determination of Ascorbic Acid, Paracetamol and Guaifenesin in Presence of Their Toxic Impurities. *Journal of Chromatographic Science* **2019**, *57*, 149–155, doi:10.1093/chromsci/bmy096.
151. Chouhan, S.; Mulani, R.; Ansari, H.; Sindhav, G.; Rao, P.; Rawal, R.M.; Saraf, M.; Goswami, D. Rapid Method for Detection, Quantification and Measuring Microbial Degradation of Pesticide-Thiram Using High Performance Thin Layer Chromatography (HPTLC). *Environ Sci Pollut Res* **2023**, *30*, 7874–7885, doi:10.1007/s11356-022-22731-4.
152. Rodrigues, R.; Oliveira, M.B.P.P.; Alves, R.C. Chlorogenic Acids and Caffeine from Coffee By-Products: A Review on Skincare Applications. *Cosmetics* **2023**, *10*, 12, doi:10.3390/cosmetics10010012.
153. Rodarte-Morales, A.I.; Feijoo, G.; Moreira, M.T.; Lema, J.M. Degradation of Selected Pharmaceutical and Personal Care Products (PPCPs) by White-Rot Fungi. *World J Microbiol Biotechnol* **2011**, *27*, 1839–1846, doi:10.1007/s11274-010-0642-x.
154. Lu, J.; Guo, C.; Li, J.; Zhang, H.; Lu, G.; Dang, Z.; Wu, R. A Fusant of Sphingomonas Sp. GY2B and Pseudomonas Sp. GP3A with High Capacity of Degrading Phenanthrene. *World J Microbiol Biotechnol* **2013**, *29*, 1685–1694, doi:10.1007/s11274-013-1331-3.

155. Das, P.; Mehra, A.; Sachan, S.G.; Chattopadhyay, S. Screening Different Solid Supports for Pseudomonas Aeruginosa Biofilm Formation and Determining Its Efficiency for Decolorization and Degradation of Congo Red. *Arch Microbiol* **2024**, *206*, 402, doi:10.1007/s00203-024-04125-x.
156. Nie, H.; Guo, D.; Wang, Y.; Wang, L.; Cao, S.; Huang, Z.; Zhao, T. Glucose Co-Metabolism Enhances Extracellular ROS-Mediated TBBPA Biodegradation by Pseudomonas Aeruginosa NY3 and Reshapes Microbial Communities in Wastewater Treatment Systems. *Journal of Water Process Engineering* **2025**, *75*, 107989, doi:10.1016/j.jwpe.2025.107989.
157. Dave, B.; Łobos-Moysa, E.; Kuznik, A.; Maqsood, A.; Appiah, A.N.S.; Krzeszowski, S.; Joshi, R. Enhancing Microbial Biodegradation of PPCPs in Wastewater via Natural Self-Purification in a Novel Constructed Wetland System. *Sustainability* **2026**, *18*, 548, doi:10.3390/su18010548.
158. Gupta, P.; Ann, T.; Lee, S.-M. Use of Biochar to Enhance Constructed Wetland Performance in Wastewater Reclamation. *Environmental Engineering Research* **2016**, *21*, 36–44, doi:10.4491/eer.2015.067.
159. Freeman, A.I.; Widdowson, S.; Murphy, C.; Cooper, D.J. Economic Assessment of Aerated Constructed Treatment Wetlands Using Whole Life Costing. *Water Science and Technology* **2019**, *80*, 75–85, doi:10.2166/wst.2019.246.
160. Snyder, B.F. The Inclusion of Ecosystem Service Valuations in Bioenergy Cost Analysis: A Case Study of Constructed Wetlands in the Neotropics. *Ecological Economics* **2019**, *156*, 196–201, doi:10.1016/j.ecolecon.2018.10.005.
161. Gebru, S.B.; Werkneh, A.A. Applications of Constructed Wetlands in Removing Emerging Micropollutants from Wastewater: Occurrence, Public Health Concerns, and Removal Performances – a Review. *South African Journal of Chemical Engineering* **2024**, *48*, 395–416, doi:10.1016/j.sajce.2024.03.004.
162. Wdowczyk, A.; Szymańska-Pulikowska, A. Effect of Substrates on the Potential of Phragmites Australis to Accumulate and Translocate Selected Contaminants from Landfill Leachate. *Water Resources and Industry* **2023**, *29*, 100203, doi:10.1016/j.wri.2023.100203.
163. Liu, N.; Shi, Y.; Li, W.; Xu, L.; Cai, Y. Concentrations and Distribution of Synthetic Musks and Siloxanes in Sewage Sludge of Wastewater Treatment Plants in China. *Science of The Total Environment* **2014**, *476–477*, 65–72, doi:10.1016/j.scitotenv.2013.12.124.
164. Javid, F.; Ali, G.; Rehman, A.; Naeem, R.; Ali, I.; Naz, I. Assessment of Plastic Degradation by Indigenous Bacteria from Waste Disposal Sites. *Emerging Contaminants* **2024**, *10*, 100323, doi:10.1016/j.emcon.2024.100323.
165. Dave, B.; Moysa, E.L.; Kuźnik, A. Nicotine Degradation by Trametes Versicolor: Insights from Diverse Environmental Stressors and Wastewater Medium. *Molecules* **2025**, *30*, 2658, doi:10.3390/molecules30122658.
166. Borman, P.; Elder, D. Q2(R1) Validation of Analytical Procedures: Text and Methodology. In *ICH Quality Guidelines*; Teasdale, A., Elder, D., Nims, R.W., Eds.; Wiley, 2017; pp. 127–166 ISBN 978-1-118-97111-6.
167. Iwai, Y.; Nagano, H.; Lee, G.S.; Uno, M.; Arai, Y. Measurement of Entrainer Effects of Water and Ethanol on Solubility of Caffeine in Supercritical Carbon Dioxide by FT-IR Spectroscopy. *The Journal of Supercritical Fluids* **2006**, *38*, 312–318, doi:10.1016/j.supflu.2005.12.005.
168. Taweetanawanit, P.; Ratpukdi, T.; Siripattanakul-Ratpukdi, S. Performance and Kinetics of Triclocarban Removal by Entrapped Pseudomonas Fluorescens Strain MC46. *Bioresource Technology* **2019**, *274*, 113–119, doi:10.1016/j.biortech.2018.11.085.

169. D'Amelio, N.; Fontanive, L.; Uggeri, F.; Suggi-Liverani, F.; Navarini, L. NMR Reinvestigation of the Caffeine–Chlorogenate Complex in Aqueous Solution and in Coffee Brews. *Food Biophysics* **2009**, *4*, 321–330, doi:10.1007/s11483-009-9130-y.
170. Tavagnacco, L.; Engström, O.; Schnupf, U.; Saboungi, M.-L.; Himmel, M.; Widmalm, G.; Cesàro, A.; Brady, J.W. Caffeine and Sugars Interact in Aqueous Solutions: A Simulation and NMR Study. *J. Phys. Chem. B* **2012**, *116*, 11701–11711, doi:10.1021/jp303910u.
171. Kent, J.E.; Bell, N.G.A. Molecular Properties of Caffeine Explored by NMR: A Benchtop NMR Experiment for Undergraduate Physical-Chemistry Laboratories. *J. Chem. Educ.* **2019**, *96*, 786–791, doi:10.1021/acs.jchemed.8b00633.
172. Atac, A.; Karabacak, M.; Karaca, C.; Kose, E. NMR, UV, FT-IR, FT-Raman Spectra and Molecular Structure (Monomeric and Dimeric Structures) Investigation of Nicotinic Acid N-Oxide: A Combined Experimental and Theoretical Study. *Spectrochimica Acta Part A: Molecular and Biomolecular Spectroscopy* **2012**, *85*, 145–154, doi:10.1016/j.saa.2011.09.048.
173. Ferreira, C.L.; Rocha, E.C.D.S.; Reis, Y.F.A.D.; Zanon Guimarães, R.; Silva, S.M.S.D.D.; Paiva, R.T.G.D.; Moraes, J.P.D.S.; Dos Santos, L.; Carvalho, L.F.D.C.E.S.D. Comparative FT-IR Spectroscopy Salivary Profiles of University Students: E-Cigarette Users vs Nonusers. *ACS Omega* **2026**, *11*, 1953–1961, doi:10.1021/acsomega.5c10219.
174. Zeng, H.; Zhang, Y.; Peng, L.-J.; Shao, H.; Menon, N.K.; Yang, J.; Salomon, A.R.; Freidland, R.P.; Zagorski, M.G. Nicotine and Amyloid Formation. *Biological Psychiatry* **2001**, *49*, 248–257, doi:10.1016/S0006-3223(00)01111-2.
175. Duell, A.K.; Pankow, J.F.; Peyton, D.H. Free-Base Nicotine Determination in Electronic Cigarette Liquids by^{1} H NMR Spectroscopy. *Chem. Res. Toxicol.* **2018**, *31*, 431–434, doi:10.1021/acs.chemrestox.8b00097.
176. Salam, S.; El-Hajj Moussa, F.; El-Hage, R.; El-Hellani, A.; Aoun Saliba, N. A Systematic Review of Analytical Methods for the Separation of Nicotine Enantiomers and Evaluation of Nicotine Sources. *Chem. Res. Toxicol.* **2023**, *36*, 334–341, doi:10.1021/acs.chemrestox.2c00310.
177. Cogo, K.; Montan, M.F.; Bergamaschi, C.D.C.; D. Andrade, E.; Rosalen, P.L.; Groppo, F.C. In Vitro Evaluation of the Effect of Nicotine, Cotinine, and Caffeine on Oral Microorganisms. *Can. J. Microbiol.* **2008**, *54*, 501–508, doi:10.1139/W08-032.
178. Huang, R.; Li, M.; Gregory, R.L. Effect of Nicotine on Growth and Metabolism of *Streptococcus Mutans*. *European J Oral Sciences* **2012**, *120*, 319–325, doi:10.1111/j.1600-0722.2012.00971.x.
179. DuBois, A.E.; Bennett, Z.C.; Khalid, U.; Khalid, A.; Meece, R.A.; Difiore, G.J.; Gregory, R.L. Nicotine: Its Stimulating and Inhibitory Effects on Oral Microorganisms. *finefocus* **2014**, *1*, 63–75, doi:10.33043/FF.1.1.63-75.
180. Del Sorbo, G.; Schoonbeek, H.; De Waard, M.A. Fungal Transporters Involved in Efflux of Natural Toxic Compounds and Fungicides. *Fungal Genetics and Biology* **2000**, *30*, 1–15, doi:10.1006/fgbi.2000.1206.
181. He, C.; Huang, Y.; Liu, P.; Wei, J.; Yang, Y.; Xu, L.; Xiao, M. Transcriptome Analysis of Genes and Metabolic Pathways Associated with Nicotine Degradation in Aspergillus Oryzae 112822. *BMC Genomics* **2019**, *20*, 86, doi:10.1186/s12864-019-5446-2.
182. Su, Y.; Xian, H.; Shi, S.; Zhang, C.; Manik, S.M.N.; Mao, J.; Zhang, G.; Liao, W.; Wang, Q.; Liu, H. Biodegradation of Lignin and Nicotine with White Rot Fungi for the Delignification and Detoxification of Tobacco Stalk. *BMC Biotechnol* **2016**, *16*, 81, doi:10.1186/s12896-016-0311-8.

183. Saeed, T.; Sun, G. A Comparative Study on the Removal of Nutrients and Organic Matter in Wetland Reactors Employing Organic Media. *Chemical Engineering Journal* **2011**, *171*, 439–447, doi:10.1016/j.cej.2011.03.101.
184. Sandle, T. Selection and Application of Culture Media. In *Biocontamination Control for Pharmaceuticals and Healthcare*; Elsevier, 2019; pp. 103–123 ISBN 978-0-12-814911-9.
185. Wang, L.; Liu, T.; Sun, H.; Zhou, Q. Transesterification of Para-Hydroxybenzoic Acid Esters (Parabens) in the Activated Sludge. *Journal of Hazardous Materials* **2018**, *354*, 145–152, doi:10.1016/j.jhazmat.2018.04.077.
186. Duc, H.D. Enhanced Degradation of Sulfamethoxazole Using Immobilized Biomass Reactor. *Environmental Engineering Research* **2022**, *28*, 220213–0, doi:10.4491/eer.2022.213.
187. Alam, P.; Shakeel, F.; Iqbal, M.; Foudah, A.I.; Alqarni, M.H.; Aljarba, T.M.; Abdel Bar, F.; Alshehri, S. Quantification of Pomalidomide Using Conventional and Eco-Friendly Stability-Indicating HPTLC Assays: A Contrast of Validation Parameters. *ACS Omega* **2023**, *8*, 30655–30664, doi:10.1021/acsomega.3c04382.
188. Jeon, J.-M.; Park, S.-J.; Choi, T.-R.; Park, J.-H.; Yang, Y.-H.; Yoon, J.-J. Biodegradation of Polyethylene and Polypropylene by Lysinibacillus Species JJY0216 Isolated from Soil Grove. *Polymer Degradation and Stability* **2021**, *191*, 109662, doi:10.1016/j.polymdegradstab.2021.109662.
189. Mali, H.; Shah, C.; Patel, D.H.; Trivedi, U.; Subramanian, R.B. Degradation Insight of Organophosphate Pesticide Chlorpyrifos through Novel Intermediate 2,6-Dihydroxypyridine by Arthrobacter Sp. HM01. *Bioresour. Bioprocess.* **2022**, *9*, 31, doi:10.1186/s40643-022-00515-5.
190. Wu, K.; Shi, M.; Pan, X.; Zhang, J.; Zhang, X.; Shen, T.; Tian, Y. Decolourization and Biodegradation of Methylene Blue Dye by a Ligninolytic Enzyme-Producing Bacillus Thuringiensis: Degradation Products and Pathway. *Enzyme and Microbial Technology* **2022**, *156*, 109999, doi:10.1016/j.enzmictec.2022.109999.
191. Mazzola, M.; De Bruijn, I.; Cohen, M.F.; Raaijmakers, J.M. Protozoan-Induced Regulation of Cyclic Lipopeptide Biosynthesis Is an Effective Predation Defense Mechanism for*Pseudomonas Fluorescens*. *Appl Environ Microbiol* **2009**, *75*, 6804–6811, doi:10.1128/aem.01272-09.
192. Miller, T.R.; Colquhoun, D.R.; Halden, R.U. Identification of Wastewater Bacteria Involved in the Degradation of Triclocarban and Its Non-Chlorinated Congener. *Journal of Hazardous Materials* **2010**, *183*, 766–772, doi:10.1016/j.jhazmat.2010.07.092.
193. Pan, H.; Shi, J.; Xu, D.; Wang, J.; Ma, Q. Environmental Occurrence, Ecological Risks, and Microbial Interactions of p-Chloro-m-Xylenol: An Emerging Ubiquitous Antimicrobial Agent. *International Biodeterioration & Biodegradation* **2026**, *207*, 106229, doi:10.1016/j.ibiod.2025.106229.
194. Liang, B.; Yun, H.; Kong, D.; Ding, Y.; Li, X.; Vangnai, A.S.; Wang, A. Bioaugmentation of Triclocarban and Its Dechlorinated Congeners Contaminated Soil with Functional Degraders and the Bacterial Community Response. *Environmental Research* **2020**, *180*, 108840, doi:10.1016/j.envres.2019.108840.
195. Wang, H.; Yun, H.; Li, M.; Cui, H.; Ma, X.; Zhang, Y.; Pei, X.; Zhang, L.; Shi, K.; Li, Z.; et al. Fate, Toxicity and Effect of Triclocarban on the Microbial Community in Wastewater Treatment Systems. *Journal of Hazardous Materials* **2022**, *440*, 129796, doi:10.1016/j.jhazmat.2022.129796.

196. Escher, B.I.; Fenner, K. Recent Advances in Environmental Risk Assessment of Transformation Products. *Environ. Sci. Technol.* **2011**, *45*, 3835–3847, doi:10.1021/es1030799.
197. Kotthoff, L.; Keller, J.; Lörchner, D.; Mekonnen, T.F.; Koch, M. Transformation Products of Organic Contaminants and Residues—Overview of Current Simulation Methods. *Molecules* **2019**, *24*, 753, doi:10.3390/molecules24040753.
198. Suman, T.-Y.; Kim, S.-Y.; Yeom, D.-H.; Jeon, J. Transformation Products of Emerging Pollutants Explored Using Non-Target Screening: Perspective in the Transformation Pathway and Toxicity Mechanism—A Review. *Toxics* **2022**, *10*, 54, doi:10.3390/toxics10020054.
199. Xu, T.; Chen, J.; Chen, X.; Xie, H.; Wang, Z.; Xia, D.; Tang, W.; Xie, H. Prediction Models on p K_a and Base-Catalyzed Hydrolysis Kinetics of Parabens: Experimental and Quantum Chemical Studies. *Environ. Sci. Technol.* **2021**, *55*, 6022–6031, doi:10.1021/acs.est.0c06891.
200. Cheng, Z.; Zhang, C.; Jiang, W.; Zhai, W.; Gao, J.; Wang, P. Effects of the Presence of Triclocarban on the Degradation and Migration of Co-Occurring Pesticides in Soil. *Environmental Pollution* **2022**, *310*, 119840, doi:10.1016/j.envpol.2022.119840.
201. Wu, J.; Zhang, S.; Chen, Y.; Zhao, J.; Prosun, T.; O'Brien, J.W.; Mueller, J.F.; Tscharke, B.J.; Coin, L.J.M.; Luby, S.P.; et al. Associations between Wastewater Microbiome and Population Smoking Rate Identified Using Wastewater-Based Epidemiology. *Environ. Health* **2023**, *1*, 394–404, doi:10.1021/envhealth.3c00105.
202. Schabacker, J.; Gerlach, J.; Münderle, M.; Dietzen, C.; Ludwigs, J.-D. Focal Bird Species and Risk Assessment Approach for Nonagricultural Grassland Scenarios in Central Europe. *Environmental Toxicology and Chemistry* **2014**, *33*, 2055–2061, doi:10.1002/etc.2652.
203. Adhikari, S.; Kumar, R.; Driver, E.M.; Perleberg, T.D.; Yanez, A.; Johnston, B.; Halden, R.U. Mass Trends of Parabens, Triclocarban and Triclosan in Arizona Wastewater Collected after the 2017 FDA Ban on Antimicrobials and during the COVID-19 Pandemic. *Water Research* **2022**, *222*, 118894, doi:10.1016/j.watres.2022.118894.
204. Mariencheck, W.I.; Alcorn, J.F.; Palmer, S.M.; Wright, J.R. *Pseudomonas Aeruginosa* Elastase Degrades Surfactant Proteins A and D. *Am J Respir Cell Mol Biol* **2003**, *28*, 528–537, doi:10.1165/rcmb.2002-0141OC.
205. Aleksic, I.; Milivojevic, D. The Plastic-Degrading Capabilities of Pseudomonas Aeruginosa. *Biotechnol Environ* **2025**, *2*, 17, doi:10.1186/s44314-025-00033-6.
206. Banar, M.; Emaneini, M.; Beigverdi, R.; Fanaei Pirlar, R.; Node Farahani, N.; Van Leeuwen, W.B.; Jabalameli, F. The Efficacy of Lyticase and β-Glucosidase Enzymes on Biofilm Degradation of Pseudomonas Aeruginosa Strains with Different Gene Profiles. *BMC Microbiol* **2019**, *19*, 291, doi:10.1186/s12866-019-1662-9.
207. Moredo, N.; Lorenzo, M.; Domínguez, A.; Moldes, D.; Cameselle, C.; Sanroman, A. Enhanced Ligninolytic Enzyme Production and Degrading Capability of Phanerochaete Chrysosporium and Trametes Versicolor. *World Journal of Microbiology and Biotechnology* **2003**, *19*, 665–669, doi:10.1023/A:1025198917474.
208. Tran, N.H.; Urase, T.; Kusakabe, O. Biodegradation Characteristics of Pharmaceutical Substances by Whole Fungal Culture Trametes Versicolor and Its Laccase. *J. of Wat. & Envir. Tech.* **2010**, *8*, 125–140, doi:10.2965/jwet.2010.125.
209. Mir-Tutusaus, J.A.; Masís-Mora, M.; Corcellas, C.; Eljarrat, E.; Barceló, D.; Sarrà, M.; Caminal, G.; Vicent, T.; Rodríguez-Rodríguez, C.E. Degradation of Selected Agrochemicals by the White Rot Fungus Trametes Versicolor. *Science of The Total Environment* **2014**, *500–501*, 235–242, doi:10.1016/j.scitotenv.2014.08.116.

210. Ellegaard-Jensen, L.; Knudsen, B.E.; Johansen, A.; Albers, C.N.; Aamand, J.; Rosendahl, S. Fungal–Bacterial Consortia Increase Diuron Degradation in Water-Unsaturated Systems. *Science of The Total Environment* **2014**, *466–467*, 699–705, doi:10.1016/j.scitotenv.2013.07.095.
211. Silva, L.C.F.; Lima, H.S.; Sartoratto, A.; Sousa, M.P.D.; Torres, A.P.R.; Souza, R.S.D.; De Paula, S.O.; Oliveira, V.M.D.; Silva, C.C.D. Effect of Salinity in Heterotrophic Nitrification/Aerobic Denitrification Performed by Acclimated Microbiota from Oil-Produced Water Biological Treatment System. *International Biodeterioration & Biodegradation* **2018**, *130*, 1–7, doi:10.1016/j.ibiod.2018.03.009.
212. Rezaei, Z.; Moghimi, H. Fungal-Bacterial Consortia: A Promising Strategy for the Removal of Petroleum Hydrocarbons. *Ecotoxicology and Environmental Safety* **2024**, *280*, 116543, doi:10.1016/j.ecoenv.2024.116543.
213. Sipahutar, M.K.; Piapukiew, J.; Vangnai, A.S. Efficiency of the Formulated Plant-Growth Promoting Pseudomonas Fluorescens MC46 Inoculant on Triclocarban Treatment in Soil and Its Effect on Vigna Radiata Growth and Soil Enzyme Activities. *Journal of Hazardous Materials* **2018**, *344*, 883–892, doi:10.1016/j.jhazmat.2017.11.046.
214. Wang, Z.; Gao, J.; Wang, S.; Zhao, Y.; Dai, H.; Li, D.; Cui, Y.; Li, Z. Triclocarban Shifted the Microbial Communities and Promoted the Spread of Antibiotic Resistance Genes in Nitrifying Granular Sludge System. *Bioresource Technology* **2022**, *347*, 126429, doi:10.1016/j.biortech.2021.126429.
215. Ilyas, H.; Van Hullebusch, E.D. Performance Comparison of Different Constructed Wetlands Designs for the Removal of Personal Care Products. *IJERPH* **2020**, *17*, 3091, doi:10.3390/ijerph17093091.
216. Iacopetta, D.; Catalano, A.; Ceramella, J.; Saturnino, C.; Salvagno, L.; Ielo, I.; Drommi, D.; Scali, E.; Plutino, M.R.; Rosace, G.; et al. The Different Facets of Triclocarban: A Review. *Molecules* **2021**, *26*, 2811, doi:10.3390/molecules26092811.
217. Löffler, P. *Impact of Antimicrobial Transformation Products on Aquatic Environments*; Acta Universitatis Agriculturae Sueciae; Swedish University of Agricultural Sciences, 2025; Vol. 2025:82; ISBN 978-91-8124-112-9.

List of Tables

List of figures

Figure 57. 1H NMR spectrum of wetland B (Trametes versicolor) 7 weeks

Figure 58. 1H NMR spectrum of wetland C (Pseudomonas aeruginosa + Trametes versicolor) 7 weeks

Figure 59. SEM images illustrating microbial colonization of porous media used in the constructed wetland system